University of Southampton Research Repository

University of Southampton

Faculty of Natural and Environmental Sciences

School of Ocean and Earth Science

The challenge of scaling up from individual physiology to population level effects: Using the Dynamic Energy Budget to describe and predict crustacean responses to climate variability

by

Sarah Elizabeth Talbot

ORCID ID: 0000-0002-5046-5143

Thesis for the degree of Doctor of Philosophy

December 2019

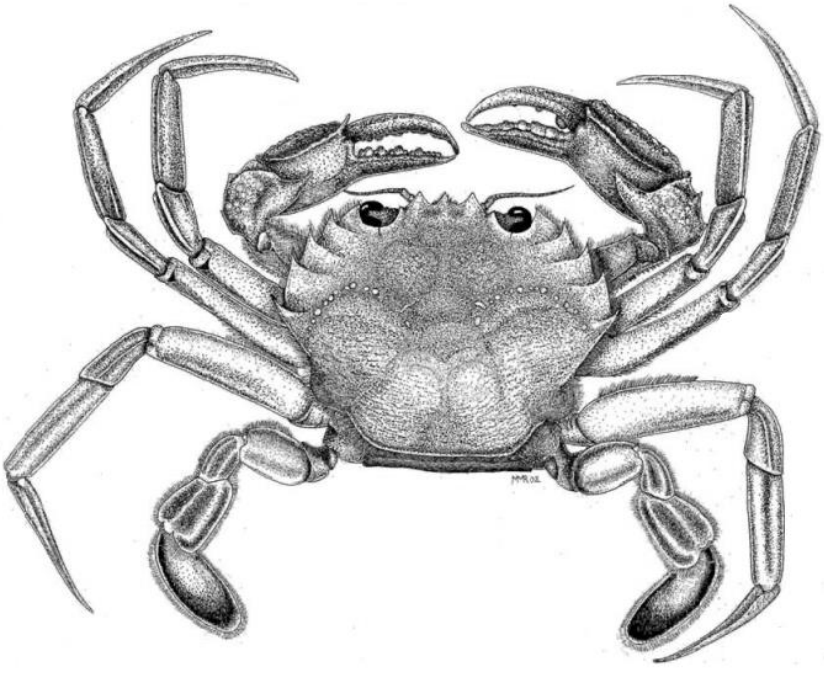

University of Southampton

Abstract

Faculty of Natural and Environmental Sciences

School of Ocean and Earth Science

Thesis for the degree of Doctor of Philosophy

The challenge of scaling up from individual physiology to population level effects: Using the Dynamic Energy Budget to describe and predict crustacean responses to climate variability

by

Sarah Elizabeth Talbot

Predicting how marine communities will be affected by environmental change is one of the most significant challenges facing researchers today. In order to tackle this challenge, a mechanistic understanding of climate impacts at the individual level is necessary, as variations in species physiological responses are often reflected in patterns at higher organisational levels such as populations and communities. In order to explore the relationship between individual physiology and higher-level dynamics more fully, the swimming crab *Liocarcinus depurator* (Linnaeus, 1758) was selected as a model species for experimental work in which whole organism responses (growth, respiration and allocation to reproduction) to climate drivers were investigated using a bio-energetic modelling approach. This species was selected as a model organism after analysis of epibenthic time-series from the Western English Channel monitoring Station L4 revealed that decapod crustaceans played a key role in structuring the benthic community, and that *L. depurator* was one of the most dominant species in the area, in terms of both abundance and biomass. A bio-energetic approach was used as the same time-series analysis identified water temperature and seasonal phytodetrital input (e.g. food) as the predominant drivers of variation in benthic community wet biomass at L4, with the two drivers appearing to primarily influence community biomass at different times of the year. It is possible that warmer water temperatures in the autumn trigger gonad development and a consequent increase in reproductive biomass, while the sedimentation of the spring phytoplankton bloom drives an increase in somatic biomass. This time-series analysis clearly highlighted the role of organism energetics, and the environmental conditions that influence energy allocation, in structuring benthic communities. Further work elucidated the relationship between environmental variables and individual energy budgets. *L. depurator* responses to climate drivers (temperature, hypoxia and ocean acidification) were tested experimentally, and a mechanistic Dynamic Energy Budget (DEB) model was parameterised to describe the life history characteristics of crustaceans. At an individual level the model was able to accurately describe and predict observed responses to environmental drivers, both in isolation and in multiple-stressor scenarios. Experimental results suggested that *L. depurator* was broadly tolerant of those climate drivers tested in the short term. Over the longer term however, model scenarios suggested that OA and the combined stressors may have an adverse effect on growth. When the multi-stressor model was forced with environmental projections from a coupled hydrodynamic-biogeochemical model (NEMO-ERSEM), it could be used to make predictions regarding ultimate carbon mass, age-at-maturity and cumulative allocation to reproduction, which were used to infer possible population level effects such as species distributions and population viability. Model scenarios suggested that, in the future, the optimum settlement time for juvenile *L. depurator* would shift forward across the north-west European shelf, and that this crustacean species may be able to expand its range further into the northern North Sea. The DEB model presented here can provide a mechanistic underpinning of observed species responses to climate drivers, and more broadly, the thesis demonstrates how multi-stressor models can be built from data collected in single stressor experiments, thereby providing a way of synthesising single stressor data into a modelling environment. This approach allows us to simulate more complex, ecologically relevant conditions. At a broader scale, the coupled DEB-ERSEM model showed that it can provide insight into why changes in species' distributions are predicted, as these distributions are an emergent property of the processes being modelled.

Dedicated to Mum

I’m sorry you never got to see me do this, but I hope I’ve made you proud.

A learning experience is one of those things that say, “You know that thing you just did? Don’t do that.”

Douglas Adams

Table of Contents

List of Tables

List of Figures

Research Thesis: Declaration of Authorship

Print name:	Sarah Elizabeth Talbot

Title of thesis:	The challenge of scaling up from individual physiology to population level effects: Using the Dynamic Energy Budget to describe and predict crustacean responses to climate variability

I declare that this thesis and the work presented in it are my own and has been generated by me as the result of my own original research.

I confirm that:

1. This work was done wholly or mainly while in candidature for a research degree at this University;
2. Where any part of this thesis has previously been submitted for a degree or any other qualification at this University or any other institution, this has been clearly stated;
3. Where I have consulted the published work of others, this is always clearly attributed;
4. Where I have quoted from the work of others, the source is always given. With the exception of such quotations, this thesis is entirely my own work;
5. I have acknowledged all main sources of help;
6. Where the thesis is based on work done by myself jointly with others, I have made clear exactly what was done by others and what I have contributed myself;
7. Parts of this work have been published as:

Talbot, E., Bruggeman, J., Hauton, C. & Widdicombe, S, 2019. Uncovering the environmental drivers of short-term temporal dynamics in an epibenthic community from the Western English Channel. *Journal of the Marine Biological Association of the UK*. **99** (7), 1476-1479.

Talbot, E., Widdicombe, S., Hauton, C. & Bruggeman, J., 2019. Adapting the Dynamic Energy Budget (DEB) approach to include non-continuous growth (moulting) and provide better predictions of biological performance in crustaceans. *ICES Journal of Marine Science,* **76** (1), 192-205.

Signature:		Date:	

Acknowledgements

I have been fortunate enough to have received the help and support of many people during the last four years. First and foremost among those, I thank my supervisors Steve Widdicombe, Jorn Bruggeman and Chris Hauton, whose support, enthusiasm and constructive suggestions never failed to buoy my spirits, and to remind me that what I was doing was actually pretty cool……... Thanks also to the benthic group at PML, particularly Ana Quierós for providing help and advice even though I wasn't your student; Jo Nunes for your good humoured and patient support of all my work in the mesocosm; Louise McNeill for sharing your taxonomic expertise when I first started working with the benthic trawls, and Sarah Dashfield for helping me organise boat trips and sort through trawl samples for crabs! Finally, a huge thank you to the skipper and crew of the *RV Plymouth Quest*: Andy, Gary, Andrew and Jim – for your expertise, your advice, your patience, and all the tea and cake I enjoyed on board – I truly appreciate it.

I will never be able to thank my family and friends enough for their kindness, love and support. To my fellow students at PML, especially Rachel Coppock-Weston, Jo Warwick-Dugdale, Becca Shellock, Sarah Nelms and Kevin Purves - we started this together, and we'll celebrate together when we're all done! Special mention also goes to Saskia Rühl: we shared a walk-in freezer (sorry, I mean lab) on board the *RRS James Clark Ross*, and one of the most enduring memories of my PhD concerns us trying to clear the water out of Steve's office after the mesocosm flood. May your cores always be easy to extract!

Thank you to the Hart and Leggatt clans for letting me decompress in your homes when I needed a break, and for listening to me ramble every time you asked how I was getting on. I couldn't have hoped for a better bunch of in-laws. Also to Dad and Gwen – you'll be delighted to hear that I can finally get a proper job - hooray!

And last, but by no means least, to my husband, Rob Hart. You deserve an award for weathering every storm with me – bearing the brunt of my frustration and dealing with the tears, the tantrums and the occasional bouts of hysteria – meeting it all with sympathy and, critically, baked goods. Thank you.

Abbreviations and notation

Common abbreviations used throughout the text

AmP	Add-my-Pet: a database containing DEB parameters for >1000 species. https://www.bio.vu.nl/thb/deb/deblab/add_my_pet/
DEB	Dynamic Energy Budget: metabolic theory and associated models
DBEM	dynamic bioclimatic envelope model: a type of species distribution model
IP	Intermoult period: the time period between moults in crustaceans
IPBES	Intergovernmental Science-Policy Platform on Biodiversity and Ecosystem Services
IPCC	Intergovernmental Panel on Climate Change
MAE	mean average error: a common model test statistic used to evaluate model performance throughout the thesis
MI	moult increment: the increase in crustacean size/mass after a moult
NEMO-ERSEM	a coupled hydrodynamic-biogeochemical model (Nucleus for European Modelling of the Ocean-European Regional Seas Ecosystem Model)
OA	ocean acidification
POC	particulate organic carbon
SDM	species distribution model
SEB	static energy budget: a range of models for exploring organism energetics and growth. Conceptually distinct from DEB

SS-DBEM	size spectrum dynamic bioclimatic envelope model: DBEM models which explicitly consider trophic interaction *via* a coupled size spectrum module
WCO	Western Channel Observatory

DEB notation

AAM	age at maturity
α (alpha)	ratio of carbon mass to wet mass. Specific to the crustacean model presented here
j_{XAm}	maximum ingestion rate
κ (kappa)	proportion of mobilised reserve allocated to somatic maintenance and growth
1-κ	proportion of mobilised reserve allocated to maturity and reproduction
k_J	maturity maintenance rate
k_M	somatic maintenance rate
M_C	carbon mass
M_E	the state variable reserve
M_R	the state variable reproductive buffer/allocation to reproduction
M_V	the state variable structure
M_W	wet mass. A state variable in the crustacean model presented here. Not a standard state variable in DEB models.
TC	Arrhenius temperature correction factor
v	reserve mobilisation rate
y_{EX}	assimilation efficiency
y_{VE}	growth efficiency

Chapter 1 Introduction

1.1 Global change impacts on marine communities

Marine habitats are under increasing threat from human activity, with pronounced ecological consequences (Doney et al., 2012; IPBES, 2019). The pressure of habitat loss, pollution, overexploitation and climate change are now almost inescapable (Halpern et al., 2015). The cumulative effects of these pressures are numerous, and include climate-related mortality events such as coral bleaching (Hoegh-Guldberg, 1999) and mass die-offs of benthic invertebrates (Boesch and Rabalais, 1991; Diaz and Rosenberg, 2008) and fish (Thronson and Quigg, 2008) in response to hypoxic events. Changes in biogeographical ranges as a response to ocean warming have been recorded, with marine crustaceans (Beaugrand et al., 2002; Mieszkowska et al., 2005), molluscs (Zacherl et al., 2003), echinoderms (Banks et al., 2010) and fish (Perry et al., 2005; Frainer et al., 2017) all shifting their ranges poleward. There have been documented changes in the strengths and types of ecological interactions (Milazzo et al., 2012; Pincebourde et al., 2012) and phenological shifts in the timing of reproductive events (Poloczanska et al., 2013). For example, decapod larvae now appear in the plankton of the southern North Sea earlier than they did in the 1980s (Lindley and Kirby, 2010). Finally, climate change has led to an erosion of biodiversity (Butchart et al., 2010; McCauley et al., 2015), with tropical biodiversity hotspots often losing species due to elevated heat stress (Worm and Lotze, 2016). Collectively, this has prompted concerns that we are approaching a planetary-scale tipping point (IPCC, 2018).

There is much work in the published literature concerning the possible physiological effects of anthropogenic change on individual species. Ocean acidification has been shown to impact upon reproductive processes in various taxa, with fertilisation success negatively affected by reduced seawater pH in echinoderms (Havenhand et al., 2008) and bivalve molluscs (Parker et al., 2009). Larval development can be impaired when seawater pCO_2 is elevated, with studies highlighting an increase in bivalve (Parker et al., 2009; Crim et al., 2011) and echinoderm (Kurihara et al., 2004; Dupont et al., 2008) larval abnormalities with decreasing pH. Research has also shown a reduction in larval growth rates in echinoderms (Dupont et al., 2008; Chan et al., 2015), decapod crustaceans (Walther et al., 2010; Rato et al., 2017) and bivalves (Barros et al., 2013) in response to elevated pCO_2. Growth rates in post-metamorphic animals can be negatively affected by ocean acidification. While much of the literature focuses on the growth reductions in calcifying organisms such as corals (Büscher et al., 2017; Mollica et al., 2018) and bivalves (Stevens and Gobler, 2018), there is some indication that crustacean growth can also be negatively impacted by increased seawater pCO_2 (Whiteley, 2011). Environmental hypoxia has been shown to negatively impact reproduction in gastropods by reducing the number of egg capsules produced (Cheung et al., 2008) and in echinoderms by delaying the development of female reproductive structures (Calder-Potts et al., 2015). There is evidence that decreasing oxygen concentrations can also reduce growth in gastropods (Cheung et al., 2008; Li and Chiu, 2013) and decapod crustaceans (Das and Stickle, 1993; Wei et al., 2008). A reduction in ingestion rate as a response to hypoxic conditions has been observed in bivalves (Artigaud et al., 2014; Sanders et al., 2014), gastropods (Liu et al., 2011) and decapod crustaceans (Baden et al., 1990; Das and Stickle, 1993) and several taxa including molluscs (Artigaud et al., 2014; Sanders et al., 2014) and echinoderms (Calder-Potts et al., 2015) are known to reduce their metabolic rate as an energy-saving mechanism. Finally, water temperature is known to be the primary driver of physiological processes in marine ectotherms (Kooijman, 2010). Ectothermic animal species are adapted to and depend upon maintenance of the characteristic temperature window of their natural environment (Pörtner, 2001), and exposure to temperatures outside of their optimal range can have a number of sub-lethal effects on marine organisms. For example, increased water temperatures resulted in reduced growth in gastropods (Vilchis et al., 2005), echinoderms (Pearce et al., 2005; Zamora and Jeffs, 2012) and decapod crustaceans (Thomas et al., 2000). Thermal stress has been shown to impact upon reproduction, with higher water temperatures causing a reduction in gonad development, gametogenesis and fecundity in gastropods (Vilchis et al., 2005; Rogers-Bennett et al., 2010) and bivalves (Fearman and Moltschaniwskyj, 2010). Reproductive success can be diminished in crustaceans exposed to higher water temperatures prior to mating (Wiklund and Sundelin, 2001), and embryonic development in echinoderms is impaired as temperatures increase towards predicted ocean warming limits (Byrne et al., 2009). A factor which can further complicate our understanding of the varying individual physiological effects of climate stressors on marine organisms is the evidence from a number of studies showing that physiological tolerance varies geographically (Place et al., 2008; Pearson et al., 2009). For example, Helmuth et al. (2006) suggested that regional tidal regimes and local patterns in wave splash on rocky shores can be more influential in driving patterns of body temperature in bivalves than large scale climate drivers, leading to complex thermal mosaics of temperature rather than simple latitudinal gradients.

1.2 Why do we need mechanistic understanding of organism responses to climate change?

Much of the literature cited above focuses on whole-organism (e.g. growth, development, reproduction) effects of environmental change. While this approach provides the advantage of directly translating the effects of stressors into the fitness consequences of an individual and the survival of its populations, it provides no insight into the mechanism of these effects, and so limits our ability to transfer results into novel or untested conditions (Sokolova, 2013). Given that the goal of environmental management is to maintain the long term health of populations, communities and ultimately, ecosystems (Jager and Klok, 2010) it is clear that a more thorough understanding of the mechanisms underlying the interactions between changes in the physical environment and organismal and ecological responses are critical if we are to predict future patterns of biodiversity, distribution and abundance (Gunderson et al., 2016). Once we have this mechanistic understanding of responses to anthropogenic change, it will be possible to make informed decisions on how best to manage marine habitats to mitigate its effects (McLeod et al., 2009; Bernhardt and Leslie, 2013; Green et al., 2014).

While there are many ways to explore the mechanisms of organism responses to environmental change, energetic approaches are arguably one of the most useful. This is because even where organismal-level impacts of stressors appear to be minimal, there can be dramatic changes in energy allocation in order to maintain compensatory mechanisms and physiological function (Pan et al., 2015). Several authors have linked observed changes in organism growth, reproduction and respiration to impacts on energy budgets (Fernández-Reiriz et al., 2011; Stumpp et al., 2012; Pan et al., 2015; Jager et al., 2016; Gray et al., 2017). For example, Stumpp et al. (2011) showed that reduced pH leads to a reduction in the scope for growth of urchin larvae, with only 39-45% of available energy spent on somatic growth in animals in acidified treatments, compared to 78-80% spent on somatic growth in animals in controls. Similarly, in their study on the effects of environmental hypoxia on gastropods, Cheung et al. (2008) noted that the energy allocated to growth and reproduction decreased by between 48-70% with reductions in oxygen concentration. Bio-energetic methods can also provide a framework for linking individual physiological responses to environmental change and long-term, population level consequences (Sokolova, 2013), due to the fact that processes such as growth, development and reproduction show great interspecific variability. These patterns of physiological variability at the species level are often reflected in patterns at higher organisational levels such as populations and ecosystems (Bozinovic et al., 2011; Bozinovic and Pörtner, 2015).

1.3 Improving our ability to predict species responses to environmental change

Models are useful tools for understanding the contributions of different environmental factors in driving species distributions patterns. They are also critical for predicting future changes in these distributions, and for providing information to aid in conservation decision-making in complex, multi-disciplinary scenarios (Serra-Diaz et al., 2013). Despite the obvious association between variations in organism physiology and species distributions, many of the most widely used species distribution models (SDMs, also known as bioclimatic envelop models and correlative ecological niche models) do not focus on the mechanisms governing species performance in a given environment. Instead, they rely on empirical statistical modelling approaches to profile the bioclimatic envelope of a species and then project these conditions onto a geographical space, allowing species distributions to be mapped (Franklin, 2010). Although these SDMs have been used to investigate a range of marine ecological, resource management and conservation questions (Reiss et al., 2011; Sundblad et al., 2011), a fundamental limitation of this approach is that the models are phenomenological (Robinson et al., 2017). Variables thought to constrain a species' distribution are selected for use in the model, but the processes by which the variables limit species' distributions remain implicit (Mathewson et al., 2017). Consequently, extrapolation to future distribution patterns resulting from changing environmental conditions confronts the statistical and ecological assumptions of these models (Elith and Leathwick, 2009; Melle et al., 2014). In order to overcome this limitation, process-based or eco-physiological models, which use mechanistic understanding of organism responses to environmental drivers, can be used to describe and predict species distributions by linking key organismal traits with environmental and spatial data (Kearney et al., 2008).

1.4 Metabolic theories, bio-energetic models and the Dynamic Energy Budget

Metabolic theories are bio-energetic methods which conceptualise how organisms obtain matter and energy from their environment and then allocate it to physiological processes such as growth, development, maintenance and reproduction (Lika et al., 2011). Mechanistic theories of metabolism based on first principles recognise the constraints placed on mass and energy fluxes through any biological system, and so have the potential to describe the energetic basis for higher level (e.g. population and ecosystem) dynamics (Nisbet et al., 2000). In principal, it is possible to develop an eco-physiological species distribution model by coupling a mechanistic model based on metabolic theory to a large scale model of physical processes and environmental drivers (Kearney et al., 2008).

The best known bio-energetic models based on metabolic theory can be broadly grouped into three categories – static energy budget (SEB) models, Dynamic Energy Budget (DEB) models and the models proposed by West et al. (2001) which later came to be associated with the “metabolic theory of ecology” (Brown et al., 2004), and which will be referred to here as WBE (for West, Brown and Enquist) models. In WBE models, a simple description of metabolic rate as a function of body size and temperature is emphasized as a powerful tool to capture variation in ecological patterns ranging from individual growth and the scaling of metabolic rate (West et al., 2001; Hou et al., 2008) to ecosystem-level patterns, such as food-web structure (Brown and Gillooly, 2003). These models have been applied to investigate general ecological questions and have been shown to predict broad-scale physiological and ecological phenomena with some accuracy (Enquist et al., 2003; Brown et al., 2004; Gillooly et al., 2005; Hou et al., 2008). However, there has been vociferous debate regarding the WBE approach, and doubt has been cast on the fundamental principles of the models (Makarieva et al., 2004; van der Meer, 2006b; O'Connor et al., 2007; Apol et al., 2008; Price et al., 2012), the universality of the mass scaling relationships they propose (based on Kleiber’s law - that the metabolic rate of an organism is proportional to its mass$^{3/4}$ - and that this relationship is underpinned by the geometry of the metabolic supply system, specifically fractally branching distribution networks such as vertebrate blood vessels or the branches of trees) (Glazier, 2005; White et al., 2007) and their predictive capacity (Algar et al., 2007). The SEB category contains a number of representatives, but the scope-for-growth approach is one of the most established. The scope-for-growth model is based on an empirical energy balance for a "standard" organism, and it uses allometric curves to extrapolate to organisms of different sizes (Filgueira et al., 2011). It assumes that assimilated energy is immediately available for catabolism (respiration and excretion), with the remainder being utilised for growth or deposited as reserves (Filgueira et al., 2011; Larsen et al., 2014). This assumption implies that energy from catabolism is lost. However, any energy from catabolism that has been reinvested in the anabolic processes of growth remains in the organism and is not subsequently lost, leading to an imbalance according to the energy conservation rule (Filgueira et al., 2011). These models are widely applied, and have been used to explore the energy budgets of a wide range of taxa including gastropods (Navarro et al., 1992; Lau and Leung, 2004), bivalves (Navarro et al., 2000; Sarà et al., 2008), echinoderms (Hill and Lawrence, 2006; Yuan et al., 2009), crustaceans (Normant and Lamprecht, 2006; Urbina et al., 2010) and fish (Peck et al., 2003). They have also been used to describe and predict somatic growth in bivalves (Filgueira et al., 2011; Larsen et al., 2014) and gastropods (Navarro et al., 2006). In contrast to SEB models, DEB models are based on the assumption that assimilated energy is first stored in reserves, which are then mobilised to fuel other metabolic purposes (van der Meer, 2006a). Reserves therefore reflect the feeding history of the organism and, as a result, the structural growth dynamics in a DEB model become different from the scope-for-growth model, particularly in environments with temporally variable food availability. Another important assumption of the DEB model is the "κ-rule" which states that a fixed fraction (κ) of mobilised energy is allocated to somatic maintenance and growth (with maintenance taking priority), and the remaining fraction (1-κ) is allocated to development and reproduction (van der Meer, 2006a).

In the standard DEB model (Figure 1-1), individuals are assumed to be isomorphs (i.e. there are no ontogenetic changes in body shape) feeding on one food source (Jager and Zimmer, 2012). They are primarily characterised by three state variables: **structure**, which determines actual size, feeding rates and maintenance costs; **reserve**, which serves as intermediate storage between feeding and metabolic mobilisation, and either **maturity** (in juvenile animals) or **reproduction buffer** (in sexually mature animals). Juvenile animals increase maturity by sinking energy into the development of reproductive structures. Once sexual maturity ("puberty" in DEB terminology) has been reached, animals will then switch energy allocation to the production of gametes (Martin et al., 2013).

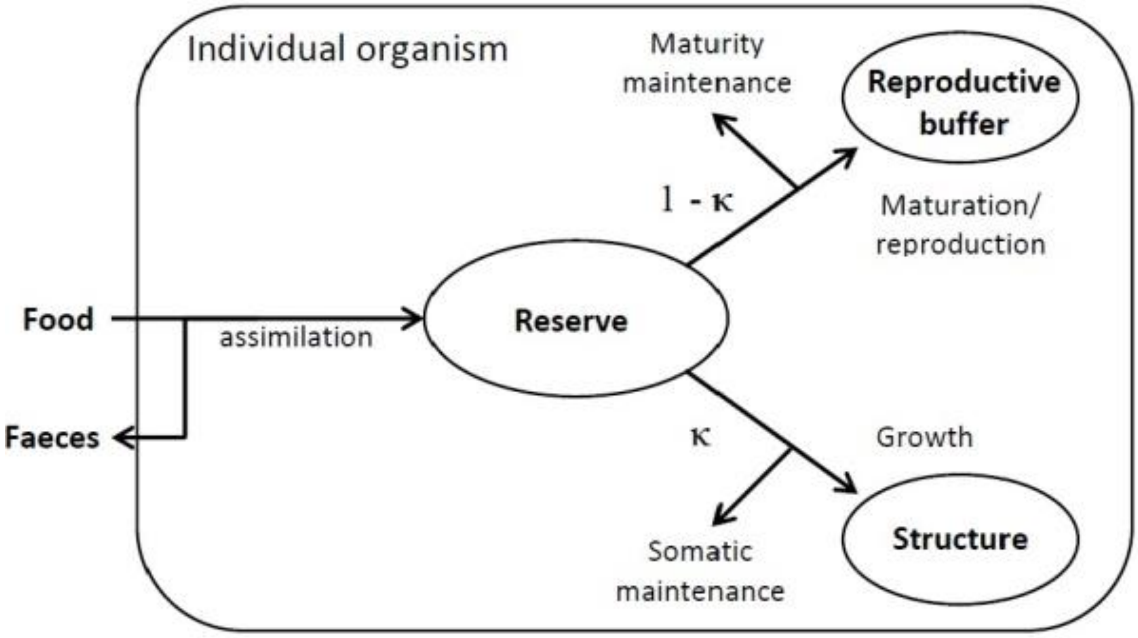

Figure 1-1: Schematic diagram of the standard DEB model. State variables are in ovals. κ (kappa) is the energy allocated to somatic maintenance and growth and represents a fixed fraction of energy mobilised from the reserve. 1-κ is the remainder of mobilised energy and is allocated to either maturation (juveniles) or reproduction (adults). Mature animals sink energy into the reproductive buffer until it is emptied during reproductive events (i.e. gamete release).

The DEB model has several advantages over other energetic models: i) it is a mechanistic model that relies on physiological principles common to all species; ii) it has a relatively small number of parameters which integrate environmental effects on the organism and iii) its structure allows comparison of energy budgeting between species, as inter-specific differences appear as different model parameter values (Alunno-Bruscia et al., 2009). DEB theory is based on precise knowledge of energy partitioning within organisms, and so can be used to investigate the effects of environmental factors on demographic responses such as growth and reproduction and, from there, effects on population dynamics can be inferred. The primary environmental drivers used by the DEB model are temperature and food availability, and numerous studies have demonstrated the skill of the DEB model in predicting development, growth, and reproductive rate in a number of different taxa under ambient conditions (Bourlès et al., 2009; Jusup et al., 2011; Augustine et al., 2014).

However, DEB models have also been forced with other (additional) variables, and used to make predictions regarding organism responses to environmental stressors. For example, Lavaud et al. (2019) used the DEB approach to disentangle the effects of hypoxia, temperature and food availability on the life-history traits of two populations of Atlantic cod (*Gadus morhua*, Linnaeus, 1758) in the Gulf of Saint Lawrence (Canada), and showed that temperature explained 48% of the difference in length and 59% of the difference in mass between the two populations. Model scenarios also suggested that a linear decrease in oxygen concentration would reduce growth and reproduction in this species (Lavaud et al., 2019). The effects of decreased oxygen concentration on bivalves has also been explored, with a DEB model parameterised for the scallop *Argopecten purpuratus* (Lamarck, 1819) accurately capturing the reductions in growth and reproduction observed under hypoxic conditions (Aguirre-Velarde et al., 2019). Klok et al. (2014b) used a DEB model to investigate the negative impact of increased pCO_2 on cockle (*Cerastoderma edule*, Lamarck, 1809) growth and concluded that the observed decrease in shell length and flesh dry weight could be attributed to increased maintenance costs and decreased assimilation efficiency. Finally, DEB models are increasingly used in ecotoxicology applications. They have been shown to be useful tools not only in predicting the effects of toxicants on growth and reproduction (Muller et al., 2009; Xie et al., 2019) but also in elucidating the mode of action of toxicants (Jager and Zimmer, 2012).

A great deal of the published literature applies the DEB model to bivalves (Pouvreau et al., 2006; Bourlès et al., 2009; Rosland et al., 2009; Alunno-Bruscia et al., 2011; Barillé et al., 2011; Bernard et al., 2011; Thomas et al., 2011; Maar et al., 2015; Aguirre-Velarde et al., 2018; Aguirre-Velarde et al., 2019) and, to a lesser extent, fish (Pecquerie et al., 2009; Jusup et al., 2011; Pecquerie et al., 2011; Kooijman and Lika, 2014; Lavaud et al., 2019). While the success of the DEB model in describing and predicting growth and reproduction in these taxa is well established, there are fewer studies which attempt to model these processes in crustaceans, particularly decapods. One of the primary challenges in applying the DEB model to crustaceans is that the standard model assumes continuous growth of structure. In most animal phyla, an increase in structure results in a concurrent increase in physical size (e.g. body length). However, this is not the case with crustaceans in which growth of structure is indeed continuous, but increase in physical size occurs periodically *via* the moult. In most of the published DEB models which have been applied to crustaceans (Campos et al., 2009; Jager and Ravagnan, 2015; Jager et al., 2015; Jager and Ravagnan, 2016) these discontinuities in physical size measures are ignored. Moulting is a difficult and energy-demanding process, which represents a major and repeated physiological change in the life history of all crustaceans (Buchholz et al., 2006; Seear et al., 2010). As such, most aspects of crustacean life history are synchronised with the moult cycle to some degree, and a DEB model which can capture this process would not only represent a novel development in the application of DEB theory to crustaceans, but also provide valuable insights into the energetics of moulting, and serve as a useful basis for exploring possible effects of environmental stressors on crustacean life history traits.

1.5 The ecological and economic importance of crustaceans

Crustaceans, particularly decapods, have important ecological roles (Boudreau and Worm, 2012). Studies have shown that decapod predation can influence the structuring of benthic communities; for example, experimental exclusion of decapods in Bonne Bay, Newfoundland resulted in an increase in benthic infaunal species richness due to the reduction of crab predation on infauna (Quijón and Snelgrove, 2005). Benthic decapods have been shown to exert top-down control upon the recruitment of other species by feeding on settling bivalve larvae (Barkai and McQuaid, 1988), or 0-group plaice (*Pleuronectes platessa,* Linnaeus, 1758) (van der Veer and Bergman, 1987). The abundance of decapod larvae in the water column has been negatively correlated with plaice and sole (*Solea solea*, Linnaeus, 1758) recruitment in the North Sea (Kirby and Beaugrand, 2009), leading those researchers to conclude that in addition to adult predation on fish recruits, decapod larval predation in the plankton may have contributed to changes in the structure of the North Sea holozooplankton which underpins fish recruitment (Beaugrand et al., 2003). It has also been suggested that some crustacean predators can be keystone species. In the NW Atlantic, blue crabs (*Callinectes sapidus,* Rathbun, 1896) were attributed with regulating marsh grass cover in salt marshes. Blue crabs preyed on the periwinkle *Littoraria irrorata* (Say, 1822), preventing it from decimating the marsh grass *Spartina* spp. and so converting this complex habitat to mudflats (Silliman and Bertness, 2002). Based on these findings, overfishing of blue crab was proposed as a possible mechanism contributing to the massive die-off of salt marshes in the south-eastern USA. Similarly, crabs are thought to contribute to the maintenance of kelp beds in the Gulf of Maine (Leland, 2002; Steneck et al., 2004). The removal of large predatory fish from kelp beds in the early 20th century reduced predation pressure on lower trophic levels, fostering an increase in the herbivorous green sea urchin *Strongylocentrotus droebachiensis* (Müller, 1776) (Harris and Tyrrell, 2001). If these urchins reach sufficiently high densities, they can denude the benthos of fleshy macroalgae, creating “urchin barrens” (Steneck, 1997). Stable algal communities are now maintained by the presence of crustacean predators, which have replaced the previously removed fish predators and can effectively keep vast regions free of sea urchins (McNaught, 1999; Leland, 2002).

Some crustacean species, such as clawed and spiny lobster, crabs and penaeid shrimp, also have significant commercial value (Smith and Addison, 2003). These decapods underpin lucrative fisheries across the globe and deliver some of the highest prices per weight of any seafood (Cawthorn and Hoffman, 2017). Global production of decapod crustaceans has doubled since 2000, reaching over 12.5 million tonnes in 2013 and accounting for approximately 8% of total global fisheries production (Cawthorn and Hoffman, 2017). While landings from decapod capture fisheries have remained relatively stable over the last decade, the rapid increase in global supply largely reflects the growth in aquaculture production, predominantly in Asia. In 2014, aquaculture production of crustaceans reached 6.9 million tonnes, worth an estimated US$36.2 million (FAO, 2016).

1.6 Thesis rationale

Given the clear ecological and economic importance of crustaceans, it is evident that a more comprehensive mechanistic understanding of their responses to climate drivers is needed if we are to improve our predictive capability in order to manage benthic ecosystems and crustacean fisheries sustainably**.** While experimental examination of drivers and responses is a well-tested and robust approach, the sheer number of drivers acting on the marine environment means that measuring all potential interactions between every combination of drivers is impossible. It is in this context that theoretical approaches such as DEB can prove useful, as models can provide a mechanistic underpinning of observed responses, which is critical if we are to predict the impacts of stressors under novel or untested conditions. The standard DEB model has been shown to be a useful tool in describing and predicting growth in bivalves and fish under ambient conditions, and in response to climate stressors such as increased CO_2 and decreased O_2 concentrations. However, it is currently lacking in its ability to accurately capture the discontinuous growth of crustaceans, which significantly limits its applications in exploring the physiological responses of crustaceans to climate change.

1.6.1 Aims and objectives

1. To investigate the drivers of natural variability in a benthic community in the Western English Channel, and to select a model crustacean species for further work
2. To investigate the feeding, growth and respiration of the model species under ambient conditions and to parameterise a simple DEB model in order to explore the energy budget of this species. More specifically, to introduce a “moult extension” into the model which will account for the discontinuous nature of crustacean growth
3. To investigate the responses of the model species to climate drivers (water temperature, moderate hypoxia and ocean acidification), and parameterise individual DEB models which describe and predict relevant physiological endpoints under these conditions
4. To develop a unified “multi-stressor” DEB model for the model species, and use it to predict changes in ecologically relevant endpoints and possible distribution across the European seas using projected environmental conditions between the present day and 2050

Chapter 2 Quantifying the environmental drivers of short-term temporal dynamics in an epibenthic community from the Western English Channel

This chapter has been published as: Talbot, E., Bruggeman, J., Hauton, C. & Widdicombe, S, 2019. Uncovering the environmental drivers of short-term temporal dynamics in an epibenthic community from the Western English Channel. *Journal of the Marine Biological Association of the UK*. **99** (7), 1476-1479.

Author contributions: ET performed taxonomic analysis of the epifaunal samples, all statistical analysis and wrote the manuscript. JB, CH and SW provided comments and feedback on written drafts. Taxonomic analysis of the epifaunal samples was also undertaken by a number of individuals besides ET: Adrien Lowenstein, Laura Briers, Bianca Maria Torre, Harry Powell, Alessandro Brunzini, Craig Dornan, Olli Ford and Jemma French. Phytoplankton data were provided by Clare Widdicombe, and meroplankton data were provided by Andrea McEvoy and Angus Atkinson.

2.1 Abstract

Benthic communities, critical to the health and function of marine ecosystems, are under increasing pressure from anthropogenic impacts such as pollution, eutrophication and climate change. In order to refine predictions of likely future changes in benthic communities resulting from these impacts, we must first better constrain their responses to natural seasonality in environmental conditions. Epibenthic time series data (July 2008 – May 2014) have been collected from Station L4, situated 7.25 nautical miles south of Plymouth in the Western English Channel. These data were analysed to establish patterns in community abundance, wet biomass and composition, and to link any observed patterns to environmental variables. A clear response to the input of organic material from phytoplankton blooms was detected, with sediment surface living deposit feeders showing an immediate increase in abundance, while predators and scavengers responded later, with an increase in biomass. I suggest that this response is a result of two factors.

The low organic content of the L4 sediment results in food limitation of the community, and the mild winter/early spring bottom water temperatures allow the benthos to take immediate advantage of bloom sedimentation. An inter-annual change in community composition was also detected, as the community shifted from one dominated by the anomuran *Anapagurus laevis* to one dominated by the gastropod *Turitella communis*. This appeared to be related to a period of high larval recruitment for *T. communis* in 2013/2014, suggesting that changes in the recruitment success of one species can affect the structure of an entire community.

2.2 Introduction

Benthic epifaunal communities are under growing pressure from anthropogenic activities in coastal seas, the strength and range of which have increased significantly over the last century with the growth in global industrialisation and urbanisation (Daan et al., 1996; Halpern et al., 2008). As a result, impacts such as pollution, eutrophication and the effects of climate change are of major concern to conservationists and resource managers alike (Capasso et al., 2010). In order to assess long-term changes in epibenthic communities as a result of these impacts, it is critical that we gain an improved understanding of the short-term temporal variability in the responses of community abundance, biomass and composition to environmental parameters (Reiss and Kröncke, 2004; Chikina et al., 2014; Włodarska-Kowalczuk et al., 2016).

While descriptions of the large-scale spatial distribution and structure of temperate, shelf-sea epibenthic communities in connection with environmental factors are relatively common, only a few studies have investigated the temporal variability of these communities. Many of those focussed on the North Sea, and concluded that sea surface temperature (SST) is a dominant factor influencing the temporal variability of epibenthic communities, particularly in the shallow, well-mixed areas of the south-eastern North Sea (Reiss and Kröncke, 2004; Neumann et al., 2008; Neumann et al., 2009b), which are characterised by strong seasonal fluctuations in temperature (Neumann et al., 2008). The influence of SST appears to be less dominant in the deeper, stratified areas of the northern North Sea however. Neumann et al. (2009a) found no correlation between overall epibenthic community structure and changing SST, although relationships were found between SST and the abundance and biomass of some individual species, in some cases with a one year lag.

Shallow-water communities are generally thought to have access to high quality (if temporally variable) food, and as a result, the influence of organic input on structuring the benthos may be secondary to other physical and biological factors (Quijón et al., 2008). Again, there are comparatively few studies which focus on the responses of benthic epifauna to bloom sedimentation, but a number have investigated macro-infaunal community structures and responses to phytodetrital inputs. The trophic structure of North Sea macrofauna communities was found to reflect differences in the relative quality of organic matter received (Dauwe et al., 1998; Wieking and Kröncke, 2005). Between 55% and 84% of year to year variability in benthic infaunal abundance off the coast of Northumberland was explained by changes in primary production (Buchanan, 1993), and a marked increase in macrofaunal abundance in the same area in the 1980s was attributed to increases in phytodetrital input (Frid et al., 1996), as were decadal-scale variations in taxonomic composition (Frid et al., 2009a; Frid et al., 2009b; Clare et al., 2017). Josefson et al. (1993) showed that the abundance, biomass and growth of macro-infaunal species were closely related to bloom sedimentation in the Skagerrak-Kattegat region. Macrofaunal deposit feeders were found to increase in abundance immediately following bloom sedimentation in the Western English Channel, while other trophic groups responded more slowly, primarily with an increase in biomass (Zhang et al., 2015). However, not all studies found a clear response to organic input. Quijon et al. (2008) found that the effects of phytodetrital input were short term, and were minor in comparison to the seasonal differences observed in the macrofaunal community, and studies of the infauna of the western Baltic (Graf et al., 1982) and of the epifauna in the German Bight area of the North Sea (Reiss and Kröncke, 2004) failed to find any response to bloom sedimentation at all.

The seasonal and interannual variability of the epibenthic community at Station L4 in the Western English Channel was investigated from July 2008 until May 2014. Since little is known about the ecology and biology of the epibenthos in the Western English Channel, these data provide valuable information on the short-term variation of several epibenthic groups. The purpose of this study was to: i) describe the seasonal and interannual variability in diversity, abundance, and biomass of the epibenthos at Station L4; ii) to identify and discuss environmental drivers in accordance with faunal patterns and iii) to identify a species to serve as a model for further investigation into the energetic costs of changing environmental conditions.

2.3 Materials and Methods

2.3.1 The L4 sampling station

Station L4 is part of the Western Channel Observatory (WCO, www.westernchannelobservatory.org.uk), and represents a long term oceanographic and marine biodiversity time series, having been routinely sampled since 1988. In 2008, a benthic series was added – an element often missing from other observatories (Smyth et al., 2015). Situated in the Western English Channel, 7.25 nautical miles south of Plymouth, UK (50°15.00’N, 4°13.02’W), it can be considered representative of a temperate coastal environment (Tait et al., 2015). Water column depth is approximately 53m, and the station is well mixed during the winter and stratified over the summer (Figure 2-1A). Bottom water temperature varies from approximately 8°C - 16°C (Figure 2-1A). Chlorophyll-*a* concentration is at its lowest during winter, and higher during the characteristic spring and autumn phytoplankton blooms (Figure 2-1B, note that these are fluorescence measurements, a proxy for chlorophyll-*a*). Phytoplankton cells can sink very quickly at L4, with high chlorophyll-*a* and phytoplankton carbon values measured at the seabed within two weeks of the start of a bloom (Tait et al., 2015; Zhang et al., 2015).

2.3.2 Animal collection and processing

Using a 60cm wide Naturalist dredge with a 22mm mesh deployed from the *RV Plymouth Quest*, three replicate samples were taken every other month during the period July 2008 - May 2014 from Station L4. For each replicate the dredge was lowered to the seabed and then towed for approximately 2 mins at a speed of approximately 0.3 knots. Total towed distance was calculated for each replicate using the formula:

$$\cos^{-1}(\cos lat_S \ * \cos\ lat_E \ + \sin lat_S \ * \sin lat_E \ \ * \cos(lon_S - \ lon_E)) \ * 6371$$

Where: lat_S is start latitude (in radians), lat_E is end latitude (in radians), lon_S is start longitude (in radians), lon_E is end longitude (in radians) and 6371 is the approximate radius of the Earth (in Km).

All organisms collected in the dredge were fixed in 10% formalin solution. Prior to analysis, samples were rinsed at 4mm and epifaunal individuals carefully picked out. All individuals were identified to species level, wherever possible, using a stereo microscope (Leica M32 Kombistereo). Individuals within each of the identified taxonomic groups were counted, carefully blotted dry and weighed on a Sartorius R220D microbalance (± 0.01 mg, European Instruments). Standardised values for abundance and biomass for each time point were calculated by dividing the total abundance (or biomass) in three replicate samples by the total area covered by the dredge.

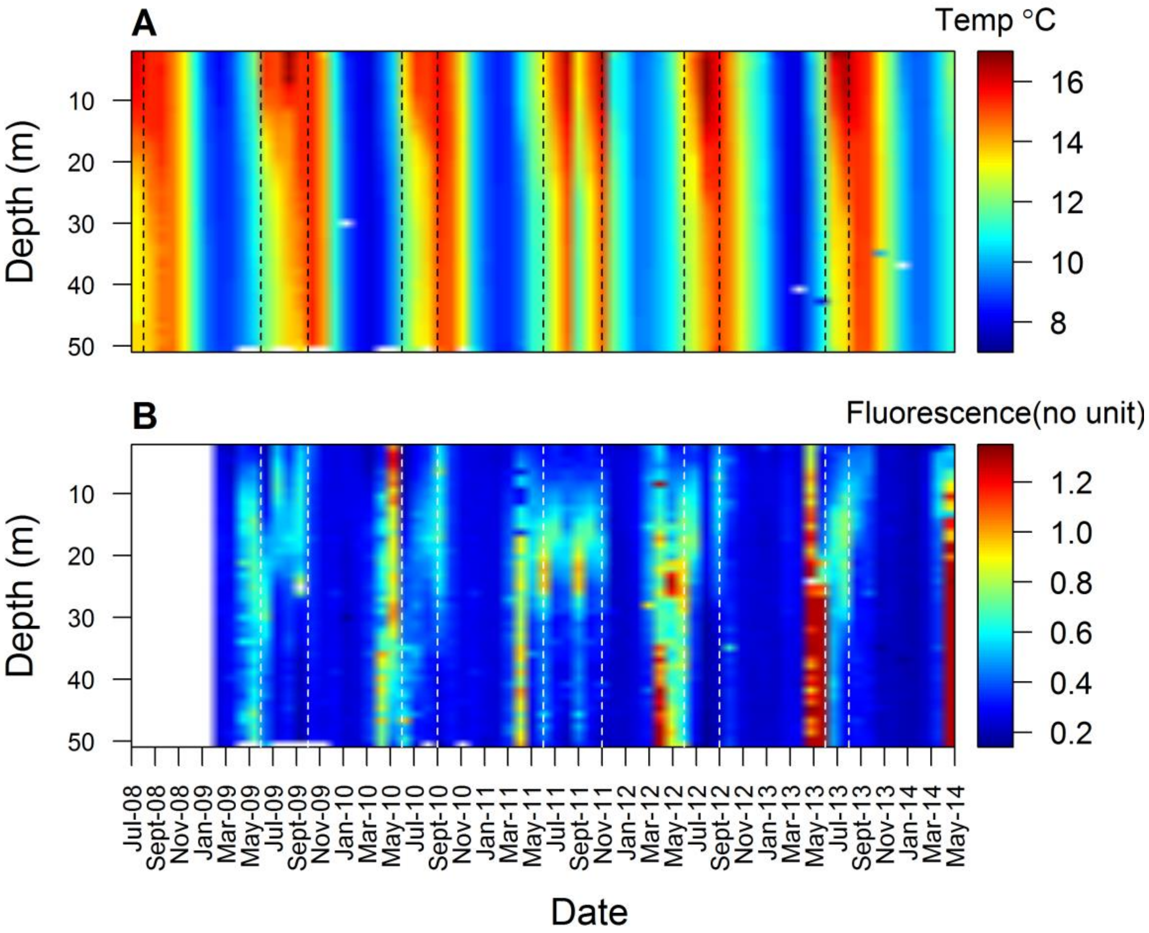

Figure 2-1 Monthly mean water temperature and fluorescence at Station L4. (A) temperature between July 2008 and May 2014. (B) fluorescence between Jan 2009 and May 2014. Data were collected weekly (weather permitting) using a Seabird SBE 19+ CTD deployed from the *RV Plymouth Quest*. Dotted vertical lines indicate periods of thermal stratification.

2.3.3 Ancillary data

During the study period (July 2008 – May 2014), a suite of environmental and biological data were collected from L4 every week (weather permitting) from the *RV Plymouth Quest*. Vertical profiles of temperature and fluorescence were measured using a SeaBird SBE 19+ CTD. Water samples for phytoplankton analysis were collected from a depth of

10m using 10L Niskin bottles attached to the CTD rosette, and zooplankton were collected in two vertical WP2 net hauls (mesh size = 200µm, mouth aperture = 57cm diameter) taken from the seabed to the surface (UNESCO, 1968).

2.3.4 Phytoplankton analysis

Paired water-bottle samples were preserved with 2% Lugol's iodine solution (Throndsen, 1978) and 4% buffered formaldehyde. Between 10 and 100 ml of sample (depending on cell density) were settled for at least 48 h (Widdicombe et al., 2010). Cell volumes were calculated according to the equations of Kovala and Larrance (1966) and converted to carbon (pgC cell^{-1}) (Menden-Deuer and Lessard, 2000) and then expressed per unit volume of seawater (mgC m^{-3}).

2.3.5 Meroplankton analysis

Haul samples were preserved and stored in 5% formalin. Two subsamples were extracted using a Folsom splitter and a Stempel pipette, to identify large and small organisms separately, then counted and identified under a microscope. Abundances in the two hauls were averaged to reduce the variability related to the sampling, and counts were converted to individuals m^{-3} (John et al., 2001). Due to the difficulties in larval identification and because different analysts have worked on the data set over the years, meroplankton are only identified to major taxonomic groups. These groups are: Decapoda, Brachyura, Cirripedia, Bivalvia, Gastropoda, Echinodermata and Polychaeta. These groups provide an overall picture of the seasonal changes in the meroplankton assemblage at L4. For this study, all groups except Cirripedia were considered, because although Cirripede larvae can dominate the meroplankton at L4 (Highfield et al., 2010) mature animals are rarely present in the epibenthic faunal samples.

2.3.6 Statistical analysis

All statistical analyses were conducted in R statistical software. Time-series of epibenthic abundance and wet biomass m^{-2} between July 2008 and May 2014 were compiled. Missing data were interpolated using the “zoo” package in R (Zeileis et al., 2018). Data for each sampling month (January, March, May, July, September and November) were pooled across the whole time series and overall means of community, major phyla and dominant species abundance and wet biomass were calculated to establish the structure of the community. Average individual body mass of the whole community and each phylum was calculated by dividing the overall mean wet biomass by the overall mean abundance for each sampling month. To establish whether responses to environmental drivers were more easily identifiable when considering functional groups rather than taxa, species were grouped into one of five feeding guilds (predator/scavenger, omnivore, surface-deposit feeder, subsurface-deposit feeder, suspension feeder). Information on polychaete feeding mode was retrieved from Jumars et al. (2015). Information on feeding mode for all other phyla was retrieved from the Marine Life Information Network's biological traits catalogue (MarLIN, 2006). Where a species exhibited more than one feeding method, it was classified by the preferred or most frequently documented method. While I appreciate that the "fuzzy coding" method (Chevene et al., 1994; Neumann and Kröncke, 2011), which uses positive scores to describe the affinity of species to trait categories, would reflect a wider range of ecological function than the method adopted here, the aim of this chapter was to provide a broad overview of the structure of the community and its responses to environmental variables, rather than an in-depth analysis of biological traits. Data on meroplanktonic larval abundance, water temperature and phytoplankton carbon for the duration of the time series were also collected and monthly means calculated.

The "vegan" package in R (Oksanen et al., 2017) was used to construct a species accumulation curve to determine whether the full diversity of Station L4 had been captured, and to calculate rarefied species richness as an indicator of changes in diversity over the course of the time series. Rarefied species richness was chosen as the measure of diversity as the total area covered by the dredge varied between sampling dates. As a consequence, it is likely that the number of species (and individuals) collected in each sample was a function of the area sampled. Rarefaction techniques can correct for this difference in sampling effort by generating the expected number of species in a small collection of n individuals drawn at random from a larger pool of N individuals (Gotelli and Colwell, 2001).

In order to identify any correlation between the biological (community, feeding guild and phyla abundance and biomass) and the environmental (water temperature, phytoplankton carbon) data series, cross correlation analysis was performed (Olden and Neff, 2001; Probst et al., 2012) in R using the "astsa" package (Stoffer, 2016). Where relationships between data series were found, linear regressions were used to quantify the relationship for a particular time lag. Cross correlation analysis was also performed on the phyla abundance and larval abundance data series. Prior to this analysis, all data series were checked for homoscedasticity by fitting a simple ordinary least squares regression model and checking the residuals against the fitted values. The community abundance and biomass series, and the larval abundance data series were found to be heteroscedastic and were log-n transformed to achieve homoscedasticity. All data series were differenced to remove any trends or seasonal effects (Probst et al., 2012), and then checked for stationarity using an Augmented Dickey-Fuller test in the “tseries” package for R (Trapletti et al., 2017). Finally, to ensure that estimates of cross correlations were not inflated by any temporal autocorrelation, series were checked for any autocorrelation by generating ACF and PACF plots (Olden and Neff, 2001).

2.4 Results

2.4.1 Variations in the epibenthic community 2008 - 2014

The species accumulation curve for Station L4 started to level off after approximately 20 samples (corresponding to a sampling period of 2.5 years) had been collected (Figure 2-2A). Rarefied species richness varied across the course of the series (Figure 2-2B) with values ranging from 7 – 24 species. Spring/summer values were generally higher than values in the preceding winter. Rarefied richness reached a maximum in spring/summer 2011, and declined steadily to the end of the series.

Community abundance over the course of the series varied from 0.13 individuals m^{-2} in May 2010, to 3.93 individuals m^{-2} in May 2014 (Figure 2-3A). Community wet biomass ranged from 0.21 g m^{-2} in September 2008 – 5.99 g m^{-2} in May 2014 (Figure 2-3B). The peak in community abundance seen in summer 2009 was largely attributable to a peak in crustacean abundance (specifically the anomuran *Anapagurus laevis* (Bell, 1845)) (Figure 2-3E). The increase in abundance in autumn 2013 was driven by increases in the crustaceans *A. laevis, Galathea nexa* (Embleton, 1834), and *Macropodia spp.*; the mollusc *Turitella communis* (Risso, 1826), and to a lesser extent, the echinoderms *Astropecten irregularis* (Pennant, 1777) and *Ophiothrix fragilis* (Abildgaard, 1789) (Figures 2-3C and 2-3E). The abundance maximum in spring 2014 was due predominantly to an increase in mollusc numbers (specifically *T. communis*) (Figure 2-3E). All but one of the observed peaks in wet biomass were driven by increases in echinoderm biomass (*Marthasterias glacialis* (Linnaeus 1758) in March 2010 and September 2012, and *Luidia ciliaris* (Philippi, 1837) in March 2011) (Figure 2-3F). The very high wet biomass maximum in spring 2014 can be attributed to increases in biomass of molluscs (*T. communis*) and crustaceans (*Liocarcinus depurator* (Linnaeus 1758) and *Atelecyclus rotundatus* (Olivi, 1792)) (Figure 2-3F). The increase in polychaete biomass in spring 2014 (Figure 2-3D) was due to the presence of a single large *Aphrodita aculeata* (Linnaeus 1758) in the sample.

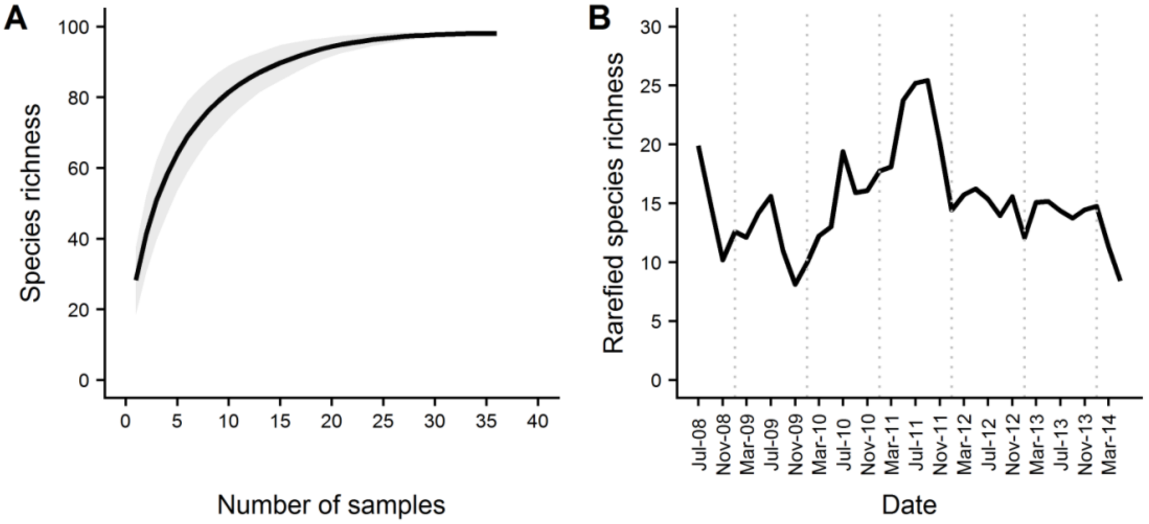

Figure 2-2 Species accumulation curve and rarefied species richness over the course of the L4 epibenthic time series, July 2008 - May 2014. The species accumulation curve (A) started to level off after approximately 20 samples (representing a sampling period of 2.5 years) were collected. Grey shading denotes standard deviation from the mean curve, generated from 1000 random permutations of the data. In terms of diversity (B), the series is characterised by a period of high species richness in late 2010/2011, with periods of lower richness at the beginning and end of the series. Dotted vertical lines denote January of each year.

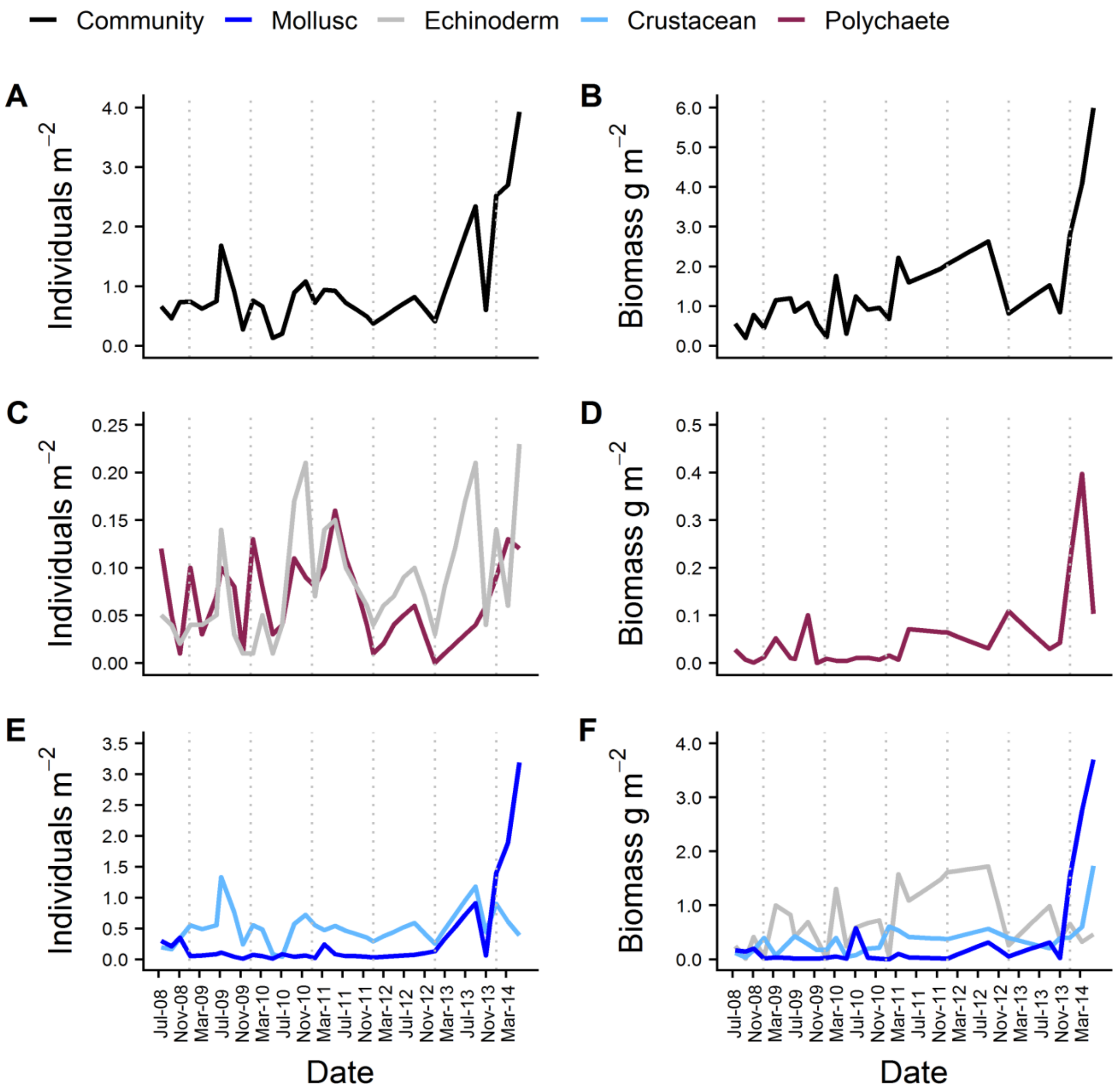

Figure 2-3 L4 epibenthic abundance and biomass over the study period July 2008 - May 2014. Abundance of the whole community (A), polychaetes and echinoderms (C) and molluscs and crustaceans (E). Biomass of the whole community (B), polychaetes (D) and echinoderms, molluscs and crustaceans (F). Dotted vertical lines denote January of each year.

Four of the five most dominant species in terms of abundance were crustaceans, although the most dominant species was the gastropod mollusc *T. communis*, accounting for 28% of total abundance over the course of the time series (Table 2-1). Biomass was dominated by the echinoderm *M. glacialis,* which accounted for 45% of community biomass over the period July 2008 – May 2014 (Table 2-1).

Table 2-1: Contributions of dominant species to L4 community abundance and biomass over the period July 2008 - May 2014.

Abundance dominant species	**% contribution to total abundance**	**Biomass dominant species**	**% contribution to total biomass**
Turitella communis	28	*Marthasterias glacialis*	45
Anapagurus laevis	19	*Liocarcinus depurator*	14
Liocarcinus depurator	6	*Turitella communis*	10
Inachus dorsettensis	5	*Atelecyclus rotundatus*	4
Macropodia tenuirostris	4	*Nucula* spp.	4

Benthic larvae were always present in the water column over the course of the time series. Abundances ranged from 12 (± 8) individuals m^{-3} in December 2009 to 2080 (± 3656) individuals m^{-3} in July 2010. In 2009, 2010 and 2011, summer abundances of benthic larvae were very high, reaching more than 1000 individuals m^{-3} (Figure 2-4A). In 2009, the majority of the benthic larvae recorded were gastropod molluscs (Figure 2-4C), while in 2010 and 2011, echinoderm larvae were the primary contributors to the observed peaks in abundance (Figure 2-4D).

Both the abundance and wet biomass of suspension and deposit feeders was relatively stable over the course of the time series, although suspension feeder abundance increased sharply in summer 2013 and spring 2014 (Figure 2-5A). Likewise, the wet biomass of suspension and deposit feeders reached a peak in spring 2014 (Figure 2-5B). In terms of abundance, omnivores were the most dominant feeding guild at L4 (Figure 2-5C), while the predator/scavenger guild dominated in terms of wet biomass (Figure 2-5F). The predators/scavengers (Figure 2-5E) exhibited an increase in abundance in spring 2014, although it was not as dramatic as that recorded for the suspension feeders.

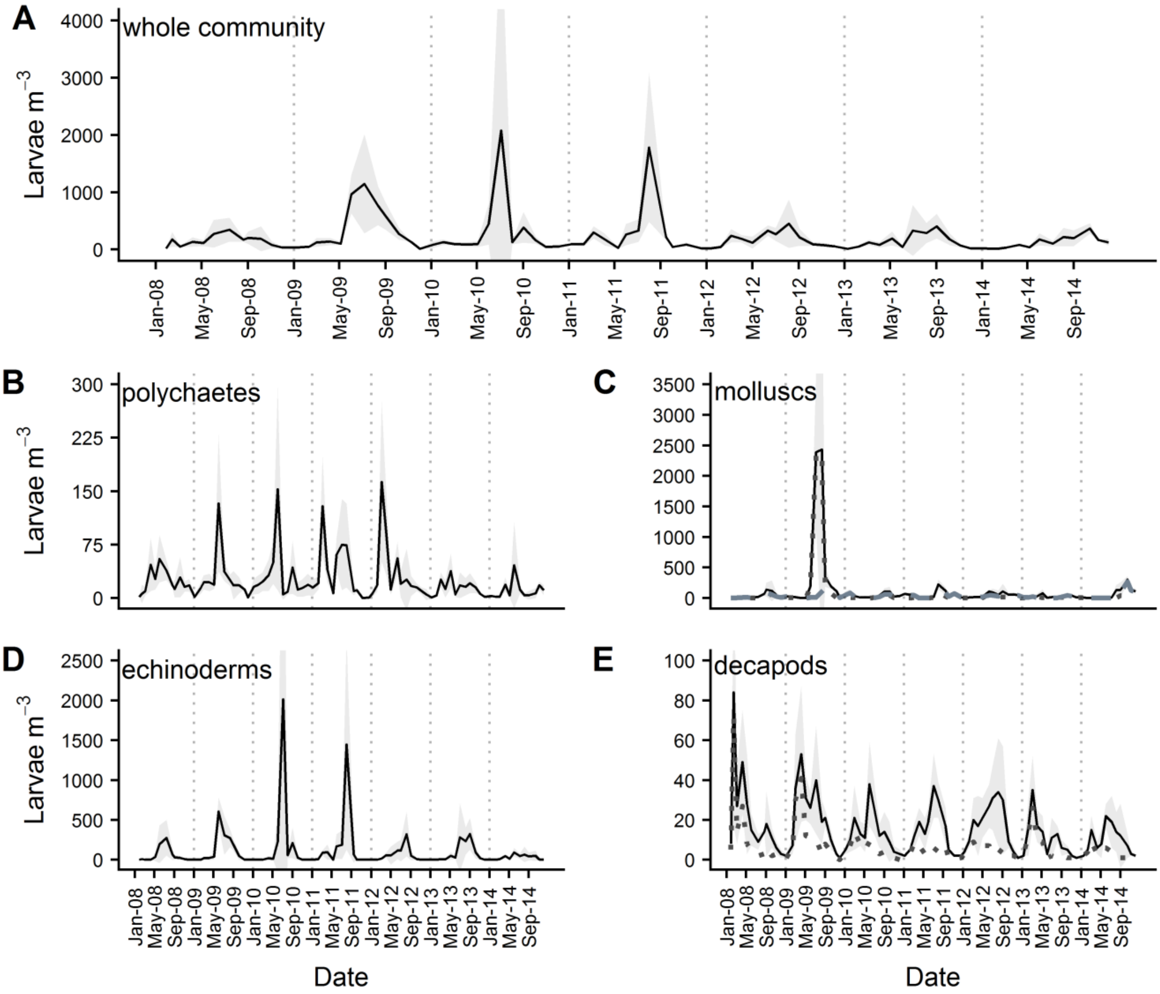

Figure 2-4 Abundance of benthic larvae in the water column at Station L4. (A) the four major benthic phyla, (B) polychaetes, (C) molluscs, (D) echinoderms and (E) decapod crustaceans during the study period July 2008 – May 2014. The grey dotted line in panel C is the abundance of gastropod larvae present, while the grey dashed line is the abundance of bivalve larvae. The grey dotted line in panel E is the abundance of brachyuran larvae present. Grey shading represents standard deviation from the mean calculated for the phyla.

.

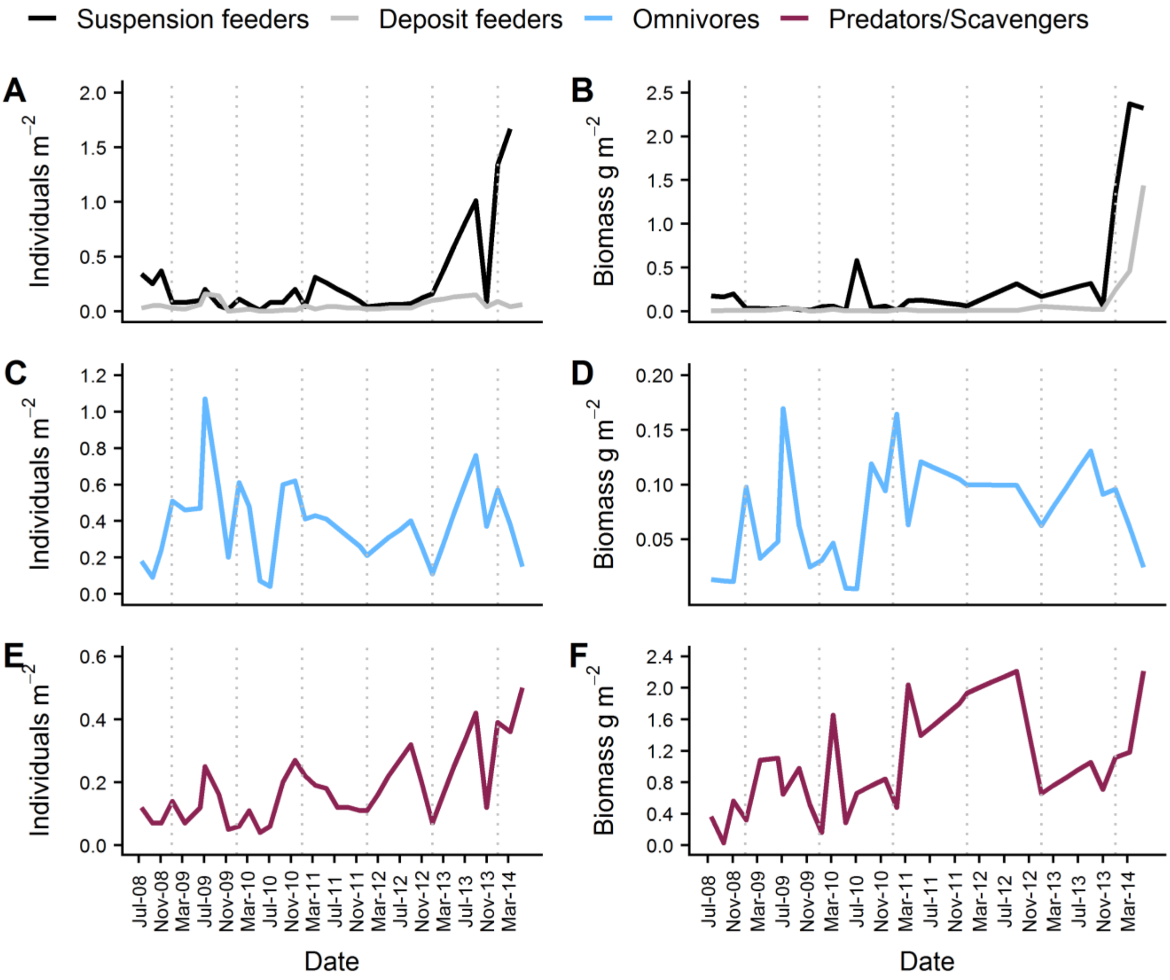

Figure 2-5 Abundance and biomass of the main feeding guilds found at Station L4. Left hand panels are abundance, right hand panels are biomass. (A) and (B) are suspension and deposit feeders, (C) and (D) are omnivores and (E) and (F) are predators/scavengers. Deposit feeders were split into surface and sub-surface feeders for the purposes of analysis, but were combined for plotting.

2.4.2 Overall structure of the epibenthic community

There was some structure apparent in the overall means of the community abundance and wet biomass series. Abundance increased from January to reach a peak in May, before declining again over the summer. There was a second, smaller increase apparent in September, and abundance then decreased steadily through the winter (Figure 2-6A). Wet biomass peaked slightly earlier than abundance, in March, and remained fairly high over the spring before declining from May onward. There was a second, smaller increase in community wet biomass in September (Figure 2-6B). The first peak in abundance can be attributed to an increase in abundance of molluscs (and to a lesser extent polychaetes and echinoderms) which, when added to an already high abundance of crustaceans, raised community abundance to ~1.2 individuals m^{-2} (Figure 2-6C, E, G and I). While mollusc abundance dropped sharply after the May maximum (Figure 2-6E), the decline in community abundance was more gradual, due to an increase in the abundance of crustaceans (Figure 2-6I), and numbers of polychaetes and echinoderms remaining relatively high (Figure 2-6C and G). This increase in crustacean abundance, which reached its maximum in September, was the primary contributor to the second community abundance peak (Figure 2-6A). The biomass maximum in March was predominantly caused by a sharp increase in biomass of echinoderms (Figure 2-6H), and polychaetes (Figure 2-6D) although molluscs (Figure 2-6F) also contribute. Both molluscs and crustaceans (Figure 2-6J) reached a biomass peak in May, ensuring that community biomass remained high throughout the spring (2-6B).

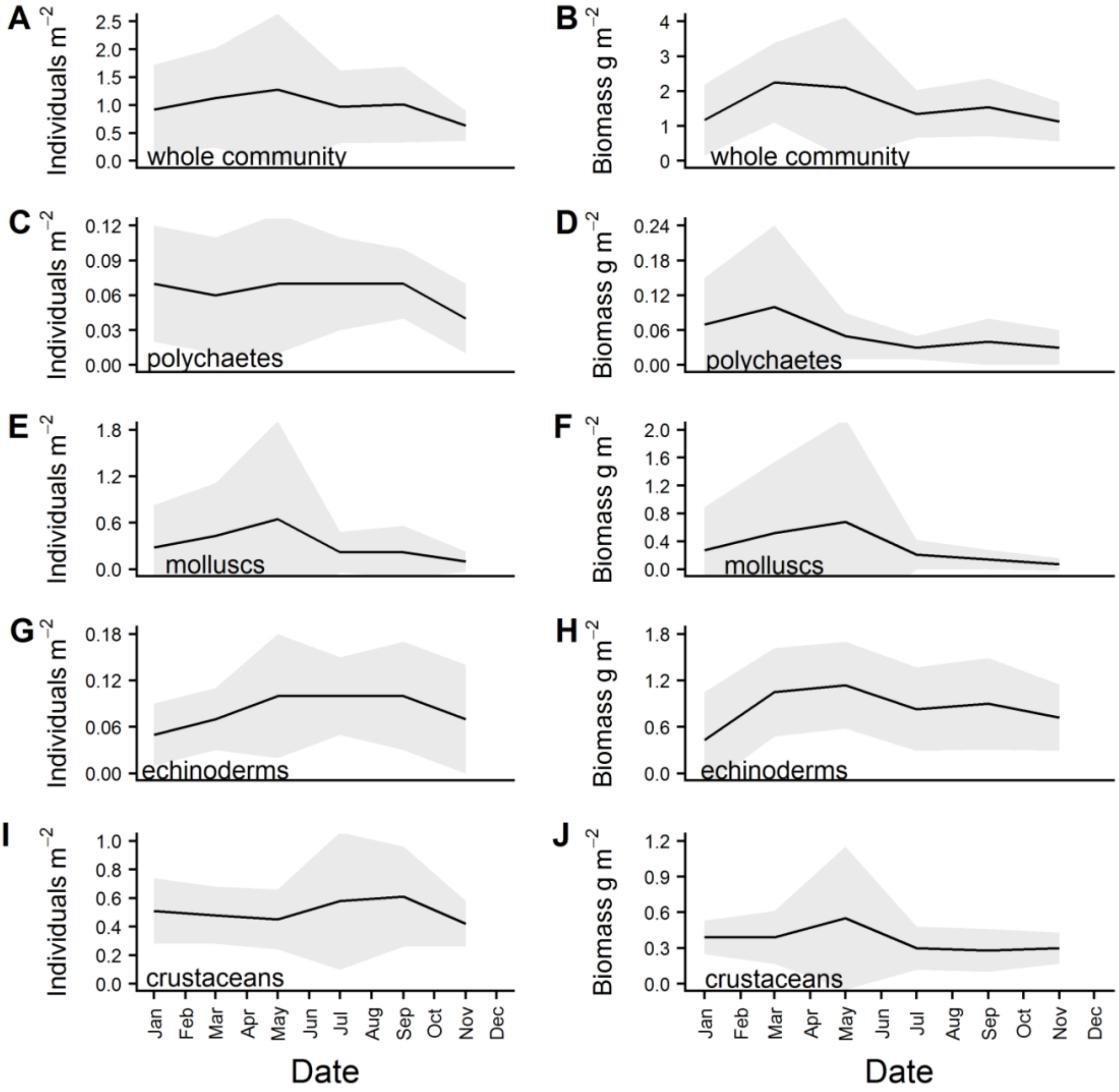

Figure 2-6 Overall means for community and major phyla abundance and wet biomass. Left hand panels are abundance, right hand panels are biomass. Data for each sampling month (Jan, Mar, May, Jul, Sept, and Nov) were pooled across the whole time series. Shaded grey area represents standard deviation from the mean.

Average individual body mass of the whole community reached a maximum in March, and then decreased steadily over the summer, before increasing again from September (Figure 2-7A). Polychaete (Figure 2-7A) individual body mass exhibited a similar pattern, although the decline after March was much steeper. Peaks in body mass for crustaceans and molluscs (Figure 2-7A) were reached in May, again with a decrease over the summer, and an increase beginning in September. Echinoderms (Figure 2-7B) reached a maximum in March, and body mass remained high into May before declining. There was a subsequent increase in echinoderm body mass although it started earlier than in other taxa, in July.

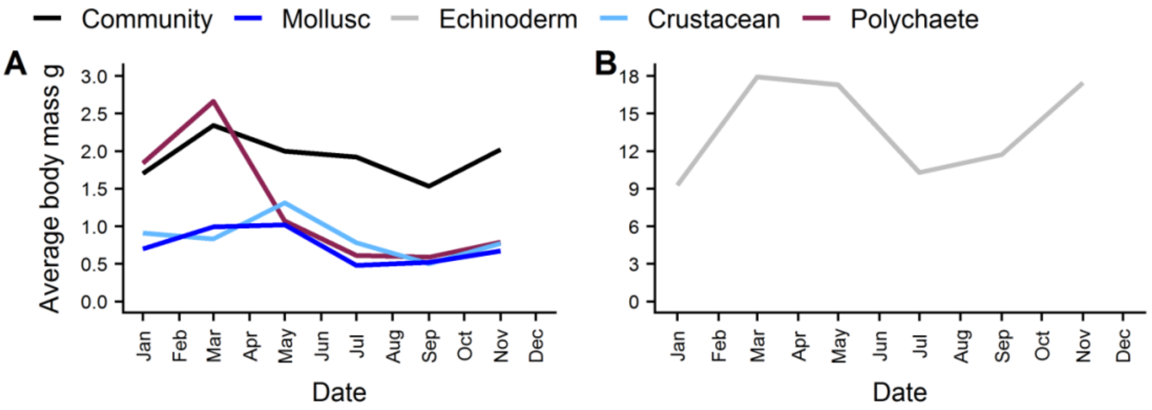

Figure 2-7 Average individual body mass of the L4 epibenthic community. (A) whole community, molluscs, polychaetes and crustaceans. (B) echinoderms.

Overall monthly means of larval abundance show that the highest numbers of benthic larvae are recorded in the water column in July/August (Figure 2-8A). While all four major phyla contribute to this peak in abundance, it is largely attributable to high abundances of molluscs (Figure 2-8C) and echinoderms (Figure 2-8D). Different classes of mollusc appear to have different spawning times at L4, with gastropod larvae abundances (grey dotted line, Figure 2-8C) in the water column peaking slightly earlier than bivalve larvae (grey dashed line, Figure 2-8C). Polychaete larvae exhibited two peaks, in March and June (Figure 2-8B), while decapod larvae abundances peaked in March/April (Figure 2-8E), and remained relatively high throughout the summer, before declining steadily from July. Much of the initial peak in decapod larval abundance can be attributed to brachyuran larvae (grey dotted line, Figure 2-8E), although this declines after April.

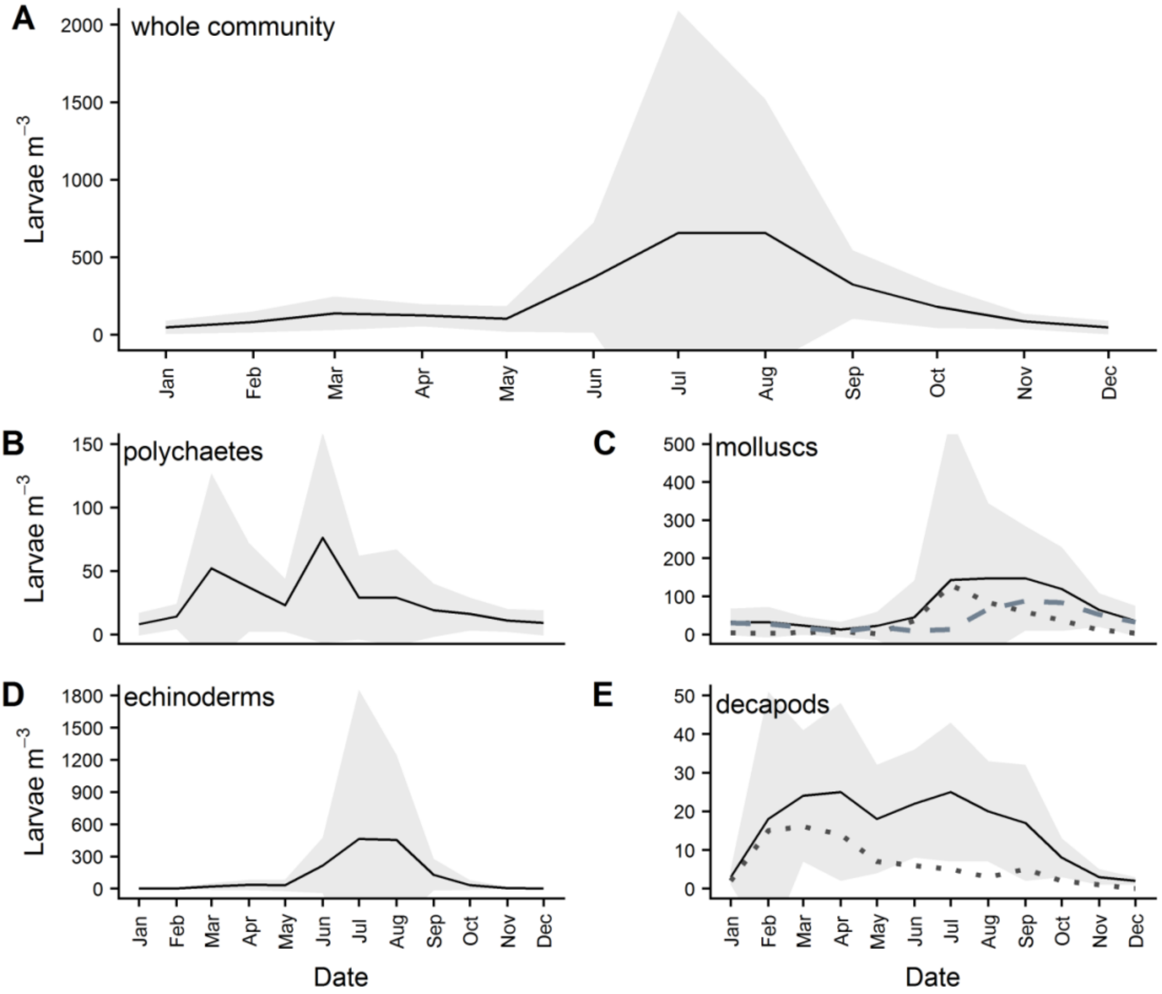

Figure 2-8 Overall monthly mean abundances of benthic larvae in the water column at Station L4. (A) the four major benthic phyla combined, (B) polychaetes, (C) molluscs, (D) echinoderms and (E) decapod crustaceans. Means were calculated for each month from data pooled across the whole time series. The grey dotted line in panel C is the abundance of gastropod larvae present, while the grey dashed line is the abundance of bivalve larvae. The grey dotted line in panel E is the abundance of brachyuran larvae present. Grey shading represents standard deviation from the mean calculated for the phyla.

2.4.3 Drivers of variation in epibenthic community structure

Non-metric multidimensional scaling (NMDS) ordination revealed that although there was no clear seasonal pattern apparent over the course of the time series in either the abundance or wet biomass data, there were some interannual differences in the abundance data. Analysis of community abundance identified 3 clusters (Figure 2-9A). Cluster 1 consists of the years 2008, 2013 and 2014. Cluster 2 contains the years 2011 and 2012, and cluster 3 contains the years 2009 and 2010. The differences between these three clusters were driven by differences in the relative abundances of the two dominant species. In cluster 1, the gastropod *T. communis* was dominant, whereas in cluster 3 the anomuran crab *Anapagurus laevis* was dominant. Cluster 2 was characterised by a more even community structure, with no single species dominant. There were no clear interannual patterns identified in the biomass data, with most data points falling into a single cluster (Figure 2-9B). The only months to fall outside this cluster were January 2010 and January 2011. This appears to be due to the fact that during these months, the asteroid *M. glacialis,* which dominated the biomass over the course of the time series, was not recorded.

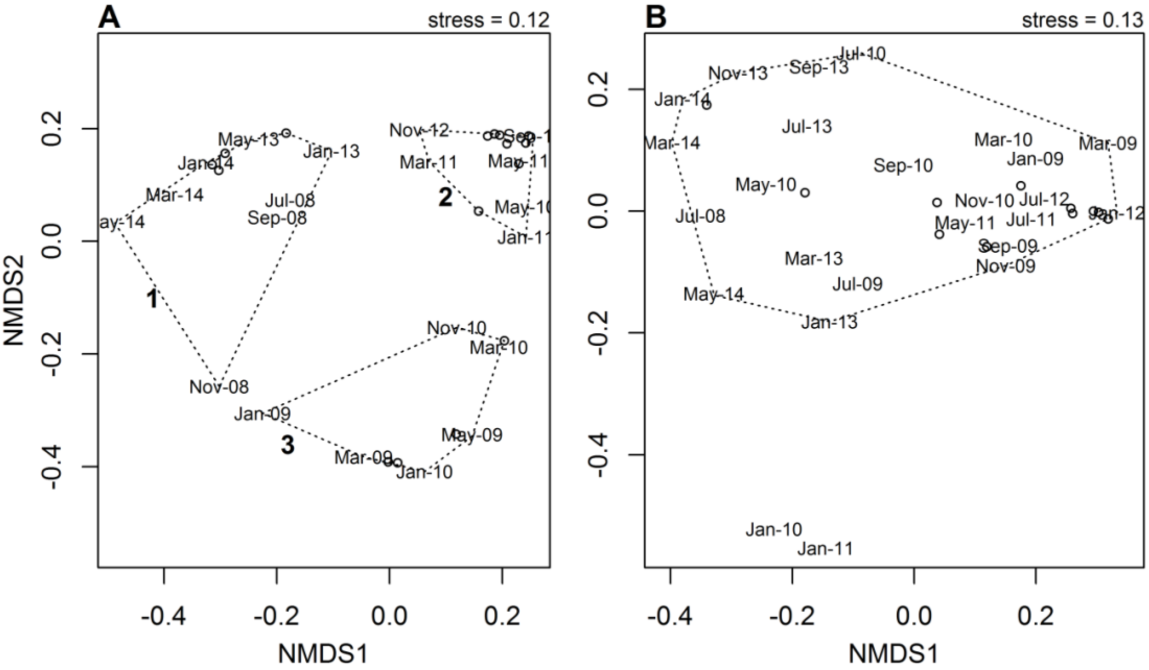

Figure 2-9 NMDS ordination of community abundance and wet biomass data over the course of the time series July 2008 - May 2014. Although there is no seasonal pattern evident in either the abundance (A) or wet biomass data (B), there is some interannual variation in the abundance data, predominantly due to the relative variations in abundance of the dominant species.

All significant results of the cross correlation analysis are shown in Table 2-2. There was no significant relationship between total community abundance and any of the explanatory environmental variables. Community wet biomass correlated with both phytoplankton carbon ($R^2 = 0.4$, $p = 0.0001$) and temperature ($R^2 = 0.46$, $p < 0.0001$), with a 6 month lag in both cases (Table 2-2). If both carbon and temperature are left in the linear model as explanatory variables, the model fit improves ($R^2 = 0.6$) and both terms remain significant (carbon $p = 0.003$, temperature $p = 0.002$, Table 2-2). There was no significant interaction effect detected between carbon and temperature ($p = 0.9$). Of the four major phyla, only echinoderm biomass exhibited significant relationships with any of the explanatory environmental variables, correlating with temperature with a 6 month lag ($R^2 = 0.37$, $p = 0.0003$, Table 2-2). Both mollusc and echinoderm abundance were correlated with larval abundance. Mollusc abundance was correlated with total mollusc larval abundance ($R^2 = 0.81$, $p = 0.001$) and gastropod larval abundance ($R^2 = 0.61$, $p =$

0.01) with a 4.5 year lag in each case (Table 2-2). Echinoderm abundance is correlated with echinoderm larval abundance with a lag of 3 years (R^2 = 0.58, *p* = 0.002, Table 2-2).

Table 2-2 Significant models identifying relationships between the epibenthic community and environmental variables. In those models where two predictors were included, the significance value for the whole model has been given in the column for R^2, and the significance value for individual predictors has been given in the coefficient column.

Response variable	Predictor	lag	R^2 (*p*)	Coefficient (*p*)
Community biomass	phytoplankton carbon	6 months	0.4 (0.0001)	0.1
Community biomass	temperature	6 months	0.43 (0.0001)	0.18
Community biomass	carbon + temperature	6 months	0.6 (<0.0001)	Carbon = 0.1(0.003) Temperature = 0.14 (0.002)
Echinoderm biomass	temperature	6 months	0.37 (0.0003)	0.11
Predator/scavenger biomass	phytoplankton carbon	6 months	0.32 (0.0006)	0.1
Predator/scavenger biomass	temperature	6 months	0.38 (0.0003)	0.13
Predator/scavenger biomass	carbon + temperature	6 months	0.53 (<0.0001)	Carbon = 0.09 (0.02) Temperature = 0.12 (0.002)
Surface-deposit feeder abundance	phytoplankton carbon	0 months	0.42 (0.02)	0.09
Mollusc abundance	mollusc larvae	4.5 years	0.81 (0.001)	0.21
Mollusc abundance	gastropod larvae	4.5 years	0.61 (0.01)	0.17
Echinoderm abundance	echinoderm larvae	3 years	0.58 (0.002)	0.1

Analysis of the community when grouped into feeding guilds (suspension feeders, surface and sub-surface deposit feeders, omnivores and predators/scavengers) showed a relationship between predator/scavenger biomass and phytoplankton carbon with a 6 month lag (R^2 = 0.32, *p* = 0.0006, Table 2-2). As with community wet biomass, this group also exhibited a relationship with temperature, again with a six month lag (R^2 = 0.38, *p* = 0.0003). If both of these terms are left in the model, they remain significant (carbon *p* =

0.02, temperature $p = 0.002$), and the overall fit improves ($R^2 = 0.53$, $p < 0.0001$, Table 2-2). There was no significant interaction effect detected however ($p = 0.5$). This analysis also showed a relationship between phytoplankton carbon and surface-deposit feeder abundance, with an immediate response from the surface-deposit feeders to phytodetrital input ($R^2 = 0.5$, $p = 0.02$, Table 2-2).

2.5 Discussion

Time series data (collected every other month during the period July 2008 – May 2014) for benthic epifauna at Station L4 were analysed to establish patterns in community abundance, wet biomass and composition, and to link any observed patterns to environmental variables. A clear response to the input of organic material from phytoplankton blooms was detected, with sediment surface living deposit feeders showing an immediate increase in abundance, while predators and scavengers responded later, with an increase in biomass. An inter-annual change in community composition was also detected, as the community shifted from one dominated by the anomuran *Anapagurus laevis* to one dominated by the gastropod *Turitella communis.*

There is some evidence for benthic-pelagic coupling at Station L4, demonstrated by the correlation between surface-deposit feeder abundance and phytoplankton carbon. This pattern has been previously observed in the macro-infauna at L4, with deposit feeders rapidly responding to phytodetrital input with an increase in abundance, while predators and scavengers responded more slowly with an increase in biomass (Zhang et al., 2015). While many studies have concluded that benthic communities can be structured by phytodetrital input over both short-term and decadal scales (Buchanan, 1993; Josefson et al., 1993; Dauwe et al., 1998; Wieking and Kröncke, 2005; Frid et al., 2009b; Frid et al., 2009a; Clare et al., 2017) clear responses to organic input from benthic fauna can be difficult to detect (Graf et al., 1982; Reiss and Kröncke, 2004). The “food bank” hypothesis suggests that large reserves of labile organic matter in sediments can sustain benthic communities at constant levels of abundance on a year round basis, and clear responses to phytodetrital input are difficult to detect as a consequence (Mincks et al., 2005; Kędra et al., 2012; Włodarska-Kowalczuk et al., 2016). This appears not to be the case at Station L4, which is fairly impoverished in terms of organic matter content, with organic carbon contributing only 0.4% to total sediment mass (Zhang et al., 2015). It is possible that this comparatively low sediment carbon content results in the epibenthic community at L4 being food limited, and so the seasonal pulses of phytodetrital input elicit measurable responses. Furthermore, spring bloom sedimentation in temperate areas can often occur when bottom water temperatures are low, and benthic faunal responses are limited as a result. Weeks can pass before water temperature increases enough to allow for macrofaunal feeding (Lopez and Levinton, 2011). It is possible that the particular hydrographic conditions in the Western English Channel, where bottom water temperatures fluctuate less than in other temperate systems, result in early spring temperatures high enough for the surface-deposit feeders in the L4 community to respond immediately.

Interestingly, there was no apparent decrease in diversity associated with the sedimentation of the spring bloom. In macrofaunal communities, enriched sediments are typically rapidly colonised by a few opportunist, fast-reproducing species (Widbom and Frithsen, 1995) which can take advantage of the fresh organic matter, generally resulting in a reduction in diversity (Chamberlain et al., 2001; Widdicombe and Austen, 2001). As noted above, epibenthic surface-deposit feeders did show an immediate increase in abundance with the arrival of phytodetritus, but rarefied richness values for May (post sedimentation) are generally equal to or higher than values for March (pre-bloom). It is possible that these values are indirect evidence of predation. Predation is thought to play a key role in marine sedimentary systems, due in part to the lack of clear evidence for competitive exclusion (Peterson, 1979; Woodin, 1999). While detection of predation is challenging, and numerous studies have found no consistent regulatory role (Thrush, 1999), it has been suggested that epibenthic predators can equalise numbers and increase evenness by preying preferentially on numerically dominant species (Quijón and Snelgrove, 2005). Given the fact that L4 community wet biomass is predominantly represented by predators and scavengers, there is a possibility that opportunistic deposit feeders are prevented from becoming dominant after sedimentation of the spring bloom by the feeding of the predator/scavenger group. This pattern in the regulation of benthic community structure has been noted before (Posey et al., 1995), with those authors concluding that the presence or absence of predation may alter the visible response of the benthos to organic enrichment. While there was no direct evidence of predator-prey interactions (e.g. a clear relationship between deposit-feeder and predator/scavenger abundance or biomass) detected in this study, the patterns in species richness observed would seem to support the proposal that epibenthic predators can be of major influence in benthic communities (Quijón and Snelgrove, 2005), and may diminish or counterbalance the changes in prey species that result from phytodetrital input.

A relationship between community wet biomass and both bottom-water temperature and phytoplankton carbon was detected at Station L4, although there was no significant interaction between the two predictors and their effects on biomass. This leads me to propose that temperature and phytoplankton carbon primarily influence biomass at different times of the year. Community wet biomass peaks in March/May, driven predominantly by an increase in biomass of echinoderms and molluscs. Individual body mass curves for these two phyla show an identical pattern, with a maximum also being reached in March/May. It is possible that this is representative of the development of the gonads in preparation for spawning. Several studies have found that ripe gonads in these two phyla can make a significant contribution to body mass (Barker and Nichols, 1983; Nichols and Barker, 1984a; Nichols and Barker, 1984b; Berthelin et al., 2000; Freeman et al., 2001; Alunno-Bruscia et al., 2011). This view would appear to be supported by the increase in benthic larvae (of which mollusc and echinoderm larvae are recorded in the highest numbers) in the water column from May onwards, while community, mollusc and echinoderm biomass decreases after May, perhaps indicating spent individuals. I suggest that this pre-spawning biomass is influenced by temperature. Several studies have noted the role of temperature in triggering gonad development in marine invertebrate species (Sastry, 1966; Sastry and Blake, 1971; Aktaş et al., 2003; Herrmann et al., 2009; Balogh et al., 2018), and it is possible that gonad development at L4 is initiated by the high water temperatures recorded in September, with full maturation and spawning occurring the following spring. Gonad development and maturation in some temperate echinoderm & mollusc species has been recorded to take up to six months, which would be in keeping with the six-month lag between peaks in temperature and biomass identified in this chapter (Bowner, 1982; Sköld and Gunnarsson, 1996; Kim et al., 2016). Although there was no significant interaction between temperature and phytoplankton carbon and their effects on biomass detected here, food availability will clearly affect gonad development as it dictates the nutritional status of an individual (Nunes and Jangoux, 2004), and the autumn bloom characteristic of Station L4, along with the carbon from seaweed detritus which contributes to winter organic matter in the area (Queirós et al., 2019) is likely to help fuel gonad development over the winter. In contrast to maximum temperatures, maximum phytoplankton carbon values are generally recorded in April/May, with a response in community biomass seen six months later. It is possible that the relationship between phytoplankton carbon and biomass is indicative of somatic growth, which occurs after spawning has taken place in the spring. The seasonal prioritisation of either sexual or somatic growth in benthic fauna is well documented, particularly in echinoderms (Greenwood, 1980; Peterson and Fegley, 1986; Guillou and Michel, 1993; Lozano et al., 1995; Coma et al., 1998). This shift in energetic prioritisation is often related to reproductive effort being concentrated at a time favourable to the survival of offspring, e.g. spawning prior to or coincident with a phytoplankton bloom (Giangrande et al., 1994). The same lagged relationship between biomass, temperature and phytoplankton carbon was also recorded in the predator/scavenger group. The biomass of this feeding guild is dominated by echinoderms (70%), so the postulated relationships outlined above could also be driving the responses of this group.

The role of larval supply as a determinant of the structure and dynamics of marine populations (i.e. supply side ecology) has long been discussed (Thorson, 1950; De Wolf, 1973; Lewin, 1986; Underwood and Fairweather, 1989), and there is much evidence to suggest that variations in recruitment can contribute to patterns of abundance and demographics in adult populations of fish (Williams, 1980; Doherty and Fowler, 1994), barnacles (Gaines and Roughgarden, 1985; Sutherland, 1990; Scrosati and Ellrich, 2017), mussels (Scrosati and Ellrich, 2017) and bryzoans (Hughes, 1990). I propose that larval recruitment of dominant species is also a key influence on benthic community structure and composition at Station L4. The dramatic increase in community and suspension feeder abundance and biomass in May 2014, and the shift in community structure (from one dominated by *A. laevis* in 2009 to one dominated by *T. communis* in 2013/2014) are likely due to the sieve recruitment (the point at which individuals recruited to the population reach a size where they would be retained on the sieve mesh) of the high numbers of gastropod larvae present in the plankton in 2009. Previous studies of benthic recruitment have stressed that sieve recruitment can be far removed in time from actual settlement (Buchanan and Moore, 1986), as many benthic macrofaunal settlers are of meiofaunal size. The lag of 4.5 years identified between mollusc abundance and gastropod larval abundance likely reflects the fact that any newly settled animal needs to reach a size both big enough to be collected by the dredge, and to be retained on the 4mm sieve used in this study.

Analysis of the first six years of the epibenthic time series at Station L4 reveals some temporal structure in community abundance and wet biomass, apparently influenced by both bottom water temperature and seasonal phytodetrital input. It is possible that the spring phytoplankton bloom fuels somatic growth, while gonad development and maturation is triggered by warmer water temperatures in the autumn, resulting in a pre-spawning biomass peak evident in early spring. Different functional groups within the community were found to respond to the bloom in specific ways, a result that is in keeping with previous studies of the L4 macro-benthos. While benthic faunal responses to changes in water temperatures have been previously recorded in other temperate systems, clear responses to phytodetrital input as seen here are less common. The reason we can detect this response is likely to be a combination of two factors: i) The relative impoverishment of the L4 sediment in terms of organic content, indicating a food limited community, and ii) the comparatively small range of bottom water temperatures, resulting in relatively mild winter/early spring conditions and a community that is able to take immediate advantage of bloom sedimentation.

This chapter demonstrates the importance of organism energetics and the environmental conditions (e.g. temperature) that influence energy allocation. The control of this process can drive seasonal and inter-annual patterns in species biomass and the relative composition of benthic communities. Any method that allows us to explore, visualise and predict an organism’s energy acquisition and allocation under different environmental conditions or in response to stressors has the potential to provide insight into population and community dynamics. In order to explore the effect of environmental conditions on organism energetics, and to provide a solid mechanistic basis for scaling up from individual physiology to population level effects, a model species, the swimming crab *L. depurator* was selected for further experimental work. As well as being among the most dominant species (in terms of both abundance and biomass) recorded at L4 over the course of the time series, *L. depurator* is also one of the most commonly found portunid crabs in the wider coastal Northeast Atlantic (Mori and Zunino, 1987; Abelló et al., 1988; Rufino et al., 2004). It occurs on several benthic sediment types and is a commonly encountered species in muddy and sandy-muddy bottoms (Minervini et al., 1982) on the continental shelf and upper continental slope (Rufino et al., 2005). Due to its abundance, it can play a key role in structuring soft-bottom communities, both by controlling the abundance of its prey species and by constituting an important prey species itself for fish and other large predators (Careddu et al., 2017). The ubiquity and ecological importance of *L. depurator* therefore makes this species an ideal candidate for further exploring the energetics of crustaceans.

Chapter 3 An adapted Dynamic Energy Budget model for the swimming crab *Liocarcinus depurator,* including explicit consideration of the moult

This chapter has been published as: Talbot, E., Widdicombe, S., Hauton, C. & Bruggeman, J., 2019. Adapting the Dynamic Energy Budget (DEB) approach to include non-continuous growth (moulting) and provide better predictions of biological performance in crustaceans. *ICES Journal of Marine Science,* **76** (1), 192-205.

Author contributions: ET designed and performed all experiments, and wrote the manuscript. ET and JB constructed the initial DEB model. JB, CH and SW provided comments and feedback on all written drafts.

3.1 Abstract

Dynamic Energy Budget (DEB) theory offers a comprehensive framework for understanding the overall physiological performance (growth, development, respiration, reproduction etc.) of an organism over the course of its life cycle. A simplified DEB model for the swimming crab *Liocarcinus depurator* (Linnaeus, 1758) is presented here, the first DEB model to be parameterised for this species. Most applications of the standard DEB model assume continuous growth in all size metrics (length, wet mass, carbon content) of the modelled species. However, in crustaceans growth, measured as an increase of carapace length/width, occurs periodically *via* moult. To account for this, the model has been extended to track the continuous increase in carbon mass as well as the episodic increase in physical size. Model predictions were consistent with the patterns in the observed data, predicting both the moult increment and the intermoult period of an individual. In addition to presenting the model itself, recommendations are made for further development.

3.2 Introduction

Chapter 2 demonstrated the importance of considering species energy acquisition and allocation when trying to understand community responses to environmental drivers. In order to explore organism energetics more fully, Dynamic Energy Budget (DEB) theory can be employed, as it offers a whole organism approach to explaining how factors in the physical environment translate into biologically and ecologically relevant responses, *via* the assumption that food and temperature are the primary drivers of an organism's metabolic machinery. To date, the majority of published DEB models for marine species are for molluscs or fish, with relatively few models parameterised for decapod crustaceans. Given that Chapter 2 showed the importance of decapods in structuring benthic communities, this chapter explores the energetics of decapod crustaceans more fully, using a common coastal portunid crab as a model species. More specifically, the work presented here focuses on a key aspect of the crustacean life cycle - the moult - which most crustacean DEB models do not adequately account for.

The moult cycle represents a major and repeated physiological change in the life history of all crustaceans (Buchholz et al., 2006; Seear et al., 2010). Given that moulting is a complex and energy-demanding process, most aspects of crustacean life history are synchronised with the moult cycle (Raviv et al., 2008). Both reproduction and metabolism are dependent on the moult stage in crustaceans, and all three phenomena – moult, reproduction and metabolism – are influenced by environmental factors such as temperature (Buchholz et al., 2006). Moult and reproduction can be coordinated in a variety of ways, with different reproductive events (e.g. mating and oviposition) coupled to different moult stages (Cuzin-Roudy and Buchholz, 1999; Buchholz et al., 2006). Since mating can indicate the onset, acceleration or completion of vitellogenesis, and since oviposition marks the beginning of egg incubation, the sequence of mating and oviposition combined with the occurrence of moulting comprise different reproductive strategies (Raviv et al., 2008). Some of these strategies can be related to a particular taxon, while others may be found in a variety of taxa. Furthermore, a single species may exhibit more than one reproductive strategy. For example, in the snow crab *Chionoecetes opilio* (Fabricius, 1788) the first reproductive cycle comprises pre-moult ovary maturation, followed by the pubertal (and terminal) moult. Copulation occurs with the female in a soft shelled condition and the cycle ends with oviposition. In all subsequent reproductive cycles mating and oviposition occur with the female in a hard shelled condition (Elner and Beninger, 1995; Sainte-Marie et al., 2008). The reproductive cycle is regulated by a combination of internal cues such as energy allocation, and external environmental cues such as season (Raviv et al., 2008).

As well as facilitating growth and reproduction, moult may also be undertaken as a response to stressors or parasite infection. For example, Antarctic krill *Euphausia superba* (Dana, 1850) have the capacity to shrink at moult under conditions of low food availability (Ettershank, 1983; Nicol et al., 1992; Nicol, 2000). It is possible that this mechanism would allow the species to survive a long period of food limitation such as that encountered during the Antarctic winter (Quetin and Ross, 1991). Similarly, the Northern Krill *Meganyctiphanes norvegica* (M. Sars, 1857) moults outside of the reproductive season, and shows negligible somatic growth. It has been proposed that these moults may remove ecto-parasites that can severely reduce swimming efficiency (Buchholz et al., 2006).

Modelling growth forms the basis for almost all quantitative fisheries stock assessment (Chang et al., 2012). Accurate estimates of growth are essential in the determination of lifespan, age at recruitment, age at maturity and cohort identification (Hoggarth et al., 2006; Chang et al., 2012). Similarly it is critical for aquaculture production of crustaceans. Not only does it allow producers to assess when a crop will be ready for harvesting, it provides a way of quantifying and evaluating the effects of different production systems (Wyban et al., 1995; Kim et al., 2014), dietary regimes (Ackefors et al., 1992) or immunostimulants (Bai et al., 2010; Sang et al., 2011) on growth.

Moulting in crustaceans causes two problems in quantifying growth: all hard parts that might be used for aging (and so for an estimation of size-at-age) are lost at each moult, and growth is discontinuous, occurring in a stepwise fashion (Chang et al., 2012). While the first of these problems may be overcome by using methods such as mark recapture data (for larger or slower growing species) or length frequency analysis (Kilada and Driscoll, 2017) to estimate relative size-at-age, the second problem of discontinuous growth has received less attention, and limited attempts have been made to model the stepwise growth of crustaceans (Chang et al., 2012).

In order to capture moult dynamics in crustaceans, information on two components is needed – the moult increment (i.e. the magnitude of the increase in size at moult), and the intermoult period (i.e. the length of time between two successive moults) (Chang et al., 2012). The moult increment (MI) is generally the simpler of the two processes to model, with much of the modelling effort focused on finding the best means of fitting pre-moult and post-moult size data. These range from the fitting of separate lines to pre- and post-moult data with an intersection corresponding roughly to the size at maturity (Somerton, 1980), to log-linear (Mauchline, 1977) or non-linear models (Easton and Misra, 1988). Modelling the intermoult period (IP) is more of a challenge, as the only way to measure it directly is by observing animals in captivity. In those studies that have recorded data on observed IP, various general functions relating IP to pre-moult size have been proposed. For example, simple and higher order linear models (Mauchline, 1977; Castro, 1992), non-linear models (Ehrhardt, 2008), and a geometric series of time intervals increasing from an initial “seed” interval by a constant proportion at each successive interval (Caddy, 2003) have all been used. In those studies that have no direct measurement of IP, an estimate of moulting probability or moulting frequency is required, and many empirical equations exist to relate moulting probability to pre-moult size (Chang et al., 2012). Once information on MI and IP has been obtained, there are various ways of quantifying the average growth versus time. The moult-process model projects the relationship between pre-moult size and MI, and pre-moult size and IP repeatedly, allowing for the prediction of growth beyond the size range of the original observations (Mauchline, 1977). This approach is deterministic however, and does not account for intrinsic variations in growth among individuals. A stochastic moult-process model has therefore been developed based on the Monte-Carlo technique to construct growth curves and their associated uncertainty (Chen and Kennelly, 1999). While both these models produce growth curves, neither of them consider the effect of environmental factors on growth.

While all of these methods have been used successfully to model growth in a number of crustacean taxa, the fact that many of them have been developed for a particular species means it is unlikely that any individual model will be applicable to all species. Additionally, while some of them explicitly consider the effects of environmental temperature on growth (Wainwright and Armstrong, 1993; Brylawski and Miller, 2006) none consider food availability. In order to simplify the process of modelling crustacean growth, and to facilitate comparisons of growth between species, a single mechanistic model that can quantify both MI and IP, relate both to environmental temperature and food availability, and which should be applicable to all crustacean species is required. The DEB model (see Chapter 1, section 1.4) should, in principle, be able to fulfil these requirements.

Application of the DEB model to crustaceans has some specific challenges however. The standard DEB model assumes continuous growth of structure (see Chapter 1, Figure 1-1). In most animal phyla, an increase in structure results in a concurrent increase in physical size (e.g. body length). However, this is not the case with crustaceans in which growth of structure is indeed continuous, but increase in physical size occurs periodically *via* the moult. In most of the published DEB models which apply to crustaceans (Campos et al., 2009; Jager and Ravagnan, 2015; Jager et al., 2015; Jager and Ravagnan, 2016) these discontinuities in physical size measures are ignored. The single exception in the published literature is the work of Ananthasubramaniam et al. (2014) which includes explicit representation of discrete moults in *Daphnia magna* using a moult development index. The assumption that model predictions are representative of overall growth over multiple moults rather than individual daily growth is not unreasonable when dealing with relatively small fast growing crustacean species that moult frequently (Campos et al., 2009; Jager and Ravagnan, 2015), but when dealing with larger bodied, longer lived species such as commercially important decapods, it is less representative. It is possible, in the case of these decapods, that any modelled process which depends upon the physical size of the animal (e.g., feeding) is not accurately represented.

In this chapter, the feeding, growth and respiration of one of the most commonly recorded crustacean species at Station L4, *L. depurator* are investigated. As a first step towards exploring the links between individual species energetics and higher-level population dynamics, a simple DEB model is parameterised in order to explore the energy budget of this species. Due to the particular challenges presented by applying the standard DEB model to crustaceans, and in order to overcome the limitations that this imposes on using DEB approaches to fully investigate the effects of environmental drivers on crustacean life history traits, the DEB model presented here focuses specifically on capturing the dynamics of the moult.

3.3 Materials and Methods

3.3.1 Animal collection

Individuals of *L. depurator* were collected on 9th June 2016 from the Western Channel Observatory (Smyth et al., 2015) sampling station L4 (50°15.00’N, 4°13.02’W) using a 2m beam trawl. Four separate trawls, each of 15 mins duration, were conducted to ensure collection of a sufficient number of individuals (N = 60). Once removed from the cod end of the trawl, all intact individuals were transferred into buckets of freshly collected seawater (vol = 5L, five individuals per bucket) and transported back to Plymouth Marine Laboratory (PML, Plymouth, UK) within 2hrs of collection.

On arrival, animals were transferred to individual plastic containers (vol = 1L) filled with filtered (10µm) seawater and placed in the mesocosm tanks, two large (vol = 600L) tanks of seawater maintained at 13°C ± 0.5°C. Each individual plastic container had a layer of aquarium gravel (Dennerle Plantahunter, 8-12mm, J & K Aquatics) for the animal to sit on, and was aerated individually, with air being finely bubbled through aquarium airstones. Once transferred to these containers, individuals were left for 48 hours prior to the start of the experiment.

3.3.2 Experimental design

In the first week of the experiment, each individual's carapace width (CW) was measured with digital Vernier callipers (± 0.05mm) and then weighed on a balance scale (Sartorius R220-D, 0.01mg, European Instruments). These measurements were repeated weekly for the duration of the experiment (10 weeks). Once a week, the containers were washed, the gravel rinsed with clean seawater, and the water was changed. *L. depurator* were fed three times per week (Monday, Wednesday and Friday) on raw squid tubes (*Illex argentinus*). Wet weight of squid (typically between 1 - 1.5g) was measured before being presented to the animals, which were then left undisturbed for 6hrs to feed. After the 6hr period, any un-ingested squid was removed and reweighed.

Oxygen consumption data were collected for randomly selected individuals during the last 3 weeks of the experiment. *L. depurator* were removed from their individual containers and placed on a platform in a 920ml static respiration chamber containing aerated seawater of the same temperature as that in the experimental aquaria. The chamber was placed on a stirrer plate and a 10mm stir bar mixed the water at 500rpm, separated from the animal by the platform. The rpm was kept at the lowest possible setting to ensure that water in the chamber would be mixed while minimising disturbance to the animal. The chamber was then covered with a black cloth and the crab left to settle for approximately 30mins (the time it took for the animal to stop moving around the chamber or displaying obvious signs of agitation such as climbing the sides). After this initial 30min period, the chamber was sealed, ensuring there were no trapped air bubbles, and an initial measurement of the percentage air saturation in the chamber was taken using an OxyMini-AOT (World Precision Instruments). Further measurements were taken every 15mins for up to 3hrs, with the chamber covered with a black cloth between measurements to ensure the crabs experienced minimal disturbance. At no point during the measurements was air saturation in the chamber allowed to drop below 70%. Percent air saturation was converted to µmol O_2 L^{-1} using the formula

$$\left[\frac{P_{atm} - P_w(T)}{P_N} \cdot \frac{\%\, air\ saturation}{100} \cdot 0.2095 \cdot \alpha(T) \cdot 920 \cdot \frac{M(O_2)}{V_m}\right] \cdot 31.25$$

Where P_{atm} is atmospheric pressure (mbar)

P_N is standard pressure (1013 mbar)

$P_w(T)$ is vapour pressure of water (Pa) at measurement temperature (K)

α is the Bunsen absorption coefficient at measurement temperature (K)

$M(O_2)$ is the molecular mass of O_2 (32g/mol)

V_m is the molar volume (22.414L/mol)

0.2095 is the volume content of O_2 in air

31.25 is the conversion factor from mg L^{-1} to µmol L^{-1}

And 920 is the volume of the respirometry chamber (ml)

Subsequently, the rate of whole animal O_2 consumption (µmol O_2 consumed min^{-1}) was determined by plotting µmol O_2 over time for each crab, and calculating the slope of the regression line. To allow for a more accurate comparison of O_2 consumption rates between individuals of different sizes, O_2 consumption was then corrected to µmol O_2 consumed g $carbon^{-1}$ min^{-1}, using pre-determined carbon mass/wet mass conversions (see below).

3.3.3 Wet mass/carbon mass conversions

Prior to collection of experimental animals, ~80 individuals were collected from the same location, following the same method outlined above. These animals were euthanised on arrival at PML by immersing them in briny water chilled to -11°C and then weighed and measured in the same way as the experimental animals. Once wet mass had been established, individuals were placed in a drying oven at 60°C and dried to a constant weight (typically 48hrs), left to cool to room temperature in a desiccator (typically 2-3hrs) and weighed again on removal to quantify dry mass. Animals were then placed in a muffle furnace at 550°C for 4 hours to be incinerated (West et al., 2004), and the remaining ash weighed. Carbon mass was calculated by subtracting the ash weight from the dry weight. The regression equation for the relationship between wet mass and carbon mass was calculated, and the ratio of carbon mass to wet mass was determined.

3.3.4 *L. depurator* DEB model structure

A simplified version of the standard DEB model (see Chapter 1, section 1.4) was implemented in the R programming environment and used to evaluate growth, ingestion and oxygen consumption in *L. depurator* (see Figure 3-1 for an outline of the model procedure). In terms of the simplification of the standard DEB model, all carbon allocated to maturation and reproduction, as defined by the “kappa rule”, was respired completely in this model. This decision was made because observations on maturity of the individuals and on the biomass of their reproductive tissues was lacking; furthermore, it allowed the same model to be used for juvenile and mature individuals, without having to detect the moment of maturation. This makes the model equivalent to that of a standard DEB juvenile animal. As a result, modelled total biomass by necessity excludes reproductive tissues; for modelled oxygen consumption, the oxygen needed to metabolize all carbon allocated to maturation/reproduction was included. For mature animals the model has the potential to slightly underestimate total mass, and overestimate respiration. However, this is a reasonable simplification, given the small size of crabs involved, and the absence of eggs in all animals.

Given the discontinuous nature of crustacean growth, and the potential difference in tissue composition that can be measured in two animals of the same carapace width, carbon mass (M_C) was identified as a more appropriate size metric to use in order to quantify the model’s continuously varying state variables, structure (M_V) and reserve (M_E)

(NB – any use of the term “structure” in this thesis refers to the state variable M_V). However, as M_C cannot be measured directly without sacrificing experimental animals, the model was extended with a variable for wet mass (M_W), an easily established measure of physical size. This variable was designed to change only through moulting. The moulting process was triggered when the modelled ratio of carbon mass to wet mass (α) exceeded a threshold calculated from observed carbon to wet mass ratios (Figure 3-2 and Section 3.4.1). It should be noted that α increased between moults due to assimilation of carbon (and increased structure and reserve), while M_W remains fixed (equation ix, Section 3.3.5). In this way, the model produced a stepwise growth curve in wet mass, even though structure and reserve increased continuously, with α as the primary link between the measured variable M_W, and the state variables M_V and M_E. This increase in M_V and M_E, taken alongside the constant M_W between moults, implies a change in water content of the animal during the inter-moult period.

In DEB theory, ingestion scales with surface area, assumed to be proportional to structure$^{2/3}$ in the standard DEB model. This reflects the theory that ingestion is a function of the surface area of organs responsible for ingestion and/or digestion. However, in moulting animals the physical size of organisms remains constant between moults, and is more appropriately measured by wet mass than the carbon mass of structure. Therefore, it was assumed that the surface areas responsible for ingestion, and thus, the maximum ingestion rate, are proportional to $M_W^{2/3}$ (equation iii). To test the validity of this assumption, the log-log relationship between wet mass and measured ingestion rate was examined (Figure 3-3), and ingestion was found to scale to $M_W^{0.65}$. Other size-dependent processes in the DEB standard model, specifically the reserve mobilisation rate and the maintenance rate, were left to scale with structure, as these are thought to relate primarily to metabolically active biomass and energy density, rather than physical size.

Additional logic to describe the feeding regime was introduced as part of the model code, in which the simulation was cut into many feeding and non-feeding periods that are individually simulated and linked through the initial and final states of the individual being modelled. The model calculated the amount of food ingested over the 6hr feeding period, based on the maximum ingestion rate scaled to $M_W^{2/3}$ (equation iii, section 3.3.5). It then compared the modelled output to the measured output.

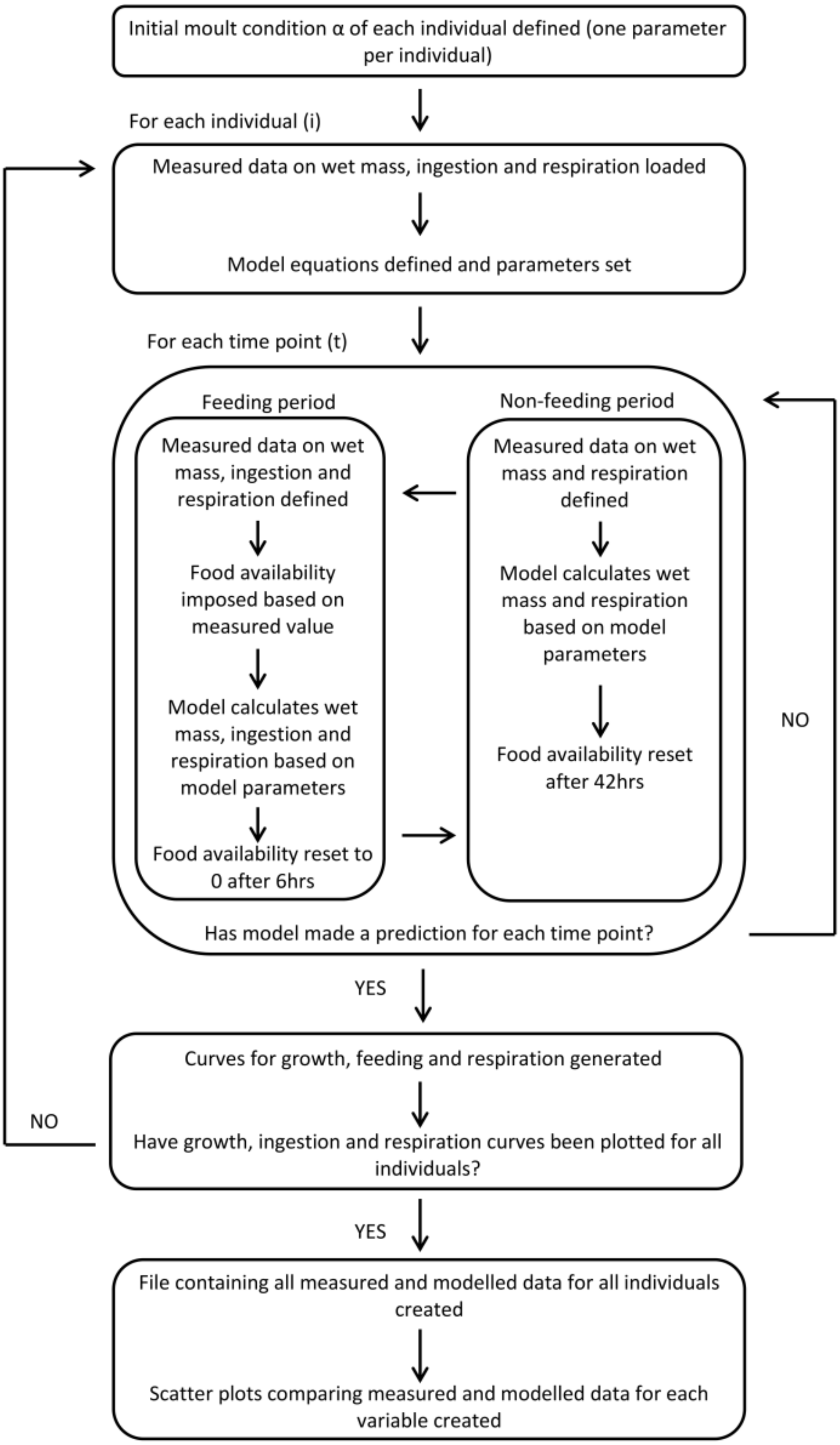

Figure 3-1: Flow chart outlining the major steps of each DEB model iteration. Initial moult condition is the parameter α. Note that the model was designed to differentiate between feeding and non-feeding periods. All code was developed *de-novo*, although the majority of the model equations are from the standard DEB model. Any exceptions are listed in section 3.3.5

3.3.5 Model equations and parameter values

Most model equations are standard DEB model equations (Kooijman, 2010), although the commonly used notation is not entirely adhered to. For example, the decision to use M_W as the measure of physical size necessitated the calculation of certain parameters (e.g. reserve mobilisation, v) in $g^{1/3}$ d^{-1}, rather than cm d^{-1}. Also, all fluxes were calculated in g d^{-1}, rather than in J or C-moles d^{-1}. Some equations needed to be adjusted to accommodate the chosen size measure. In equation (iii), ingestion scales with M_W rather than surface area, and equation (viii) is a cubic function (not part of standard DEB) to calculate the initial state of structure M_V. Equation (ix) is a new equation which calculates the magnitude of wet mass increase during a moult.

State variables are structure $\boldsymbol{M_V}$ and reserve $\boldsymbol{M_E}$

(i) Reserve density (gC gC^{-1})

$$m_E = \frac{M_E}{M_V}$$

(ii) Functional response for ingestion

$$f = \frac{X}{X + K}$$

where X is food and K is the half saturation coefficient. At ad libitum food, $f = 1$

(iii) Ingestion (gM_W d^{-1})

$$J_{XA} = \{j_{XAm}\}\, M_W^{\frac{2}{3}}\, f$$

Where $\{j_{XAm}\}$ is the maximum ingestion rate scaled to $M_W^{2/3}$

(iv) Assimilation (gC d^{-1})

$$J_{EA} = y_{EX}\, J_{XA}$$

Where y_{EX} is the assimilation efficiency

(v) Specific growth rate (d^{-1}) of structure M_V (gC)

$$r = \frac{y_{VE}\left[\kappa\, m_E \frac{v}{L} - k_M\right]}{1 + y_{VE}\, \kappa\, m_E}$$

Where y_{VE} is growth efficiency when turning reserve into structure and

v (g$^{1/3}$ d^{-1}) is the reserve mobilisation rate

L is the structural length (g⅓), which equals $\sqrt[3]{M_V}$

k_M is the maintenance cost (d^{-1}) and

κ (kappa) is the energy allocated to somatic maintenance and growth

(vi) Catabolic flux (gC d^{-1})

$$J_{EC} = M_E\left(\frac{v}{L} - r\right)$$

(vii) Respiration (CO$_2$ flux in gC d^{-1}) is equal to all carbon mobilized from the reserve, minus the carbon used in growth (i.e., fixed in structural biomass)

$$resp = J_{EC} - (r\, M_V)$$

Note that this includes all carbon allocated to maturation and/or reproduction.

(viii) Due to the use of M_W as an indicator of physical size, the calculation used in the standard DEB model to determine the initial state of structure M_V is not applicable and is replaced with the cubic function

$$x^3 + c_1\, x - c_2 = 0$$

Where $x = {M_V}^{1/3}$ and

$$c_1 = \frac{\{j_{XAm}\}{M_W}^{\frac{2}{3}} f}{v}$$

$$c_2 = \frac{M_W}{(M_W/M_C)}$$

For full derivation and assumptions, see Appendix A, section A.3.

(ix) During a moult, triggered by the ratio of carbon (structure + reserve) to wet mass (α) reaching the predefined maximum α_{pre}, water is taken in until α reaches the predefined minimum α_{post}. Therefore, M_W post moult is calculated as

$$M_{W_{new}} = \frac{M_W \cdot \alpha_{pre}}{\alpha_{post}}$$

Parameter values are listed in Table 3-1. Initial values for reserve mobilisation (v), fraction of allocation to soma (κ) and volume specific maintenance costs (k_M) were obtained from the DEB species explorer (Bruggeman, 2019). Ingestion rate $\{j_{XAm}\}$ was calculated for each animal from observed data. Initial values for assimilation efficiency (y_{EX}) and growth efficiency (y_{VE}) were estimated from the literature (Klein Breteler, 1975; Paul and Fuji, 1989; Iguchi and Ikeda, 1995; Lemos et al., 2001; Taylor and Peck, 2004; Iguchi and Ikeda, 2005; McGaw and Whiteley, 2012). As there is little data on assimilation and growth efficiency in *L. depurator* specifically, these values were estimated from assimilation and growth efficiency data from a range of predatory decapod crustaceans.

Table 3-1: Mean DEB parameter values for *L. depurator* along with values for *Carcinus maenas* for comparison. Values for *C. maenas* were taken from the Add-my-Pet database. https:/www.bio.vu.nl/thb/deb/deblab/add_my_pet/species_list.html

Parameter	**Symbol**	**Values (± SD)**	***Carcinus maenas* values**	**Unit**
Maximum ingestion rate scales to $M_W^{2/3}$	$\{j_{XAm}\}$	1.41 (0.24)	-	$g^{1/3}$ Mw d^{-1}
Assimilation efficiency	y_{EX}	0.87 (0.08)	0.8	-
Reserve mobilisation rate	v	0.025 (0.01)	0.02	$g^{1/3}$ C d^{-1}
Fraction of energy allocated to somatic maintenance and growth	κ	0.85 (0.02)	0.9	-
Somatic maintenance coefficient	k_M	0.17 (0.03)	0.1	d^{-1}
Growth efficiency	y_{VE}	0.5 (0.04)	0.8	-

The model was run with these parameters and predictions for growth, ingestion and O_2 consumption were compared to measured values for each individual crab. Model performance was assessed using mean absolute error (MAE), a standard model test statistic which gives equal weight to all errors and as such is easy to interpret. All parameters except $\{j_{XAm}\}$ (for which there was a calculated value for each crab) were then tuned, by hand, the model iterated again, and performance assessed using MAE for each individual. This process was repeated until a parameter set was found for each individual which minimised the deviation between predictions and observations for the three metrics investigated (growth, ingestion and O_2 consumption), based on the MAE. The mean values of all parameters were then calculated, and the model run for a final time using these mean parameter values and observations from all experimental animals. Validity of the parameters was assessed by comparing them to a parameter set for the related portunid crab *Carcinus maenas* (Linnaeus, 1758), taken from the Add-my-Pet database (AmP, 2017). While a certain level of deviation between parameter estimates for the two species is to be expected, it was assumed that their relative taxonomic proximity would result in similar values (e.g. for the values for *C. maenas* to be within 1 standard deviation of the mean parameter values for *L. depurator*).

In order to facilitate a comparison between this model, in which moult dynamics are explicitly considered, and the standard DEB model, in which physical size is allowed to increase constantly alongside the increase in structure and reserve, the model was run again without the “moult extension” applied. In this version of the model, ingestion was scaled to structure, rather than $M_W^{2/3}$.

3.4 Results

3.4.1 Carbon mass/wet mass

Carbon mass/wet mass ratios (α) in animals collected from the field were found to range from ~0.13 – ~0.2 (Figure 3-2. For full derivation of the fitting procedure for the upper and lower envelope see Appendix A, section A.1). These extremes describe the “moult condition” in *L. depurator,* with newly moulted individuals having a α of ~0.13, and individuals approaching a moult having a α of ~0.2. These ratios were imposed in the DEB model, where they control both the timing of the moult and the magnitude of the increase in wet mass.

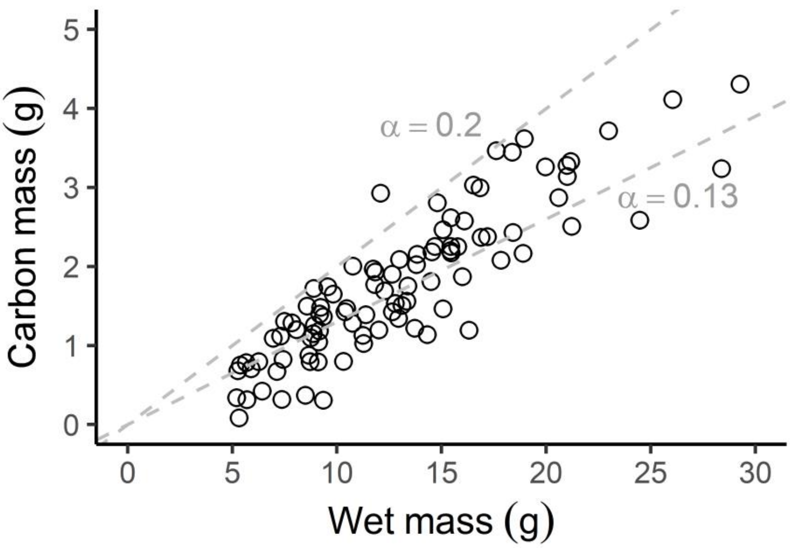

Figure 3-2: Carbon mass/wet mass ratio (α) for *L. depurator.* The lower dashed line represents the approximate α of a newly moulted crab (0.13); the upper dashed line represents the "moult threshold" of 0.2. Once an animal reaches this threshold it will moult in the model.

3.4.2 Scaling of ingestion to wet mass

Measured ingestion was found to scale approximately with $M_W^{2/3}$. The actual exponent was 0.65 (Figure 3-3).

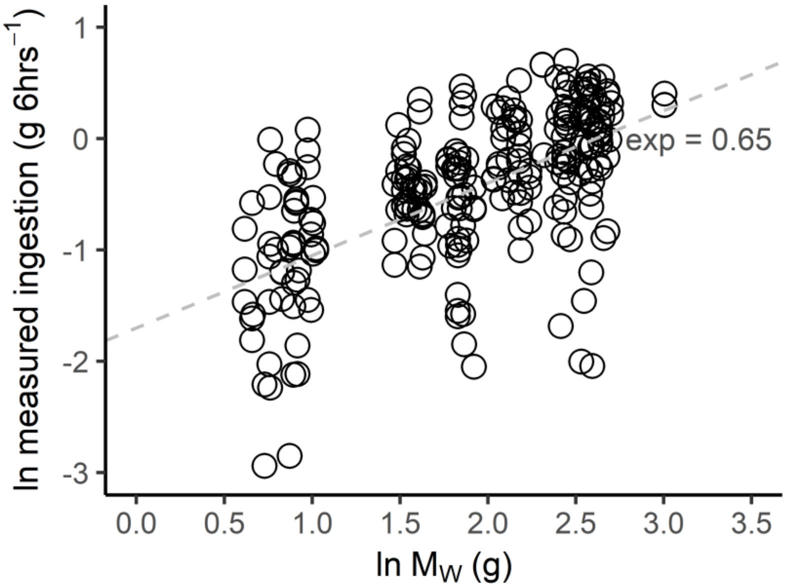

Figure 3-3: Scaling relationship between wet mass (M_W) and ingestion *in L. depurator.*

3.4.3 Growth, ingestion and oxygen consumption

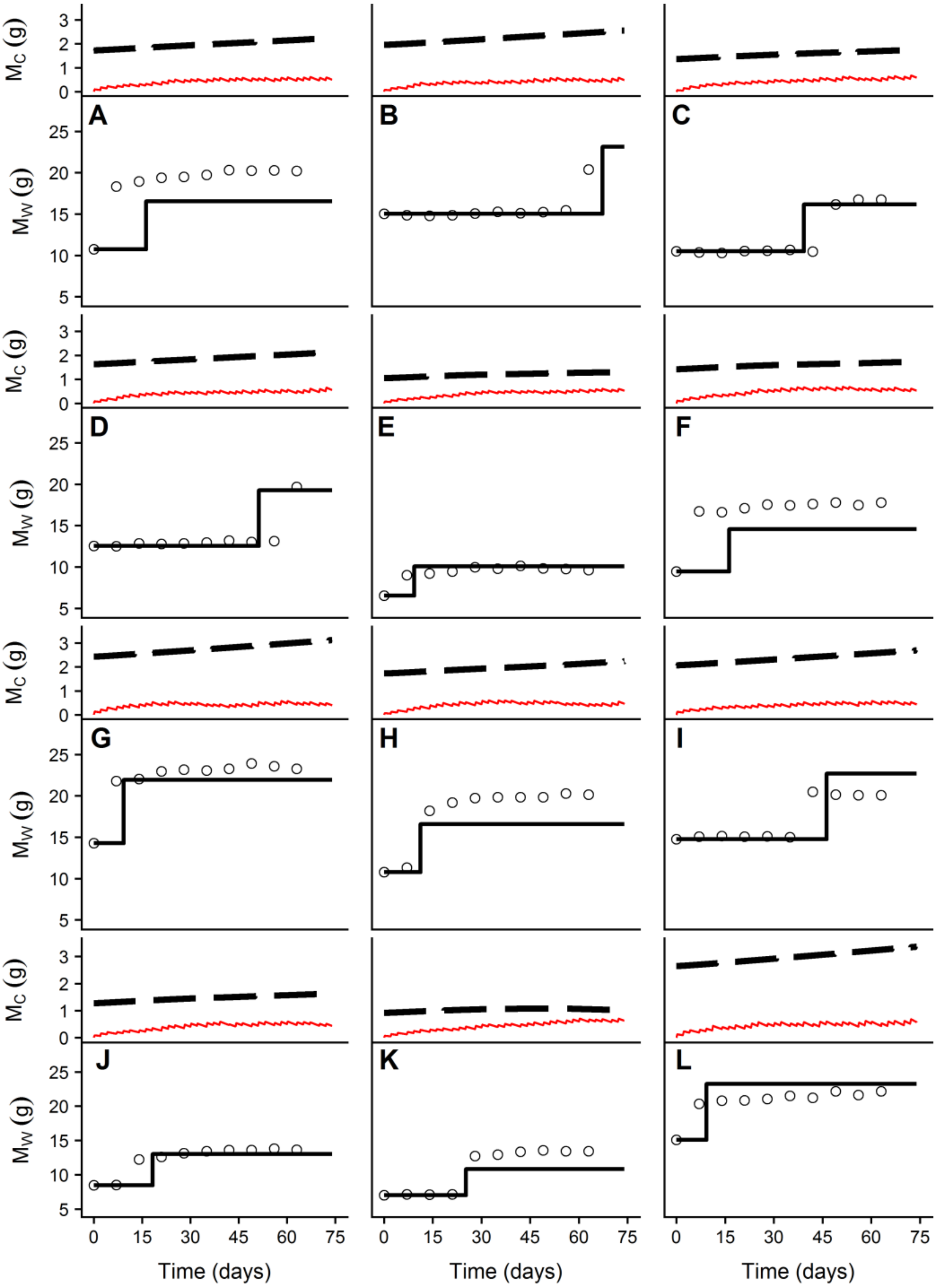

Figure 3-4: Growth curves for those animals which moulted over the course of the experiment. Black circles are measured wet mass (M_W), solid black line is modelled wet mass. Dotted black line is modelled structure, and solid red line is modelled reserve (both measured in g carbon). The zig-zag appearance of the red line is a reflection of the reserve dynamics. Reserve increases as food is assimilated, and decreases as it is mobilised for somatic growth and maintenance. The upward trend of the dotted black line is the overall increase in structure. Note how structure increases smoothly while wet mass increases in a stepwise fashion.

Figure 3-4 illustrates the skill of the DEB model in predicting both the timing of the moult and the magnitude of the increase in wet mass for all of those individuals which moulted over the course of the experiment. The structure of the animal (dotted black line) changes smoothly between moults, while wet mass increases in a stepwise manner. The dynamics of the reserve are also apparent (red line), with reserve increasing after food has been assimilated, and decreasing as it is mobilised for somatic growth and maintenance. In some cases, the model underestimates the increase in wet mass (Figure 3-4A, F, H and K). In two cases, it lacks accuracy in predicting the timing of the moult (Figure 3-4A and F). As noted in section 3.3.4, the model does have the capacity to slightly underestimate total biomass due to the fact that modelled biomass excludes reproductive tissues.

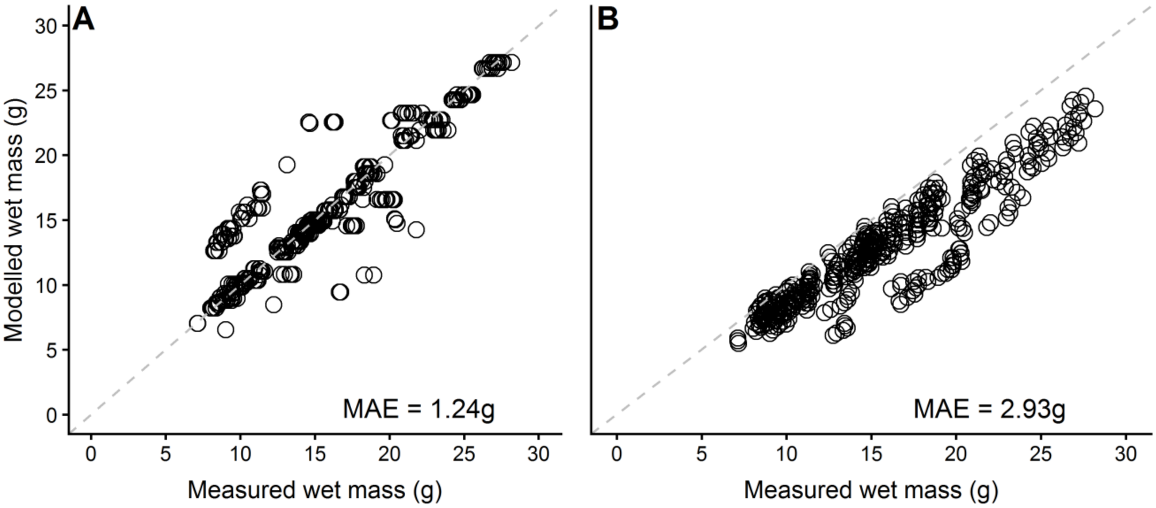

Figure 3-5: Measured versus modelled wet mass in *L. depurator.* (A) shows performance of the model with the “moult extension” presented in this chapter. (B) is the performance of the model when run as a standard DEB model, without the dynamics of the moult considered. Dashed line is a 1:1 reference line. Modelled values were calculated using the parameter values in Table 3-1. Mean average error (MAE) is shown.

A direct comparison of modelled and measured wet masses for all experimental animals (N = 52, data for those animals which died over the course of the experiment were not considered) shows overall model skill is good, with a MAE of 1.24g (Figure 3-5A). Those points which sit on the 1:1 reference line represent each time step at which measured and modelled wet masses matched. The points sitting above and below the reference line represent those time steps at which modelled and measured wet masses differed. These mismatches are largely due to the model either underestimating wet biomass (Figure 3-4A, F, H and K), or a lack of accuracy in predicting moult timing (Figure 3-4A and F). The performance of the model when run as a standard, if simplified, DEB model (i.e. without the “moult extension”, allowing M_W to increase continuously) is poorer, with a MAE of 2.93g (Figure 3-5B).

The model showed considerably less skill in predicting *L. depurator* ingestion rate (Figure 3-6). Observed ingestion rate showed a great deal of variation over the course of the experiment, which is not captured in the model; measured ingestion over a six hour feeding period varied between 0 - 1.96g wet mass squid ingested, whereas model predictions ranged from 0.29 – 1.84g wet mass squid ingested. The vertical line of points at 0 on the x axis represents the animals that did not feed during at least one of the 6 hour feeding periods – some of these animals would have moulted over the course of the experiment and would not have fed immediately before or after ecdysis (Figure 3-6). The slope of points visible just under the 1:1 reference line (Figure 3-6) represents those animals that ingested all the food that was presented to them.

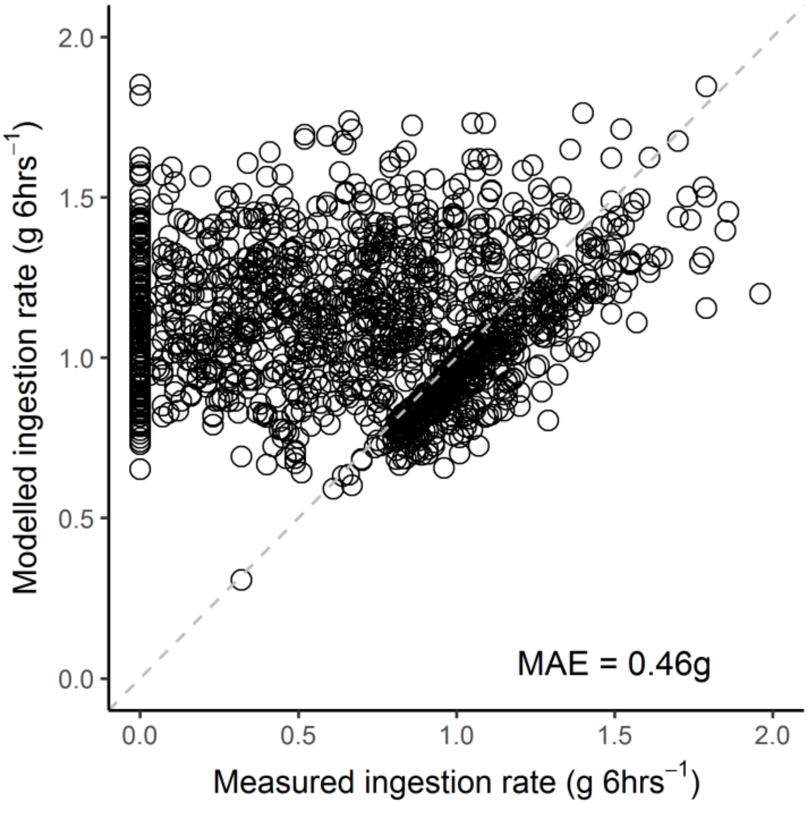

Figure 3-6: Measured versus modelled ingestion rate in *L. depurator.* Dashed line is a 1:1 reference line. Modelled values were calculated using the parameters in Table 3-1. Mean average error (MAE) is shown.

Modelled rates of oxygen consumption demonstrated less variability than the measured rates (Figure 3-7). Of the eight animals measured, 6 were assumed to be in the intermoult stage of the moult cycle, while 2 had moulted within 48hrs prior to having O_2

consumption measured (blue filled circles, Figure 3-7). However, one of the animals assumed to be in the intermoult period had a very high rate of O_2 consumption (red filled circle, Figure 3-7) perhaps suggesting that it was approaching a moult. Measurements for this individual were taken on the last day of the experiment so it is unknown whether or not it moulted soon after these observations were made. An independent test of model skill when considering all eight animals measured showed a discrepancy between measured and modelled rates (MAE 0.06 µmol O_2 gC^{-1} min^{-1} consumed). When excluding the animals with higher rates, however, MAE dropped to 0.02 µmol O_2 consumed gC^{-1} min^{-1}).

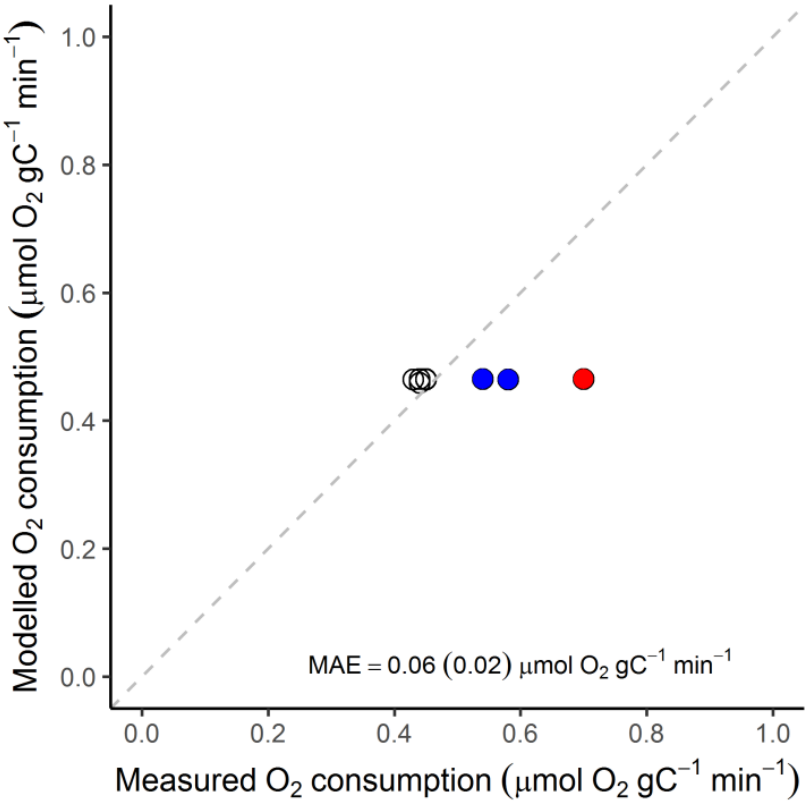

Figure 3-7: Measured versus modelled O_2 consumption rate in experimental *L. depurator.* Modelled values were calculated using the parameters in Table 3-1. Unfilled circles are animals that were assumed to be intermoult. Blue filled circles represent animals that moulted within 48hrs previous to having O_2 consumption measured. Red filled circle represents an animal that had not moulted over the course of the experiment, but was assumed to have been approaching a moult due to the very high rate of O_2 consumption measured. Mean average error (MAE) is shown. Figure in parentheses is the value of MAE when the three animals represented by filled circles are not considered. Dashed line is a 1:1 reference line.

3.5 Discussion

3.5.1 Model performance

A simple Dynamic Energy Budget model was successfully parameterised for the decapod species *L. depurator*. Statistical tests of the model showed that it made good predictions for the increase in wet mass during a moult, and for oxygen consumption, but lacked skill in predicting ingestion rates. By combining the DEB framework with empirical data collected specifically for modelling purposes, a set of parameters were estimated that describe the dynamics of physiological processes related to growth and maintenance, in particular the dynamics of the moult.

A critical factor for moult dynamics in this model was the carbon mass/wet mass ratio (α), with animals being assigned a pre/post moult threshold of 0.13 and 0.2 respectively. This ratio was also used to calculate the moult increment (MI) and intermoult period (IP) of an individual crab. The independent statistic used to assess model skill in capturing moult dynamics found an acceptably low deviation (MAE = 1.24g) between predicted and observed values for wet mass in all experimental individuals, which suggests that α is not only a simple indicator of an individual's moult stage, but is also a powerful tool in constraining the upper limits of wet mass increase during a moult. Furthermore, when the model was run again without the "moult extension" – in effect run as a standard, if simplified, DEB model – deviations between predicted and observed values for wet mass increased. This would lend credence to the notion that this simple extension to DEB theory can improve predictions of growth in crustaceans by accounting for the dynamics of the moult. Once parameterised, the standard DEB model generates properties of the individual such as maximum body size. This allows the validity of the parameters to be evaluated, based on whether these "implied properties" are consistent with what is known about the life history of the species. The model presented here does not generate these data, so the parameters cannot be evaluated in this way, but comparison between the parameters presented here with those of the related portunid *Carcinus maenas* showed that most parameters for *C. maenas* were within 1 standard deviation of the mean of those for *L. depurator*. This would suggest that the model parameters are valid, but a further iteration of the model in which life history properties are generated would be useful.

Model skill with regards to ingestion was fairly poor, with a MAE of 0.46g. This is a reflection of the fact that observed ingestion rate was very variable, which was not captured in the model. This is perhaps unsurprising when considering the fact that the ingestion rate used in the model was a mean rate for all experimental animals. When there is substantial variation between individuals, the ingestion rate of the average crab can deviate considerably from the mean rate of the whole group. There is significant evidence that feeding activity in crustaceans is driven by circadian rhythms, particularly light (Reymond and Lagardère, 1990; Cannicci et al., 1996; Focken et al., 1998; Soares et al., 2005) and tidal (Hunter and Naylor, 1993; Chatterton and Williams, 1994; Cannicci et al., 1996) rhythms, which was not accounted for in the model. While these circadian rhythms may account for any temporal variations in maximum ingestion, they do not explain the differences in individual ingestion observed. However, it has been documented that feeding activity can be triggered or inhibited in individual animals depending on metabolic requirements. For example, it is well established that crustaceans in the premoult stage stop feeding (O'Halloran and O'Dor, 1988; Mantelatto and Christofoletti, 2001; Endo and Yamano, 2006). It is evident that further work is needed to better understand the variability exhibited in feeding behaviour in *L. depurator*, so that this variability can be better accounted for in the model. While it is unlikely that that the model will ever capture the full variability of feeding behaviour in crustaceans, it is likely that accounting for the moult duration and the associated suppression in feeding regime may improve the modelled output to some degree.

The range of values measured for oxygen consumption in this experiment is indicative of the fact that respiration in decapods changes depending on the moult stage of an individual, with animals immediately pre and post moult exhibiting high O_2 consumption, and individuals mid cycle showing lower values (Alcaraz and Sardà, 1981; Penkoff and Thurberg, 1982; Stern and Cohen, 1982; Carvalho and Phan, 1998). Of the animals measured here, two had moulted within the 48 hours previous to measurements being taken, which would explain the higher rates of O_2 consumption measured, and which the model failed to capture. Similarly, the individual with the highest value for O_2 consumption may have been approaching a moult. However, oxygen consumption can vary for reasons besides moult stage, such as disease or parasite burden (Schuwerack et al., 2001), and it is possible that the very high oxygen consumption recorded in this individual was a reflection of some kind of disease related physiological stress. Equally, while those crabs with the lower oxygen consumption rates were assumed to be mid cycle (i.e. intermoult stage C based on the Drach staging system (Drach et al., 1967)), and while there is a method for moult staging *L. depurator* (Abelló, 1989), due to practical considerations (i.e. the need for destructive sampling to accurately identify the premoult D_2-D_4 stage) and time constraints, none of the experimental animals were formally moult staged. Finally it should be noted that relatively few measurements were taken, and more data would be useful to better constrain the model.

The model predictions for oxygen consumption showed good agreement with observed values for those animals with the lower rates, with a MAE of 0.02 µmol O_2 consumed gC^{-1} min^{-1} when the three outliers were not considered in the analysis. When all eight animals were considered however, model skill decreased, and MAE increased to 0.06 µmol O_2 gC^{-1} min^{-1} consumed. Clearly, further development is needed to ensure that the variability in oxygen consumption exhibited by crustaceans over the course of the moult cycle is accurately captured in the model.

3.5.2 Future model development

While this model represents a promising start to modelling crustacean moult dynamics, it requires further development. The primary limitations relate to the fact that the model currently does not capture the changes in ingestion and oxygen consumption rate that occur as an animal progresses through the moult cycle. In order to improve model performance in these areas it is necessary to build a true “moulting period” into the model code, which causes the suppression of feeding and an increase in O_2 consumption. While O_2 consumption is an output of the model, and so cannot be coupled to the moult cycle directly, model parameters affecting O_2 consumption (e.g. maintenance rate k_M) can be. By coupling maintenance and ingestion rates to α both ingestion and O_2 consumption will change with the increase in α as an animal approaches moult.

The model in its current form does not follow the mobilised flux from the reserve to the reproductive buffer (1-kappa) once it has been allocated – in effect, the model is representative for juvenile individuals that allocate to maturation but not reproduction. In order to explore this more fully, the next iteration must utilise the existing DEB framework to track the energy allocated to the reproductive buffer, as well as the reproduction process itself. Again, an accurate model of moulting will be essential to get this right. Moult is critical to reproduction in many crustacean taxa, with the two being coordinated in a variety of ways (Raviv et al., 2008), and influenced by environmental conditions. For example, there is evidence to suggest seasonal moulting as a precursor to a breeding season in some species. In the spiny lobster *Jasus edwardsii* (Hutton, 1875) in northeast New Zealand, both males and females had seasonal moulting periods (October/November for males, April/June for females). Females would moult immediately prior to mating, while males moulted earlier to ensure that they were in intermoult during the mating season (MacDiarmid, 1989). In temperate areas, the presence of a maximum number of brachyuran crabs of several species undergoing ecdysis in the summer has been observed by various authors (Abelló, 1989; Fernández et al., 1991) and the number of ovigerous females is often inversely proportional to the number of females in the moult stage (Abelló, 1989; Fernández et al., 1991), suggesting that these species may have a “fixed” seasonal moult in which copulation takes place. Additionally, ovigerous females do not moult, so the number of egg batches a female releases can affect moult timing. Several species (including *L. depurator*) can spawn multiple times between moults, so the intermoult period becomes dependent on egg incubation time, which is itself influenced by temperature (Hamasaki, 2003; Wehrtmann and López, 2003). Given the strength of this link between reproduction and moult, it is possible that, in some species, moult is not solely dependent on energetic factors (e.g. α). It may be that, during “fixed” seasonal moults, the reproductive buffer plays a role in moult dynamics. This is perhaps more likely in those species exhibiting parturial moults, in which the ovaries begin to develop during the previous moult cycle and mature ovaries are carried through ecdysis, so that oviposition can occur immediately after mating. The implementation of the equations governing this reproductive buffer would allow further exploration of the role (if any) it plays in crustacean moulting. Development of the reproductive side of the model will also provide a direct link to population level processes, such as fecundity and reproductive output, as well as the effects of stressors (environmental and anthropogenic) on reproduction. This could be useful in stock assessments of crustacean fisheries, as well as having broader applications in the fields of benthic ecology and ecological modelling. For example, it could be used to explore population and ecosystem level consequences of changes in temperature and food availability under climate change.

This chapter demonstrates that the standard DEB model can be easily modified to better describe the physiological processes related to crustacean growth and maintenance under ambient conditions. However, it is becoming increasingly important for researchers to be able to assess and predict the impacts of changing environmental conditions on marine species. In order to fully test the capabilities of the new DEB model, it necessary to evaluate its performance in describing and predicting crustacean responses to climate drivers such as changing water temperatures, ocean acidification and hypoxia.

Chapter 4 Modelling *Liocarcinus depurator* responses to multiple stressors in marine environments

4.1 Abstract

A pressing issue facing marine biologists today is to understand, and critically, to predict, how marine organisms will be impacted by a rapidly changing environment. To date, many single factor experiments have been conducted to assess organism performance in response to a specific stressor. In reality however, organisms will be exposed to environments in which multiple stressors are acting simultaneously. Consequently, researchers need a method by which data generated from single stressor experiments can be synthesised in order to improve our predictive understanding of organism responses in a complex environment. Here I demonstrate that a Dynamic Energy Budget (DEB) model, parameterised using results from three separate single stressor (temperature, ocean acidification and moderate environmental hypoxia) experiments, and validated using data collected in multi-stressor experiments, can be used to predict responses of the swimming crab *Liocarcinus depurator* (Linnaeus, 1758) to multiple stressor scenarios. Results from the single stressor experiments showed that *L. depurator* oxygen consumption increased in both the hypoxic and ocean acidification (OA) treatments, while ingestion decreased in the hypoxic treatment. An independent test of model skill showed that the multi-stressor model, which combined the parameters estimated using data from the single factor experiments, was able to accurately describe *L. depurator* responses to multiple-factor (temperature + OA and temperature + environmental hypoxia) experimental conditions, leading me to propose that any predictions made with this model are likely to be robust. The multi-stressor model predicted an increase in the intermoult period at 10°C in hypoxic conditions. This effect was less pronounced at 13°C and 16°C, suggesting that effects of hypoxia on growth can be mitigated by higher temperatures. At all temperatures OA alone and OA + hypoxia increased the intermoult period. The results of these model scenarios support further investigation of *L. depurator* responses to OA and OA + hypoxia at varying temperatures to see if the predicted effects on growth are observed. I contend that the DEB model has several advantages: i) Predicted responses are based on the effects of stressors on model

parameters, providing a mechanistic insight into stressor mode of action. ii) Results allow the identification of stressors with the greatest predicted impact, aiding in the development of testable hypotheses and the design of logistically challenging multi-stressor experiments. iii) Finally, DEB can provide a modelling environment in which organism responses to more stressors than it is possible to investigate experimentally can be explored, using data generated from single factor experiments.

4.2 Introduction

One of the problems currently facing the development of robust predictions about biological responses to anthropogenic change is the sheer number of stressors acting on natural systems (Côté et al., 2016). Depending on location, organisms can face changes including, but not limited to, increased water temperature (Burrows et al., 2011; Gleckler et al., 2012; Cheung et al., 2013), decreased pH (Doney et al., 2009; Hofmann et al., 2011), lowered oxygen availability (Diaz and Rosenberg, 2008; Keeling et al., 2009), changes in salinity (Curry et al., 2003; Korhonen et al., 2013) and increased pollution (Fowler, 1990; Nizzetto et al., 2010). There exists a huge body of data generated from single stressor experiments, which represent a relatively simple approach to assessing organism performance under changing conditions (Todgham and Stillman, 2013). While these single stressor investigations have undoubtedly been critical in providing a solid foundation for the understanding of organism responses to environmental change, the number of possible interactions between stressors means that researchers are increasingly focussed on the investigation of the cumulative impacts of multiple stressors (Wernberg et al., 2012; Stevens and Gobler, 2018; Whiteley et al., 2018). Over the last decade the impacts of rising seawater temperature in combination with at least one other factor (and in a range of different taxa) have been explored. One of the most commonly investigated secondary factors is ocean acidification (Martin and Gattuso, 2009; Munday et al., 2009; Parker et al., 2009; Findlay et al., 2010a; Findlay et al., 2010b; Wood et al., 2010; Edmunds et al., 2012; Arnberg et al., 2013; Melatunan et al., 2013; Duarte et al., 2014; Paganini et al., 2014; Miller et al., 2015), although the effects of increased water temperature combined with environmental hypoxia (Schurmann and Steffensen, 1994; Claireaux et al., 2000; Wiklund and Sundelin, 2001; Alexander and McMahon, 2004; McBryan et al., 2013), varying salinity (Motes et al., 1998; Purcell et al., 1999; Fockedey et al., 2005; Re et al., 2005; Wang et al., 2008) and heavy metal pollution (Sokolova, 2004;

Khan et al., 2006) also appear in the literature. Researchers have also investigated other combinations of these factors, although they are less common. For example, recently published work concerns the impacts of ocean acidification in combination with environmental hypoxia (Mukherjee et al., 2013; Frieder et al., 2014; Gobler et al., 2014; DePasquale et al., 2015; Sui et al., 2016) and heavy metal pollution (Lewis et al., 2013; Roberts et al., 2013; Biscéré et al., 2015; Ivanina and Sokolova, 2015).

This experimental research is clearly invaluable however, the complexity of the situation - that for a given set of stressors, interaction type will differ across focal species (Muthukrishnan and Fong, 2014) and response metrics (Boyd and Brown, 2015), and may change over time or with varying severity of the stressors (Gunderson et al., 2016), along with the limited resources available for research and the logistical difficulty in designing complex multi-factor trials - means that experimental examination of all possible combinations is impractical (Griffen et al., 2016). It is likely that the level of complex synthesis required to explore these interactions is only truly practicable in models, and the wealth of data generated by both single and multi-stressor experiments can be a valuable resource in this regard. It is in this context that Dynamic Energy Budget (DEB) models can prove useful. DEB models are mechanistic models which offer a whole organism approach to explaining how factors in the physical environment translate into biologically and ecologically relevant responses (van der Meer, 2006a). They have also been successfully used to model organism responses to stressors based on the assumption that stressors influence the acquisition and/or use of energy, which in turn affects measurable endpoints e.g. growth, reproduction, calcification (Jager and Zimmer, 2012; Muller and Nisbet, 2014; Lavaud et al., 2019). While many of these are single stressor models (although see Baas et al. (2010) for a review of using DEB to predict the physiological effects of multiple toxins), the fact that predicted responses are a function of the stressors' effects on model parameters means that multi-stressor models can be built from data collected in single stressor experiments.

Crustacean responses to broad scale climate drivers such as hypoxia, ocean acidification (OA) and ocean warming are diverse. While many decapod crustaceans have effective regulatory mechanisms which can compensate for acute (Hagerman and Uglow, 1985) and chronic hypoxia, (McMahon, 2001), and exposure to pCO_2 levels expected by 2100 (at least in the short to medium term) (Whiteley, 2011), the energetic cost of these mechanisms are likely to be high (Spicer et al., 2007), reducing aerobic scope (Pörtner, 2010; Whiteley, 2011). Aerobic scope is likely to decrease further once exposure to hypoxia and/or OA is added to ocean warming, which up-regulates metabolism (Kooijman, 2010) and increases oxygen demand (Manush et al., 2004). Elevated pCO_2 in seawater has been shown to have negative effects on growth rates, moulting frequency, and embryonic development (Whiteley, 2011), while hypoxia has been shown to decrease prey handling efficiency (Brante and Hughes, 2001) and ingestion rates (Shin et al., 2005; Wei et al., 2008). Clearly, any persistent suppression of ingestion will have implications for energy budgets and growth in the long term. These climate-related reductions in growth are of particular concern, as changes could affect species survival, distribution and abundance (Whiteley, 2011).

The work in this chapter demonstrates that a DEB model parameterised using results from three separate single stressor experiments can be used to make predictions about the responses of *L. depurator* to multiple stressor scenarios. In doing so, several important points are addressed: i) Predicted responses are based on the effects of stressors on model parameters, giving us a mechanistic insight into the mode of action of stressors; ii) the results allow us to identify those stressors which are predicted to have the greatest impact, therefore aiding in the development of testable hypotheses and the design of logistically challenging multiple stressor experiments, which in turn allows us to validate model predictions and iii) DEB can provide a modelling environment in which organism responses to more stressors than it is possible to investigate experimentally can be explored, using data generated from single factor experiments.

4.3 Materials and Methods

4.3.1 Single stressor experiments

Three separate experiments were conducted to investigate the responses of *L. depurator* to each individual stressor (temperature, ocean acidification and moderate environmental hypoxia). Animals were collected on 19th January 2017 for the ocean acidification (OA) experiment (N = 48), 27th June 2017 for the temperature experiment (N = 52) and 1st November 2017 for the moderate hypoxia experiment (N = 45). All individuals were collected from the Western Channel Observatory (Smyth et al., 2015) sampling station L4 (50°15.00’N, 4°13.02’W) using a 2m beam trawl towed for 15 mins.

Once removed from the cod end of the trawl, all intact individuals were transferred into buckets of freshly collected seawater (vol = 5L, five individuals per bucket) and transported back to Plymouth Marine Laboratory (PML, Plymouth, UK) within 2hrs of collection. On arrival, animals were transferred to individual plastic mesh-sided containers (245mm x 160mm x 60mm, mesh = 10mm). Each individual plastic container had a layer of aquarium gravel (Dennerle Plantahunter, 8-12mm, J & K Aquatics) for the animal to sit on. In the temperature and OA experiments, these containers were placed in the mesocosm tanks, four large (vol = 600L) tanks of filtered (10µm) seawater. The mesh of the containers allowed free water exchange with the surrounding seawater, and the mesocosm tanks were aerated with air continuously bubbled through aquarium airstones. Once transferred to these containers, individuals in all experiments were left for 48 hours before conditions in the tanks were manipulated.

4.3.1.1 Temperature tolerance experimental design

Nominal temperatures for this experiment were 10°C, 13°C, 16°C and 19°C (Table 4-1). Bottom water temperature at Station L4 was ~13°C at the time of collection, so ambient temperature in the PML mesocosm was maintained at 13°C for the duration of the experiment. The 13°C treatment tank therefore required no further temperature manipulation. Water in the 10°C treatment tank was chilled to the required temperature using a marine aquarium chiller (Boyu L-500). Water in the 16°C and 19°C treatment tanks were warmed using aquarium heaters (Tetratec Heaterstat 300W). Temperatures in the treatment tanks were changed at a rate of 1°C per day until the required temperature was reached.

4.3.1.2 Ocean acidification experimental design

Ambient temperature at Station L4 at the time of animal collection was ~11.5°C, so the water temperature in the mesocosm tanks was kept as close to this as possible for the duration of the experiment (Table 4-1). Mesocosm tanks were assigned to one of two CO_2 levels (400ppm or 1000ppm), and seawater CO_2 concentration was increased to the nominal experimental level (decreasing the pH to 7.8) in the 2 elevated CO_2 treatment tanks over a one week period. CO_2 was mixed into the airlines supplying the 2 treatment tanks following methods described by Findlay et al. (2008) and gas concentrations were logged and recorded continuously using a CO_2 gas analyser (Licor LI-820). All treatment tanks contained submersible pumps to aid water circulation and mixing, and all were tightly covered with 2mm thick clear PVC sheeting to allow the headspace to equilibrate and to reduce gas exchange with the atmosphere (Queirós et al., 2015). Measurements of seawater pH were recorded daily, and alkalinity samples (A_T, 250ml) were taken weekly. These samples were poisoned with 50µl saturated solution of mercuric chloride ($HgCl_2$) and analysed using potentiometric open cell titration (Dickson et al., 2007). The carbonate system variables total Dissolved Inorganic Carbon (DIC) and saturation states of calcite (Ωcal) and aragonite (Ωarag) were calculated from measured pH, CO_2 concentration and A_T data using the "seacarb" package in R (Gattuso et al., 2018), and the solubility constants of Mehrbach et al. (1973) (See Appendix B for carbonate chemistry parameters).

4.3.1.3 Environmental hypoxia experimental design

Ambient temperature at Station L4 at the time of animal collection was ~13.5°C, so the water temperature in the mesocosm tanks was kept as close to this as possible for the duration of the experiment (Table 4-1). Crabs were placed in one of four experimental aquaria (vol = 145L), each one of which was assigned to one of two O_2 levels (normoxia – 8mg O_2 L^{-1} or moderate environmental hypoxia – 4mg O_2 L^{-1}). Hypoxic and normoxic seawater were held in 2 separate header tanks (vol = 450L). To produce hypoxic seawater, dissolved oxygen (DO) levels were manipulated using a computerised control system (Walchem Webmaster Series) which regulated the addition of O_2-free nitrogen gas (Calder-Potts et al., 2015). Seawater DO concentrations in the hypoxic header tank were monitored using a submersible DO sensor (Sensorex DO6441-T) while nitrogen gas was finely bubbled through aquarium airstones. Once DO had fallen to the required level, the supply of nitrogen was stopped with an automated feedback relay system. The addition of fresh seawater caused the DO in the header tank to increase, which triggered the release of nitrogen until the DO sensor detected the pre-set value. In the hypoxic header tank, small plastic spheres floated on top of the water to reduce gas exchange with the atmosphere, while seawater in the normoxic header tank was kept aerated with a continuous air supply bubbled through airstones. Both header tanks contained submersible pumps to aid water circulation and mixing, and both were shielded with a hard top cover. Each header tank was connected to its respective experimental aquaria via a peristaltic pump (Watson Marlow 2058), which supplied a constant flow of seawater (60 ± 0.5 ml min^{-1}). As the volume of water within each header tank decreased, seawater was replenished from a large reservoir (vol = 15000 L). After the initial 48 hour holding period, the water supply feeding 2 of the 4 experimental aquaria was transferred from the normoxic to the hypoxic header tank. It took ~48 hours for the water in these aquaria to reach the desired experimental levels of DO.

Table 4-1: Experimental treatments and treatment conditions for the single stressor experiments

Experiment	**Nominal treatment value**	**Mean temp °C (± SD)**	**Mean pH (± SD)**	**Mean [O_2] mg L^{-1} (± SD)**
Temperature 1	10°C	10.4 (0.5)	7.97 (0.02)	8.19 (0.2)
Temperature 2	13°C	12.7 (0.2)	8.1 (0.03)	8.14 (0.23)
Temperature 3	16°C	16.0 (0.2)	8.09 (0.02)	8.12 (0.18)
Temperature 4	19°C	19.6 (0.3)	7.99 (0.01)	8.1 (0.21)
Normocapnia	400ppm CO_2	12.11 (0.17)	8.1 (0.01)	8.15 (0.39)
Ocean acidification	1000ppm CO_2	12.65 (0.35)	7.77 (0.06)	8.11 (0.37)
Normoxia	8mg O_2 L^{-1}	13.1 (0.3)	8.0 (0.02)	8.00 (0.22)
Moderate hypoxia	4mg O_2 L^{-1}	13.4 (0.2)	8.15 (0.02)	4.43 (0.64)

In the temperature and OA experiments, the mesocosm tanks had weekly 50% water changes, using seawater from 4 header tanks (vol = 450L) maintained at the same conditions as the 4 treatment tanks. In all experiments, the temperature, salinity, pH and DO of all experimental and header tanks were checked and recorded daily (Table 4-1) using a multiprobe (WTW Multi-3420).

4.3.2 Multiple stressor experiments

Individuals were collected from sampling station L4, transported back to the PML mesocosm, and transferred into mesh containers following the methods outlined in section 4.3.1. In the control and temperature + OA experiments, the containers were placed in the mesocosm tanks, six large (vol = 600L) tanks of filtered (10µm) seawater. The mesh of the containers allowed free water exchange with the surrounding seawater, and the mesocosm tanks were aerated with air continuously bubbled through aquarium airstones. Once transferred to these containers, individuals in all experiments (N= 86) were left for 48 hours before conditions in the tanks were manipulated.

4.3.2.1 *Temperature + ocean acidification experimental design*

Mesocosm tanks were assigned to one of two CO_2 (400ppm or 1000ppm) and temperature (10°C or 16°C) levels (two replicate tanks at each temperature for the 1000ppm treatments, a single tank at each temperature for the 400ppm control treatment). Seawater experimental conditions were achieved by manipulating temperature and CO_2 concentration over a one-week period until the desired levels had been reached. CO_2 concentration in each tank was regulated using the method outlined for the single stressor CO_2 experiment in section 4.3.1.2. Water in the 10°C treatment tanks was chilled to the required temperature using a marine aquarium chiller (Boyu L-500). Water in the 16°C treatment tanks was warmed using aquarium heaters (Tetratec Heaterstat 300W). Mesocosm tanks had weekly 50% water changes, using seawater from six header tanks (vol = 450L) maintained at the same conditions as the eight treatment tanks. In all treatments, the temperature, salinity, pH and DO of all experimental and header tanks were checked and recorded daily (Table 4-2) using a multiprobe (WTW Multi-3420). Alkalinity samples (250ml) were taken weekly, and treated and analysed using the method outlined in section 4.3.1.2. The carbonate system variables total DIC, Ωcal and Ωarag were calculated from measured pH, CO_2 concentration and A_T data using the "seacarb" package in R (Gattuso et al., 2018), and the solubility constants of Mehrbach et al. (1973) (See Appendix B for carbonate chemistry parameters).

4.3.2.2 *Temperature + environmental hypoxia experimental design*

Crabs were placed in one of 4 experimental aquaria (vol = 145L), each one of which was assigned to one of two O_2 (normoxia – 8mg O_2 L^{-1} or moderate hypoxia – 3mg O_2 L^{-1}) and temperature (10°C or 16°C) levels. Hypoxic and normoxic seawater were held in 2 separate header tanks (vol = 450L). Hypoxic seawater was produced in the same way as in the single stressor hypoxia experiment (see section 4.3.1.3.). After the initial 48 hour holding period, the water supply feeding 2 of the 4 experimental aquaria was transferred from the normoxic to the hypoxic header tank. It took ~48 hours for the water in these aquaria to reach the desired experimental levels of DO. Water in the 10°C treatment aquaria was chilled to the required temperature using a marine aquarium chiller (Boyu L-500). Water in the 16°C treatment aquaria was warmed using aquarium heaters (Tetratec Heaterstat 300W).

Table 4-2: Nominal and mean (± standard deviation) seawater conditions in the multi-stressor experimental treatments

Treatment	Nominal temperature °C	Mean temperature °C (±SD)	Nominal [O_2] mg L^{-1}	Mean [O_2] mg L^{-1} (±SD)	Nominal pH	Mean pH (±SD)
400ppm CO_2- cool (CC)	10	10.15 (1.17)	8.0	8.15 (0.39)	8.0	8.1 (0.01)
400ppm CO_2– warm (CW)	16	16.64 (0.87)	8.0	7.98 (0.26)	8.0	8.01 (0.01)
Hypoxic-cool (HyC)	10	10.62 (1.02)	3.0	3.47 (0.22)	8.0	8.08 (0.02)
Hypoxic-warm (HyW)	16	15.88 (0.85)	3.0	3.02 (0.61)	8.0	7.96 (0.01)
1000ppm CO_2-cool (OAC)	10	10.06 (0.97)	8.0	8.19 (0.42)	7.8	7.78 (0.04)
1000ppm CO_2-warm (OAW)	16	17.27 (1.05)	8.0	8.11 (0.37)	7.8	7.81 (0.05)

4.3.3 Measurement of wet mass and oxygen consumption

In the first week of the experiments, each individual’s carapace width (CW) was measured with digital Vernier callipers (± 0.05mm) and then weighed on a balance scale (Sartorius R220-D, 0.01mg, European Instruments). These measurements were repeated weekly for the duration of the experiments (7 weeks in all the single stressor experiments, 5 weeks in the multi-stressor experiments. NB – The duration of the multi-stressor experiments was two weeks shorter than the single stressor experiments due to technical difficulties with the experimental set up). *L. depurator* were fed every weekday on raw squid tubes (*Illex argentinus*). Wet weight of squid (typically between 1 - 1.5g) was measured before being presented to the animals, which were then left undisturbed for 6hrs to feed. After the 6hr period, any un-ingested squid was removed and reweighed. Ingestion rates (g squid ingested 6hr^{-1}) were compared between treatments in order to establish whether feeding was affected by changing environmental conditions. Ingestion was scaled to wet mass to account for differences in ingestion between animals of different sizes using the formula:

$$\frac{LN(ingestion)}{LN(wet\ mass^{2/3}\ )}$$

Differences in ingestion rate between treatments were tested for statistical significance using repeated measures ANOVA, which accounts for within group differences due to time in addition to between group differences.

Oxygen consumption data were collected for randomly selected individuals during the last 2 weeks of the experiments. *L. depurator* were removed from their individual containers and placed on a platform in a 920ml static respiration chamber containing seawater of the same conditions as those in the experimental tanks. The chamber was placed on a stirrer plate and a 10mm stir bar mixed the water at 500rpm, separated from the animal by the platform. The chamber was then covered with a black cloth and the crab left to settle for approximately 30mins (the time it took for the animal to stop moving around the chamber or displaying obvious signs of agitation such as climbing the sides). After this initial 30min period, the chamber was sealed, ensuring there were no trapped air bubbles, and an initial measurement of the percentage air saturation in the chamber was taken using an OxyMini-AOT (World Precision Instruments). Further measurements were taken every 15mins for up to 3hrs, with the chamber covered with a black cloth between measurements to ensure the crabs experienced minimal disturbance. Air saturation in the chamber was kept above 70% of the starting value at all times, and percent air saturation was then converted to µmol O_2 L^{-1} (for formula see section 3.3.2). The rate of whole animal O_2 consumption (µmol O_2 consumed min^{-1}) was determined by plotting O_2 consumption over time for each crab, and calculating the slope of the regression line. To allow for a more accurate comparison of O_2 consumption rates between individuals of different sizes, O_2 consumption was then corrected to µmol O_2 consumed g $carbon^{-1}$ min^{-1}, using previously calculated wet mass/carbon mass conversions for *L. depurator* (see section 3.3.3). Differences in oxygen consumption between treatments were tested for statistical significance using one way ANOVA and Tukey's post hoc tests (for treatments groups in the temperature experiment).

4.3.4 DEB model structure

In the standard DEB model, individuals are characterised by three state variables: structure, which determines actual size, feeding rates and maintenance costs; reserve, which serves as intermediate storage between feeding and metabolic mobilisation, and either maturation (in juvenile animals) or reproduction (in sexually mature animals) (Martin et al., 2013). The DEB model used here was the simplified version of the standard DEB model with the crustacean moult extension outlined in Chapter 3. Parameters for the DEB model run in control conditions for both the single and multiple stressor experiments were those previously estimated for *L. depurator* (see Table 3-1). According to DEB theory, all physiological rates are affected by temperature in the same way, which is accounted for in the model *via* the Arrhenius-based temperature correction factor (Schoolfield et al., 1981; Kooijman, 2010), shown below.

$$\left(1 + \exp\left(\frac{T_{AL}}{T} - \frac{T_{AL}}{T_L}\right) + \exp\left(\frac{T_{AH}}{T_H} - \frac{T_{AH}}{T}\right)\right)^{-1}$$

where T_L and T_H are the lower and upper boundaries of the temperature tolerance range, and T_{AL} and T_{AH} are the Arrhenius temperatures for the rate of decrease at both boundaries. This automatically applied temperature correction factor means that changes in temperature do not affect the values of DEB model parameters. As a result, parameters for all temperature treatments are identical to those in the above control treatments. Parameters for animals in the high CO_2 and low O_2 treatments were adjusted by hand for each treatment condition until the minimum deviation between observations and predictions were found, based on the model skill metric mean absolute error (MAE). Statistical comparisons of model estimates or predictions (P_i) with pairwise matched observations (O_i) are among the most basic means of assessing model performance in the climatic and environmental sciences (Willmott and Matsuura, 2005). Individual model prediction errors usually are defined as $e_i = P_i - O_i$. Measures of average error or model performance are then based on statistical summaries of e_i. Calculation of MAE is relatively simple:

$$MAE = n^{-1} \sum_{i=1}^{n} |e_i|$$

Where n is the number of errors and $|e_i|$ is the absolute value of the error. MAE provides an unambiguous and easy to interpret measure of average error magnitude, and as such, it is one of the most commonly used model test statistics (Monaco *et al.*, 2014). Finally, parameter values from the single stressor models were combined in order to make a new multi-stressor DEB model. In order to validate this new model, I used it to describe the growth and oxygen consumption of *L. depurator* in the experimental multiple stressor conditions (temperature + OA and temperature + environmental hypoxia). Once validated, the multi-stressor model was run once more, and used to predict *L. depurator* growth and oxygen consumption under three multiple stressor scenarios, using wet mass and ingestion data from the animals used in the single stressor temperature sensitivity experiment. The model scenarios ran for a simulated period of 98 days (a period chosen because it was double the length of any of the experimental work) and the scenarios explored were: temperature + OA and temperature + moderate environmental hypoxia at 10°C, 13°C, 16°C and 19°C (e.g. two levels more than were used in the experimental multi-stressor treatments), and a "combined stressor" scenario (temperature + OA + hypoxia at the same four temperature levels) which was not tested experimentally.

4.4 Results

4.4.1 *L. depurator* responses to warming, OA and environmental hypoxia

Single stressor experiments showed significant differences in *L. depurator* oxygen consumption with increasing temperature ($F = 12.6_{3, 12}$, $p < 0.001$). Post-hoc tests showed that O_2 consumption at the two lower temperatures (10°C and 13°C) was lower than at the two higher temperatures (16°C and 19°C, Figure 4-1A). Mean oxygen consumption increased from 0.36 µmol $O_2\,gC^{-1}\,min^{-1}$ in normoxic conditions to 0.43 µmol $O_2\,gC^{-1}\,min^{-1}$ in moderate hypoxia (Figure 4-1B), although the difference in the means was not significant. Mean oxygen consumption in the ocean acidification (OA) treatment was significantly higher than in control conditions, increasing from 0.23 µmol $O_2\,gC^{-1}\,min^{-1}$ to 0.34 µmol $O_2\,gC^{-1}\,min^{-1}$ (Figure 4-1C, $F = 11.14_{1, 12}$, $p < 0.01$).

L. depurator mean ingestion was very variable across all treatments, with no significant differences detected between treatments in the temperature (Figure 4-2A) and OA experiments (Figure 4-2C). However, there was a significant decrease in ingestion in the moderate environmental hypoxia treatment (Figure 4-2B) ($F = 7.587_{1, 326}$, $p<0.01$).

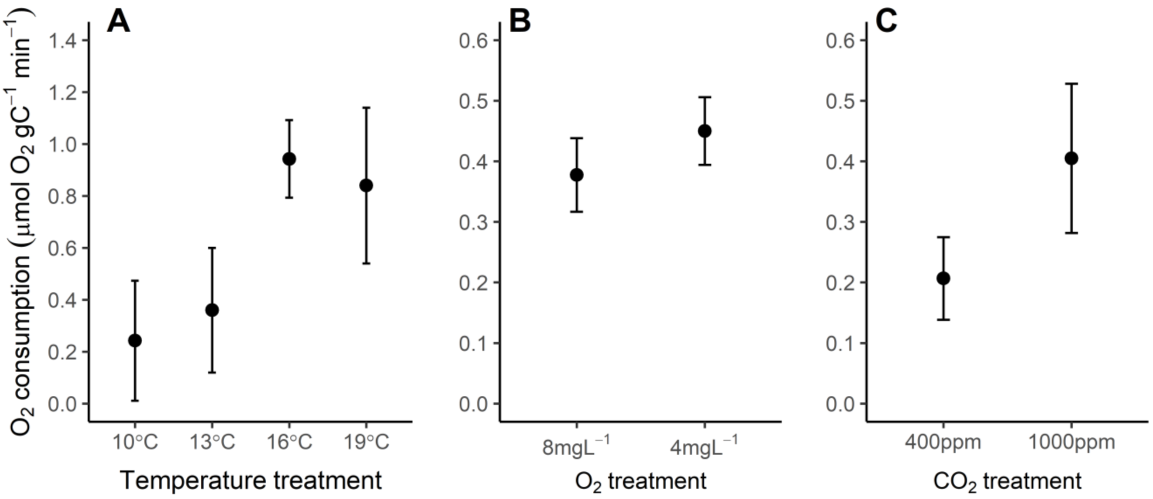

Figure 4-1: *L. depurator* mean oxygen consumption in (A) different temperature treatments; (B) different O_2 concentrations and (C) different CO_2 concentrations. Error bars represent the 95% confidence interval. N per treatment: Temperature = 9; O_2 = 7, OA = 9.

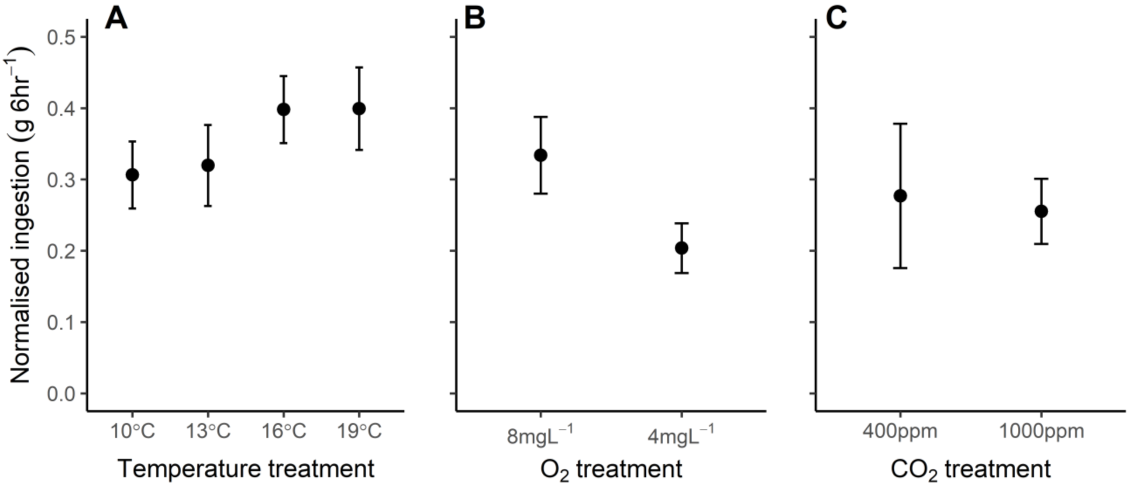

Figure 4-2: *L. depurator* mean ingestion normalised to wet mass in (A) different temperature treatments; (B) different O_2 concentrations and (C) different CO_2 concentrations. Error bars represent the 95% confidence interval. N per treatment: Temperature = 13, O_2 – normoxia = 22, hypoxia = 21, OA = 24.

4.4.2 DEB model skill in single stressor conditions

Figure 4-3 illustrates the skill of the DEB model in predicting *L. depurator* wet mass and oxygen consumption in different temperature, CO_2 and O_2 conditions. Mean average error in all conditions was low, ranging from 0.57 – 0.95g for wet mass data, and from 0.03 – 0.04 μmol O_2 gC^{-1} min^{-1} consumed for the oxygen consumption data. The model predicted wet mass equally well across all treatment conditions (Figure 4-3A). Oxygen consumption in crabs under high CO_2 or low O_2 conditions was higher than those animals in control conditions, and there was evidence of metabolic depression in those animals in the 19°C treatment, which the model captured (Figure 4-3B).

Two model parameters were affected under moderate environmental hypoxia – the scaled maximum ingestion rate $\{j_{XAm}\}$, which decreased to 1.2 $g^{1/3}$ M_W d^{-1} and the somatic maintenance coefficient k_M, which increased to 0.19 d^{-1} (Table 4-3). The maintenance coefficient also increased to 0.19 d^{-1} in the OA treatment, along with reserve mobilisation rate (v) which increased to 0.045 $g^{1/3}$ C d^{-1} (Table 4-3). Ingestion rate was not affected by an increase in CO_2 concentration.

Table 4-3: DEB parameter values for *L. depurator* in control, single stressor and multi-stressor models

Parameter	Symbol	Unit	Control/ Temperature	High CO_2	Low O_2	Multi-stressor
Maximum ingestion rate scaled to wet mass$^{2/3}$	$\{j_{XAm}\}$	$g^{1/3}$ M_W d^{-1}	1.41	1.41	1.2	1.2
Assimilation efficiency	y_{EX}	-	0.87	0.87	0.87	0.87
Reserve mobilisation rate	v	$g^{1/3}$ C d^{-1}	0.025	0.045	0.025	0.045
Fraction of energy allocated to somatic maintenance and growth	κ	-	0.85	0.85	0.85	0.85
Somatic maintenance coefficient	k_M	d^{-1}	0.17	0.19	0.19	0.19
Maturity maintenance rate	k_J	gCM_E^{-1} gC maturity^{-1} d^{-1}	0.01	0.01	0.01	0.01
Growth efficiency	y_{VE}	-	0.5	0.5	0.5	0.5

4.4.3 Experimental validation of multi-stressor DEB model

Figure 4-4 illustrates the skill of the multi-stressor DEB model (parameterised using data from the single factor experiments) in predicting *L. depurator* wet mass and oxygen consumption in different temperature + OA and temperature + moderate hypoxia conditions. Mean average error in all conditions was low, 0.5g for wet mass data and 0.03 µmol O_2 gC^{-1} min^{-1} consumed for the oxygen consumption data. The model predicted wet mass equally well across all treatment conditions and was able to capture the timing of moults and the increase in wet mass post moult with a fair degree of accuracy (Figure 4-4A). Oxygen consumption in crabs at 10°C under high CO_2 (OAC) or low O_2 (HyC) conditions was higher than those animals in cool control (CC) conditions. At 16°C, oxygen consumption rates in all treatments were virtually identical (Figure 4-4B).

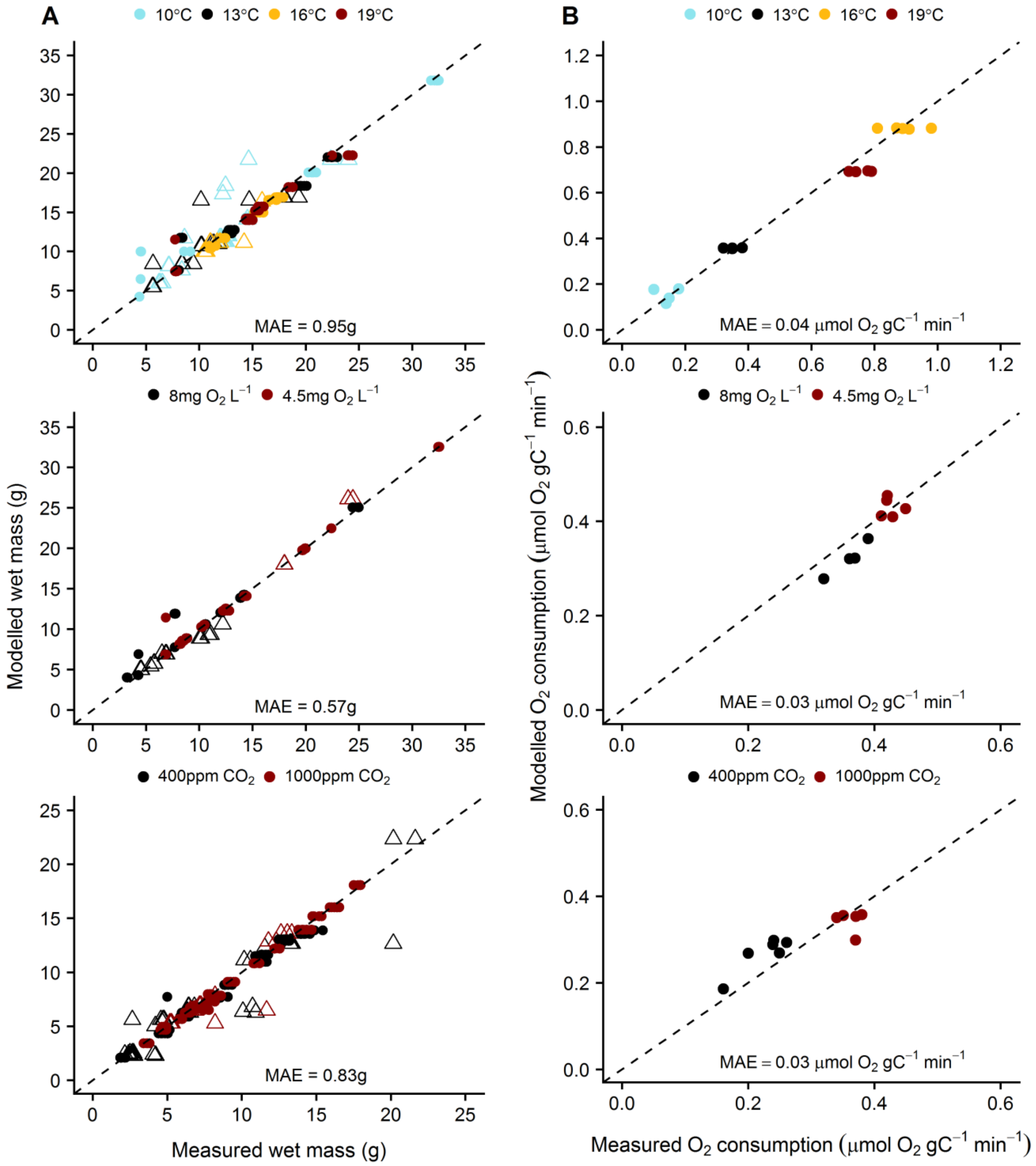

Figure 4-3: Measured vs. modelled wet mass and oxygen consumption in each of the experimental conditions. Unfilled triangles in panel (A) represent animals which moulted over the course of the experiment. Filled circles are those animals which did not moult. Triangle outline colour denotes treatment condition.

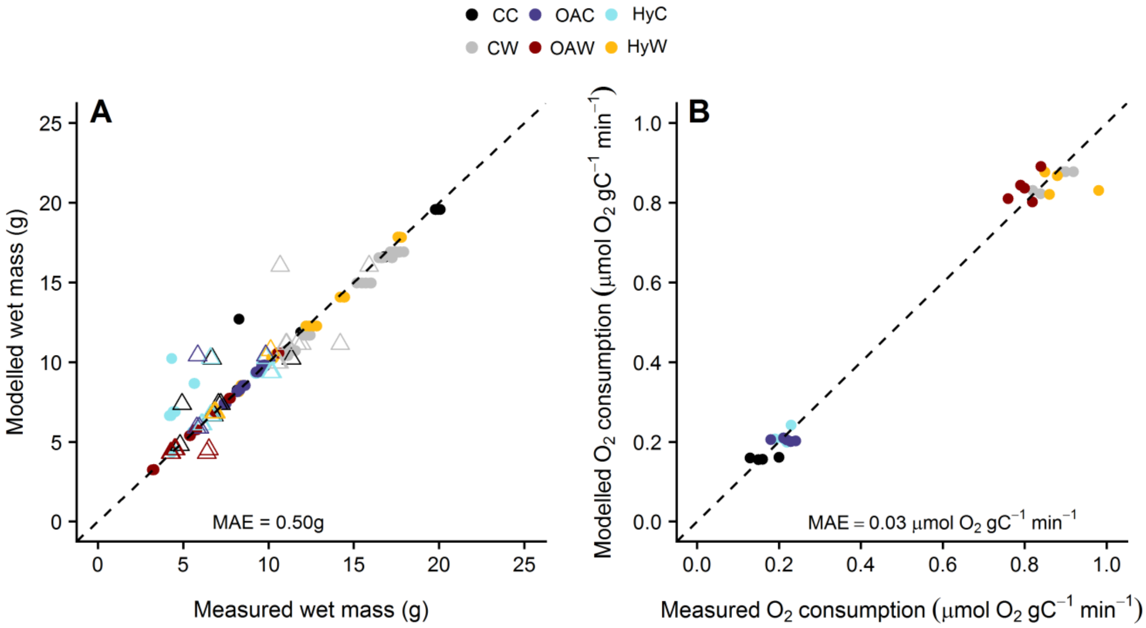

Figure 4-4: DEB model skill in predicting wet mass (A) and O_2 consumption (B) under multi-stressor conditions. CC – cool control (water at 10°C, no further manipulation); OAC – ocean acidification, 10°C; HyC – moderate hypoxia, 10°C; CW – warm control (water at 16°C, no further manipulation); OAW – ocean acidification , 16°C; HyW – moderate hypoxia, 16°C. Unfilled triangles in (A) represent those animals that moulted over the course of the experiment. Triangle outline colour denotes treatment. Dashed line is a 1:1 line, MAE is mean average error.

4.4.4 Predictions for *L. depurator* responses under multiple stressor conditions

Figure 4-5 shows wet mass predictions for a randomly selected individual, a small animal with a starting wet mass of 5.96g. At 10°C the predicted effects of increased CO_2 on growth were almost identical to the effects of temperature alone up to the first moult (Figure 4-5). Moderate environmental hypoxia and the three combined stressors increased the intermoult period (IP) by approximately 7 days. After this, all stressors (both individually and combined) increased the IP, with increased CO_2 and the combined stressors exhibiting the greatest impact. In all cases, the predicted wet mass at the end of the 98 day period was ~21g. At 13°C, the IP was increased by all stressors. A second moult was predicted under moderate hypoxia, but not under increased CO_2 concentrations or in the multiple stressor scenario (Figure 4-5). At 16°C, the effects on growth of lower O_2 concentrations were identical to the effects of temperature alone (Figure 4-5), but higher CO_2 and the three combined stressors increased the IP. At 19°C, the IP increased from that of temperature alone under all stressor scenarios (Figure 4-5), but a moult was only predicted under conditions of moderate hypoxia.

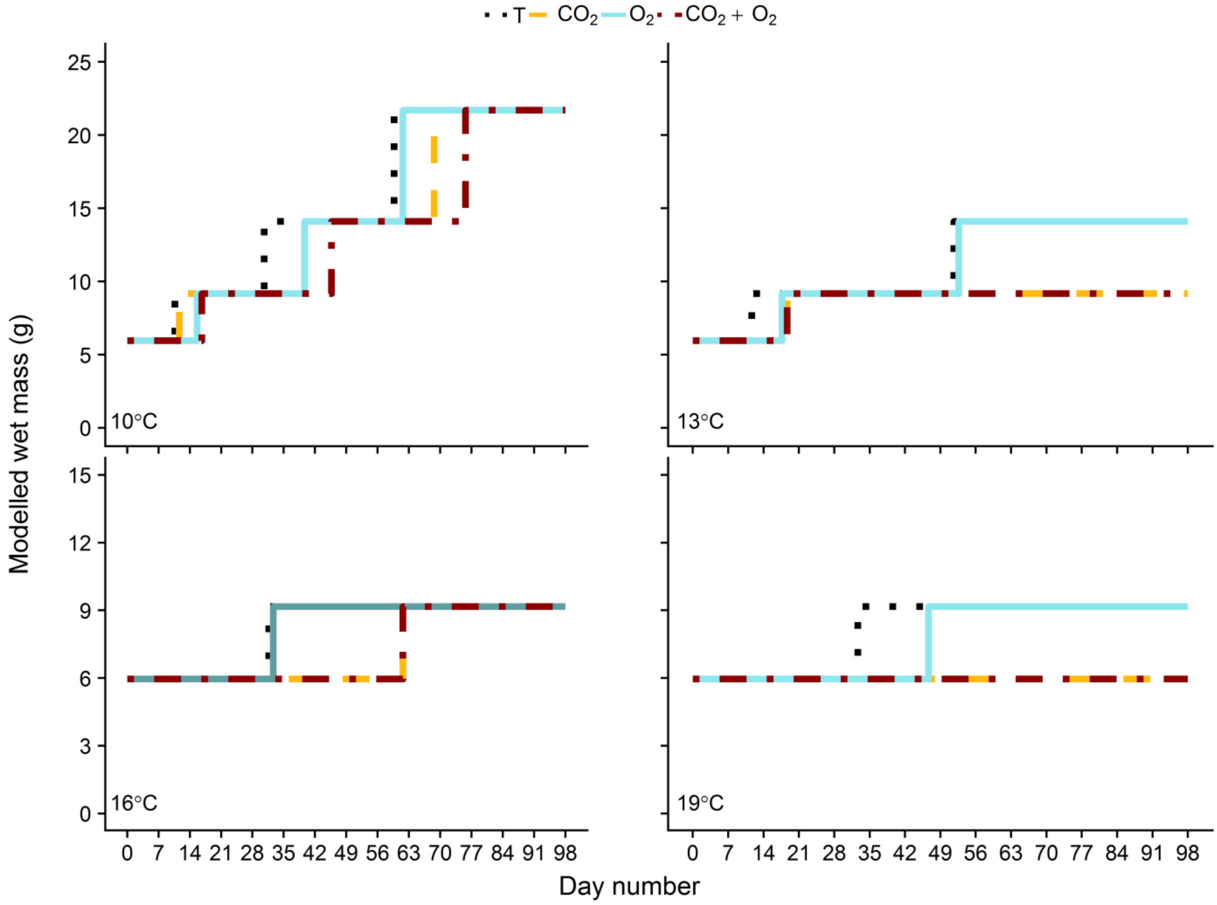

Figure 4-5: Predicted wet mass in a randomly selected individual *L. depurator* over a 98 day simulation period under multiple stressor scenarios. The temperature of each experimental treatment is given in the bottom left of each panel. “T” is the predicted effect on growth of that experimental temperature alone, “CO_2” is the predicted effect of elevated pCO_2 at that temperature, “O_2” is the predicted effect of environmental hypoxia at that temperature, and “$CO_2 + O_2$” is the predicted effect of elevated pCO_2 and environmental hypoxia at that temperature. The crab had a starting wet mass of 5.96g;

Figure 4-6 shows predictions for the combined state variables structure and reserve for the same animal, providing an insight into the changes in carbon mass (M_C) between moults. At 10°C the predicted effects on M_C of all stressor combinations are very similar until approximately day 60 of the model scenario (Figure 4-6). After this, the more severe impact of CO_2 and the three combined stressors become apparent as the growth of M_C slows. In contrast to the predictions for wet mass, there is a difference of ~1gC between the temperature alone/temperature + hypoxia treatments and the temperature + OA/three combined stressor treatments by the end of the 98 day simulation period. This decrease in the growth rate of structural mass under the temperature + OA and combined stressor treatments is the reason for the predicted increase in IP (Figure 4-5), as moult in the model is triggered by the ratio of carbon mass: wet mass (α) reaching a given threshold (See Chapter 3, section 3.3.4). Environmental hypoxia appears to affect the growth of structure, as it affected predictions of wet mass, and as with wet mass, this effect is less apparent at higher temperatures. A similar pattern is seen at 13°C, 16°C and 19°C, with a clear difference in severity of effect observable between the temperature alone/temperature + hypoxia treatments, and the temperature + OA/ three combined stressors. In the latter two treatments, carbon mass is lower at the end of the simulated period than in the first two treatments. At 16°C and 19°C, all modelled scenarios result in a reduction in structural mass at day 84 which continues until day 97, where it begins to recover (Figure 4-6).

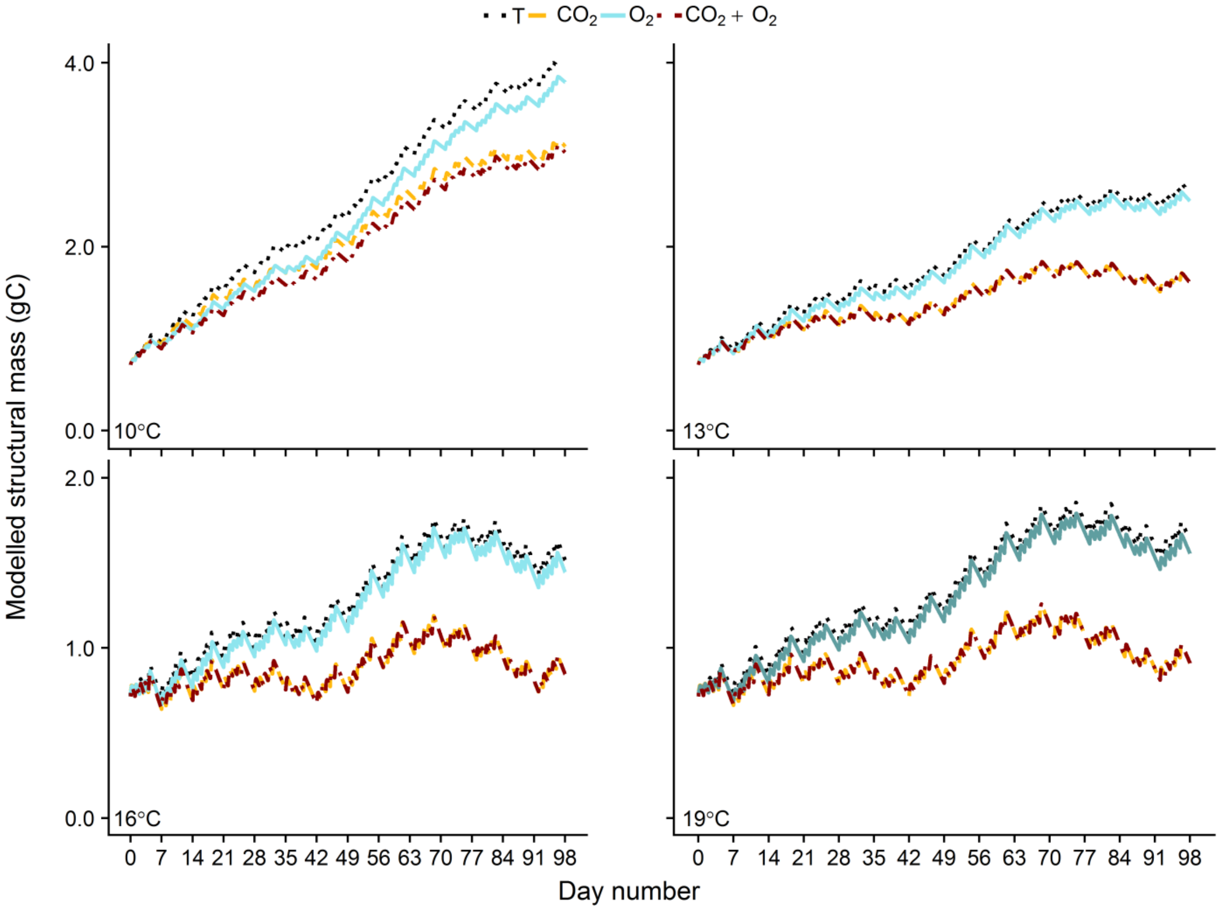

Figure 4-6: Predicted carbon mass (g) in a randomly selected individual *L. depurator* over a 98 day simulation period under multiple stressor scenarios. The temperature of each experimental treatment is given in the bottom left of each panel. "T" is the predicted effect on growth of that experimental temperature alone, "CO_2" is the predicted effect of elevated pCO_2 at that temperature, "O_2" is the predicted effect of environmental hypoxia at that temperature, and "$CO_2 + O_2$" is the predicted effect of elevated pCO_2 and environmental hypoxia at that temperature. The crab had a starting wet mass of 5.96g.

Modelled oxygen consumption rates in low O_2 conditions are very similar to those under control conditions at all temperatures. In all cases the addition of increased CO_2 or the combination of all stressors resulted in an increase in O_2 consumption (Figure 4-7). There was little difference in rates between the single stressor OA scenario and the multiple stressor scenario at any temperature.

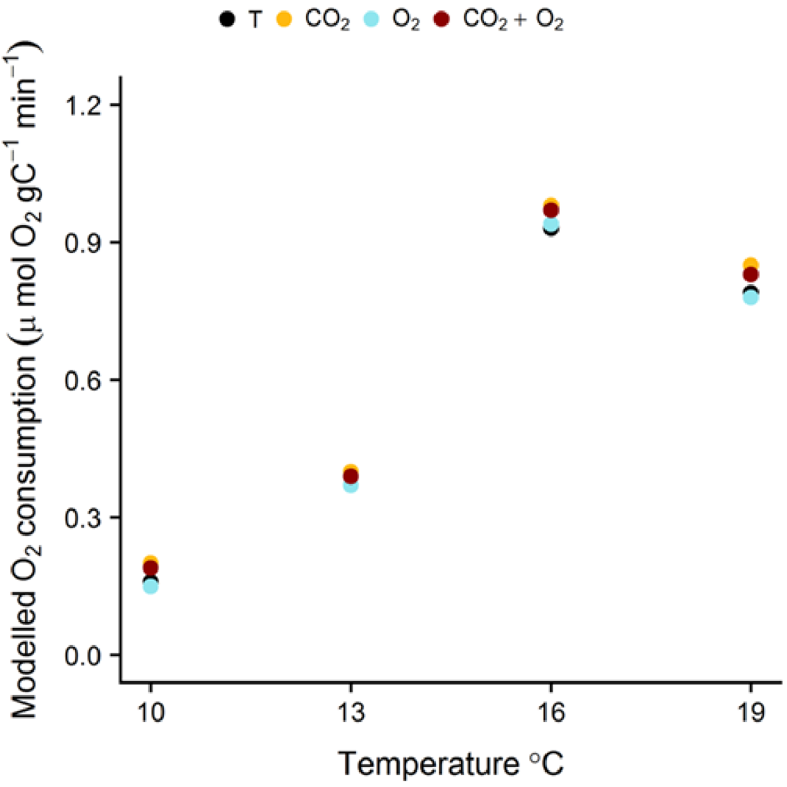

Figure 4-7: Predicted oxygen consumption in a randomly selected *L. depurator* under multiple stressor scenarios. Predicted rates were virtually identical for all animals, so only one is shown here.

4.5 Discussion

Three individual DEB models were parameterised using data collected from three separate single stressor experiments. These parameter sets were then combined to produce a new multi-stressor model, which was used to make predictions concerning the growth and oxygen consumption of *L. depurator* under more complex and realistic multi-stressor scenarios. The parameters and predictions made by this multi-stressor model were validated using data collected in multiple factor experiments. The single stressor experiments showed that *L. depurator* oxygen consumption increased in both the hypoxic and ocean acidification (OA) treatments, while ingestion decreased in the hypoxic treatment. An independent test of model skill showed that the multi-stressor model was able to accurately describe *L. depurator* responses to multiple-factor (temperature + OA and temperature + environmental hypoxia) experimental conditions. The multi-stressor model predicted an increase in the intermoult period at 10°C in hypoxic conditions. This effect was less pronounced at 13°C and 16°C, suggesting that effects of hypoxia on growth can be mitigated by higher temperatures. At all temperatures OA alone and OA + hypoxia increased the intermoult period.

4.5.1 Single stressor experiments and model predictions

The results of the single stressor experiments are in keeping with other published examples of decapod responses to climate drivers. As expected, oxygen consumption increases with increasing temperature up to 16°C, then decreases with further temperature increase, indicating metabolic depression. Although ingestion was very variable at all temperatures, it was noticeably higher at 16°C and 19°C than at 10°C and 13°C. The temperature dependence of physiological rates in poikilotherms is well documented (Huntley and Lopez, 1992; van der Have and de Jong, 1996; Dell et al., 2011) as is the reduction of rates at high and low temperatures outside the temperature tolerance range (Pörtner and Knust, 2007). This is accounted for in the DEB model by the Arrhenius temperature correction factor, which ensures that any temperature driven change in metabolic activity is reflected in concurrent changes in all modelled rates (e.g. ingestion, maintenance and reserve mobilisation rates).

The experimental work showed that moderate environmental hypoxia slightly increased oxygen consumption rate in *L. depurator*. This increase in oxygen consumption was reflected in the increase in the model parameter k_M (somatic maintenance coefficient). While several other model processes contribute to oxygen consumption, it was only necessary in this case to increase k_M to ensure the model reproduced the observed increase in O_2 consumption. In physiological terms, this increase in k_M (and so O_2 consumption rate) is related to any compensatory mechanisms that maintain respiration and sustain the standard metabolic rate in spite of the environmental O_2 reduction, such as increased ventilation and/or heart rate (Thomas et al., 2019). There is good evidence that crustaceans possess such compensatory mechanisms. Many decapod crustaceans are oxy-regulators (Leiva et al., 2018). They can compensate for both acute (Hagerman and Uglow, 1985) and chronic hypoxia (McMahon, 2001), either with increased ventilation and subsequent increase in haemocyanin O_2 affinity due to respiratory alkalosis (McMahon and Burnett, 1990), the increase of haemocyanin concentration in the haemolymph (Baden et al., 2003) or *via* the build-up of metabolites such as lactate and urate, which also increases haemocyanin O_2 binding affinity and maintains effective uptake of O_2 across the gills (McMahon, 2001). In addition to the increased O_2 consumption rate, ingestion rate decreased in hypoxic conditions, reflected in the lower value of the scaled maximum ingestion rate $\{j_{XAm}\}$ in the model. The negative effects of hypoxia on ingestion recorded here have been documented in numerous marine organisms (Siikavuopio et al., 2007; Brandt et al., 2009; Aguirre-Velarde et al., 2018), including crustaceans (Desai and Prakash, 2009). For example, prey handling efficiency, specifically the time taken to consume a fixed-sized item of food, was negatively affected by hypoxia in the shore crab *Carcinus maenas* (Linnaeus, 1758), and the study's authors concluded that hypoxia would likely decrease the feeding rate due to increased prey handling time (Brante and Hughes, 2001). The ingestion rates of the swimming crab *Thalamita danae* (Stimpson, 1858) (Shin et al., 2005) and the shrimp *Fenneropenaeus chinensis* (Osbeck, 1765) (Wei et al., 2008) were also shown to decrease in low oxygen environments. These decreases in feeding rate are an oxygen saving strategy. The reduction in energetically costly processes such as ingestion, digestion and absorption of food (i.e. specific dynamic action, SDA) reduces the energy demand, and thereby the O_2 requirements of the organism (Thomas et al., 2019). DEB models applied to animals in hypoxic conditions have reflected this effect on feeding by reducing the parameter $\{j_{XAm}\}$, as is reported in this chapter (Thomas et al., 2019). In contrast to the model presented here however, some of these DEB models also assumed an effect on reserve dynamics caused by this decrease in ingestion. For example, in models published for both bivalves (Aguirre-Velarde et al., 2019) and fish (Thomas et al., 2019), the authors argue that a negative effect of hypoxia on ingestion results in a decrease in energy available for assimilation. Consequently, the parameter y_{EX} (assimilation efficiency) was modified in these models. Similarly, reserve (M_E) mobilisation was also affected. Under hypoxic conditions, ATP production through aerobic pathways is impaired, and less efficient anaerobic pathways are activated (da Silva-Castiglioni et al., 2010; Martinez-Cruz et al., 2012). In DEB terms, this may result in organisms which are limited in their ability to mobilise M_E, which is reflected in a decrease in the model parameter v (reserve mobilisation rate). Taken together, the reductions in y_{EX} and v restrict both reserve entry and output (Aguirre-Velarde et al., 2019; Thomas et al., 2019). In the present work, modifications of assimilation efficiency and reserve mobilisation rate were unnecessary, as fine-tuning of the model parameters showed that any decrease in y_{EX} or v actually made the model fit worse. It is likely that the reason these parameters were not affected is because the level of hypoxia that experimental animals were exposed to did not cross a critical threshold where oxy-regulatory capacity was impaired and anaerobic ATP production was necessary. This notion is supported by the fact that there was no decrease in oxygen consumption exhibited by any of the individuals in the study, and the maintenance coefficient k_M actually increased, suggesting that *L. depurator* can maintain effective compensatory mechanisms at the levels of dissolved O_2 concentration tested here.

L. depurator oxygen consumption increased in the ocean acidification (OA) treatment, indicating an increase in metabolic rate. This is reflected in the increase in the values of two model parameters, the somatic maintenance coefficient k_M and reserve mobilisation rate v. As in the hypoxia treatment discussed above, the increase in k_M recorded here is reflective of the energetic cost of maintaining compensatory mechanisms. This increase in k_M as a response to reduced pH has been noted in previously published DEB models applied to organisms in OA scenarios (Klok et al., 2014b; Jager et al., 2016), along with a possible negative effect on assimilation efficiency y_{EX} (Klok et al., 2014b). While there was no effect of OA on y_{EX} found in this study, it was necessary to increase the reserve mobilisation rate (v) in order to ensure the model captured the observed patterns in *L. depurator* oxygen consumption and growth. The reserve mobilisation rate represents the amount of carbon mobilised from the reserve and used in all modelled processes (e.g. somatic maintenance, growth, maturity maintenance, reproduction). Increasing k_M increases modelled oxygen consumption and decreases growth, and any increase in this parameter beyond the value of 0.19 d^{-1} results in the modelled growth of *L. depurator* being slower than measured growth. Increasing v also increases modelled oxygen consumption (though to a lesser degree than increasing k_M), but without the negative effect on growth, as the increase in reserve mobilisation rate means that somatic maintenance costs can be met with enough energy still available for growth. Taken together, the increases in both of these parameters are indicative of the increased energetic costs incurred by *L. depurator* under OA scenarios due to maintenance of effective compensatory mechanisms. It has been demonstrated that many crustaceans are efficient acid-base regulators (Melzner et al., 2009; Dissanayake et al., 2010; Paganini et al., 2014; Knapp et al., 2015), and are able to compensate for the increase in CO_2 in the haemolymph caused by the changes in seawater carbonate chemistry associated with OA (Whiteley, 2011; Whiteley et al., 2018). However, the energetic costs of this are likely to be significant, particularly in the medium to long term (Spicer et al., 2007; Whiteley, 2011).

The skill of each single stressor model in predicting wet mass and oxygen consumption in *L. depurator* is good, with acceptably low deviations between measured and modelled values under all experimental conditions apparent. The skill of this adapted DEB model in predicting changes in crustacean wet mass and oxygen consumption under ambient conditions was demonstrated in Chapter 3, and DEB models have been used to successfully describe responses to hypoxia (Aguirre-Velarde et al., 2019; Lavaud et al., 2019), OA (Klok et al., 2014b; Jager et al., 2016) and toxicants (Jager and Zimmer, 2012) in several species, suggesting that in general, DEB theory is well suited to exploring the effects of stressors on the physiological responses of a range of marine organisms. The parameters estimated for the single stressor models were combined to create a new multi-stressor DEB model. This new model was successfully validated when it accurately captured the growth and oxygen consumption of *L. depurator* under experimental multi-stressor conditions. I would therefore argue that any predictions made by this multi-stressor DEB model are likely to be robust.

4.5.2 Predictions under multi-stressor conditions

The new multi-stressor model predicts that the effects of moderate environmental hypoxia on mass-specific oxygen consumption in *L. depurator* are minimal at all temperatures. As discussed in detail in section 4.5.1., this is due to the fact that crustaceans are efficient oxy-regulators, and the predictions are in keeping with the effects of lower O_2 concentrations recorded in the published literature. The effects on growth (in terms of both wet mass and carbon mass M_C) are predominantly seen at 10°C, when the intermoult period (IP) increases under moderate hypoxia, and there is a small, but noticeable difference in the growth rate of structure. This reduction in growth rate is very likely due to the decrease in ingestion recorded in the hypoxic treatments. This reduction in feeding is a commonly observed response to low dissolved oxygen concentrations, and a subsequent negative effect on growth has been recorded in some species (Llobrera and Neill, 1987; Chabot and Dutil, 1999; Cheung et al., 2008). Indeed, the decrease in feeding related to low dissolved oxygen appears to be one of the most sensitive processes determining growth. For example, Chabot and Dutil (1999) showed that 97% of the reduction in growth of Atlantic cod *Gadus morhua* (Linnaeus, 1758) in hypoxic conditions could be explained by the reduction in ingestion rate. A similar observation was made for the Pacific oyster (*Crassostrea gigas*, Thunberg, 1793) (Le

Moullac et al., 2007). Interestingly, this effect is less pronounced at 13°C and 16°C, suggesting that temperature can mediate the negative effects of hypoxia on growth. While I am aware of no published evidence for this in crustaceans, a model of Atlantic cod suggested that growth rate of animals is better at 50% O_2 saturation and 6°C than 100% O_2 saturation and 2°C (Claireaux et al., 2000).

Generally, the predicted effects on growth of increased CO_2 alone and the three combined stressors are identical, with the addition of moderate hypoxia having no further effect beyond that of OA in isolation. The only exception is at 10°C, in which the three combined stressors increase the IP beyond that of OA alone, and M_C is slightly lower throughout the 98 day period in the three stressor scenario. This is perhaps due to the negative effect of moderate hypoxia on growth, likely caused by the decrease in ingestion, as discussed above. At all other temperatures, IP increases in the same way under OA and three stressor scenarios, with animals predicted to attain smaller ultimate wet masses and structural masses at 13°C, 16°C and 19°C (compared to 10°C) by the end of the 98 day simulation. The fact that the addition of moderate hypoxia is predicted to have no additional impact beyond that of OA alone at higher temperatures may be due to the possible temperature mediation of any adverse effects on growth of hypoxia (Claireaux et al., 2000). It is also possible that the increase in CO_2 concentration could itself have mediated any effect of hypoxia. Molecular CO_2 has been shown to improve O_2 saturation at the gills in some crustaceans, as it improves haemocyanin O_2 affinity independently of, and in opposition to, the CO_2 driven effects of respiratory acidosis (Weber and Hagerman, 1981; Mangum and Burnett, 1986; Lehtonen and Burnett, 2016).

The DEB models presented here predict that *L. depurator* is broadly tolerant of the climate drivers tested, both in isolation and combined, in the short term. In the medium to long term however, it suggests that OA and the combined stressors may have an adverse effect on growth. It is worth noting that these effects are apparent under the assumption that *L. depurator* can maintain its regulatory capacity for the whole 98 day simulation period, which may not be the case (Whiteley et al., 2018). The model simulation therefore supports further investigation of *L. depurator* responses to OA and OA + moderate hypoxia at varying temperatures over longer time frames to see if the predicted effects on growth are observed, and if compensatory mechanisms can be maintained. Model simulations also raised an interesting question regarding the temperature dependent effects of hypoxia on growth – does the negative effect disappear at higher temperatures because the temperature driven increase in ingestion outweighs the suppression of ingestion caused by hypoxia? Evidently, more experimental work is required in order to explore this further.

4.5.3 Benefits of using DEB modelling approaches

Until relatively recently, single stressor experimental design was the most prevalent method to investigate the effects of climate change on marine life, primarily because the logistics required in tackling a range of experiments across a broad representation of species or groups are relatively simple. These single stressor experiments also provide a straightforward conceptual platform to launch more logistically challenging multiple stressor designs (Boyd et al., 2018). While the research community is now focussed on multi-stressor experimental work, the huge number of stressors acting on the marine environment means that measuring all potential interactions between every combination of stressors is impossible (Boyd and Ellwood, 2010). For example, Côté et al. (2016) estimate that many of the world’s oceans have upwards of 10 two-way interactions. The number of experimental treatments required to quantify these interactions is impractical, even when implementing specifically designed statistical methods, e.g. collapsed factorial designs (Boyd et al., 2016), and this is before we even consider higher order interactions. In this context, modelling approaches are essential, as the kind of complex synthesis required is only truly practicable in models.

The DEB model presented here can provide a mechanistic underpinning of observed responses, an understanding that is essential if we are to be able to predict the impacts of multiple stressors under novel or untested conditions (Griffen et al., 2016). In this approach, predicted responses are a function of the stressors’ effects on model parameters, and as a consequence, multi-stressor models can be built from data collected in single stressor experiments. Indeed, single factor experimental work has already generated a wealth of data that could be used to parameterise single stressor DEB models, and those parameters combined to create multi-stressor models, as demonstrated here. The model may also be a useful tool in helping to elucidate the general type of interactions that can be expected between multiple stressors. For example, if two stressors act on the same physiological process (e.g. model parameter), then co-tolerance could be expected (tolerance to one stressor confers tolerance to another) when those stressors act in concert. Conversely, when different stressors act on different model parameters, species may be equipped to resist a small number, but not all stressors, which may result in additive cumulative effects (Côté et al., 2016).

4.5.4 Future work

The single stressor DEB models described *L. depurator* responses to stressors with some skill, and the predictions made by the multi-stressor DEB model which combined those parameters, and was validated by experimental work, are broadly supported by the published literature on crustacean responses to multiple climate drivers. While there is undoubtedly a need for further, robust experimental research on the combined impacts of multiple stressors, I contend that the modelling approach presented here can not only be a useful tool in helping to prioritise the most relevant stressors to carry forward into that experimental work, but a way of synthesising single stressor data into a mechanistic modelling environment that can simulate more complex, ecologically relevant conditions. In this way, research can be focussed on achieving the ultimate goal of improving our ability to predict organism responses to rapidly changing conditions.

The work in this chapter demonstrates that the DEB model is undoubtedly a useful tool in the development of experimental climate change work at the individual level. It is also necessary however, to put that experimental work into a broader environmental and ecological context. Given that patterns of physiological variability at the individual level can be reflected in patterns at higher organisational levels, the DEB model has potential as a means to scale up from the individual and explore the energetic basis for population dynamics.

Chapter 5 Using physiological processes to improve predictions of large scale responses to climate change

5.1 Abstract

A significant challenge in global ocean change research is in predicting organism responses to anthropogenic change. In order to tackle this, a mechanistic understanding of climate impacts on the focal organism is necessary, to provide sufficient knowledge of cause and effect at the individual level to increase predictive power. NEMO-ERSEM projections for environmental conditions in two time periods (2006-2016, 2038-2048) across the north-west European shelf were used to force a mechanistic Dynamic Energy Budget (DEB) model parameterised for the common swimming crab *Liocarcinus depurator* (Linnaeus, 1758) after previous experimental work investigating growth, ingestion and oxygen consumption under multiple stressor (temperature + ocean acidification, temperature + moderate environmental hypoxia) conditions. This DEB model made predictions on any changes in ultimate carbon mass, age-at-maturity and cumulative allocation to reproduction. These physiological endpoints were used to infer the non-lethal consequences of climate change, such as the optimum settlement window for juvenile animals, species distribution, and potential population viability. The optimum settlement time was predicted to shift forward across the whole of the north-west European shelf. Cumulative allocation to reproduction showed only minimal increases – it is possible that the temperature driven increase in allocation driven by higher metabolic rates is offset by a corresponding increase in mortality. Estimates of population viability and species distribution suggest that *L. depurator* may be able to expand its range further into the northern North Sea in the future. It can be argued that the DEB model presented here represents a step forward in the methodology of species distribution modelling, as it uses mechanistic physiological understanding, rather than statistical dependence between environmental and distributional data, to predict organism responses to changing environmental conditions. Furthermore, the mechanistic nature of the model negates the risk of erroneous extrapolation when transferring into novel conditions, which is a key issue for some correlative species distribution models.

5.2 Introduction

Marine organisms are increasingly faced with multiple, interacting ecosystem-level stressors associated with global environmental change (Boyd et al., 2014; Boyd et al., 2018). The Intergovernmental Panel on Climate Change (IPCC) has identified temperature, pH, oxygen concentration and food availability as the principal climate drivers affecting marine ecosystem structure, functioning and adaptive capacity (IPCC, 2014). The effects on marine organisms of changes in some of these properties have already been recorded. For example, shifts in species distributions in response to changing ocean temperatures have been observed (Wiltshire et al., 2009) and phenological processes may be influenced *via* changes in reproduction, the onset of spawning, and embryonic and gonad development (Birchenough et al., 2015). Hypoxic events, the extension, duration and severity of which are on the increase (Breitburg et al., 2018) have been shown to trigger mass mortalities (Diaz and Rosenberg, 2008; Altieri et al., 2017). Surviving organisms are also affected through sub-lethal stresses such as reduced growth (Hrycik et al., 2017; Jeppesen et al., 2018) effects on reproduction and recruitment (Breitburg, 1992; Miller et al., 2002) and increased vulnerability to predators (Decker et al., 2004; Riedel et al., 2008). The effects of ocean acidification vary between and among taxa (Kroeker et al., 2013), but experimental studies have demonstrated that survival (Talmage and Gobler, 2010), calcification (Zhao et al., 2017), and growth and development (Dupont et al., 2008) can all be negatively affected by decreased seawater pH.

A significant challenge in global ocean change research is in predicting organism responses to anthropogenic change. Species distribution models (SDMs, also known as ecological niche models or bioclimatic envelope models) are a commonly used method to link organism distribution to environmental variables. Many of these models are phenomenological, relying on statistical dependence between environmental and distributional data to estimate a species' realised niche (Robinson et al., 2017).Variables thought to constrain a species' distribution are selected for use in the model, but the processes by which the variables limit species' distributions remain implicit (Mathewson et al., 2017). Consequently, extrapolation to future distribution patterns resulting from changing environmental conditions confronts the statistical and ecological assumptions of these models (Elith and Leathwick, 2009; Melle et al., 2014). Some models, such as dynamic bioclimatic envelope models (DBEMs) (Cheung et al., 2011) go one step further, by accounting for the role organism physiology plays in constraining species distributions. DBEMs calculate changes in growth and other life history traits in response to changes in environmental conditions based on algorithms derived from empirical growth and metabolic functions (Fernandes et al., 2013). It can be argued that the predictions made by these DBEMs are likely to be more robust than those made by other SDMs due to the fact that projected species' distributions are limited by more than just the distribution of suitable habitat (Queirós et al., 2015). However, they are still limited by the fact that they do not incorporate a fully mechanistic physiological understanding of species' responses to changing conditions.

In order to provide sufficient knowledge of cause and effect at the individual level to increase predictive power, a mechanistic understanding of environmental impacts on the focal organism is necessary (Helmuth et al., 2005; Kearney and Porter, 2009; Griffen et al., 2016). Mechanistic approaches offer the ability to extend experimental results beyond the specific study conditions to different species or environmental conditions (Griffen et al., 2016), and should result in more robust predictions of range shifts in in ecosystems where anthropogenic environmental change has already altered a specie's observed range, or where distribution data is not fully representative of important environmental gradients due to historical effects (e.g. through localised species depletion due to fishing pressure) (Fordham et al., 2013). These mechanistic models do not rely on known species distributions; instead, predicted distributions are an emergent property of the process being modelled (Fordham et al., 2013; Mathewson et al., 2017). Models which focus on the energetics of organisms may be useful as a means to integrate organismal responses to a wide range of environmental drivers (Boyd et al., 2018). Dynamic Energy Budget (DEB) models are mechanistic models which offer a whole organism approach to explaining how factors in the physical environment translate into biologically and ecologically relevant responses (van der Meer, 2006a). The published literature, along with the work presented in Chapter 4, has demonstrated that DEB models can be used to successfully model organism responses to stressors based on the assumption that stressors influence the acquisition and/or use of energy, which in turn affects measurable endpoints such as growth and reproduction (Jager and Zimmer, 2012; Lavaud et al., 2019).

To use physiological models in a realistic setting, they need to be provided with a complete description of the local environment as experienced by the target organism. This includes local abiotic conditions and ecosystem properties such as food availability. To relate environmental conditions experienced by marine biota to large-scale climatic drivers, results from a coupled hydrodynamic-biogeochemical model, NEMO-ERSEM were used. This model describes physical and biological properties of the marine ecosystem over the north-west European Shelf at 7 km horizontal resolution with 50 vertical layers (Skákala et al., 2018). By describing water transports and mixing as well ecosystem processes, it captures essential rates and flows of matter and energy in space and time and links them to the environment and biota. This allows it to project the bulk properties of ecosystems into the future and the past (Allen et al., 2010; Queirós et al., 2015). The large-scale environmental patterns projected by NEMO-ERSEM can be used to force a DEB model, which consequently makes predictions for ecologically relevant endpoints e.g. growth, age-at-maturity, energy allocated to reproduction etc., for any species of interest.

The DEB model parameterised from the single stressor experiments and validated in the multi-stressor experiments in Chapter 4 was forced with NEMO-ERSEM projections of environmental conditions over the north-west European shelf (Kröger et al., 2018) at a spatial resolution of 28 km over two time periods, (2006-2016 and 2038-2048), in order to explore any predicted changes in *L. depurator* responses. Forecasts for future conditions were made using the RCP 8.5 (business-as-usual emissions) scenario.

5.3 Materials and Methods

5.3.1 DEB model parameters and model scenarios

Model parameters (Table 5-1) were those previously estimated for *L. depurator* under single stressor conditions and validated by the experimental work presented in Chapter 4. As the aim of this chapter was to explore possible population level effects of changing environmental conditions on *L. depurator*, the DEB model equation governing reproductive processes and not used in previous versions of the model, was implemented in this iteration, and the carbon allocated to maturity maintenance and reproduction was tracked (equation i).

(i) Catabolic flux (gC d^{-1}):

The total energy mobilised from the reserve and allocated down either the somatic (κ) or reproductive ($1\text{-}\kappa$) pathway. The κ pathway is detailed in Chapter 3, section 3.3.5, equation (x). The $1\text{-}\kappa$ pathway is detailed below.

$$J_{ER} = 1 - \kappa(J_{EC} - k_J \cdot M_H)$$

Where J_{EC} is reserve mobilised to the κ pathway in gC d^{-1}

k_J is the maturity maintenance rate in gCM_E^{-1} gC $maturity^{-1}$ d^{-1}

and M_H is the energy from the reserve (in gC) already invested in maturity. If M_H is below the threshold $M_H{}^p$ the animal is juvenile and allocates energy to increase maturity. If M_H is above the threshold $M_H{}^p$ the animal is mature and allocates energy to reproduction.

Table 5-1: Model parameters for the coupled DEB-ERSEM model. Parameters were estimated from responses to stressors in single stressor experiments and validated in the multi-stressor experiments presented in Chapter 4.

Parameter	**Symbol**	**Unit**	**Control**	**High CO_2**	**Low O_2**
Maximum ingestion rate scaled to wet $mass^{2/3}$	$\{j_{XAm}\}$	$g^{1/3}$ M_W d^{-1}	1.41	1.41	1.2
Assimilation efficiency	y_{EX}	-	0.87	0.87	0.87
Reserve mobilisation rate	v	$g^{1/3}$ C d^{-1}	0.025	0.045	0.025
Fraction of energy allocated to somatic maintenance and growth	κ	-	0.85	0.85	0.85
Somatic maintenance rate	k_M	d^{-1}	0.17	0.19	0.19
Maturity maintenance rate	k_J	gCM_E^{-1} gC $maturity^{-1}$ d^{-1}	0.01	0.01	0.01
Growth efficiency	y_{VE}	-	0.5	0.5	0.5

For projections of *L. depurator* responses to climate drivers across the UK shelf, the DEB model was run on a single individual *L. depurator* of 0.5g wet mass. This individual represented a newly settled, sexually immature animal which had to allocate energy to increasing maturity before it could allocate to reproduction. The model made predictions for three physiological endpoints – ultimate size M_C (measured as carbon mass, g), age-at-maturity AAM (days) and cumulative allocation to reproduction over the whole of the modelled time period M_R (gC). The maximum AAM was set as 1000 days (~3 years), based on the assumption that any area in which animals took longer than this to mature would likely not be able to support a viable population. As any increase in temperature will lead to an increase in metabolic rates, it was assumed that M_R (allocation to reproduction integrated over a fixed time period) would likely increase in the future due to predicted ocean warming. However, increased metabolism will also lead to increased natural (and possibly predation) mortality, which may negate any temperature driven gains in M_R. While survival is not explicitly modelled, future estimates of M_R were temperature corrected to try and account for this. DEB models use a temperature correction factor (TC) to describe the temperature dependency of physiological rates (Schoolfield et al., 1981; Kooijman, 2010)(see Chapter 4, section 4.3.4). For each NEMO-ERSEM model grid cell a "metabolic speedup factor" was calculated ($TC_{future}/TC_{present}$). Future predictions of M_R were divided by this factor. The model does not directly predict *L. depurator* presence/absence or population dynamics – it evaluates an individual's potential to grow and allocate energy to maturation and reproduction over the whole model domain. However, population level inferences can be made using the reproductive endpoints AAM and M_R. I estimated the possible distribution of *L. depurator* populations in each time period by allocating the values of each of these endpoints in each model grid cell a "viability score" (Table 5-2). These scores were based on the notion that individual fitness is determined by the amount of carbon an individual invests in reproduction over its lifetime. Areas in which animals mature early and are able to invest heavily in reproduction therefore produce individuals with the greatest fitness, and so have the highest viability scores. Individual scores were summed and normalised using the equation:

$$\frac{(value - min)}{(max - min)}$$

to give an overall viability score for each grid cell between 0 and 1, with 0 indicating that the area would be unlikely to support a population, and 1 indicating an area would be very likely to support a population.

The model was forced with temperature, sediment particulate organic carbon (POC, a proxy for food availability), dissolved oxygen and pH inputs provided by NEMO-ERSEM for the periods 08/03/2006 – 14/01/2016 and 16/09/2038 – 24/07/2048. It was run a total of

94 times across the two time periods (47 model runs in each decade). In each time period, the first model run started on the first date of the input time series (08/03/2006 and 16/09/2038) and run for a total of 6 years. Each subsequent run started on the first day of the next month (e.g. 01/04/2006 and 01/10/2038). In this way, I could explore any effect of seasonal and interannual environmental variability on the modelled endpoints.

Table 5-2: Viability scores assigned to values of AAM and M_R. These individual scores were summed and normalised to provide an overall viability score for each model grid cell.

Individual viability score	**AAM (days)**	**M_R (gC)**
0	>1000	<2
0.25	751 – 1000	2.01 – 4
0.5	501 – 750	4.01 – 8
0.75	251 – 500	8.01 – 12
1	<250	>12

5.4 Results

5.4.1 Environmental conditions – decadal means

The temperature of near-bottom water was predicted to increase across most of the model domain by between 0.5°C – 1.5°C, with the greatest warming trend apparent in the southern North Sea and Irish Sea (Figures 5-1A, B & C). Model predictions for near-bottom pH showed decreases in all areas, with pH in the northern North Sea and Celtic Sea dropping to ~7.8 by 2048 (Figure 51D, E & F). The greatest decrease in pH (~0.14 pH units) was projected for the central part of the northern North Sea (Figure 5-1F).

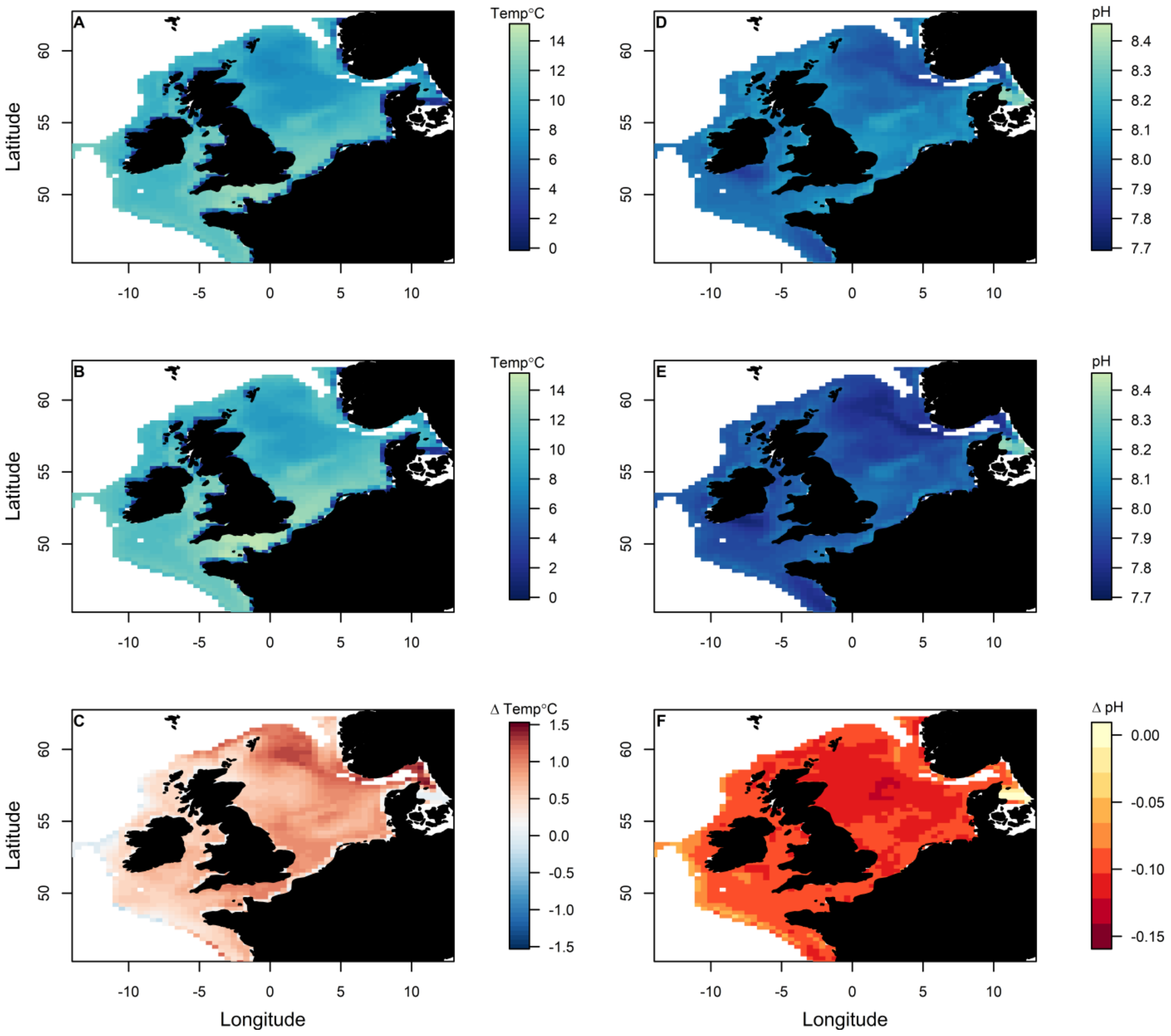

Figure 5-1: NEMO-ERSEM projections of mean near-bottom seawater temperature in °C (left hand panel) and pH (right hand panel) in the period 2006-2016 (A & D), 2038-2048 (B & E) and difference in temperature (C) and pH (F) between the two periods.

Mean oxygen concentration in the North Sea was predicted to decrease in the future, although absolute values in the model projections for the period 2038-2048 remained high at ~7mg L^{-1} (Figure 5-2A, B & C). Benthic particulate organic carbon (POC) ranged from 0.02g to ~11.5g in both time periods (Figure 5-2D & E), and changes were predicted to be fairly minor, with slight decreases apparent in the North Sea and off the west coasts of Scotland and Ireland, and increases in the English Channel and southern Celtic Sea (Figure 5-2F).

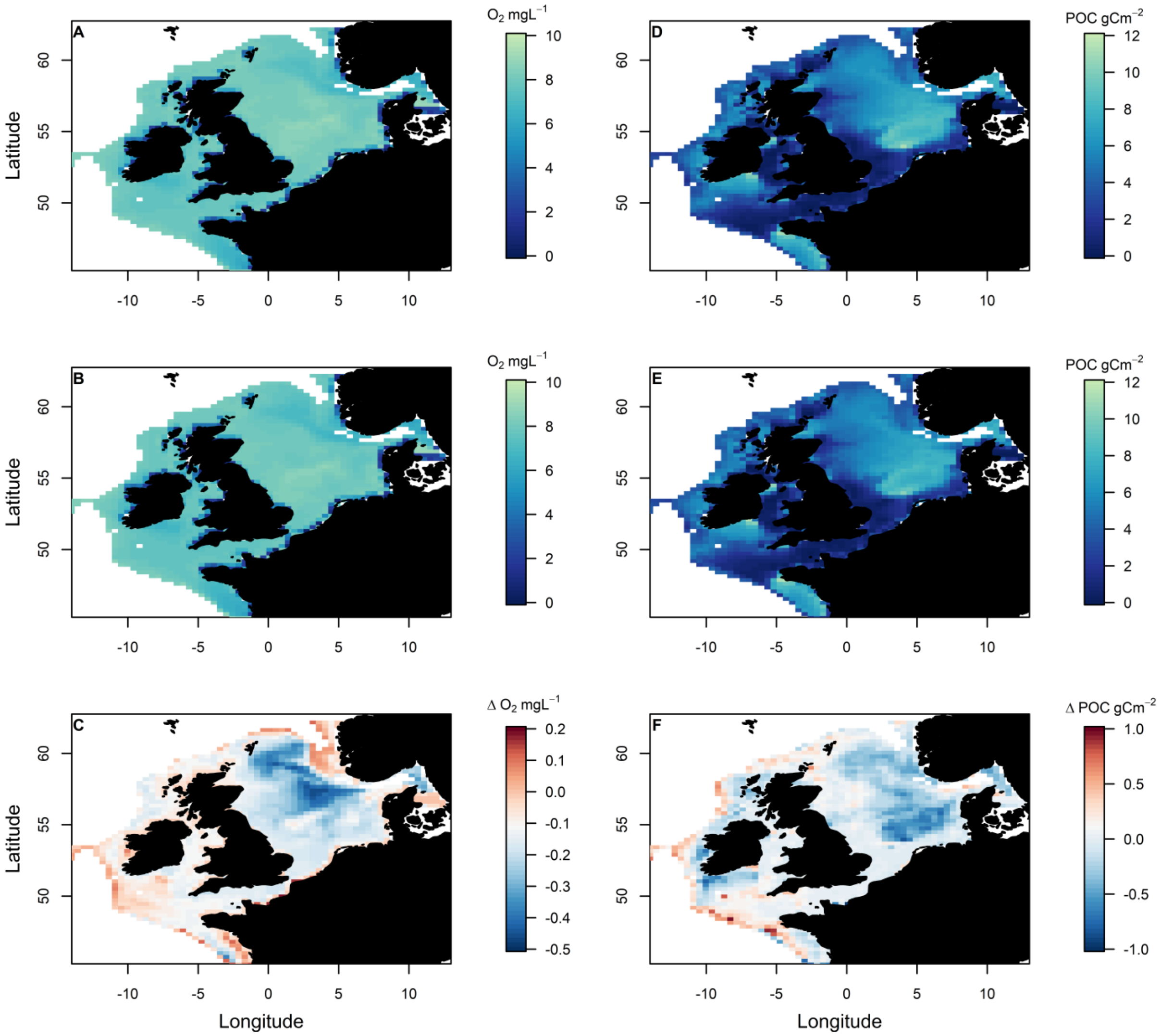

Figure 5-2: NEMO-EREM projections of mean O_2 concentration in mg L^{-1} (left hand panel) and benthic POC in g (right hand panel) in the period 2006-2016 (A & D), 2038-2048 (B & E) and difference in O_2 concentration (C) and POC (F) between the two periods.

5.4.2 Physiological endpoints – decadal means

Comparison of present day (2006-2016) and future (2038-2048) decadal means showed that predicted *L. depurator* ultimate carbon mass (M_C) ranged from ~0.3g in the English Channel, to ~4.5g in the southern North Sea and Celtic Sea (Figure 5-3A). M_C was predicted to change little around the UK shelf in the future. The only exception is in the northern North Sea, where animals were predicted to increase in mass by approximately 1gC, from ~3gC (Figure 5-3A) to ~4gC (Figure 5-3B & C). Mean predicted age-at-maturity (AAM) ranged from 160 – 1000 days from settlement. The greatest difference in AAM between the two time periods was seen in the northern North Sea. During the period 2006-2016, AAM was predicted to be over 1000 days (Figure 5-3D) in some parts of the northern North Sea. For the period 2038-2048, AAM was predicted to decrease to ~1000 days in the same area (Figure 5-3E & F).

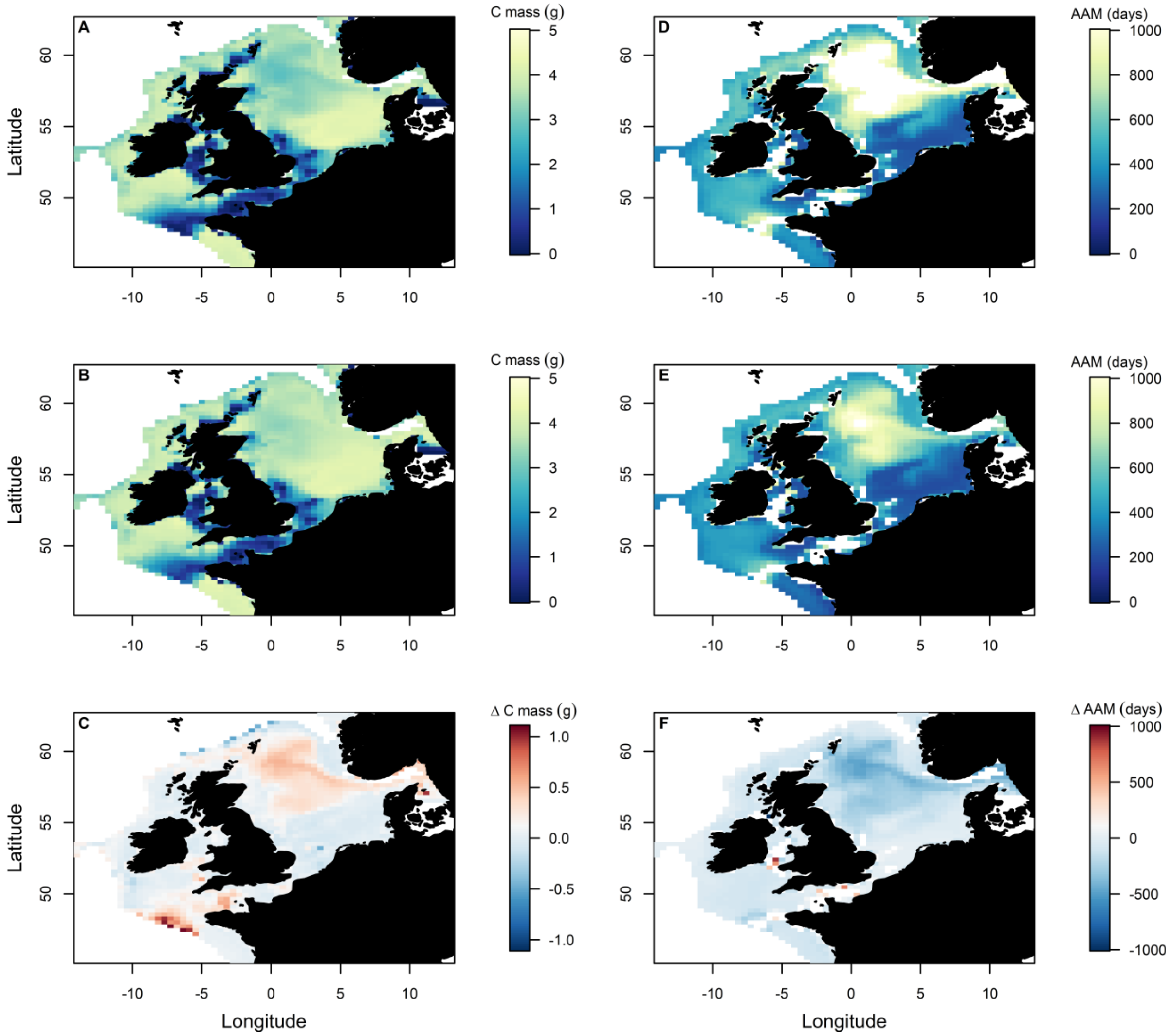

Figure 5-3: Predicted *L. depurator* ultimate carbon mass (MC) in g (left hand panel) and age-at-maturity (AAM) in days (right hand panel) in the period 2006-2016 (A & D), 2038-2048 (B & E) and difference in M_C (C) and AAM (F) between the two periods. The upper limit for age-at-maturity has been set at 1000 days (~3 years), as a viable population likely could not be maintained if animals took longer than that to mature. Any areas where age-at-maturity is predicted to be >1000 days are shown as white areas in (D & E).

Mortality corrected cumulative allocation to reproduction over the 6 year period (M_R) was predicted to increase in some parts of the central North Sea, increasing from ~10gC in the period 2006-2016 (Figure 5-4A) to ~12gC during the period 2038-2048 (Figure 5-4B). Conversely, M_R is predicted to decrease slightly in the southern North Sea, dropping ~2gC from ~18gC in the present day, to ~16gC in the period 2038-2048 (Figure 5-4B & C).

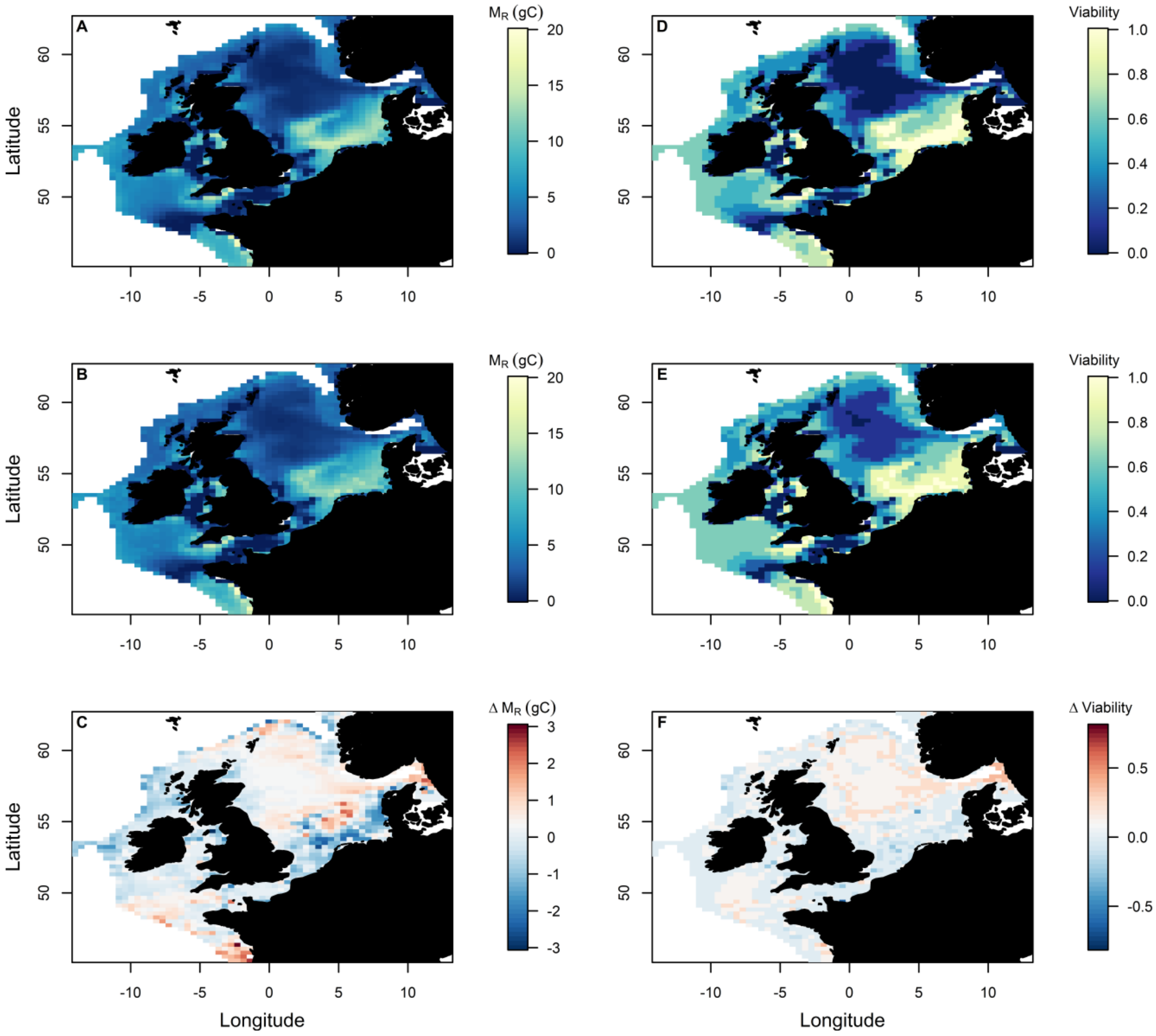

Figure 5-4: Predicted *L. depurator* cumulative allocation to reproduction (MR) in gC (left hand panel) and population viability (right hand panel) in the period 2006-2016 (A & D), 2038-2048 (B & E) and difference in M_C (C) and viability (F) between the two periods. Future allocation to reproduction has been temperature corrected using the “metabolic speedup factor”. Viability is an aggregate score based on predicted age-at-maturity and mortality corrected cumulative allocation to reproduction. See main text for full details and calculations.

Viability scores based on the reproductive endpoints of AAM and M_R suggested that *L. depurator* populations were likely to be widely distributed around the UK in both simulated time periods. The southern North Sea, Celtic Sea shelf, coastal areas of the Western English Channel and Bay of Biscay are all predicted to have suitable conditions in the period 2006-2016 (Figure 5-4D) with viability scores over 0.5. In contrast, central areas of the northern North Sea and English Channel had much lower viability scores (<0.2), suggesting that conditions were not ideal for the establishment of *L. depurator* populations. In the period 2038-2048 viability scores increased from ~0.4 - ~0.6 in the deeper parts of the Celtic Sea (Figure 5-4E & F). In the deeper central parts of the northern North Sea, scores increased, but remained low at ~0.2. In coastal areas of the northern North Sea, scores increased from ~0.2 to ~0.4 (Figure 5-4E & F).

Predictions for M_C and M_R varied little regardless of the month in which the simulation started (assumed time of settlement, see Appendix C for figures demonstrating this). Based on AAM however, the DEB model predicted a shift in the optimum time for settlement (e.g. the settlement month which results in the least time taken for an individual to mature). The optimum time for settlement shifted across the whole of the NEMO-ERSEM model domain (Figure 5-5). The shift was particularly noticeable in the southern North Sea, where optimum settlement time was in the summer/autumn (July – September) in the period 2006-2016 (Figure 5-5A), but was predicted to move to winter/spring (February-April) in the period 2038-2048 (Figure 5-5B).

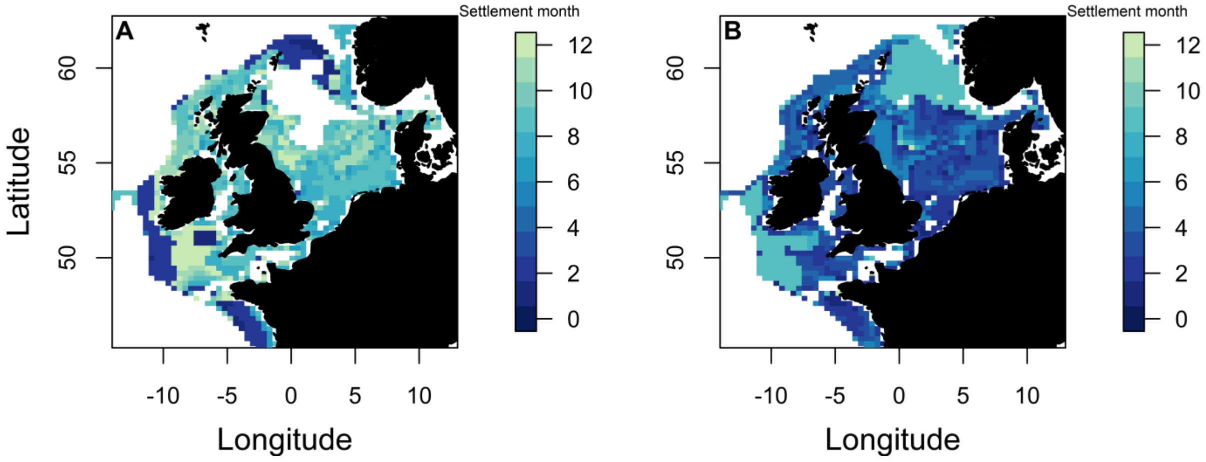

Figure 5-5: Predicted optimum settlement month based on age-at-maturity for *L. depurator*. The 12 colours on the scale bar represent a different month, with January in dark blue and December in yellow. (A) is the period 2006-2016, (B) is the period 2038-2048. The modelled period was clipped to 1000 days (~3 years) based on the assumption that individuals would likely not be present in any area in which maturity took >1000 days to achieve. White patches are areas in which AAM is predicted to be >1000 days.

5.5 Discussion

Predicting the future distribution and performance of marine species under climate change is of paramount importance. In this chapter a new method is presented, in which existing model projections for seawater temperature, pH and dissolved O_2 concentration and benthic particulate organic carbon (POC) across the north-western European shelf were used to force a mechanistic DEB model for the swimming crab *L. depurator*. This DEB model was used to make predictions regarding changes in carbon mass (M_C), age-at-maturity (AAM) and cumulative allocation to reproduction (M_R), and by extension, species distribution and population viability. The optimum settlement time, based on estimates of AAM, was predicted to shift forward across the whole of the NEMO-ERSEM model domain. M_R showed only minimal increases – it is possible that the temperature driven increase in allocation driven by higher metabolic rates is offset by a corresponding increase in mortality. Estimates of population viability and species distribution suggest that *L. depurator* may be able to expand its range further into the northern North Sea in the future.

5.5.1 Model performance

The published literature appears to support the likely distribution of *L. depurator* in the present day (2006-2016) which was inferred from AAM and M_R. Viability scores in the central English Channel and central northern North Sea and are low, although coastal areas of the northern North Sea have higher scores, suggesting that conditions in shallower areas may be more suitable for population persistence. *L. depurator* has been recorded in coastal locations east of Scotland, around the Moray Firth (Basford et al., 1989), south of Aberdeen (Pan et al., 2008) and in the shallower waters off the coast of north-east England, (Catchpole et al., 2006). Those model grid cells with high viability scores all correspond to areas in which *L. depurator* is regularly recorded, e.g. central and southern North Sea (Jennings et al., 1999; Zühlke et al., 2001; Hinz et al., 2004; CHARM, 2012; Depestele et al., 2014), the Celtic Sea shelf (Ellis et al., 2013), the eastern (Bremner et al., 2003) and western English Channel (Kaiser et al., 1998), the Bay of Biscay (Blanchard et al., 2004; Trenkel et al., 2007), the Clyde Sea (Bergmann and Moore, 2001; Bergmann et al., 2001; Moore and Bergmann, 2001; Bergmann et al., 2002) and the Bristol Channel (Ellis et al., 2000).

Model predictions of AAM and M_R (and their associated viability scores) for the period 2038-2048 suggest that conditions in parts of the coastal northern North Sea may become more favourable for *L. depurator* in the future. Given that the predicted changes in O_2 concentration, pH and benthic POC are minimal in the area, it is likely that changes in *L. depurator* responses are driven by increasing seawater temperatures. This temperature increase might allow an offshore range extension into slightly deeper waters off the east coast of Scotland. Climate-related range extension for crustaceans is well documented globally (Sorte et al., 2010), and in the North Sea specifically (Neumann et al., 2013). *L. depurator* itself has already expanded its range in the southern North Sea (Franke and Gutow, 2004). There is a predicted decrease in M_R in the southern North Sea in the period 2038-2048, which is likely due to increased temperatures causing an increase in all metabolic processes, including mortality, any increase in which will clearly affect cumulative allocation to reproduction. This decrease does not appear to have any significant impact on estimated population viability or distribution in the future however, with viability scores for the southern North Sea remaining high despite the predicted decrease in M_R. Interestingly, the model predicts a change in the optimum settlement window (based on AAM) for *L. depurator* between the present day and 2038-2048, with a particularly dramatic shift predicted in the Southern North Sea window (July- Sept in 2006-2016 to Feb-April in 2038-2048). DEB theory states that all physiological rates, including energy allocation to maturity in juvenile animals, increase in the same way with increasing temperatures (Kooijman, 2010), so a decrease in AAM is perhaps to be expected with predicted ocean warming. However, once a thermal tolerance limit is reached, rates will begin to decrease (Pörtner and Knust, 2007), and AAM will increase as a result. It is likely that some of the predicted changes in optimum settlement time are as a result of this phenomenon, with summer temperatures in some areas increasing beyond *L. depurator* thermal tolerance windows and impeding development, while winter temperatures increase enough to allow faster growth and earlier maturity. This is not unprecedented, as temperature driven changes in decapod phenology have already been documented in the literature. For example, decapod larvae occur in the North Sea plankton earlier in recent years than in the early 1980s (Lindley and Kirby, 2010), and the hatch timing of the northern shrimp in the North East Atlantic has been affected by increasing temperatures (Richards, 2012).

It is worth noting that the DEB model in its current form does not explicitly model survival. While the potential impact on M_R of temperature driven mortality is accounted for via the “metabolic speed-up factor”, it is clear that further research is needed to fully explore the effects of temperature on both natural and predation driven mortality. In its present iteration, the DEB model predicts an increase in somatic maintenance and a decrease in ingestion once dissolved oxygen concentrations drop below 4mg L^{-1}. However, severe environmental hypoxia or anoxia will not result in mortality in the model. Short-term hypoxic conditions, as is sometimes recorded in the German Bight area of the North Sea (Brockmann et al., 2018), could therefore have significant consequences for survival, and so population persistence, that are not currently captured in the model. Further experimental work with *L. depurator* will enable the identification of two critical dissolved oxygen (DO) thresholds: i) when oxy-regulation cannot be maintained, and oxygen consumption decreases linearly with the O_2 saturation of the surrounding water, and ii) the DO concentration at which mortality can be expected. This will allow a correction factor to be calculated (Aguirre-Velarde et al., 2019; Lavaud et al., 2019; Thomas et al., 2019), which can be applied to those model parameters (somatic maintenance k_M and ingestion $\{j_{XAm}\}$) which were shown in Chapter 4 to be affected by hypoxia.

5.5.2 Benefits of the DEB-ERSEM approach

To date, most species distribution modelling efforts have used a correlative SDM approach, which relies on statistical dependencies between biotic and environmental data in order to predict future distributions (Mathewson et al., 2017). There are a number of reasons for this – SDMs are relatively easy to use and widely available, their data requirements are generally easily met, and the range of biotic and abiotic interactions they can (implicitly) capture is good (Robinson et al., 2011). However, these models provide little insight into *why* changes in species' distributions are predicted, limiting their ability to inform conservation responses. Consequently, climate adaptation actions in response to species' declines are reduced to trial and error. Furthermore, transferring correlative SDMs into novel conditions risks erroneous extrapolation, which is a key issue for studies of climate change effects (Evans et al., 2015; Mathewson et al., 2017). It is clear that alternative modelling approaches to SDMs should be explored where possible (Robinson et al., 2011). The mechanistic DEB model presented here represents just such an alternative to correlative SDMs. Rather than relying on empirical statistical relationships between environmental conditions and species distributions, the distributions predicted by this model are an emergent property of the process being modelled, in this case AAM and M_R.

While the benefits of using non-lethal modelled endpoints to infer species distributions are clear, understanding how these endpoints respond to changing conditions is useful in its own right. For example, this DEB model, which predicts changes in ultimate body size and reproductive investment, may prove to be useful in stock assessments of economically important crustacean fisheries such as those for *Cancer pagurus* (Linnaeus 1758), *Maja squinado* (Herbst 1788), *Homarus gammarus* (Linnaeus, 1758) and *Nephrops norvegicus* (Linnaeus, 1758), and could be a valuable addition to the modelling toolkit of fisheries managers. To the best of my knowledge there are no published DEB models for any of these species, although the Add-my-Pet database has model parameters for *C. pagurus* and *H. gammarus* estimated from the literature (AmP, 2017), and inferred DEB parameters (based on all parameter values of all species, weighted according to taxonomic proximity) for *M. squinado* and *N. norvegicus* can be acquired through phylogenetic inference (Bruggeman, 2019). There is also the potential to provide better understanding of organism vulnerability to stressors or disturbances in addition to large scale climate drivers, such as localised sources of pollutants. These additional stressors may not result in mortality, but they may have detrimental effects on sub-lethal endpoints such as those modelled here (Verslycke et al., 2004; Saravanan et al., 2018). A tool which provides a better understanding of the non-lethal effects of anthropogenic stressors on crustaceans also has value outside of the fisheries sector. For example, the DEB model can provide us with an insight into the potential impacts of changing environmental conditions on species which are globally important in ecological terms, such as krill.

Climate change is shifting organism distributions and phenologies, but understanding how these changes are driven by climate effects on organism responses is still a significant challenge (Deutsch et al., 2015). Although there are examples of SDMs which explicitly incorporate organism physiology or life history traits into modelled processes (Fernandes et al., 2013; Queirós et al., 2015), they are still relatively uncommon in the marine literature and, as far as I am aware, none have a fully mechanistic physiological model at the centre of the approach (although see Mathewson et al, 2017 for an example in a terrestrial ecosystem). The mechanistic DEB-ERSEM method presented here may be of use in providing insight into why changes in species' distributions are predicted, as these distributions are an emergent property of the processes being modelled. Furthermore, the ability to model non-lethal endpoints, rather than just species' presence/absence, provides an opportunity to better understand the effects of changing conditions on ecologically relevant processes which may make focal species more vulnerable to future disturbances. As such, it can be argued that this model represents a step forward in the methodology of species distribution modelling, and that it can be a useful tool in scaling up the results of experimental climate change research and placing them in an ecosystem context.

Chapter 6 General discussion and conclusions

Marine ecosystems are some of the most diverse on Earth (Solan et al., 2004). This biodiversity is predominantly attributable to the number of invertebrates living in or on sediments; indeed, it has been estimated that the benthic environment provides habitat for 98% of all marine species (May and Godfrey, 1994; Snelgrove, 1999). While the macro-infauna receive much of the attention in the published literature due to their roles in mediating biogeochemical cycles (Lohrer et al., 2004; Laverock et al., 2011), benthic epifauna also play critical roles in the health and function of marine benthic ecosystems. Decapod crustaceans are often among the most dominant species recorded in terms of both abundance and biomass in the epifauna (Chapter 2; Neumann et al., 2017) and their ubiquity means that they are often key components of marine benthic ecosystems, playing significant roles in structuring communities (Chapter 2; Quijón & Snelgrove, 2005) or acting as keystone species, maintaining complex habitats such as salt marshes and kelp forests (Silliman and Bertness, 2002; Steneck et al., 2004). Furthermore, many decapod species have significant economic value in both capture fisheries and as cultured species in aquaculture operations (Cawthorn and Hoffman, 2017).

Benthic ecosystems are under increasing threat from human activity, with pronounced ecological consequences (Doney et al., 2012; IPBES, 2019). The principal climate drivers affecting marine ecosystem structure and functioning have been identified as water temperature, pH, oxygen concentration and food availability (IPCC, 2014). Changes in species' distributions (Wiltshire et al., 2009) and phenological processes (Birchenough et al., 2015) have been identified as a response to changing temperatures. Mass mortalities as a result of hypoxic events have been recorded (Diaz and Rosenberg, 2008; Altieri et al., 2017), and sub-lethal stresses affecting surviving organisms include reduced growth (Hrycik et al., 2017; Jeppesen et al., 2018) effects on reproduction and recruitment (Breitburg, 1992; Miller et al., 2002) and increased vulnerability to predators (Decker et al., 2004; Riedel et al., 2008). The effects of ocean acidification (OA) vary between and among taxa (Kroeker et al., 2013), but experimental studies have demonstrated that survival (Talmage and Gobler, 2010), calcification (Zhao et al., 2017), and growth and development (Dupont et al., 2008) can all be negatively affected by decreased seawater pH.

A significant challenge in marine climate change research is in predicting organism responses to this anthropogenic change. Once we have predictive understanding, it will be possible to make informed decisions on how best to manage marine habitats to mitigate climate change effects. It has been demonstrated that a focus on organism energetics is useful as a means of integrating organismal responses to a wide range of environmental drivers (Boyd et al, 2018), and the mechanistic Dynamic Energy Budget (DEB) model in particular offers a whole organism approach to explaining how factors in the physical environment translate into biologically and ecologically relevant responses (Chapters 3, 4, 5; van der Meer, 2006)

6.1 DEB at the individual level

At the individual level, the DEB model presented in this thesis has shown that it can successfully describe and predict crustacean growth and oxygen consumption under ambient conditions, and that a critical part of crustacean life history – the moult – can be captured (Chapter 3). It also makes good predictions for organism responses under ecologically relevant climate stressors such as hypoxia and OA in decapods (Chapter 4) and a number of other taxa (Klok et al., 2014a; Muller and Nisbet, 2014; Lavaud et al., 2019). Perhaps most interestingly, the mechanistic nature of the DEB model (e.g. measured responses such as growth are a function of stressor effects on model parameters) means that, by combining parameter sets estimated under single stressor conditions, multi-stressor models can be developed (Chapter 4). This provides a number of advantages. Results from multi-stressor model scenarios can allow researchers to identify those stressors with the greatest predicted impact aiding in the development of testable hypotheses and the design of logistically challenging multi-stressor experiments. Given the huge number of stressors acting on marine environments (Côté et al., 2016), and the fact that the number of experimental treatments required to quantify all possible interactions of these stressors is unreasonable (Boyd et al., 2016), the kind of complex synthesis required to fully explore the interacting effects of multiple stressors is really only practicable in models. The DEB model presented in Chapter 4 provides a way of synthesising single stressor data into a mechanistic modelling environment that can simulate the effects of stressors under novel or untested conditions, and make predictions under more complex, ecologically relevant conditions.

Applications of the model at the individual level are numerous. It can be used in aquaculture operations to assess which production method (e.g., feeding regime) is likely to produce the fastest growth. Similarly, it can provide insights into optimal conditions (e.g. temperature) for production. It is possible that this model could be used for assessing suitable sites for sea based container culture projects for crustaceans, such as the Lobster Grower 2 (LG2) project (www.lobstergrower.co.uk). A bio-energetic model such as the one presented here, which specifically links crustacean moulting and growth to environmental parameters, may be very useful in selecting sites that would offer the best possible conditions in which to rear juvenile lobsters. The standard DEB model is already proven to be useful in this regard, having been previously applied to evaluate the carrying capacities of marine ecosystems and evaluate their potential for bivalve aquaculture (Thomas et al., 2011).

A serious problem in crustacean aquaculture is disease (Stentiford et al., 2012). While the model presented in this thesis cannot elucidate the specific responses of the crustacean immune system to pathogens, it may be of assistance in mitigating their effects. The model can be used to quantify the effects of infection on the energy budget of the host, as has been shown for the standard DEB model in previous studies on bivalves (Flye-Sainte-Marie et al., 2009). Once an effect on a DEB parameter has been quantified, can a change in feeding regime or food quality compensate to ensure continued growth? Similarly, how do commonly used immunostimulants affect parameters? Immunostimulants are proposed to enhance disease resistance in cultured species, but it is clear that their effectiveness varies with different host species, delivery methods and types of pathogen (Rowley and Pope, 2012; Traifalgar et al., 2013). Additionally, there are cogent reasons why the use of these compounds over prolonged periods may actually be detrimental to the host animal (Smith et al., 2003). It may be possible to use the model to balance prophylactic efficacy of a given compound against its effect on model parameters.

The crustacean DEB model could also be useful in providing more accurate estimates of growth for use in stock assessment models for crustacean capture fisheries. Growth models currently used as a basis for stock assessment do not consider food availability, and only a small number consider environmental temperature (Wainwright and Armstrong, 1993; Brylawski and Miller, 2006). As both of these factors are critical drivers of growth in crustaceans, a model that can account for changing food availability and environmental conditions would be a useful addition to the modelling toolkit of fisheries managers.

Finally, this model could also be useful in ecotoxicology studies, where *Daphnia magna* is a standard test species. Many toxicological endpoints, including effects on reproductive output, are potentially affected by variations in moult dynamics (Ananthasubramaniam et al., 2014), so a DEB model which can account for these variations has potential advantages.

There are a number of ways in which the individual model could be further refined. At present, the model does not capture the changes in ingestion and oxygen consumption rate that occur as an individual progresses through the moult cycle. In order to fine-tune model performance in these areas it is necessary to build a true “moulting period” into the model, which causes the suppression of feeding and an increase in O_2 consumption. While O_2 consumption is the result of a combination of modelled processes, and so cannot be coupled to the moult cycle directly, model parameters affecting O_2 consumption (e.g. the maintenance coefficient k_M) can be. By coupling maintenance and ingestion rates to the carbon mass/wet mass ratio α (the parameter which controls the moult in the DEB model), both ingestion and O_2 consumption will change with the increase in α as an animal approaches moult.

The first iteration of the model did not track the mobilised flux from the reserve to the reproductive buffer (1-kappa), after it had been allocated. Later iterations of the model (Chapters 4 & 5) do, but the link between reproduction and moult has still not been fully explored. Moult is critical to reproduction in many crustacean taxa, with the two being coordinated in a variety of ways (Raviv et al., 2008), and influenced by environmental conditions. There is evidence of seasonal moulting as a precursor to breeding in some species (Abelló, 1989; MacDiarmid, 1989; Fernández et al., 1991), and in those species (including *Liocarcinus depurator*) which can spawn multiple times between moults, the intermoult period becomes dependent on egg incubation time, which is itself temperature driven (Hamasaki, 2003; Wehrtmann and López, 2003). Given the strength of this link between reproduction and moult, it is possible that, in some species, moult is not solely dependent on energetic factors (e.g. α), but is also influenced by the reproductive buffer.

6.2 DEB at the population level

Despite being defined at the individual level, the DEB model proved useful to infer population-level properties. When coupled to NEMO-ERSEM, the model predicted plausible present-day distributions of *L. depurator* in the present day (Chapter 5). The level of skill the model demonstrated in making these predictions for the period 2006-2016 would lead to the conclusion that predictions for population distribution in the period 2038-2048 are also reliable. This model represents a significant step forward in the methodology of species distribution modelling, as it places mechanistic physiological understanding at the heart of the process. Unlike most species distribution models (SDMs), which are correlative and rely on statistical dependencies between environmental and biological data (Robinson et al., 2017), projected distributions in the DEB-ERSEM model are an emergent property of the processes being modelled. Much like the DEB model when used to predict responses to environmental drivers at the individual level, this mechanistic approach negates the issue of extraneous extrapolation in novel circumstances, which is a significant issue in some SDMs (Elith and Leathwick, 2009; Melle et al., 2014).

It is worth stressing again that the DEB-ERSEM model presented in Chapter 5 is not a population model. However, it is possible to make population level inferences *via* the modelled reproductive endpoints, and there are some refinements that could be made to ensure the accuracy of predictions made regarding species' distributions. The most obvious extension to the DEB-ERSEM method is to include survival as a modelled endpoint, and to investigate the effects of e.g. short term hypoxia on population viability in areas where periodic low oxygen minima are a feature of the habitat. In order to make more robust predictions at higher levels of biological organisation, it is necessary to couple the DEB model to a population model. Published examples of coupled DEB-population models include matrix models, which assign individuals to classes based on size, age or developmental stage (Jager and Klok, 2010), or physiologically structured population (PSP) models. Less commonly, DEB models are coupled to individual based models (IBMs) (Martin et al., 2012). In matrix models individuals can move into the next class or die with a certain probability (depending on age, stage or size); some classes can also produce offspring. In this way, the model calculates the intrinsic rate of population growth *(r).* The major drawback of this approach is that it assumes that each individual in every generation follows the same life history, thereby excluding maternal or trans-generational effects (Jager et al., 2014). Although this might be a reasonable assumption for a short term toxicology study (to which DEB coupled matrix models are most commonly applied), they are not representative of field conditions, and present a serious limitation to the wider application of this method.

Physiologically structured population (PSP) models also distinguish age, life-stage or size classes within a population, but unlike matrix models, they explicitly relate the transfer beween these classes to the physiological characteristics of the individual and the condition of its wider environment (De Roos et al., 2001). This makes them particularly suited to those studies in which the temporal variations in population structure are of interest. Theoretical studies have used PSP models in a DEB framework to explore the size structured dynamics of fish populations (Maury and Poggiale, 2013), and general PSP models (i.e. not used in a DEB framework) are often used in fisheries studies (Persson et al., 2004; Persson and De Roos, 2006; Hartvig and Andersen, 2013). PSP models are well suited to modelling fish populations as they analyse size dependent interactions between organisms, and body size is often considered as a defining physiological trait when modelling fish (Maury, 2010; Hartvig et al., 2011). While body size is clearly a useful trait when considering trophic interactions (i.e. predation), it is not the only key physiological trait for benthic organisms, where traits such as motility can be critical (Clare et al., 2015).

Finally, individual-based models (IBMs) represent individual organisms as unique entities that are different from each other and change over their life cycles. Population dynamics emerge from their interactions with each other and their environment (Martin et al., 2012). DEB has been proposed as a building block for IBMs, although it has rarely been used as one (Martin et al., 2012; Martin et al., 2013). The fact that IBMs explicity follow all individuals in a population means that an essential feature of DEB is preserved – the dynamic response of an individual's life history to environmental changes (Jager et al., 2014). Additionally, IBMs place no limit on the number of state variables for individuals, bringing them closer conceptually to DEB than other population models (Martin et al., 2012; Jager et al., 2014). Arguably, IBMs are the natural link to the population level for DEB as both approaches focus on the physiological performance of individuals as a key aspect in understanding higher levels of biological complexity. IBMs do have some drawbacks however. When compared to other models, IBMs are computationally expensive, particularly when modelling large populations or populations in complex environments. Furthermore, certain types of interactions (e.g. schooling or spawning aggregation behaviour) can increase model execution time exponentially when run with field realistic numbers of individuals (Breckling, 2002). This can make running repeat simulations, in order to estimate parameters or explore uncertainty, problematic.

The model as it stands is a single species model, but interspecific interactions may regulate high-level impacts of climate change on any focal organism. Consequently, the individual-based responses of a single species may not suffice to understand long-term responses in complex ecological environments where species interact (Harley, 2011). In order to take these species interactions into account, the DEB model could be used as a mechanistic component in a macro-scale species distribution model such as a size spectrum dynamic bioclimatic envelope model (SS-DBEM) (Queirós et al., 2015). These SS-DBEMs specifically account for trophic interactions by using the size spectrum component to determine resource limits in a given geographical area. These limits, along with habitat suitability for a given species determined by the DEB model, can be used together to determine the biomass of that species that can be supported across the model domain (Fernandes et al., 2013).

In conclusion, this thesis has shown that:

- Crustaceans are a key component of the benthos and can be instrumental in structuring benthic communities and driving community responses to biotic and abiotic drivers
- Modelling the energetics of individual organisms is an effective way of integrating organism responses to environmental and climate drivers
- The standard DEB model can be easily adapted to account for a key process in the crustacean life-cycle - the moult - thereby improving model predictions of crustacean growth

- DEB model parameters estimated from singe stressor experiments can be combined and used to predict organism responses under multi-stressor scenarios
- When coupled to a hydrodynamic-biogeochemical model, the DEB model can be used to make inferences about population level responses to environmental change across large spatial scales, including possible species distributions and optimum juvenile settlement times
- The DEB model can be a useful tool at both the individual level (e.g. aiding in the development of experimental climate change research, better growth models for crustacean aquaculture and capture fisheries stock assessment) and at the population level (e.g. improvements in species distribution modelling)

Appendix A Supplementary material for Chapter 3

A.1 Inferring carbon : wet mass thresholds from observations

The fitting of the upper and lower envelopes for the carbon mass/wet mass thresholds, the description that follows, and the production of Figure A-1 was done by Dr Jorn Bruggeman

Carbon mass increases continually due to assimilation of food. This ultimately leads to moulting, which we assume to be triggered when the carbon to wet mass ratio reaches a particular maximum value. During moulting, wet mass increases due to intake of water, while carbon mass remains approximately unchanged (loss of total carbon due to respiration and carapace loss/resynthesis is assumed small). We assume that wet mass increases until a minimum carbon : wet mass ratio is reached. Thus, the new wet mass is

$$M_{Wnew} = \frac{M_C}{\alpha_{min}} = \frac{\alpha_{max}}{\alpha_{min}} M_{Wold}$$

The relative change in wet mass during a moult is $\frac{\alpha_{max}}{\alpha_{min}}$. Assuming isomorphy, the relative change in any linear dimension (e.g., carapace width) is $\left(\frac{\alpha_{max}}{\alpha_{min}}\right)^{\frac{1}{3}}$. For simplicity, we assume that both minimum and maximum $M_C : M_W$ remain unchanged over the life span of a crab. That implies that pre-moult body composition, including water content, will always be the same, as will the post-moult body composition. This is in line with DEB's weak homeostasis assumption. It also implies that the relative size increase during a moult is constant. This is a first-order approximation; a moderate decrease in this increment with increasing size has been observed in some species which implies the difference between minimum and maximum α is greater at smaller size. Together, these assumptions set an envelope for observable carbon-wet mass combinations: for any given carbon mass M_C, wet mass can only take values between M_C/α_{max} and M_C/α_{min}. In a constant environment, all wet masses within this range have an equal likelihood of being observed, as long as there are no differences in survival or catch probability among crabs with the same M_C. While this is to a degree supported by field observations (fig 1), the contours of the envelope are not as sharply defined as would be implied by a universal minimum and maximum $M_C : M_W$. The apparent fuzziness of the envelope observed is likely in part caused by intraspecific variability: different crabs have slightly different $M_C : M_W$ ratios at which moulting is triggered and/or terminated.

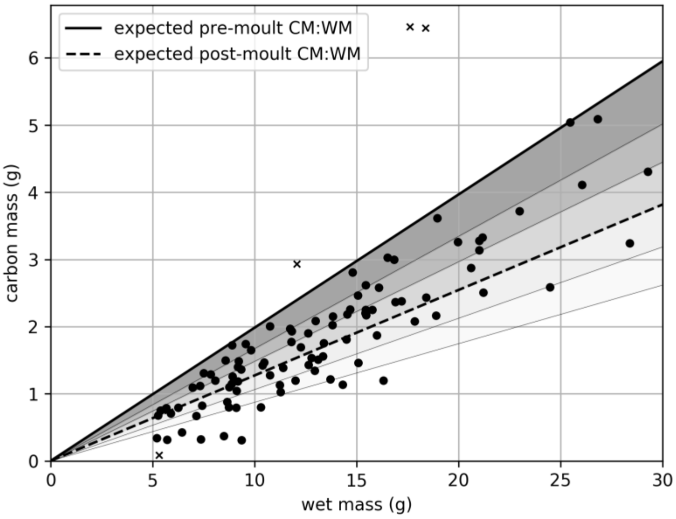

Figure A-1. Observed combinations of wet mass and carbon mass, along with the best fitting model for the upper and lower envelope. The solid black line indicates the maximum $M_C : M_W$ ratio (0.20), the dashed black line the expected minimum $M_C : M_W$ ratio (0.13). For any wet mass, the shaded regions show the density of crabs as function of their M_C, with increasing density indicated by darker shades. The lower bounds of the shaded regions are the 10th, 25th, 50th, 75th and 90th percentiles. Observations with extreme $M_C : M_W$ values were excluded during analysis; these are shown as crosses.

If we formalize this by assuming α_{min} and α_{max} are normally distributed within a population, we know that for a crab with wet mass M_W, the probability density of initial M_C is given by a normal distribution with mean $\alpha_{min}M_W$ and standard deviation $\sigma_{min}M_W$; conversely, the probability density of the final value of M_C is given by a normal distribution with mean $\alpha_{max}M_W$ and standard deviation $\sigma_{max}M_W$. The probability density of M_C for any crab with known wet mass is then given by the difference between the fraction of crabs having reached this carbon mass (individuals moulting into this M_W at larger M_C are excluded) and those already having moved on to larger M_W by moulting at lower M_C. That is the difference between two cumulative normal distributions:

$$P(\alpha) = \frac{\Phi\left(\frac{\alpha - \alpha_{min}}{\sigma_{min}}\right) - \Phi\left(\frac{\alpha - \alpha_{max}}{\sigma_{max}}\right)}{\int_{-\infty}^{\infty} \Phi\left(\frac{\alpha' - \alpha_{min}}{\sigma_{min}}\right) - \Phi\left(\frac{\alpha' - \alpha_{max}}{\sigma_{max}}\right) d\alpha'}$$

Let us assume the actual number of crabs observed within a particular wet mass/carbon mass bin follows a Poisson distribution. To avoid having to deal with variable survival/catch probability, we group all sampled individuals in bins of similar carbon mass

(20 per bin; 5 bins). Within each i^{th} M_C bin, we distinguish 100 equally spaced M_W intervals, covering all observed $M_W : M_C$ ratios (5.0 – 30.1). For each of these intervals, we compute the probability density of observing an individual according to the above equation. We then normalize the resulting 100 values to have their sum equal the total number of observed individuals for the current M_C bin (typically 20). Each of the resulting 100 values is treated as the expected number of observed crabs per M_W interval, λ_{ij}. The log likelihood of the combined M_C/M_W observations is then given by

$$\Lambda = \sum_{i=1}^{5} \sum_{j=1}^{100} k_{ij} \ln \lambda_{ij} - \lambda_{ij} - \ln k_{ij}!$$

Here, k_{ij} denotes the number of observed crabs per M_C/M_W combination. We now estimate the parameters describing the $M_C : M_W$ envelope by maximizing the log likelihood using the Nelder-Mead Simplex algorithm. The values that optimize the log-likelihood are $\alpha_{min} = 0.13$, $\alpha_{max} = 0.20$, $\sigma_{min} = 0.03$ and $\sigma_{max} = 0$. These estimates are robust under a wide range of bin counts for M_C and M_W (resp. 5-20, 20-1000).

The results imply an increase in wet mass during a moult of $\frac{\alpha_{max}}{\alpha_{min}} - 1 = 56\%$, and an increase in linear dimensions of $\left(\frac{\alpha_{max}}{\alpha_{min}}\right)^{\frac{1}{3}} - 1 = 16\%$. Estimated values for the standard deviation suggest that variability in $M_C : M_W$ thresholds occurs predominantly around the lower threshold, i.e., the quantity of water taken in to inflate the body; the upper bound on $M_C : M_W$ values is well constrained.

A.2 Consideration of the carapace

In DEB theory, the carapace of a crustacean is neither structure nor reserve, but product. However, in this model, we have included the mass of the carapace in our measures of wet mass, which implicitly places it with structure and reserve. Due to the fact that the carapace is relevant in feeding, and that, in this model ingestion scales with wet mass$^{2/3}$, we assume that carapace scales with wet mass. After a moult, the new carapace has an energy requirement as it hardens (predominantly related to the calcification of the new cuticle). Once the new carapace is hard, any energy requirement is minimal. Structure and reserve increase to fill the carapace, replacing water as they do so.

A.3 Calculation of initial state of structure M_V and reserve M_E

Each modelled crab has 3 variables – reserve (M_E), structure (M_V) and wet mass (M_W), only one of those is measurable (M_W). In order to constrain the other 2 variables as much as possible, and to simplify the model as much as possible, we assumed that all crabs encountered the same food prior to collection, and so the initial reserve density m_E was in a steady state. This premise allowed us to calculate the initial state of M_V and M_E for the first time point of the model using m_E , the ingestion rate J_{XA}, an estimation of carbon mass (M_C), which can be made using the carbon mass/wet mass conversions calculated prior to the start of the main experiment, and energy conductance v, the value of which was derived from the DEB species explorer (Bruggeman, 2019, see main text for full reference). Once the initial state of M_V and M_E had been calculated, both these state variables and m_E were allowed to fluctuate. We assume that wet mass is proportional to structural volume, and the primary link between wet mass and the state variable structure and reserve in this DEB model is the carbon mass/wet mass ratio α.

Change in reserve density:

$$\frac{d}{dt} m_E = \frac{J_{XA}}{M_V} - \frac{v}{M_V^{\frac{1}{3}}} \; m_E = 0$$

Where J_{XA} is ingestion rate, which now scales to wet mass$^{2/3}$ not structure

$$J_{XA} = \{j_{XAm}\} \, M_W^{\frac{2}{3}} f$$

Initial state of structure using m_E and J_{XA}

$$J_{XA} - v \, m_E \, M_V^{\frac{2}{3}} = 0$$

$$\{j_{XAm}\} \, M_W^{2/3} f - v \, m_E \, M_V^{\frac{2}{3}} = 0$$

$$\{j_{XAm}\} \, M_W^{2/3} f - v \frac{M_E}{M_V^{\frac{1}{3}}} = 0$$

There are three possible solutions. General cubic function to solve

$$x^3 + c_1 x - c_2 = 0$$

Where $x = \sqrt[3]{M_V}$

$$c_1 = \frac{\{j_{XAm}\}\, M_W^{\frac{2}{3}}\, f}{v}$$

$$c_2 = \frac{M_W}{(M_W/M_C)}$$

$$M_W = (M_W/M_C)(M_E + M_V)$$

$$M_E = \frac{M_W}{(M_W/M_C)} - M_V$$

Algebraic solution – calculate the discriminant first to establish the number of real roots

$$\Delta = 18\, abcd - 4b^3 d + b^2 c^2 - 4ac^3 - 27a^2 d^2$$

Where $a = 1,\ b = 0,\ c = c_1,\ d = c_2$

$$\therefore\ \Delta = -4{c_1}^3 - 27{c_2}^2$$

$\Delta < 0$ so only one real root

General solution requires the calculations

$$\Delta_0 = b^2 - 3ac$$

$$\therefore \Delta_0 = -3c_1$$

$$\Delta_1 = 2b^3 - 9abc + 27a^2 d$$

$\therefore \Delta_1 = -27c_2$

$$C = \sqrt[3]{\frac{\Delta_1 \pm \sqrt[2]{-27\Delta}}{2}}$$

$$x = -\frac{1}{3}\,(C + \frac{\Delta_0}{C})$$

$$if\ x = \sqrt[3]{M_V}\ then\ M_V = x^3$$

Appendix B Carbonate chemistry parameters for OA experiments

Table B-1: Carbonate chemistry parameters for all ocean acidification experiments. Temperature, salinity, pH, CO_2 concentration and total alkalinity (A_T) were measured for all experimental treatments and controls. Total dissolved inorganic carbon (DIC), calcite saturation state (Ωcal) and aragonite saturation state (Ωarag) were calculated in "seacarb" in R, using the mean values of the measured parameters and saturation constants from Mehrbach et al. (1973)

Experiment	Nominal CO_2 concentration ppm	Measured CO_2 concentration ppm (± SD)	Temperature °C (± SD)	Salinity (± SD)	pH (± SD)	A_T µmol kg^{-1} (± SD)	DIC µmol kg^{-1}	Ωcal	Ωarag
Control – single stressor	400	411.2 (48.6)	12.11 (0.17)	35.4 (0.1)	8.1 (0.01)	1525.21 (48.4)	1421.91	2.7	1.7
OA – single stressor	1000	10911.1 (148.1)	12.95 (0.35)	35.6 (0.2)	7.77 (0.06)	1972.82 (68.3)	1923.62	1.8	1.2
Control/cool – multi-stressor	400	406.09 (52.7)	10.15 (1.17)	35.3 (0.1)	8.1 (0.01)	1433.47 (15.8)	1343.93	2.4	1.5
Control/warm – multi-stressor	400	425.6 (98.3)	16.64 (0.87)	35.3 (0.1)	8.01 (0.01)	1374.16 (29.7)	1284.91	2.3	1.5
OA/cool – multi-stressor	1000	1036 (137.6)	10.06 (0.97)	35.6 (0.2)	7.78 (0.04)	1864.02 (94.6)	1824.87	1.6	1.0
OA/warm – multi-stressor	1000	1043 (129.4)	17.27 (1.05)	35.5 (0.2)	7.81 (0.05)	1448.61 (112.8)	1355.84	1.7	0.9

Appendix C Supplementary material for Chapter 5

C.1 Seasonal variation in the predicted physiological endpoints of *Liocarcinus depurator*

In order to ensure that predictions for decadal means were not sensitive to the month the model scenario was started in (e.g. the settlement month), overall monthly means of each physiological endpoint (ultimate carbon mass, age at maturity and cumulative allocation to reproduction) were calculated. The figures below demonstrate that predictions for each endpoint varied little, regardless of the settlement month. The only exception was age at maturity, which did vary depending on settlement month, and which is discussed in detail in Chapter 5.

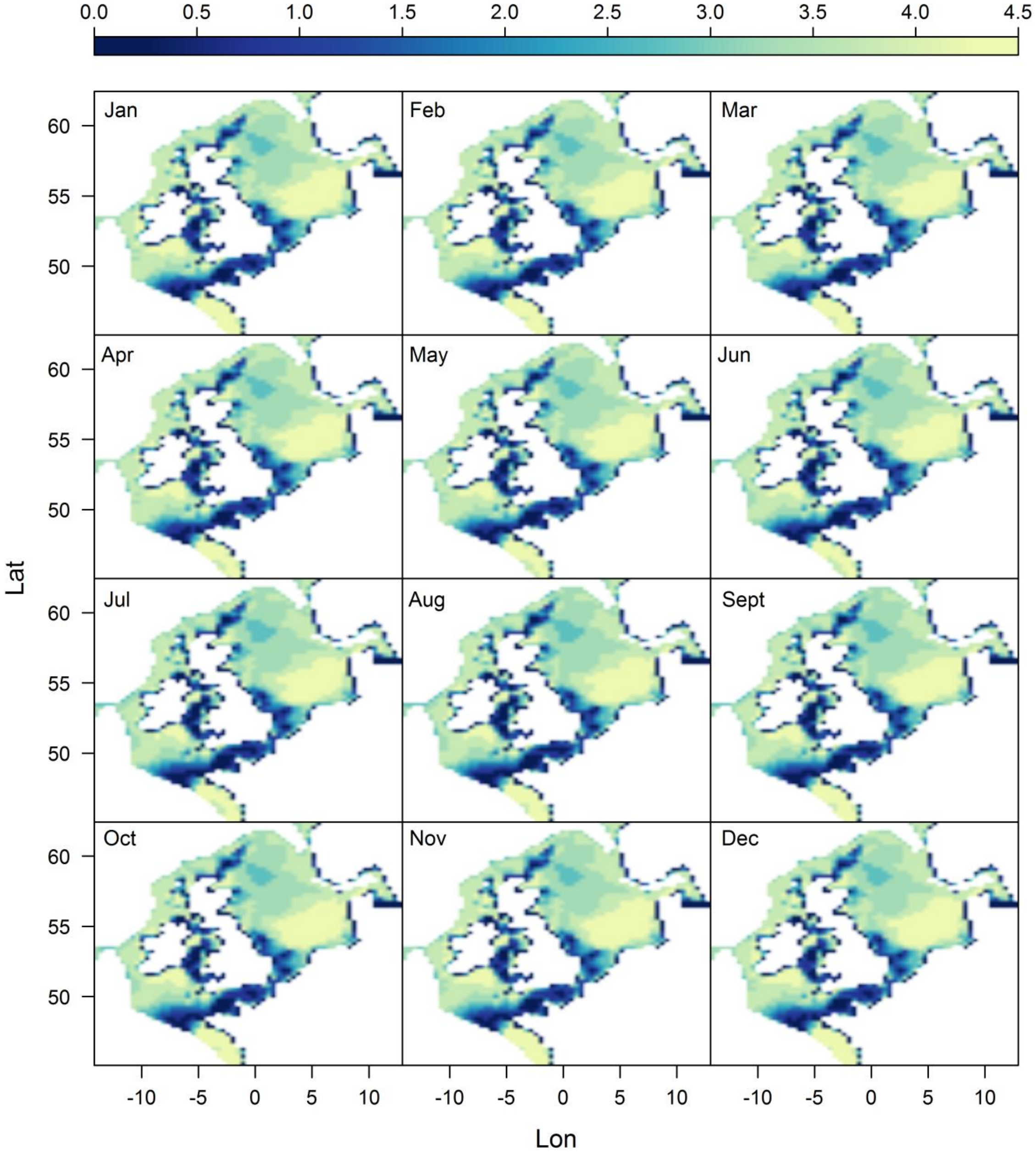

Figure C-1: *L. depurator* ultimate carbon mass (g) over the period 2006-2016. Values for each month are overall means of ultimate carbon mass at the end of the six year model run period when the model was initialised at the start of that month – e.g. four model runs were initialised in January (2007, 2008, 2009, 2010), therefore January values are the overall means of ultimate *L. depurator* carbon mass at the end of those four model simulations, and represent the ultimate size of an individual *L. depurator* had that animal settled to the benthos in January.

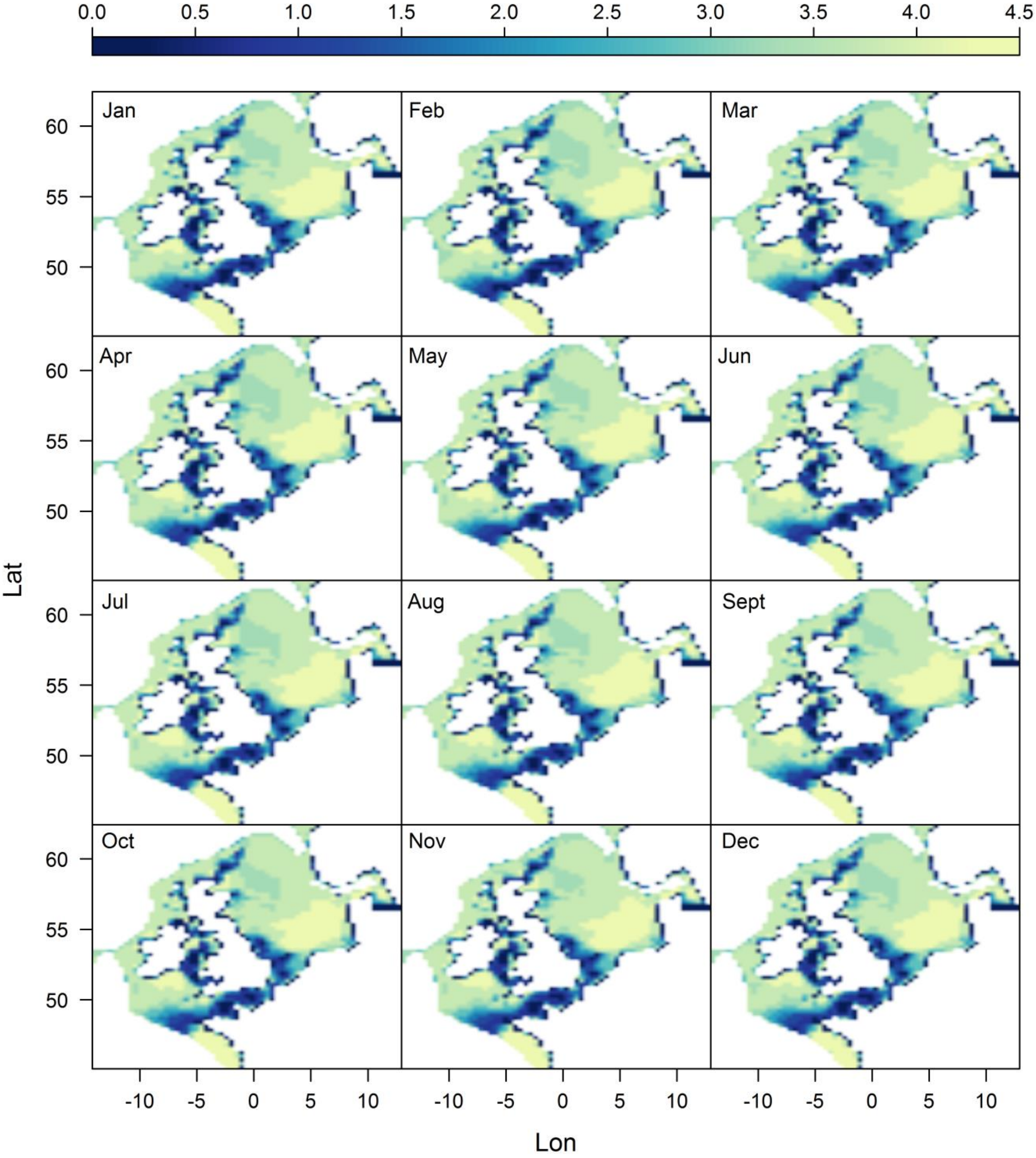

Figure C-2: *L. depurator* ultimate carbon mass (g) over the period 2038-2048. Values for each month are overall means of ultimate carbon mass at the end of the six year model run period when the model was initialised at the start of that month – e.g. four model runs were initialised in January (2039, 2040, 2041, 2042), therefore January values are the overall means of ultimate *L. depurator* carbon mass at the end of those four model simulations, and represent the ultimate size of an individual *L. depurator* had that animal settled to the benthos in January.

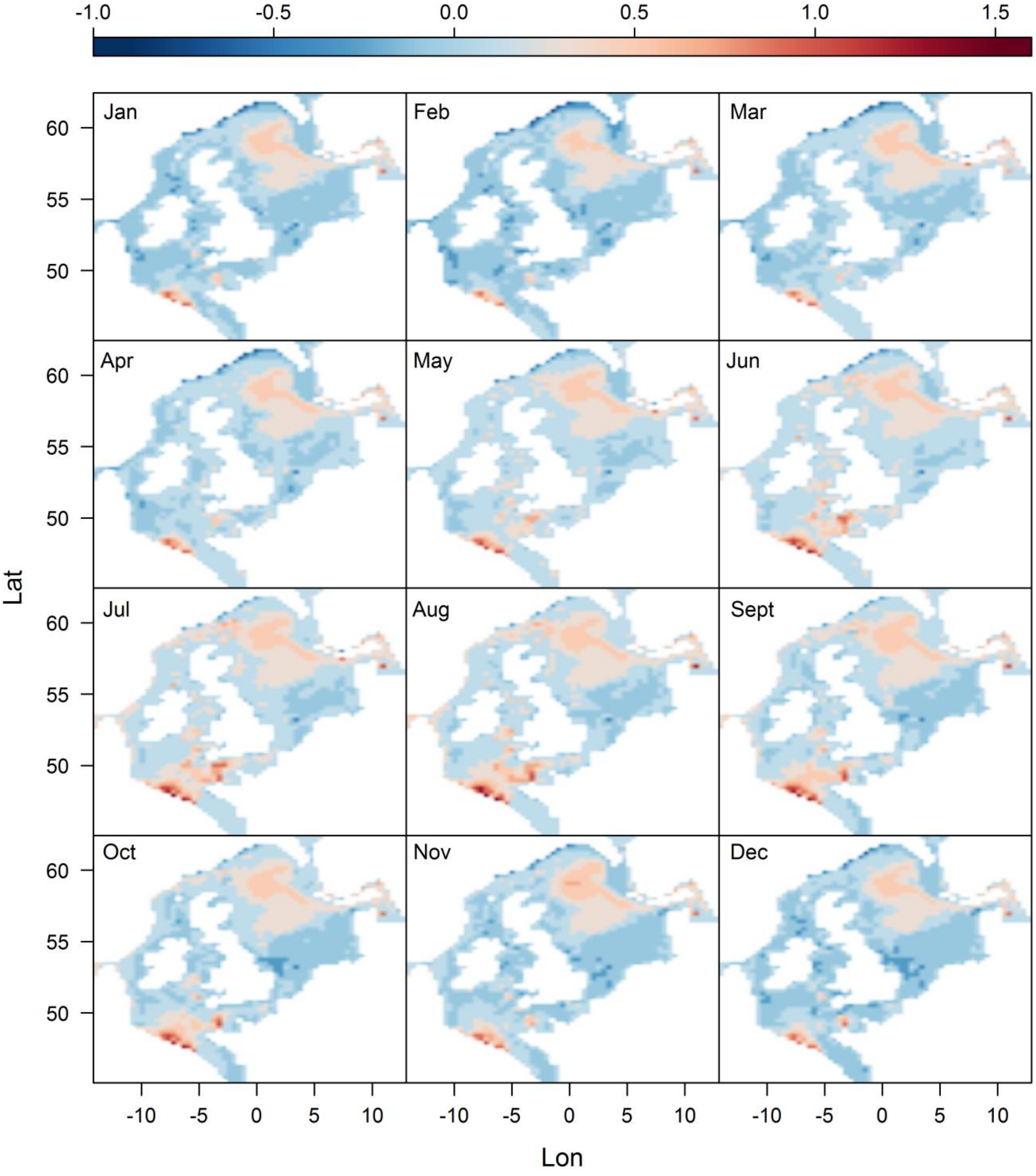

Figure C-3: Difference in predicted *L. depurator* ultimate carbon mass (g) between the periods 2006-2016 and 2038-2048.

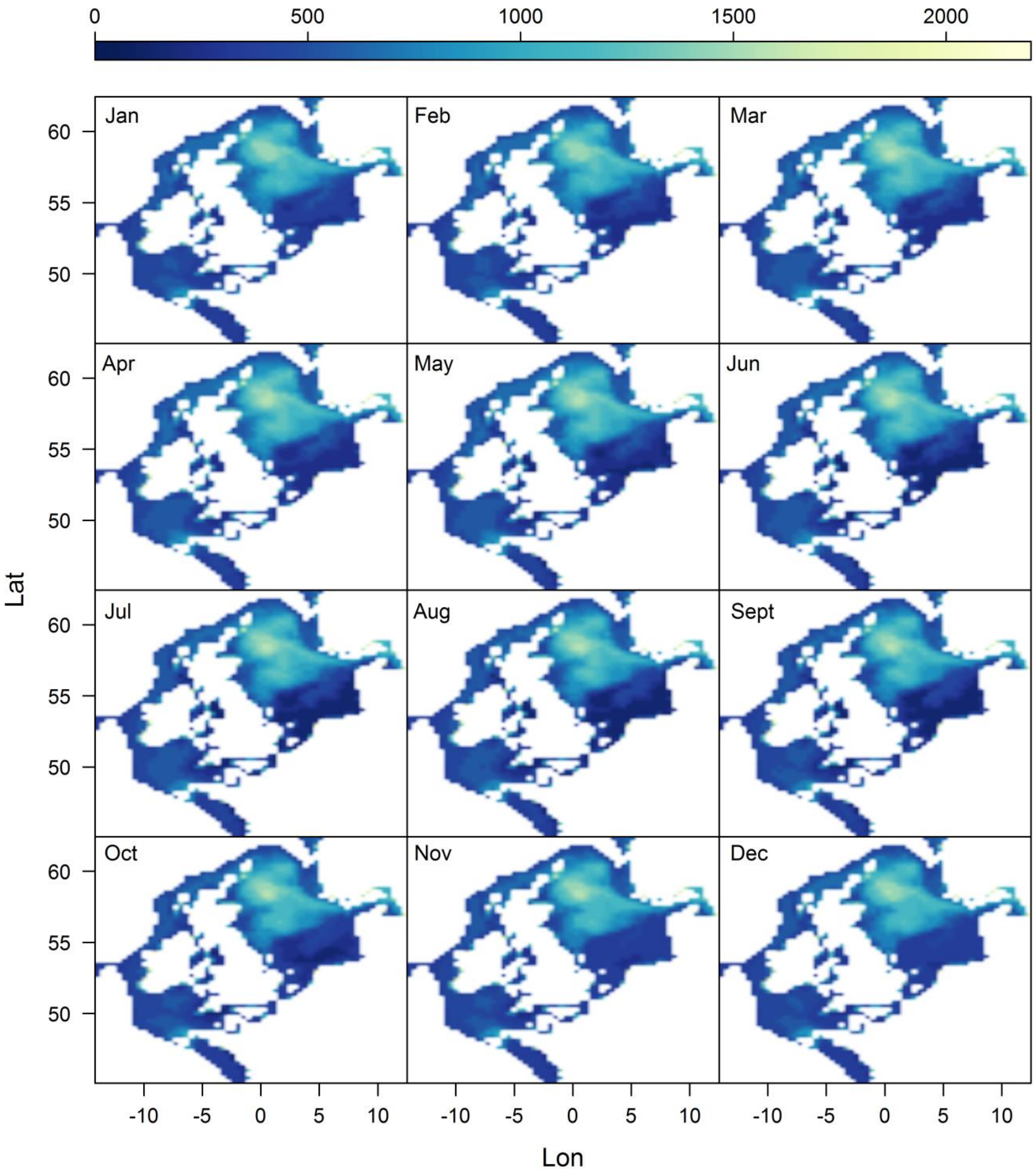

Figure C-4: *L. depurator* age-at-maturity (days) over the period 2006-2016. Values for each month are overall means of age-at-maturity at the end of the six year model run period when the model was initialised at the start of that month – e.g. four model runs were initialised in January (2007, 2008, 2009, 2010), therefore January values are the overall means of *L. depurator* age-at-maturity at the end of those four model simulations, and represent the age-at-maturity of an individual *L. depurator* had that animal settled to the benthos in January. White areas in the English Channel and Irish Sea are areas where *L. depurator* was not predicted to reach maturity within the modelled period of six years.

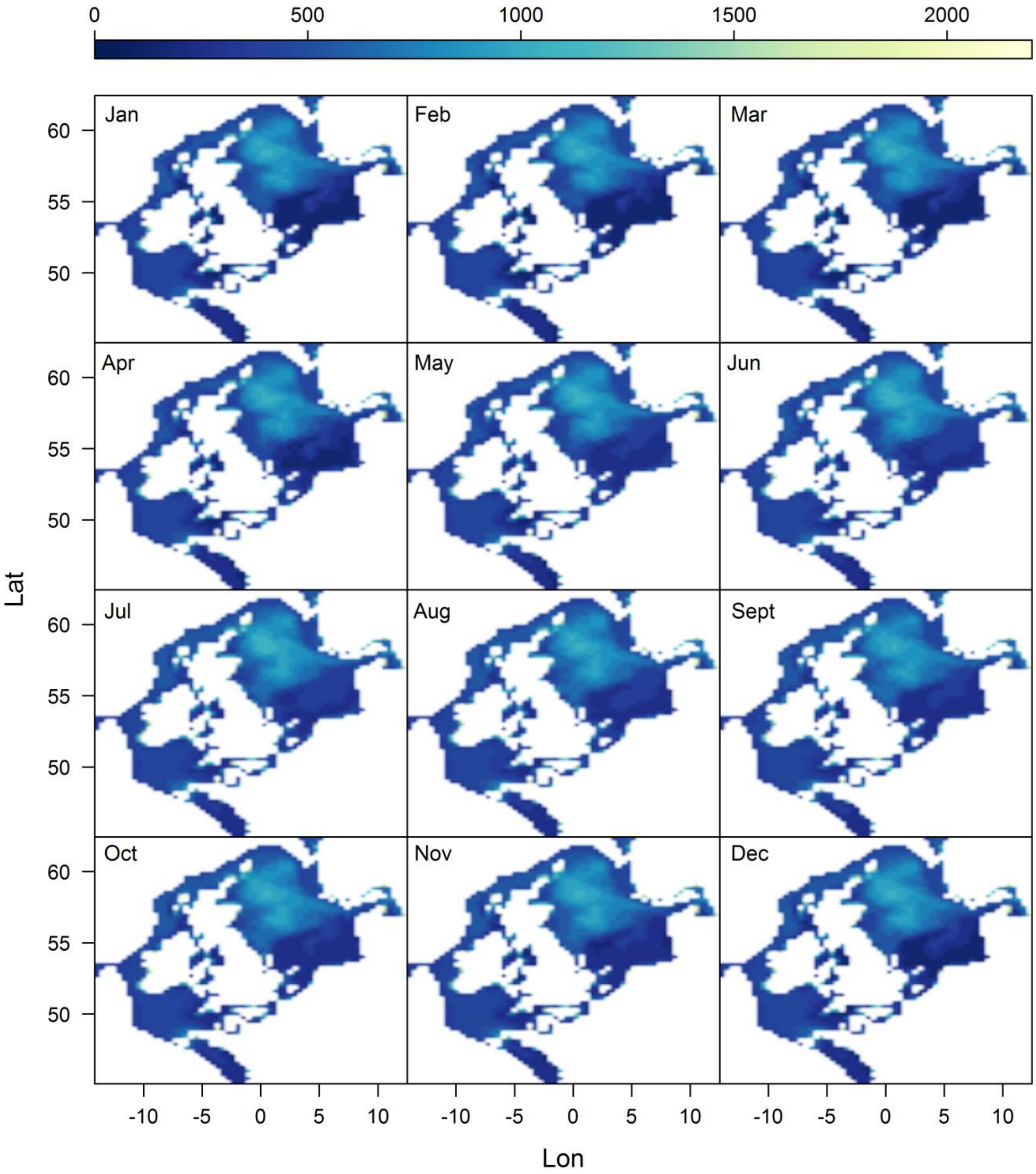

Figure C-5: *L. depurator* age-at-maturity (days) over the period 2038-2048. Values for each month are overall means of age-at-maturity at the end of the six year model run period when the model was initialised at the start of that month – e.g. four model runs were initialised in January (2039, 2040, 2041, 2042), therefore January values are the overall means of *L. depurator* age-at-maturity at the end of those four model simulations, and represent the age-at-maturity of an individual *L. depurator* had that animal settled to the benthos in January. White areas in the English Channel and Irish Sea are areas where *L. depurator* was not predicted to reach maturity within the modelled period of six years.

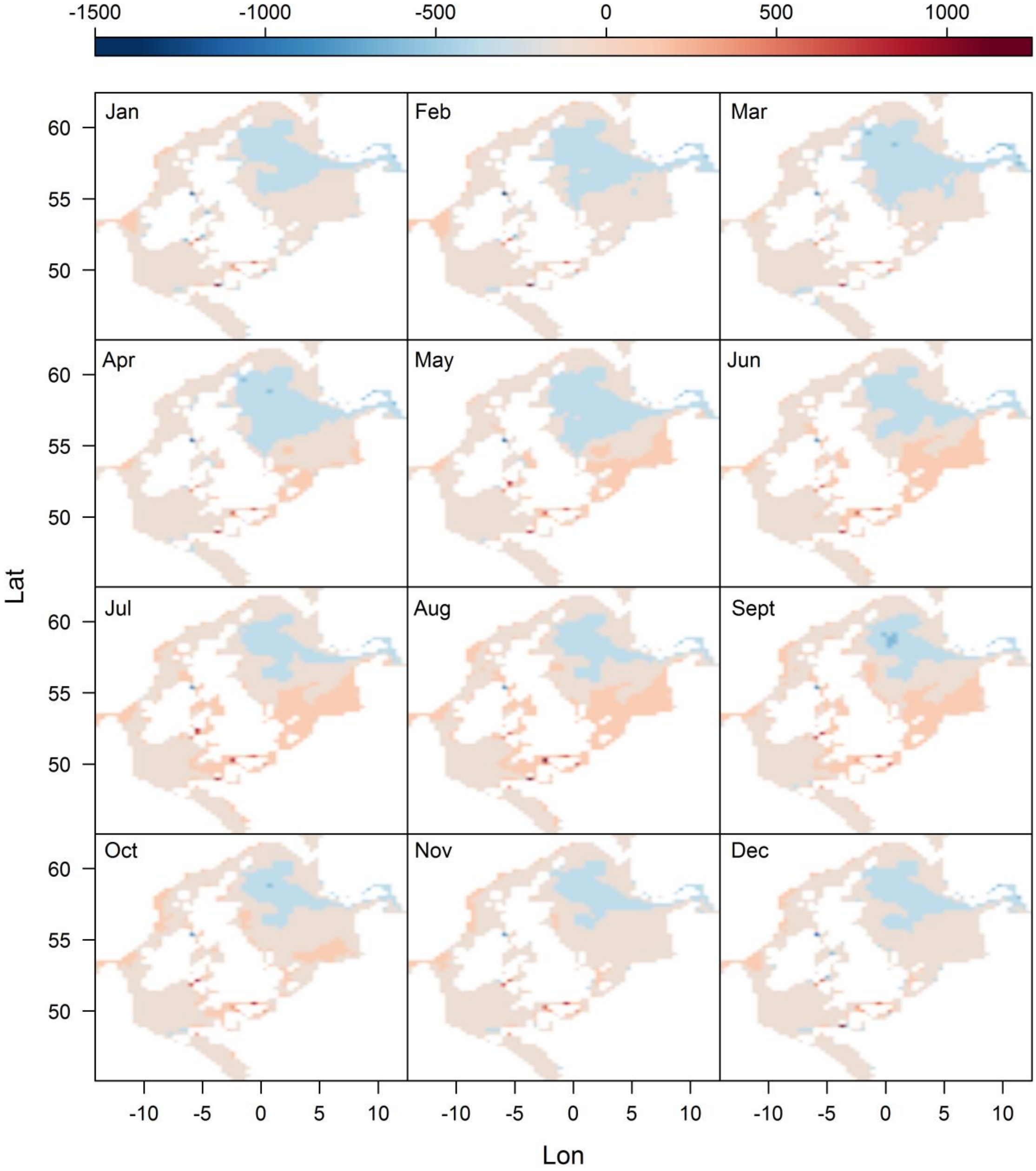

Figure C-6: Difference in predicted *L. depurator* age-at-maturity (days) between the periods 2006-2016 and 2038-2048. White areas in the English Channel and Irish Sea are areas where *L. depurator* was not predicted to reach maturity within the modelled period of six years.

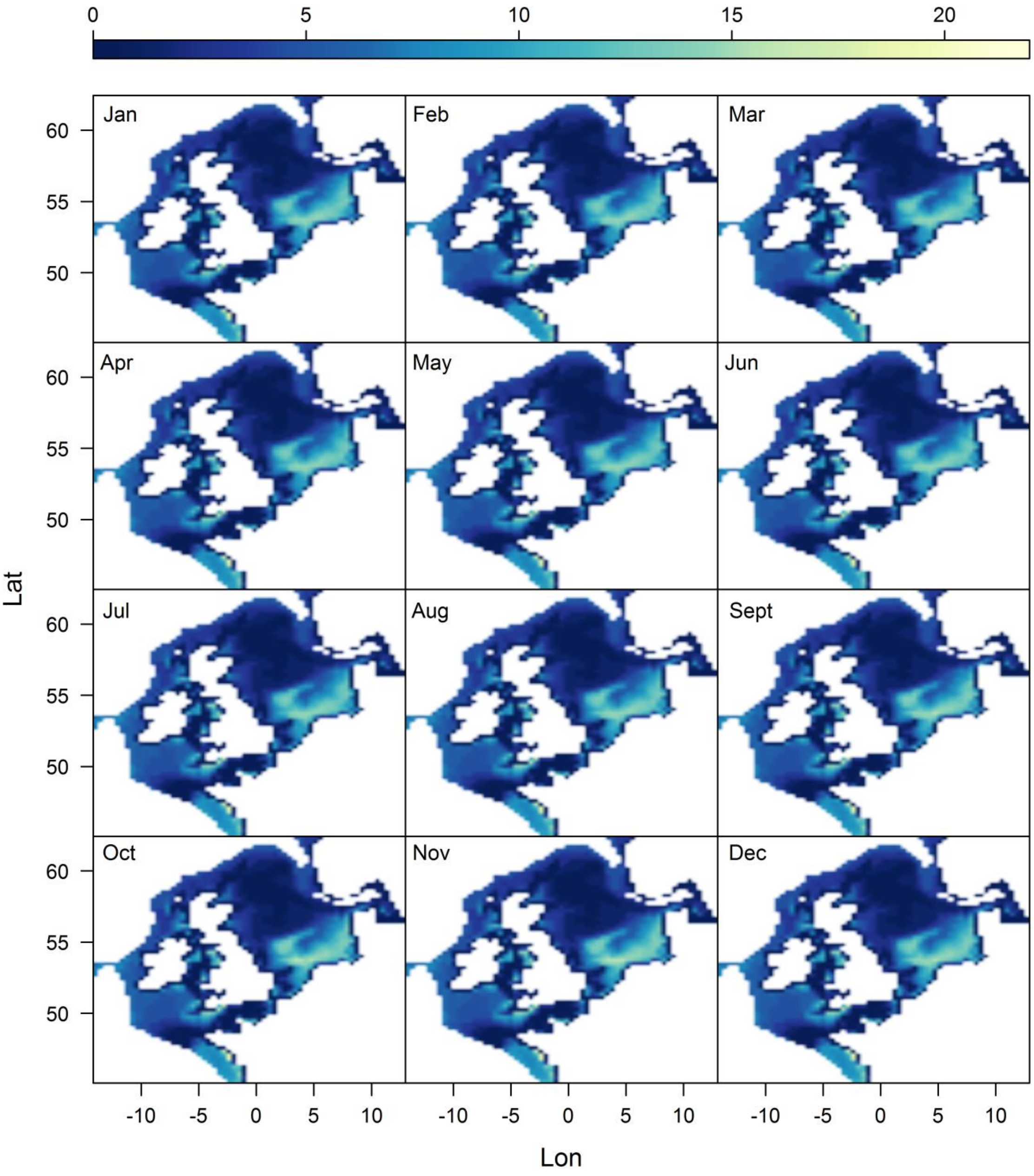

Figure C-7: *L. depurator* lifetime allocation to reproduction (gC) over the period 2006-2016. Values for each month are overall means of allocation at the end of the six year model run period when the model was initialised at the start of that month – e.g. four model runs were initialised in January (2007, 2008, 2009, 2010), therefore January values are the overall means of *L. depurator* allocation to reproduction at the end of those four model simulations, and represent the lifetime allocation to reproduction of an individual *L. depurator* had that animal settled to the benthos in January.

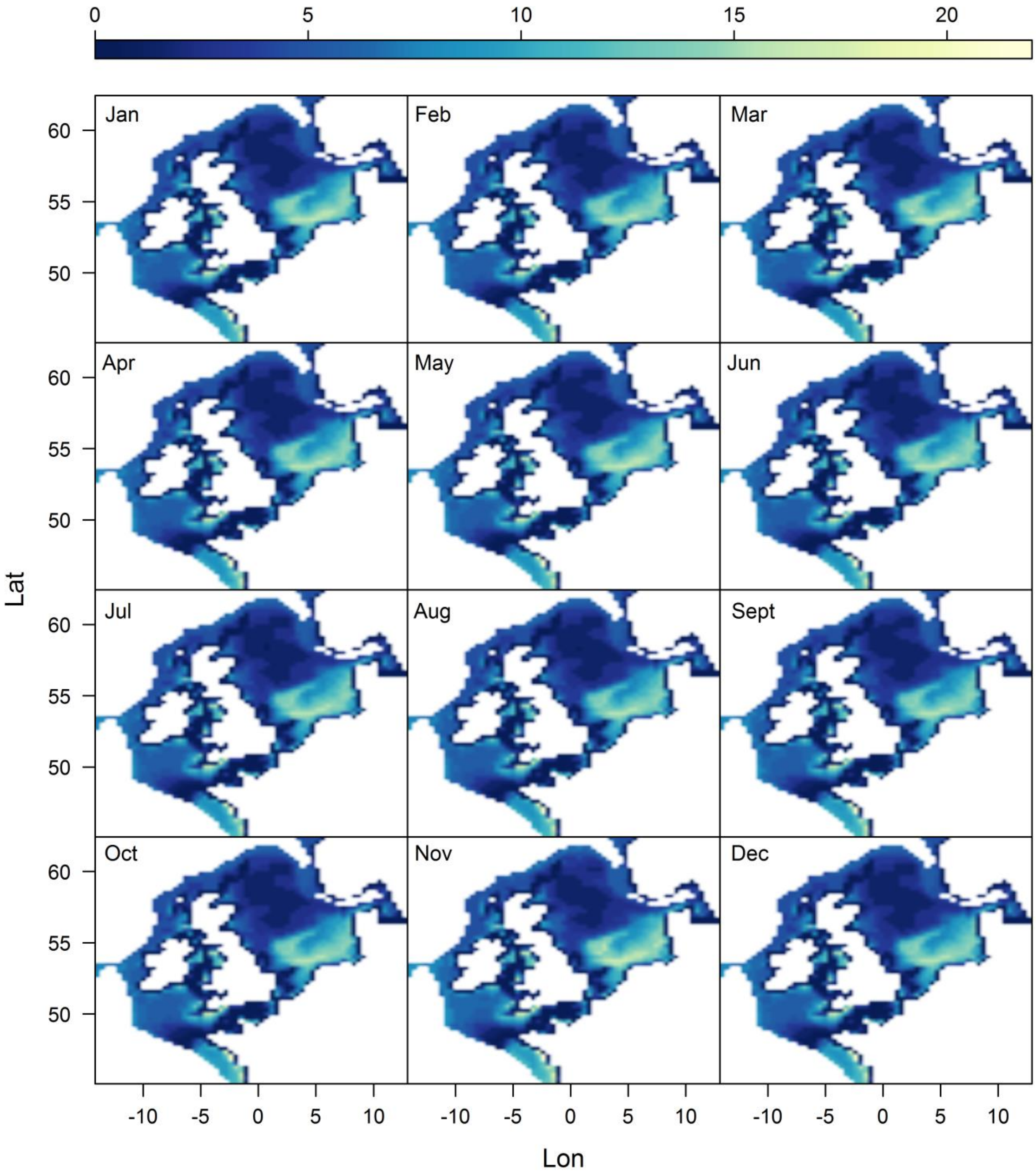

Figure C-8: *L. depurator* lifetime allocation to reproduction (gC) over the period 2038-2048. Values for each month are overall means of allocation at the end of the six year model run period when the model was initialised at the start of that month – e.g. four model runs were initialised in January (2039, 2040, 2041, 2042), therefore January values are the overall means of *L. depurator* allocation to reproduction at the end of those four model simulations, and represent the lifetime allocation to reproduction of an individual *L. depurator* had that animal settled to the benthos in January.

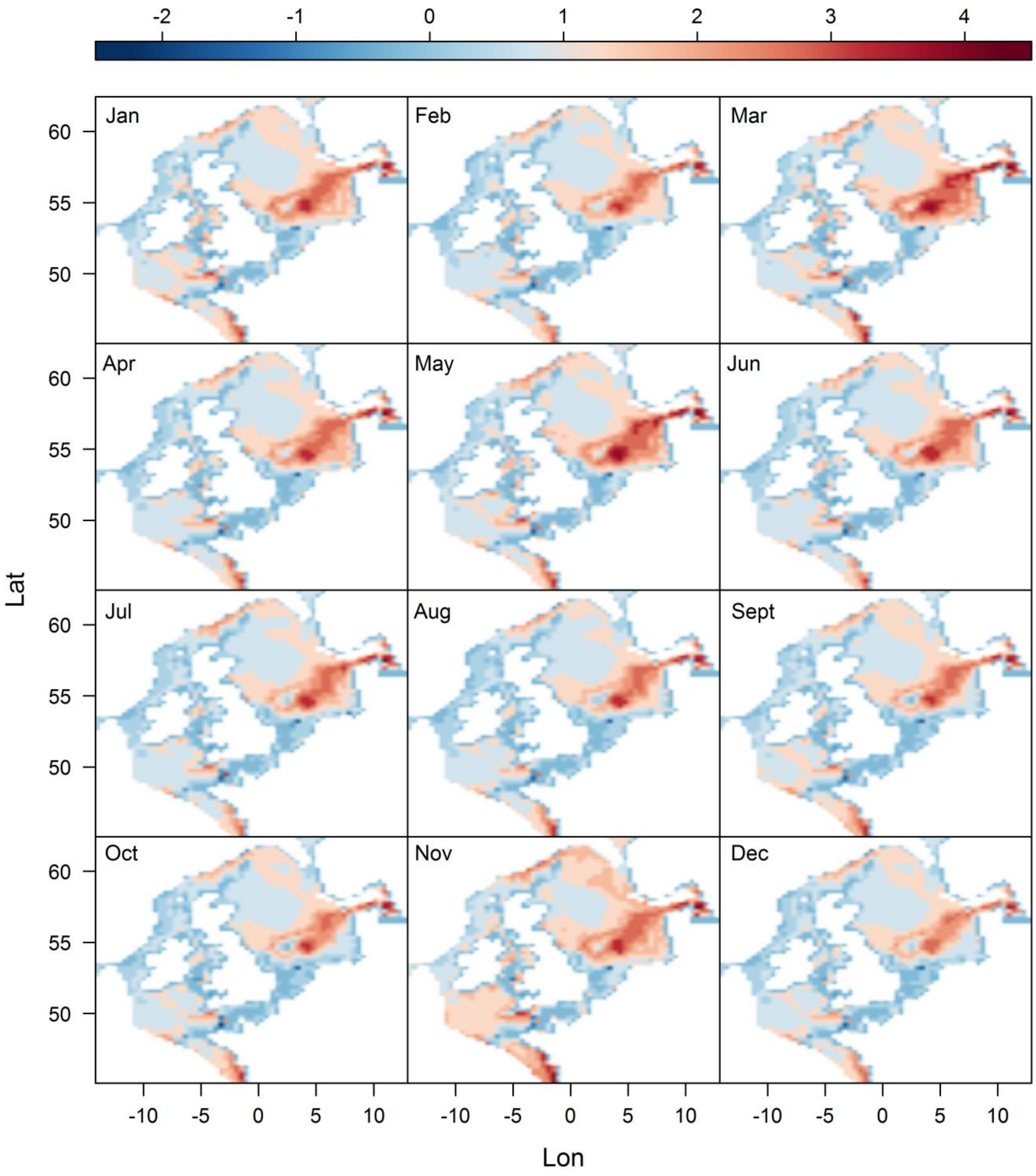

Figure C-9: Difference in predicted *L. depurator* lifetime allocation to reproduction (gC) between the periods 2006-2016 and 2038-2048

List of References

Abelló, P. 1989. Reproduction and moulting in *Liocarcinus depurator* (Linnaeus, 1758) (Brachyura: Portunidae) in the Northwestern Mediterranean sea. Scientia Marina, 53: 127-134.

Abelló, P., Sardá, R., and Masales, D. 1988. Infestation of some Mediterranean brachyuran crabs by the polychaete *Iphitime cuenoti*. Cahiers de Biologie Marine, 29: 149-162.

Ackefors, H., Castell, J. D., Boston, L. D., Räty, P., and Svensson, M. 1992. Standard experimental diets for crustacean nutrition research. II. Growth and survival of juvenile crayfish *Astacus astacus* (Linné) fed diets containing various amounts of protein, carbohydrate and lipid. Aquaculture, 104: 341-356.

Aguirre-Velarde, A., Jean, F., Thouzeau, G., and Flye-Sainte-Marie, J. 2018. Feeding behaviour and growth of the Peruvian scallop (*Argopecten purpuratus*) under daily cyclic hypoxia conditions. Journal of Sea Research, 131: 85-94.

Aguirre-Velarde, A., Pecquerie, L., Jean, F., Thouzeau, G., and Flye-Sainte-Marie, J. 2019. Predicting the energy budget of the scallop *Argopecten purpuratus* in an oxygen–limiting environment. Journal of Sea Research, 143: 254-261.

Aktaş, M., Kumlu, M., and Eroldogan, O. 2003. Off-season maturation and spawning of *Penaeus semisulcatus* by eyestalk ablation and/or temperature–photoperiod regimes. Aquaculture, 228: 361-370.

Alcaraz, M., and Sardà, F. 1981. Oxygen consumption by *Nephrops norvegicus* (L.), (Crustacea, Decapoda) in relationship with its moulting stage. Journal of Experimental Marine Biology and Ecology, 54: 113-118.

Alexander, J. E., and McMahon, R. F. 2004. Respiratory response to temperature and hypoxia in the zebra mussel *Dreissena polymorpha*. Comparative Biochemistry and Physiology Part A: Molecular & Integrative Physiology, 137: 425-434.

Algar, A. C., Kerr, J. T., and Currie, D. J. 2007. A test of Metabolic Theory as the mechanism underlying broad-scale species-richness gradients. Global Ecology and Biogeography, 16: 170-178.

Allen, J. I., Aiken, J., Anderson, T. R., Buitenhuis, E., Cornell, S., Geider, R. J., Haines, K., et al. 2010. Marine ecosystem models for earth systems applications: The MarQUEST experience. Journal of Marine Systems, 81: 19-33.

Altieri, A. H., Harrison, S. B., Seemann, J., Collin, R., Diaz, R. J., and Knowlton, N. 2017. Tropical dead zones and mass mortalities on coral reefs. Proceedings of the National Academy of Sciences, 114: 3660-3665.

Alunno-Bruscia, M., Bourlès, Y., Maurer, D., Robert, S., Mazurié, J., Gangnery, A., Goulletquer, P., et al. 2011. A single bio-energetics growth and reproduction model for the oyster *Crassostrea gigas* in six Atlantic ecosystems. Journal of Sea Research, 66: 340-348.

Alunno-Bruscia, M., van der Veer, H. W., and Kooijman, S. 2009. The AquaDEB project (phase I): Analysing the physiological flexibility of aquatic species and connecting physiological diversity to ecological and evolutionary processes by using Dynamic Energy Budgets. Journal of Sea Research, 62: 43-48.

AmP 2017. Add-my-Pet database of DEB parameters. 09/02/2016 edn.

Ananthasubramaniam, B., McCauley, E., Gust, K. A., Kennedy, A. J., Muller, E. B., Perkins, E. J., and Nisbet, R. M. 2014. Relating suborganismal processes to ecotoxicological and population level endpoints using a bioenergetic model. Ecological Applications, 25: 1691-1710.

Apol, M. E. F., Etienne, R. S., and Olff, H. 2008. Revisiting the evolutionary origin of allometric metabolic scaling in biology. Functional Ecology, 22: 1070-1080.

Arnberg, M., Calosi, P., Spicer, J. I., Tandberg, A. H. S., Nilsen, M., Westerlund, S., and Bechmann, R. K. 2013. Elevated temperature elicits greater effects than decreased pH on the development, feeding and metabolism of northern shrimp (*Pandalus borealis*) larvae. Marine Biology, 160: 2037-2048.

Artigaud, S., Lacroix, C., Pichereau, V., and Flye-Sainte-Marie, J. 2014. Respiratory response to combined heat and hypoxia in the marine bivalves *Pecten maximus* and *Mytilus* spp. Comparative Biochemistry and Physiology Part A: Molecular & Integrative Physiology, 175: 135-140.

Augustine, S., Rosa, S., Kooijman, S. A. L. M., Carlotti, F., Poggiale, J.-C., and 2014. Modeling the eco-physiology of the purple mauve stinger, *Pelagia noctiluca* using Dynamic Energy Budget theory. Journal of Sea Research, 94: 52-64.

Baas, J., Jager, T., and Kooijman, B. 2010. A review of DEB theory in assessing toxic effects of mixtures. Science of The Total Environment, 408: 3740-3745.

Baden, S., L. J. Håkansson, C., and Spicer, J. 2003. Between-individual variation in haemocyanin concentrations in the Norway lobster *Nephrops norvegicus* following exposure to hypoxia and manganese. Marine Biology, 143: 267-273.

Baden, S. P., Pihl, L., and Rosenberg, R. 1990. Effects of oxygen depletion on the ecology, blood physiology and fishery of the Norway lobster *Nephrops norvegicus*. Marine Ecology Progress Series, 67: 141-155.

Bai, N., Zhang, W., Mai, K., Wang, X., Xu, W., and Ma, H. 2010. Effects of discontinuous administration of β-glucan and glycyrrhizin on the growth and immunity of white shrimp *Litopenaeus vannamei*. Aquaculture, 306: 218-224.

Balogh, R., Wolfe, K., and Byrne, M. 2018. Gonad development and spawning of the vulnerable commercial sea cucumber, *Stichopus herrmanni*, in the southern Great Barrier Reef. Journal of the Marine Biological Association of the United Kingdom, 99: 1-9.

Banks, S. C., Ling, S. D., Johnson, C. R., Piggott, M. P., Williamson, J. E., and Beheregaray, L. B. 2010. Genetic structure of a recent climate change-driven range extension. Molecular Ecology, 19: 2011-2024.

Barillé, L., Lerouxel, A., Dutertre, M., Haure, J., Barillé, A.-L., Pouvreau, S., and Alunno-Bruscia, M. 2011. Growth of the Pacific oyster (*Crassostrea gigas*) in a high-turbidity environment: Comparison of model simulations based on scope for growth and dynamic energy budgets. Journal of Sea Research, 66: 392-402.

Barkai, A., and McQuaid, C. 1988. Predator-prey role reversal in a marine benthic ecosystem. Science, 242: 62-64.

Barker, M. F., and Nichols, D. 1983. Reproduction, recruitment and juvenile ecology of the starfish, *Asterias rubens* and *Marthasterias glacialis*. Journal of the Marine Biological Association of the United Kingdom, 63: 745-765.

Barros, P., Sobral, P., Range, P., Chícharo, L., and Matias, D. 2013. Effects of sea-water acidification on fertilization and larval development of the oyster *Crassostrea gigas*. Journal of Experimental Marine Biology and Ecology, 440: 200-206.

Basford, D. J., Eleftheriou, A., and Raffaelli, D. 1989. The epifauna of the northern North Sea (56°–61°N). Journal of the Marine Biological Association of the United Kingdom, 69: 387-407.

Beaugrand, G., Brander, K. M., Alistair Lindley, J., Souissi, S., and Reid, P. C. 2003. Plankton effect on cod recruitment in the North Sea. Nature, 426: 661-664.

Beaugrand, G., Reid, P. C., Ibañez, F., Lindley, J. A., and Edwards, M. 2002. Reorganization of North Atlantic marine copepod biodiversity and climate. Science, 296: 1692-1694.

Bergmann, M., and Moore, P. G. 2001. Survival of decapod crustaceans discarded in the *Nephrops* fishery of the Clyde Sea area, Scotland. ICES Journal of Marine Science, 58: 163-171.

Bergmann, M., Taylor, A. C., and Moore, P. G. 2001. Physiological stress in decapod crustaceans (*Munida rugosa* and *Liocarcinus depurator*) discarded in the Clyde Nephrops fishery. Journal of Experimental Marine Biology and Ecology, 259: 215-229.

Bergmann, M., Wieczorek, S. K., Moore, P. G., and Atkinson, R. J. A. 2002. Discard composition of the *Nephrops* fishery in the Clyde Sea area, Scotland. Fisheries Research, 57: 169-183.

Bernard, I., de Kermoysen, G., and Pouvreau, S. 2011. Effect of phytoplankton and temperature on the reproduction of the Pacific oyster Crassostrea gigas: Investigation through DEB theory. Journal of Sea Research, 66: 349-360.

Bernhardt, J. R., and Leslie, H. M. 2013. Resilience to climate change in coastal marine ecosystems. Annual Review of Marine Science, 5: 371-392.

Berthelin, C., Kellner, K., and Mathieu, M. 2000. Storage metabolism in the Pacific oyster (*Crassostrea gigas*) in relation to summer mortalities and reproductive cycle (West Coast of France). Comparative Biochemistry and Physiology Part B: Biochemistry and Molecular Biology, 125: 359-369.

Birchenough, S. N. R., Reiss, H., Degraer, S., Mieszkowska, N., Borja, Á., Buhl-Mortensen, L., Braeckman, U., Craeymeersch, J., De Mesel, I., Kerckhof, F., Kröncke, I., Parra, S., Rabaut, M., Schröder, A., Van Colen, C., Van Hoey, G., Vincx, M., and Wätjen, K. 2015. Climate change and marine benthos: a review of existing research and future directions in the North Atlantic. Wiley Interdisciplinary Reviews: Climate Change, 6: 203-223.

Biscéré, T., Rodolfo-Metalpa, R., Lorrain, A., Chauvaud, L., Thébault, J., Clavier, J., and Houlbrèque, F. 2015. Responses of two scleractinian corals to cobalt pollution and ocean acidification. PLoS ONE, 10: e0122898.

Blanchard, F., LeLoc'h, F., Hily, C., and Boucher, J. 2004. Fishing effects on diversity, size and community structure of the benthic invertebrate and fish megafauna on the Bay of Biscay coast of France. Marine Ecology Progress Series, 280: 249-260.

Boesch, D. F., and Rabalais, N. N. 1991. Effects of hypoxia on continental shelf benthos: comparisons between the New York Bight and the Northern Gulf of Mexico. Geological Society, London, Special Publications, 58: 27-34.

Boudreau, S. A., and Worm, B. 2012. Ecological role of large benthic decapods in marine ecosystems: a review. Marine Ecology Progress Series, 469: 195-213.

Bourlès, Y., Alunno-Bruscia, M., Pouvreau, S., Tollu, G., Leguay, D., Arnaud, C., Goulletquer, P., Kooijman, S.A.L.M. 2009. Modelling growth and reproduction of the Pacific oyster *Crassostrea gigas*: Advances in the oyster-DEB model through application to a coastal pond. Journal of Sea Research, 62: 62-71.

Bowner, T. 1982. Reproduction in *Amphiura filiformis* (Echinodermata: Ophiuroidea): Seasonality in gonad development. Marine Biology, 69: 281-290.

Boyd, P., Dillingham, P., McGraw, C., Armstrong, E., Cornwall, C., Feng, Y.-y., Hurd, C., Gault-Ringold, M., Roleda, M.Y., Timmins-Schiffman, E., and Nunn, B.L. 2016. Physiological responses of a Southern Ocean diatom to complex future ocean conditions. Nature Climate Change, 6: 207-213.

Boyd, P., and Ellwood, M. 2010. The biogeochemical cycle of iron in the ocean. Nature Geoscience, 3: 675-682.

Boyd, P. W., and Brown, C. J. 2015. Modes of interactions between environmental drivers and marine biota. Frontiers in Marine Science, 2: DOI=10.3389/fmars.2015.00009.

Boyd, P. W., Collins, S., Dupont, S., Fabricius, K., Gattuso, J.-P., Havenhand, J., Hutchins, D. A., Riebesell, U., Rintoul, M., Vichi, M., Biswas, H., Ciotti, A., Gao, K., Gehlan, M., Hurd, C.L., Kurihara, H., McGraw, C.M., Navarro, J.M., Nilsson, G.E., Passow, U., and Pörtner, H-O. 2018. Experimental strategies to assess the biological ramifications of multiple drivers of global ocean change—A review. Global Change Biology, 24: 2239-2261.

Boyd, P. W., Lennartz, S. T., Glover, D. M., and Doney, S. C. 2014. Biological ramifications of climate-change-mediated oceanic multi-stressors. Nature Climate Change, 5: 71.

Bozinovic, F., Calosi, P., and Spicer, J. I. 2011. Physiological Correlates of Geographic Range in Animals. Annual Review of Ecology, Evolution, and Systematics, 42: 155-179.

Bozinovic, F., and Pörtner, H.-O. 2015. Physiological ecology meets climate change. Ecology and Evolution, 5: 1025-1030.

Brandt, S., Gerken, M., Hartman, K., and Demers, E. 2009. Effects of hypoxia on food consumption and growth of juvenile striped bass (*Morone saxatilis*). Journal of Experimental Marine Biology and Ecology, 381(S1): S143-S149.

Brante, A., and Hughes, R., N 2001. The effect of hypoxia on the prey-handling behaviour of *Carcinus maenas* feeding on *Mytilus edulis*. Marine Ecology Progress Series, 209: 301-305.

Breckling, B. 2002. Individual-Based Modelling Potentials and Limitations. The Scientific World Journal, 2: 1044-1062.

Breitburg, D. L. 1992. Episodic hypoxia in Chesapeake Bay: Interacting effects of recruitment, behavior, and physical disturbance. Ecological Monographs, 62: 525-546.

Breitburg, D. L., Levin, L. A., Oschlies, A., Grégoire, M., Chavez, F. P., Conley, D. J., Garçon, V., Gilbert, D., Gutiérrez, D., Isensee, K., Jacinto, G.S., Limburg, K.E., Montes, I., Naqvi, S.W.A., Pitcher, G.C., Rabalais, N., Roman, M.R., Rose, K., Seibel, B., Telszewski, M., Yasuhara, M., and Zhang, J. 2018. Declining oxygen in the global ocean and coastal waters. Science, 359: eaam7240.

Bremner, J., Rogers, S. I., and Frid, C. L. J. 2003. Assessing functional diversity in marine benthic ecosystems: a comparison of approaches. Marine Ecology Progress Series, 254: 11-25.

Brockmann, U., Topcu, D., Schütt, M., and Leujak, W. 2018. Eutrophication assessment in the transit area German Bight (North Sea) 2006–2014 – Stagnation and limitations. Marine Pollution Bulletin, 136: 68-78.

Brown, J. H., and Gillooly, J. F. 2003. Ecological food webs: High-quality data facilitate theoretical unification. Proceedings of the National Academy of Sciences, 100: 1467-1468.

Brown, J. H., Gillooly, J. F., Allen, A. P., Savage, V. M., and West, G. B. 2004. Toward a metabolic theory of ecology. Ecology, 85: 1771-1789.

Bruggeman, J. 2019. Debber: build a Dynamic Energy Budget model for any species. Plymouth Marine Laboratory. https://deb.bolding-bruggeman.com/

Brylawski, B. J., and Miller, T. J. 2006. Temperature-dependent growth of the blue crab (*Callinectes sapidus*): a molt process approach. Canadian Journal of Fisheries and Aquatic Sciences, 63: 1298-1308.

Buchanan, J. B. 1993. Evidence of benthic pelagic coupling at a station off the Northumberland coast. Journal of Experimental Marine Biology and Ecology, 172: 1-10.

Buchanan, J. B., and Moore, J. J. 1986. Long-term studies at a benthic station off the coast of Northumberland. Hydrobiologia, 142: 121-127.

Buchholz, C. M., Buchholz, F., and Tarling, G. A. 2006. On the timing of moulting processes in reproductively active Northern krill *Meganyctiphanes norvegica*. Marine Biology, 149: 1443-1452.

Burrows, M. T., Schoeman, D. S., Buckley, L. B., Moore, P., Poloczanska, E. S., Brander, K. M., Brown, C., Bruno, J.F., Duarte, C.M., Halpern, B.S., Holding, J., Kappel, C.V., Kiessling, W., O'Connor, M.I., Pandolfi, J.M., Parmesan, C., Schwing, F.B., Sydeman, W.J., and Richardson, A.J. 2011. The pace of shifting climate in marine and terrestrial ecosystems. Science, 334: 652-655.

Büscher, J. V., Form, A. U., and Riebesell, U. 2017. Interactive effects of ocean acidification and warming on growth, fitness and survival of the cold-water coral *Lophelia pertusa* under different food availabilities. Frontiers in Marine Science, 4. https://doi.org/10.3389/fmars.2017.00101

Butchart, S. H. M., Walpole, M., Collen, B., van Strien, A., Scharlemann, J. P. W., Almond, R. E. A., Baillie, J. E. M., Bomhard, B., Brown, C., Bruno, J., Carpenter, K.E., Carr, G., Chanson, J., Chenery, A., Csirke, J., Davidson, N., Dentener, F., Foster, M., Galli, A., Galloway, J.N., Genovesi, P., Gregory, R.D., Hockings, M., Kapos, V., Lamarque, J-F., Leverington, F., Loh, J.,McGeoch, M.A., McRae, L., Minasyan, A., Hernández Morcillo, M., Oldfield, T.E.E., Pauly, D., Quader, S., Revenga, C., Sauer, J.R., Skolnik, B., Spear, D., Stanwell-Smith, D., Stuart, S.N., Symes, A., Tierney, M., Tyrrell, T., Vié, J-C., and Watson, R . 2010. Global biodiversity: Indicators of recent declines. Science, 328: 1164-1168.

Byrne, M., Ho, M., Selvakumaraswamy, P., Nguyen, H. D., Dworjanyn, S. A., and Davis, A. R. 2009. Temperature, but not pH, compromises sea urchin fertilization and early development under near-future climate change scenarios. Proceedings of the Royal Society of London B: Biological Sciences, 276: 1883-1888.

Caddy, J. F. 2003. Scaling elapsed time: an alternative approach to modelling crustacean moulting schedules? Fisheries Research, 63: 73-84.

Calder-Potts, R., Spicer, J. I., Calosi, P., Findlay, H. S., and Widdicombe, S. 2015. A mesocosm study investigating the effects of hypoxia and population density on respiration and reproductive biology in the brittlestar *Amphiura filiformis*. Marine Ecology Progress Series, 534: 135-147.

Campos, J., Van der Veer, H. W., Freitas, V., and Kooijman, S. A. L. M. 2009. Contribution of different generations of the brown shrimp *Crangon crangon* (L.) in the Dutch Wadden Sea to commercial fisheries: A dynamic energy budget approach. Journal of Sea Research, 62: 106-113.

Cannicci, S., Dahdouh-Guebas, F., Dyane, A., and Vannini, M. 1996. Natural diet and feeding habits of *Thalamita Crenata* (Decapoda: Portunidae). Journal of Crustacean Biology, 16: 678-683.

Capasso, E., Jenkins, S. R., Frost, M., and Hinz, H. 2010. Investigation of benthic community change over a century-wide scale in the western English Channel. Journal of the Marine Biological Association of the United Kingdom, 90: 1161-1172.

Careddu, G., Calizza, E., Costantini, M. L., and Rossi, L. 2017. Isotopic determination of the trophic ecology of a ubiquitous key species – The crab *Liocarcinus depurator* (Brachyura: Portunidae). Estuarine, Coastal and Shelf Science, 191: 106-114.

Carvalho, P. S. M., and Phan, V. N. 1998. Oxygen consumption and ammonia excretion during the moulting cycle in the shrimp *Xiphopenaeus kroyeri*. Comparative Biochemistry and Physiology Part A: Molecular & Integrative Physiology, 119: 839-844.

Castro, M. 1992. A methodology for obtaining information on the age structure and growth rates of the Norway Lobster, *Nephrops norvegicus* (L.) (Decapoda, Nephropoidea). Crustaceana, 63: 29-43.

Catchpole, T. L., Frid, C. L. J., and Gray, T. S. 2006. Importance of discards from the English *Nephrops norvegicus* fishery in the North Sea to marine scavengers. Marine Ecology Progress Series, 313: 215-226.

Cawthorn, D.-M., and Hoffman, L. C. 2017. Deceit with decapods? Evaluating labelling accuracy of crustacean products in South Africa. Food Control, 73: 741-753.

Chabot, D., and Dutil, J., D. 1999. Reduced growth of Atlantic cod in non-lethal hypoxic conditions. Journal of Fish Biology, 55: 472-491.

Chamberlain, J., Fernandes, T. F., Read, P., Nickell, T. D., and Davies, I. M. 2001. Impacts of biodeposits from suspended mussel (*Mytilus edulis* L.) culture on the surrounding surficial sediments. ICES Journal of Marine Science, 58: 411-416.

Chan, K. Y. K., García, E., and Dupont, S. 2015. Acidification reduced growth rate but not swimming speed of larval sea urchins. Scientific Reports, 5: 9764. https://dx.doi.org/10.1038%2Fsrep09764

Chang, Y.-J., Sun, C.-L., Chen, Y., and Yeh, S.-Z. 2012. Modelling the growth of crustacean species. Reviews in Fish Biology and Fisheries, 22: 157-187.

CHARM. 2012. Species and habitats - *Liocarcinus depurator* - Presence probability (2006-2012). https://sextant.ifremer.fr/record/2986ee88-c827-4e90-803a-502d13e2fd28/

Chatterton, T. D., and Williams, B. G. 1994. Activity patterns of the New Zealand cancrid crab *Cancer novaezelandiae* (Jacquinot) in the field and laboratory. Journal of Experimental Marine Biology and Ecology, 178: 261-274.

Chen, Y., and Kennelly, S. 1999. Growth of spanner crabs, *Ranina ranina*, off the east coast of Australia. Marine and Freshwater Research, 50: 319-325.

Cheung, S. G., Chan, H. Y., Liu, C. C., and Shin, P. K. S. 2008. Effect of prolonged hypoxia on food consumption, respiration, growth and reproduction in marine scavenging gastropod *Nassarius festivus*. Marine Pollution Bulletin, 57: 280-286.

Cheung, W. W. L., Dunne, J., Sarmiento, J. L., and Pauly, D. 2011. Integrating ecophysiology and plankton dynamics into projected maximum fisheries catch potential under climate change in the Northeast Atlantic. ICES Journal of Marine Science, 68: 1008-1018.

Cheung, W. W. L., Watson, R., and Pauly, D. 2013. Signature of ocean warming in global fisheries catch. Nature, 497: 365-368.

Chevene, F., Doléadec, S., and Chessel, D. 1994. A fuzzy coding approach for the analysis of long-term ecological data. Freshwater biology, 31: 295-309.

Chikina, M. V., Spiridonov, V. A., and Mardashova, M. V. 2014. Spatial and temporal variability of coastal benthic communities in the Keretsky Archipelago area and in the Velikaya Salma Strait (Karelian coast, the White Sea). Oceanology, 54: 54-65.

Claireaux, G., Webber, D. M., Lagardère, J. P., and Kerr, S. R. 2000. Influence of water temperature and oxygenation on the aerobic metabolic scope of Atlantic cod (*Gadus morhua*). Journal of Sea Research, 44: 257-265.

Clare, D. S., Robinson, L. A., and Frid, C. L. J. 2015. Community variability and ecological functioning: 40 years of change in the North Sea benthos. Marine Environmental Research, 107: 24-34.

Clare, D. S., Spencer, M., Robinson, L. A., and Frid, C. L. J. 2017. Explaining ecological shifts: the roles of temperature and primary production in the long-term dynamics of benthic faunal composition. Oikos, 126: 1123-1133.

Coma, R., Ribes, M., Gili, J.-M., and Zabala, M. 1998. An energetic approach to the study of life-history traits of two modular colonial benthic invertebrates. Marine Ecology Progress Series, 162: 89-103.

Côté, I. M., Darling, E. S., and Brown, C. J. 2016. Interactions among ecosystem stressors and their importance in conservation. Proceedings of the Royal Society B: Biological Sciences, 283: 20152592. https://dx.doi.org/10.1098%2Frspb.2015.2592

Crim, R. N., Sunday, J. M., and Harley, C. D. G. 2011. Elevated seawater CO_2 concentrations impair larval development and reduce larval survival in endangered northern abalone (*Haliotis kamtschatkana*). Journal of Experimental Marine Biology and Ecology, 400: 272-277.

Curry, R., Dickson, B., and Yashayaev, I. 2003. A change in the freshwater balance of the Atlantic Ocean over the past four decades. Nature, 426: 826-829.

Cuzin-Roudy, J., and Buchholz, F. 1999. Ovarian development and spawning in relation to the moult cycle in Northern krill, *Meganyctiphanes norvegica* (Crustacea: Euphausiacea), along a climatic gradient. Marine Biology, 133: 267-281.

da Silva-Castiglioni, D., Oliveira, G. T., and Buckup, L. 2010. Metabolic responses of *Parastacus defossus* and *Parastacus brasiliensis* (Crustacea, Decapoda, Parastacidae) to hypoxia. Comparative Biochemistry and Physiology Part A: Molecular & Integrative Physiology, 156: 436-444.

Daan, N., Richardson, K., and Pope, J. G. 1996. Changes in the North Sea ecosystem and their causes: Aarhus 1975 revisited. ICES Journal of Marine Science, 53: 879-883

Das, T., and Stickle, W. B. 1993. Sensitivity of crabs *Callinectes sapidus* and *C. similis* and the gastropod *Stramonita haemastoma* to hypoxia and anoxia. Marine Ecology Progress Series, 98: 263-263.

Dauwe, B., Herman, P. M. J., and Heip, H. R. 1998. Community structure and bioturbation potential of macrofauna at four North Sea stations with contrasting food supply. Marine Ecology Progress Series, 173: 67-83.

De Roos, A., Xe, M, and Persson, L. 2001. Physiologically structured models: From versatile technique to ecological theory. Oikos, 94: 51-71.

De Wolf, P. 1973. Ecological observations on the mechanisms of dispersal of barnacle larvae during planktonic life and settling. Netherlands Journal of Sea Research, 6: 1-129.

Decker, M. B., Breitburg, D. L., and Purcell, J. E. 2004. Effects of low dissolved oxygen on zooplankton predation by the ctenophore *Mnemiopsis leidyi*. Marine Ecology Progress Series, 280: 163-172.

Dell, A. I., Pawar, S., and Savage, V. M. 2011. Systematic variation in the temperature dependence of physiological and ecological traits. Proceedings of the National Academy of Sciences, 108: 10591-10596.

DePasquale, E., Baumann, H., and Gobler, C. J. 2015. Vulnerability of early life stage Northwest Atlantic forage fish to ocean acidification and low oxygen. Marine Ecology Progress Series, 523: 145-156.

Depestele, J., Desender, M., Benoît, H. P., Polet, H., and Vincx, M. 2014. Short-term survival of discarded target fish and non-target invertebrate species in the “eurocutter” beam trawl fishery of the southern North Sea. Fisheries Research, 154: 82-92.

Desai, D., and Prakash, S. 2009. Physiological responses to hypoxia and anoxia in *Balanus amphitrite* (Cirripedia: Thoracica). Marine Ecology Progress Series, 390: 157-166.

Deutsch, C., Ferrel, A., Seibel, B., Pörtner, H.-O., and Huey, R. B. 2015. Climate change tightens a metabolic constraint on marine habitats. Science, 348: 1132-1135.

Diaz, R. J., and Rosenberg, R. 2008. Spreading Dead Zones and consequences for marine ecosystems. Science, 321: 926-929.

Dickson, A., Sabine, C., and Christian, J. 2007. Guide to best practices for ocean CO2 measurements, PICES Spec. Publ, 3: IOCCP Report no. 8. 191pp.

Dissanayake, A., Clough, R., Spicer, J. I., and Jones, M. B. 2010. Effects of hypercapnia on acid–base balance and osmo-/iono-regulation in prawns (Decapoda: Palaemonidae). Aquatic Biology, 11: 27-36.

Doherty, P., and Fowler, A. 1994. Demographic consequences of variable recruitment to coral reef fish populations: a congeneric comparison of two damselfishes. Bulletin of Marine Science, 54: 297-313.

Doney, S. C., Fabry, V. J., Feely, R. A., and Kleypas, J. A. 2009. Ocean Acidification: The other CO_2 problem. Annual Review of Marine Science, 1: 169-192.

Doney, S. C., Ruckelshaus, M., Duffy, J. E., Barry, J. P., Chan, F., English, C. A., Galindo, H. M., Grebmeier, J.M., Hollowed, A.B., Knowlton, N., Polovina, J., Rabalais, N, N., Sydeman, W.J., and Talley, L. D. 2012. Climate change impacts on marine ecosystems. Annual Review of Marine Science, 4: 11-37.

Drach, P., and Tchernigovtzeff, C. 1967. Sur la methode de détermination des stades d'intermue et son application générale aux crustacés. Vie milieu, 18: 595-607.

Duarte, C., Navarro, J., Acuña, K., Torres, R., Manríquez, P., Lardies, M., Vargas, C., Lagos, N.A., and Aguilera, V. 2014. Combined effects of temperature and ocean acidification on the juvenile individuals of the mussel *Mytilus chilensis*. Journal of Sea Research, 85: 308-314.

Dupont, S., Havenhand, J., Thorndyke, W., Peck, L., and Thorndyke, M. 2008. Near-future level of CO_2-driven ocean acidification radically affects larval survival and development in the brittlestar *Ophiothrix fragilis*. Marine Ecology Progress Series, 373: 285-294.

Easton, M. D. L., and Misra, R. K. 1988. Mathematical representation of crustacean growth. ICES Journal of Marine Science, 45: 61-72.

Edmunds, P. J., Brown, D., and Moriarty, V. 2012. Interactive effects of ocean acidification and temperature on two scleractinian corals from Moorea, French Polynesia. Global Change Biology, 18: 2173-2183.

Ehrhardt, N. M. 2008. Estimating growth of the Florida spiny lobster, *Panulirus argus*, from molt frequency and size increment data derived from tag and recapture experiments. Fisheries Research, 93: 332-337.

Elith, J., and Leathwick, J. R. 2009. Species distribution models: ecological explanation and prediction across space and time. Annual Review of Ecology, Evolution, and Systematics, 40: 677-697.

Ellis, J. R., Martinez, I., Burt, G. J., and Scott, B. E. 2013. Epibenthic assemblages in the Celtic Sea and associated with the Jones Bank. Progress in Oceanography, 117: 76-88.

Ellis, J. R., Rogers, S. I., and Freeman, S. M. 2000. Demersal assemblages in the Irish Sea, St George's Channel and Bristol Channel. Estuarine, Coastal and Shelf Science, 51: 299-315.

Elner, R. W., and Beninger, P. G. 1995. Multiple reproductive strategies in snow crab, *Chionoecetes opilio*: Physiological pathways and behavioral plasticity. Journal of Experimental Marine Biology and Ecology, 193: 93-112.

Endo, Y., and Yamano, F. 2006. Diel vertical migration of *Euphausia pacifica* (Crustacea, Euphausiacea) in relation to molt and reproductive processes, and feeding activity. Journal of Oceanography, 62: 693-703.

Enquist, B. J., Economo, E. P., Huxman, T. E., Allen, A. P., Ignace, D. D., and Gillooly, J. F. 2003. Scaling metabolism from organisms to ecosystems. Nature, 423: 639-642.

Ettershank, G. 1983. Age structure and cyclical annual size change in the Antarctic krill, *Euphausia superba* dana. Polar Biology, 2: 189-193.

Evans, T. G., Diamond, S. E., and Kelly, M. W. 2015. Mechanistic species distribution modelling as a link between physiology and conservation. Conservation Physiology, 3: cov056. https://doi.org/10.1093/conphys/cov056

FAO. 2016. The State of World Fisheries and Aquaculture. Contributing to food security and nutrition for all. Rome,200 pp. http://www.fao.org/3/a-i5555e.pdf

Fearman, J., and Moltschaniwskyj, N. A. 2010. Warmer temperatures reduce rates of gametogenesis in temperate mussels, *Mytilus galloprovincialis*. Aquaculture, 305: 20-25.

Fernandes, J. A., Cheung, W. W. L., Jennings, S., Butenschön, M., de Mora, L., Frölicher, T. L., Barange, M., and Grant, A. 2013. Modelling the effects of climate change on the distribution and production of marine fishes: accounting for trophic interactions in a dynamic bioclimate envelope model. Global Change Biology, 19: 2596-2607.

Fernández-Reiriz, M. J., Range, P., Álvarez-Salgado, X. A., and Labarta, U. 2011. Physiological energetics of juvenile clams *Ruditapes decussatus* in a high CO_2 coastal ocean. Marine Ecology Progress Series, 433: 97-105.

Fernández, L., González-Gurriarán, E., and Freire, J. 1991. Population biology of *Liocarcinus depurator* (Brachyura: Portunidae) in mussel raft culture areas in the Ria de Arousa (Galicia, NW Spain). Journal of the Marine Biological Association of the United Kingdom, 71: 375-390.

Filgueira, R., Rosland, R., and Grant, J. 2011. A comparison of scope for growth (SFG) and dynamic energy budget (DEB) models applied to the blue mussel (*Mytilus edulis*). Journal of Sea Research, 66: 403-410.

Findlay, H. S., Kendall, M. A., Spicer, J. I., Turley, C., and Widdicombe, S. 2008. Novel microcosm system for investigating the effects of elevated carbon dioxide and temperature on intertidal organisms. Aquatic Biology, 3: 51-62.

Findlay, H. S., Kendall, M. A., Spicer, J. I., and Widdicombe, S. 2010a. Post-larval development of two intertidal barnacles at elevated CO_2 and temperature. Marine Biology, 157: 725-735.

Findlay, H. S., Kendall, M. A., Spicer, J. I., and Widdicombe, S. 2010b. Relative influences of ocean acidification and temperature on intertidal barnacle post-larvae at the northern edge of their geographic distribution. Estuarine, Coastal and Shelf Science, 86: 675-682.

Flye-Sainte-Marie, J., Jean, F., Paillard, C., and Kooijman, S. A. L. M. 2009. A quantitative estimation of the energetic cost of brown ring disease in the Manila clam using Dynamic Energy Budget theory. Journal of Sea Research, 62: 114-123.

Fockedey, N., Mees, J., Vangheluwe, M., Verslycke, T., Janssen, C. R., and Vincx, M. 2005. Temperature and salinity effects on post-marsupial growth of *Neomysis integer* (Crustacea: Mysidacea). Journal of Experimental Marine Biology and Ecology, 326: 27-47.

Focken, U., Groth, A., Coloso, R. M., and Becker, K. 1998. Contribution of natural food and supplemental feed to the gut content of *Penaeus monodon* Fabricius in a semi-intensive pond system in the Philippines. Aquaculture, 164: 105-116.

Fordham, D. A., Mellin, C., Russell, B. D., Akçakaya, R. H., Bradshaw, C. J., Aiello-Lammens, M. E., Caley, J. M., Connell, S.D., Mayfield, S., Shepherd, S.A., and Brook, B.W. 2013. Population dynamics can be more important than physiological limits for determining range shifts under climate change. Global Change Biology, 19: 3224-3237.

Fowler, S. W. 1990. Critical review of selected heavy metal and chlorinated hydrocarbon concentrations in the marine environment. Marine Environmental Research, 29: 1-64.

Frainer, A., Primicerio, R., Kortsch, S., Aune, M., Dolgov, A. V., Fossheim, M., and Aschan, M. M. 2017. Climate-driven changes in functional biogeography of Arctic marine fish communities. Proceedings of the National Academy of Sciences, 114: 12202-12207.

Franke, H.-D., and Gutow, L. 2004. Long-term changes in the macrozoobenthos around the rocky island of Helgoland (German Bight, North Sea). Helgoland Marine Research, 58: 303-310.

Franklin, J. 2010. Mapping species distributions: spatial inference and prediction*,* Cambridge University Press, 340pp.

Freeman, S. M., Richardson, C. A., and Seed, R. 2001. Seasonal Abundance, Spatial Distribution, Spawning and Growth of *Astropecten irregularis* (Echinodermata: Asteroidea). Estuarine, Coastal and Shelf Science, 53: 39-49.

Frid, C. L. J., Buchanan, J. B., and Garwood, P. R. 1996. Variability and stability in benthos: twenty-two years of monitoring off Northumberland. ICES Journal of Marine Science, 53: 978-980.

Frid, C. L. J., Garwood, P. R., and Robinson, L. A. 2009a. The North Sea benthic system: a 36 year time-series. Journal of the Marine Biological Association of the United Kingdom, 89: 1-10.

Frid, C. L. J., Garwood, P. R., and Robinson, L. A. 2009b. Observing change in a North Sea benthic system: A 33 year time series. Journal of Marine Systems, 77: 227-236.

Frieder, C. A., Gonzalez, J. P., Bockmon, E. E., Navarro, M. O., and Levin, L. A. 2014. Can variable pH and low oxygen moderate ocean acidification outcomes for mussel larvae? Global Change Biology, 20: 754-764.

Gaines, S., and Roughgarden, J. 1985. Larval settlement rate: A leading determinant of structure in an ecological community of the marine intertidal zone. Proceedings of the National Academy of Sciences, 82: 3707-3711.

Gattuso, J.-P., Epitalon, J.-M., Lavigne, H., and Orr, J. 2018. seacarb:seawater carbonate chemistry. 3.2.10 edn.

Giangrande, A., Geraci, S., and Belmonte, G. 1994. Life—cycle and life—history diversity in marine invertebrates and the implications in community dynamics. Oceanography and Marine Biology: An Annual Review, 32: 305-333.

Gillooly, J. F., Allen, A. P., Brown, J. H., Elser, J. J., del Rio, C. M., Savage, V. M., West, G. B., Woodruff, W.H., and Woods, H.A. 2005. The metabolic basis of whole-organism RNA and phosphorus content. Proceedings of the National Academy of Sciences of the United States of America, 102: 11923-11927.

Glazier, D. S. 2005. Beyond the '3/4-power law': variation in the intra-and interspecific scaling of metabolic rate in animals. Biological Reviews, 80: 611-662.

Gleckler, J. P., Santer, B., Domingues, C., W. Pierce, D., P. Barnett, T., Church, J. A., E. Taylor, K., Achuta-Roa, K., Boyer, T., Ishii, M., and Caldwell, P. 2012. Human-induced global ocean warming on multidecadal timescales. Nature Climate Change, 2: 524-529.

Gobler, C. J., DePasquale, E. L., Griffith, A. W., and Baumann, H. 2014. Hypoxia and acidification have additive and synergistic negative effects on the growth, survival, and metamorphosis of early life stage bivalves. PLoS ONE, 9: e83648.

Gotelli, N. J., and Colwell, R. K. 2001. Quantifying biodiversity: procedures and pitfalls in the measurement and comparison of species richness. Ecology Letters, 4: 379-391.

Graf, G., Bengtsson, W., Diesner, U., Schulz, R., and Theede, H. 1982. Benthic response to sedimentation of a spring phytoplankton bloom: Process and budget. Marine Biology, 67: 201-208.

Gray, M. W., Langdon, C. J., Waldbusser, G. G., Hales, B., and Kramer, S. 2017. Mechanistic understanding of ocean acidification impacts on larval feeding physiology and energy budgets of the mussel *Mytilus californianus*. Marine Ecology Progress Series, 563: 81-94.

Green, A. L., Fernandes, L., Almany, G., Abesamis, R., McLeod, E., Aliño, P. M., White, A. T., Salm, R., Tanzer, J., and Pressey, R. 2014. Designing marine reserves for fisheries management, biodiversity conservation, and climate change adaptation. Coastal Management, 42: 143-159.

Greenwood, P. J. 1980. Growth, respiration and tentative energy budgets for two populations of the sea urchin *Parechinus angulosus* (Leske). Estuarine and Coastal Marine Science, 10: 347-367.

Griffen, B. D., Belgrad, B. A., Cannizzo, Z. J., Knotts, E. R., and Hancock, E. R. 2016. Rethinking our approach to multiple stressor studies in marine environments. Marine Ecology Progress Series, 543: 273-281.

Guillou, M., and Michel, C. 1993. Reproduction and growth of *Sphaerechinus granularis* (Echinodermata: Echinoidea) in southern Brittany. Journal of the Marine Biological Association of the United Kingdom, 73: 179-192.

Gunderson, A. R., Armstrong, E. J., and Stillman, J. H. 2016. Multiple stressors in a changing world: The need for an improved perspective on physiological responses to the dynamic marine environment. Annual Review of Marine Science, 8: 357-378.

Hagerman, L., and Uglow, R. F. 1985. Effects of hypoxia on the respiratory and circulatory regulation of *Nephrops norvegicus*. Marine Biology, 87: 273-278.

Halpern, B. S., Frazier, M., Potapenko, J., Casey, K. S., Koenig, K., Longo, C., Lowndes, J. S., Rockwood, R.C., Selig, E.R., Selkoe, K.A., and Walbridge, S. 2015. Spatial and temporal changes in cumulative human impacts on the world's ocean. Nature Communications, 6: 7615. https://dx.doi.org/10.1038%2Fncomms8615

Halpern, B. S., Walbridge, S., Selkoe, K. A., Kappel, C. V., Micheli, F., D'Agrosa, C., Bruno, J. F., CAsey, K., Ebert, C., Fox, H.E., Fujita, R., Heinemann, D., Lenihan, H.S., Madin, E., Perry, M., Selig, E., Spalding, M., Stenek, R., and Watson, R. 2008. A global map of human impact on marine ecosystems. Science, 319: 948-952.

Hamasaki, K. 2003. Effects of temperature on the egg incubation period, survival and developmental period of larvae of the mud crab *Scylla serrata* (Forskål) (Brachyura: Portunidae) reared in the laboratory. Aquaculture, 219: 561-572.

Harley, C. D. G. 2011. Climate change, keystone predation, and biodiversity loss. Science, 334: 1124-1127.

Harris, L. G., and Tyrrell, M. C. 2001. Changing community states in the Gulf of Maine: synergism between invaders, overfishing and climate change. Biological Invasions, 3: 9-21.

Hartvig, M., and Andersen, K. H. 2013. Coexistence of structured populations with size-based prey selection. Theoretical Population Biology, 89: 24-33.

Hartvig, M., Andersen, K. H., and Beyer, J. E. 2011. Food web framework for size-structured populations. Journal of Theoretical Biology, 272: 113-122.

Havenhand, J. N., Buttler, F.-R., Thorndyke, M. C., and Williamson, J. E. 2008. Near-future levels of ocean acidification reduce fertilization success in a sea urchin. Current Biology, 18: R651-R652.

Helmuth, B., Broitman, B. R., Blanchette, C. A., Gilman, S., Halpin, P., Harley, C. D. G., O'Donnell, M. J., Hofmann, G., Menge, B., and Strickland, D. 2006.Mosaic patterns of thermal stress in the rocky intertidal zone: Implications for climate change. Ecological Monographs, 76: 461-479.

Helmuth, B., Kingsolver, J. G., and Carrington, E. 2005. Biophysics, physiological ecology and cliamte change: Does mechanism matter? Annual Review of Physiology, 67: 177-201.

Herrmann, M., Alfaya, J. E. F., Lepore, M. L., Penchaszadeh, P. E., and Laudien, J. 2009. Reproductive cycle and gonad development of the Northern Argentinean *Mesodesma mactroides* (Bivalvia: Mesodesmatidae). Helgoland Marine Research, 63: 207-218.

Highfield, J. M., Eloire, D., Conway, D. V. P., Lindeque, P. K., Attrill, M. J., and Somerfield, P. J. 2010. Seasonal dynamics of meroplankton assemblages at station L4. Journal of Plankton Research, 32: 681-691.

Hill, S. K., and Lawrence, J. M. 2006. Interactive effects of temperature and nutritional condition on the energy budgets of the sea urchins *Arbacia punctulata* and *Lytechinus variegatus* (Echinodermata: Echinoidea). Journal of the Marine Biological Association of the United Kingdom, 86: 783-790.

Hinz, H., Kröncke, I., and Ehrich, S. 2004. Seasonal and annual variability in an epifaunal community in the German Bight. Marine Biology, 144: 735-745.

Hoegh-Guldberg, O. 1999. Climate change, coral bleaching and the future of the world's coral reefs. Marine and Freshwater Research, 50: 839-866.

Hofmann, G. E., Smith, J. E., Johnson, K. S., Send, U., Levin, L. A., Micheli, F., Paytan, A., Price, N., Peterson, B., Takeshita, Y., Matson, P., Derse Crook, E., Kroeker, K., Gambi, M.C., Rivest, E., Frieder, C., Yu, P., and Martz, T. 2011. High-frequency dynamics of ocean pH: A multi-ecosystem comparison. PLoS ONE, 6: e28983.

Hoggarth, D. D., Abeyasekera, S., Arthur, R. I., Beddington, J. R., Burn, R. W., Halls, A. S., Kirkwood, G. P., McAllister, M., Medley, P., Meeds, C., Parkes, G., Pilling, G., Wakeford, R., and Welcomme, R. 2006. Stock assessment for fishery management : a framework guide to the stock assessment tools of the Fisheries Management Science Programme. FAO Fisheries Technical Paper 487. Food and Agriculture Organization of the United Nations, Rome, Italy.

Hou, C., Zuo, W., Moses, M. E., Woodruff, W. H., Brown, J. H., and West, G. B. 2008. Energy uptake and allocation during ontogeny. Science, 322: 736-739.

Hrycik, A. R., Almeida, L. Z., and Höök, T. O. 2017. Sub-lethal effects on fish provide insight into a biologically-relevant threshold of hypoxia. Oikos, 126: 307-317.

Hughes, T. P. 1990. Recruitment limitation, mortality, and population regulation in open systems: A case study. Ecology, 71: 12-20.

Hunter, E., and Naylor, E. 1993. Intertidal migration by the shore crab *Carcinus maenas*. Marine Ecology Progress Series, 101: 131-138.

Huntley, M. E., and Lopez, M. D. G. 1992. Temperature-dependent production of marine copepods: A global synthesis. The American Naturalist, 140: 201-242.

Iguchi, N., and Ikeda, T. 1995. Growth, metabolism and growth efficiency of a euphasiis crustacean *Euphausia pacifica* in the southern Japan Sea, as influenced by temperature. Journal of Plankton Research, 17: 1757–1769.

Iguchi, N., and Ikeda, T. 2005. Effects of temperature on metabolism, growth and growth efficiency of *Thysanoessa longipes* (Crustacea: Euphausiacea) in the Japan Sea. Journal of Plankton Research, 27: 1-10.

IPBES. 2019. Global Assessment Report on Biodiversity and Ecosystem Services: Summary for policymakers. IPBES secretariat, Bonn, Germany

IPCC 2014. Climate Change 2014 – Impacts, Adaptation and Vulnerability: Part A: Global and Sectoral Aspects: Working Group II Contribution to the IPCC Fifth Assessment Report: Volume 1: Global and Sectoral Aspects, Cambridge University Press, Cambridge.

IPCC. 2018. Global Warming of 1.5°C. An IPCC Special Report on the impacts of global warming of 1.5°C above pre-industrial levels and related global greenhouse gas emission pathways, in the context of strengthening the global response to the threat of climate change, sustainable development, and efforts to eradicate poverty.

Ivanina, A. V., and Sokolova, I. M. 2015. Interactive effects of metal pollution and ocean acidification on physiology of marine organisms. Current Zoology, 61: 653-668.

Jager, T., Barsi, A., Hamda, N. T., Martin, B. T., Zimmer, E. I., and Ducrot, V. 2014. Dynamic energy budgets in population ecotoxicology: Applications and outlook. Ecological Modelling, 280: 140-147.

Jager, T., and Klok, C. 2010. Extrapolating toxic effects on individuals to the population level: the role of dynamic energy budgets. Philosophical Transactions of the Royal Society of London B: Biological Sciences, 365: 3531-3540.

Jager, T., and Ravagnan, E. 2015. Parameterising a generic model for the dynamic energy budget of Antarctic krill *Euphausia superba*. Marine Ecology Progress Series, 519: 115-128.

Jager, T., and Ravagnan, E. 2016. Modelling growth of northern krill (*Meganyctiphanes norvegica*) using an energy-budget approach. Ecological Modelling, 325: 28-34.

Jager, T., Ravagnan, E., and Dupont, S. 2016. Near-future ocean acidification impacts maintenance costs in sea-urchin larvae: Identification of stress factors and tipping points using a DEB modelling approach. Journal of Experimental Marine Biology and Ecology, 474: 11-17.

Jager, T., Salaberria, I., Hansen, B. H., and 2015. Capturing the life history of the marine copepod *Calanus sinicus* into a generic bioenergetics framework. Ecological Modelling, 299: 114-120.

Jager, T., and Zimmer, E. I. 2012. Simplified Dynamic Energy Budget model for analysing ecotoxicity data. Ecological Modelling, 225: 74-81.

Jennings, S., Lancaster, J., Woolmer, A., and Cotter, J. 1999. Distribution, diversity and abundance of epibenthic fauna in the North Sea. Journal of the Marine Biological Association of the United Kingdom, 79: 385-399.

Jeppesen, R., Rodriguez, M., Rinde, J., Haskins, J., Hughes, B., Mehner, L., and Wasson, K. 2018. Effects of hypoxia on fish survival and oyster growth in a highly eutrophic estuary. Estuaries and Coasts, 41: 89-98.

John, E. H., Batten, S. D., Harris, R. P., and Hays, G. C. 2001. Comparison between zooplankton data collected by the Continuous Plankton Recorder survey in the English Channel and by WP-2 nets at station L4, Plymouth (UK). Journal of Sea Research, 46: 223-232.

Josefson, A. B., Jensen, J. N., and Ærtebjerg, G. 1993. The benthos community structure anomaly in the late 1970s and early 1980s — a result of a major food pulse? Journal of Experimental Marine Biology and Ecology, 172: 31-45.

Jumars, P. A., Dorgan, K. M., and Lindsay, S. M. 2015. Diet of worms amended: An update of polychaete feeding guilds. Annual Review of Marine Science, 7: 497-520.

Jusup, M., Klanjscek, T., Matsuda, H., and Kooijman, S. A. L. M. 2011. A full lifecycle bioenergetic model for Bluefin Tuna. PLoS ONE, 6: e21903.

Kaiser, M., Armstrong, P. J., Dare, P. J., and Flatt, R. P. 1998. Benthic communities associated with a heavily fished scallop ground in the English Channel. Journal of the Marine Biological Association of the United Kingdom, 78: 1045-1059.

Kearney, M., Phillips, B. L., Tracy, C. R., Christian, K. A., Betts, G., and Porter, W. P. 2008. Modelling species distributions without using species distributions: the cane toad in Australia under current and future climates. Ecography, 31: 423-434.

Kearney, M., and Porter, W. 2009. Mechanistic niche modelling: combining physiological and spatial data to predict species’ ranges. Ecology Letters, 12: 334-350.

Kędra, M., Kuliński, K., Walkusz, W., and Legeżyńska, J. 2012. The shallow benthic food web structure in the high Arctic does not follow seasonal changes in the surrounding environment. Estuarine, Coastal and Shelf Science, 114: 183-191.

Keeling, R. F., Körtzinger, A., and Gruber, N. 2009. Ocean deoxygenation in a warming world. Annual Review of Marine Science, 2: 199-299.

Khan, M., Ahmed, S., Catalin, B., Khodadoust, A., Ajayi, O., and Vaughn, M. 2006. Effect of temperature on heavy metal toxicity to juvenile crayfish, *Orconectes immunis* (Hagen). Environmental Toxicology: An International Journal, 21: 513-520.

Kilada, R., and Driscoll, J. G. 2017. Age determination in crustaceans: a review. Hydrobiologia, 799: 21-36.

Kim, H., Kim, B. H., Son, M. H., Jeon, M. A., Lee, Y. G., and Lee, J. S. 2016. Gonadal development and reproductive cycle of cultured abalone, *Haliotis discus hannai* (Gastropoda: Haliotidae) in Korea: Implications for seed production. Journal of Shellfish Research, 35: 653-659.

Kim, S. K., Pang, Z., Seo, H. C., Cho, Y. R., Samocha, T., and Jang, I. K. 2014. Effect of bioflocs on growth and immune activity of Pacific white shrimp, *Litopenaeus vannamei* postlarvae. Aquaculture Research, 45: 362-371.

Kirby, R. R., and Beaugrand, G. 2009. Trophic amplification of climate warming. Proceedings of the Royal Society B: Biological Sciences, 276: 4095-4103.

Klein Breteler, W. C. M. 1975. Food consumption, growth and energy metabolism of juvenile shore crabs *Carcinus maenas*. Netherlands Journal of Sea Research, 9: 255–272.

Klok, C., Nordtug, T., and Tamis, J. C. 2014a. Estimating the impact of petroleum substances on survival in early life stages of cod (*Gadus morhua*) using the Dynamic Energy Budget theory. Marine Environmental Research, 101: 60-68.

Klok, C., Wijsman, J. W. M., Kaag, K., and Foekema, E. 2014b. Effects of CO_2 enrichment on cockle shell growth interpreted with a Dynamic Energy Budget model. Journal of Sea Research, 94: 111-116.

Knapp, J. L., Bridges, C. R., Krohn, J., Hoffman, L. C., and Auerswald, L. 2015. Acid–base balance and changes in haemolymph properties of the South African rock lobsters, *Jasus lalandii*, a palinurid decapod, during chronic hypercapnia. Biochemical and Biophysical Research Communications, 461: 475-480.

Kooijman, S. A. L. M. 2010. Dynamic Energy Budget theory for metabolic organisation*,* Cambridge University Press, Cambridge.

Kooijman, S. A. L. M., and Lika, K. 2014. Comparative energetics of the 5 fish classes on the basis of dynamic energy budgets. Journal of Sea Research, 94: 19-28.

Korhonen, M., Rudels, B., Marnela, M., Wisotzki, A., and Zhao, J. 2013. Time and space variability of freshwater content, heat content and seasonal ice melt in the Arctic Ocean from 1991 to 2011. Ocean Science Discussions, 9: 1015-1055.

Kovala, P. E., and Larrance, J. D. 1966. Computation of phytoplankton cell numbers, cell volume, cell surface and plasma volume per litre, from microscopic count. University of Washington Deprtment of Oceanography Special Report.

Kroeker, K. J., Kordas, R. L., Crim, R., Hendriks, I. E., Ramajo, L., Singh, G. S., Duarte, C. M., and Gattuso, J-P. 2013. Impacts of ocean acidification on marine organisms: quantifying sensitivities and interaction with warming. Global Change Biology, 19: 1884-1896.

Kröger, S., Parker, R., Cripps, G., and Williamson, P. 2018. Shelf Seas: The engine of productivity. Underpinning science for policy and management, Policy Report on NERC-Defra Shelf Sea Biogeochemistry programme.

Kurihara, H., Shimode, S., and Shirayama, Y. 2004. Sub-lethal effects of elevated concentration of CO_2 on planktonic copepods and sea urchins. Journal of Oceanography, 60: 743-750.

Larsen, P. S., Filgueira, R., and Riisgård, H. U. 2014. Somatic growth of mussels *Mytilus edulis* in field studies compared to predictions using BEG, DEB, and SFG models. Journal of Sea Research, 88: 100-108.

Lau, D. C. P., and Leung, K. M. Y. 2004. Feeding physiology of the carnivorous gastropod *Thais clavigera* (Kuster): do they eat “soup”? Journal of Experimental Marine Biology and Ecology, 312: 43-66.

Lavaud, R., Thomas, Y., Pecquerie, L., Benoît, H. P., Guyondet, T., Flye-Sainte-Marie, J., and Chabot, D. 2019. Modeling the impact of hypoxia on the energy budget of Atlantic cod in two populations of the Gulf of Saint-Lawrence, Canada. Journal of Sea Research, 143: 243-253.

Laverock, B., Gilbert, Jack A., Tait, K., Osborn, A. M., and Widdicombe, S. 2011. Bioturbation: impact on the marine nitrogen cycle. Biochemical Society Transactions, 39: 315-320.

Le Moullac, G., Quéau, I., Le Souchu, P., Pouvreau, S., Moal, J., René Le Coz, J., and François Samain, J. 2007. Metabolic adjustments in the oyster *Crassostrea gigas* according to oxygen level and temperature. Marine Biology Research, 3: 357-366.

Lehtonen, M. P., and Burnett, L. E. 2016. Effects of hypoxia and hypercapnic hypoxia on oxygen transport and acid–base status in the Atlantic blue crab, *Callinectes sapidus*, during exercise. Journal of Experimental Zoology Part A: Ecological Genetics and Physiology, 325: 598-609.

Leiva, F. P., Garcés, C., Verberk, W. C. E. P., Care, M., Paschke, K., and Gebauer, P. 2018. Differences in the respiratory response to temperature and hypoxia across four life-stages of the intertidal porcelain crab *Petrolisthes laevigatus*. Marine Biology, 165: 146.

Leland, A. V. 2002. A new apex predator in the Gulf of Maine? Large, mobile crabs (*Cancer borealis*) control benthic community structure. University of Maine electronic theses and dissertations. http://digitalcommons.library.umaine.edu/cgi/viewcontent.cgi?article=1150&context=etd

Lemos, D., Phan, V. N., and Alvarez, G. 2001. Growth, oxygen consumption, ammonia-N excretion, biochemical composition and energy content of *Farfantepenaeus paulensis* Pérez-Farfante (Crustacea, Decapoda, Penaeidae) early postlarvae in different salinities. Journal of Experimental Marine Biology and Ecology, 261: 55–74.

Lewin, R. 1986. Supply-Side Ecology. Existing models of population structure and dynamics of ecological communities have tended to ignore the effect of the influx of new members into the communities. Science, 234: 25-27.

Lewis, C., Clemow, K., and Holt, W. V. 2013. Metal contamination increases the sensitivity of larvae but not gametes to ocean acidification in the polychaete *Pomatoceros lamarckii* (Quatrefages). Marine Biology, 160: 2089-2101.

Li, A., and Chiu, J. M. Y. 2013. Latent effects of hypoxia on the gastropod *Crepidula onyx*. Marine Ecology Progress Series, 480: 145-154.

Lika, K., Kearney, M. R., Freitas, V., van der Veer, H. W., van der Meer, J., Wijsman, J. W. M., Pecquerie, L., and Kooijman, S.A.L.M. 2011. The “covariation method” for estimating the parameters of the standard Dynamic Energy Budget model I: Philosophy and approach. Journal of Sea Research, 66: 270-277.

Lindley, J. A., and Kirby, R. R. 2010. Climate-induced changes in the North Sea Decapoda over the last 60 years. Climate Research, 42: 257-264.

Liu, C. C., Chiu, J. M. Y., Li, L., Shin, P. K. S., and Cheung, S. G. 2011. Physiological responses of two sublittoral nassariid gastropods to hypoxia. Marine Ecology Progress Series, 429: 75-85.

Llobrera, J. A., and Neill, W. H. 1987. Growth, moulting, food ingestion and absorption in juvenile *Macrobrachium rosebergii* in relation to dissolved oxygen. *In* Aquaculture - A Biotechnology in Progress. N. De Pauw, E. Jaspers, H. Ackefors, and N. Wilkins (Eds.). European Aquaculture Society, Amsterdam, The Netherlands.

Lohrer, A. M., Thrush, S. F., and Gibbs, M. M. 2004. Bioturbators enhance ecosystem function through complex biogeochemical interactions. Nature, 431: 1092-1095.

Lopez, G. R., and Levinton, J. S. 2011. Particulate organic detritus and detritus feeders in coastal food webs. *In* Treatise on Estuarine and Coastal Science, 1 edn, pp. 5-21. Ed. by E. Wolanski, and D. S. McLusky. Academic Press, Waltham.

Lozano, J., Galera, J., López, S., Turon, X., and Palacín, C. 1995. Biological cycles and recruitment of *Paracentrotus lividus* (Echinodermata: Echinoidea) in two contrasting habitats. Marine Ecology Progress Series, 122: 179-191.

Maar, M., Saurel, C., Landes, A., Dolmer, P., and Petersen, J. K. 2015. Growth potential of blue mussels (*M. edulis*) exposed to different salinities evaluated by a Dynamic Energy Budget model. Journal of Marine Systems, 148: 48-55.

MacDiarmid, A. B. 1989. Moulting and reproduction of the spiny lobster *Jasus edwardsii* (Decapoda: Palinuridae) in northern New Zealand. Marine Biology, 103: 303-310.

Makarieva, A. M., Gorshkov, V. G., and Li, B.-L. 2004. Ontogenetic growth: models and theory. Ecological Modelling, 176: 15-26.

Mangum, C. P., and Burnett, L. E. 1986. The CO_2 sensitivity of the hemocyanins and its relationship to Cl-sensitivity. The Biological Bulletin, 171: 248-263.

Mantelatto, F. L. M., and Christofoletti, R. A. 2001. Natural feeding activity of the crab *Callinectes ornatus* (Portunidae) in Ubatuba Bay (São Paulo, Brazil): influence of season, sex, size and molt stage. Marine Biology, 138: 585-594.

Manush, S. M., Pal, A. K., Chatterjee, N., Das, T., and Mukherjee, S. C. 2004. Thermal tolerance and oxygen consumption of *Macrobrachium rosenbergii* acclimated to three temperatures. Journal of Thermal Biology, 29: 15-19.

MarLIN 2006. BIOTIC - Biological Traits Information Catalogue. Marine Biological Association of the United Kingdom, Plymouth.

Martin, B. T., Jager, T., Nisbet, R. M., Preuss, T. G., and Grimm, V. 2013. Predicting population dynamics from the properties of individuals: A cross-level test of Dynamic Energy Budget theory. The American Naturalist, 181: 506-519.

Martin, B. T., Zimmer, E. I., Grimm, V., and Jager, T. 2012. Dynamic Energy Budget theory meets individual-based modelling: a generic and accessible implementation. Methods in Ecology and Evolution, 3: 445-449.

Martin, S., and Gattuso, J.-P. 2009. Response of Mediterranean coralline algae to ocean acidification and elevated temperature. Global Change Biology, 15: 2089-2100.

Martinez-Cruz, O., Calderon de la Barca, A. M., Uribe-Carvajal, S., and Muhlia-Almazan, A. 2012. The function of mitochondrial FOF1 ATP-synthase from the whiteleg shrimp *Litopenaeus vannamei* muscle during hypoxia. Comparative Biochemistry and Physiology Part B: Biochemistry and Molecular Biology, 162: 107-112.

Mathewson, P. D., Moyer-Horner, L., Beever, E. A., Briscoe, N. J., Kearney, M., Yahn, J. M., and Porter, W. P. 2017. Mechanistic variables can enhance predictive models of endotherm distributions: the American pika under current, past, and future climates. Global Change Biology, 23: 1048-1064.

Mauchline, J. 1977. Growth of shrimps, crabs and lobsters – an assessment. ICES Journal of Marine Science, 37: 162-169.

Maury, O. 2010. An overview of APECOSM, a spatialized mass balanced “Apex Predators ECOSystem Model” to study physiologically structured tuna population dynamics in their ecosystem. Progress in Oceanography, 84: 113-117.

Maury, O., and Poggiale, J.-C. 2013. From individuals to populations to communities: A dynamic energy budget model of marine ecosystem size-spectrum including life history diversity. Journal of Theoretical Biology, 324: 52-71.

May, R. M., and Godfrey, J. 1994. Biological Diversity: Differences between land and sea [and discussion]. Philosophical Transactions of the Royal Society of London B: Biological Sciences, 343: 105-111.

McBryan, T., Anttila, K., Healy, T., and Schulte, P. 2013. Responses to temperature and hypoxia as interacting stressors in fish: implications for adaptation to environmental change. Integrative and Comparative Biology, 53: 648-659.

McCauley, D., L Pinsky, M., R Palumbi, S., A Estes, J., Joyce, F., and Warner, R. 2015. Marine defaunation: Animal loss in the global ocean. Science, 347: 1255641.

McGaw, I. J., and Whiteley, N. M. 2012. Effects of acclimation and acute temperature change on specific dynamic action and gastric processing in the green shore crab, *Carcinus maenas*. Journal of Thermal Biology, 37: 570–578.

McLeod, E., Salm, R., Green, A., and Almany, J. 2009. Designing marine protected area networks to address the impacts of climate change. Frontiers in Ecology and the Environment, 7: 362-370.

McMahon, B. R. 2001. Respiratory and circulatory compensation to hypoxia in crustaceans. Respiration Physiology, 128: 349-364.

McMahon, B. R., and Burnett, L. E. 1990. The crustacean open circulatory system: A reexamination. Physiological Zoology, 63: 35-71.

McNaught, D. C. 1999. The indirect effects of macroalgae and micropredation on the post-settlement success of the green sea urchin in Maine. Doctoral dissertation, University of Maine.

Mehrbach, C., Culberson, C. H., Hawley, J. E., and Pytkowicx, R. M. 1973. Measurement of the apparent dissociation constants of carbonic acid in seawater at atmospheric pressure. Limnology and Oceanography, 18: 897-907.

Melatunan, S., Calosi, P., Rundle, S. D., Widdicombe, S., and Moody, A. J. 2013. Effects of ocean acidification and elevated temperature on shell plasticity and its energetic basis in an intertidal gastropod. Marine Ecology Progress Series, 472: 155-168.

Melle, W., Runge, J., Head, E., Plourde, S., Castellani, C., Licandro, P., Pierson, J., Jonasdottir, S., Johnson, C., Broms, C., Debes, C., Falkenhaug, T., Gaard, E., Gislason, A., Heath, M., Niehoff, B., Nielsen, T., Pepin, P., Stenevik, E., and Chust, G. 2014. The North Atlantic Ocean as habitat for *Calanus finmarchicus*: Environmental factors and life history traits. Progress in Oceanography, 129: 244-284.

Melzner, F., Gutowska, M. A., Langenbuch, M., Dupont, S., Lucassen, M., Thorndyke, M. C., Bleich, M., and Pörtner, H-O. 2009. Physiological basis for high CO_2 tolerance in marine ectothermic animals: pre-adaptation through lifestyle and ontogeny? Biogeosciences, 6: 2313-2331.

Menden-Deuer, S., and Lessard, E. J. 2000. Carbon to volume relationships for dinoflagellates, diatoms, and other protist plankton. Limnology and Oceanography, 45: 569-579.

Mieszkowska, N., Leaper, R., Moore, P., Kendall, M., Burrows, M., Lear, D., Poloczanska, E., Hiscock, K., Moschella, P., Thompson, R., Herbert, R., Laffoley, D., Baxter, J., Southward, A., and Hawkins, S. 2005. Assessing and predicting the influence of climatic change using rocky shore biota. Marine Biological Association Occasional Publication No. 20. 55 pp.

Milazzo, M., Mirto, S., Domenici, P., and Gristina, M. 2012. Climate change exacerbates interspecific interactions in sympatric coastal fishes. Journal of Animal Ecology, 82: 468-477.

Miller, D., Poucher, S., and Coiro, L. 2002. Determination of lethal dissolved oxygen levels for selected marine and estuarine fishes, crustaceans, and a bivalve. Marine Biology, 140: 287-296.

Miller, G. M., Kroon, F. J., Metcalfe, S., and Munday, P. L. 2015. Temperature is the evil twin: effects of increased temperature and ocean acidification on reproduction in a reef fish. Ecological Applications, 25: 603-620.

Mincks, S. L., Smith, C. R., and DeMaster, D. J. 2005. Persistence of labile organic matter and microbial biomass in Antarctic shelf sediments: evidence of a sediment ‘food bank’. Marine Ecology Progress Series, 300: 3-19.

Minervini, R., Giannotta, M., and Falciai, L. 1982. A preliminary report on the decapod crustaceans in the estuarine area of the Tiber. Quaderni del Laboratorio per la Tecnologia della Pesca, 3: 305-318.

Mollica, N. R., Guo, W., Cohen, A. L., Huang, K.-F., Foster, G. L., Donald, H. K., and Solow, A. R. 2018. Ocean acidification affects coral growth by reducing skeletal density. Proceedings of the National Academy of Sciences, 115: 1754-1759.

Monaco, C., Wethey, D., and Helmuth, B. 2014. A Dynamic Energy Budget (DEB) model for the keystone predator *Pisaster ochraceus*. PLoS ONE, 9. https://dx.doi.org/10.1371%2Fjournal.pone.0104658

Moore, P. G., and Bergmann, M. 2001. Survival of decapod crustaceans discarded in the *Nephrops* fishery of the Clyde Sea area, Scotland. ICES Journal of Marine Science, 58: 163-171.

Mori, M., and Zunino, P. 1987. Aspects of the biology of *Liocarcinus depurator* (L.) in the Ligurian Sea. Investigacion Pesquera, 51: 135-145.

Motes, M., DePaola, A., Cook, D., Veazey, J., Hunsucker, J., Garthright, W., Blodgett, R., and Chirtel, S. J. 1998. Influence of water temperature and salinity on *vibrio vulnificus* in northern gulf and atlantic coast oysters (*Crassostrea virginica*). Applied and Environmental Microbiology, 64: 1459-1465.

Mukherjee, J., Wong, K. K., Chandramouli, K. H., Qian, P.-Y., Leung, P. T., Wu, R. S., and Thiyagarajan, V. 2013. Proteomic response of marine invertebrate larvae to ocean acidification and hypoxia during metamorphosis and calcification. Journal of Experimental Biology, 216: 4580-4589.

Muller, E. B., and Nisbet, R. M. 2014. Dynamic energy budget modeling reveals the potential of future growth and calcification for the coccolithophore *Emiliania huxleyi* in an acidified ocean. Global Change Biology, 20: 2031-2038.

Muller, E. B., Nisbet, R. M., and Berkley, H. A. 2009. Sublethal toxicant effects with dynamic energy budget theory: model formulation. Ecotoxicology, 19: 48-60.

Munday, P. L., Crawley, N. E., and Nilsson, G. E. 2009. Interacting effects of elevated temperature and ocean acidification on the aerobic performance of coral reef fishes. Marine Ecology Progress Series, 388: 235-242.

Muthukrishnan, R., and Fong, P. 2014. Multiple anthropogenic stressors exert complex, interactive effects on a coral reef community. Coral Reefs, 33: 911-921.

Navarro, E., Iglesias, J. I. P., and Ortega, M. M. 1992. Natural sediment as a food source for the cockle *Cerastoderma edule* (L.): effect of variable particle concentration on feeding, digestion and the scope for growth. Journal of Experimental Marine Biology and Ecology, 156: 69-87.

Navarro, J. M., Leiva, G. E., Martinez, G., and Aguilera, C. 2000. Interactive effects of diet and temperature on the scope for growth of the scallop *Argopecten purpuratus* during reproductive conditioning. Journal of Experimental Marine Biology and Ecology, 247: 67-83.

Navarro, J. M., Urrutia, G. X., and Carrasco, C. 2006. Scope for growth versus actual growth in the juvenile predatory gastropod *Chorus giganteus*. Journal of the Marine Biological Association of the United Kingdom, 86: 1423-1428.

Neumann, H., de Boois, I., Kröncke, I., and Reiss, H. 2013. Climate change facilitated range expansion of the non-native angular crab *Goneplax rhomboides* into the North Sea. Marine Ecology Progress Series, 484: 143-153.

Neumann, H., Diekmann, R., Emeis, K.-C., Kleeberg, U., Moll, A., and Kröncke, I. 2017. Full-coverage spatial distribution of epibenthic communities in the south-eastern North Sea in relation to habitat characteristics and fishing effort. Marine Environmental Research, 130: 1-11.

Neumann, H., Ehrich, S., and Kröncke, I. 2008. Effects of cold winters and climate on the temporal variability of an epibenthic community in the German Bight. Climate Research, 37: 241-251.

Neumann, H., Ehrich, S., and Kröncke, I. 2009a. Variability of epifauna and temperature in the northern North Sea. Marine Biology, 156: 1817-1826.

Neumann, H., and Kröncke, I. 2011. The effect of temperature variability on ecological functioning of epifauna in the German Bight. Marine Ecology, 32: 49-57.

Neumann, H., Reiss, H., Rakers, S., Ehrich, S., and Kröncke, I. 2009b. Temporal variability in southern North Sea epifauna communities after the cold winter of 1995/1996. ICES Journal of Marine Science, 66: 2233-2243.

Nichols, D., and Barker, M. F. 1984a. A comparative study of reproductive and nutritional periodicities in two populations of *Asterias rubens* (Echinodermata: Asteroidea) from the English Channel. Journal of the Marine Biological Association of the United Kingdom, 64: 471-484.

Nichols, D., and Barker, M. F. 1984b. Reproductive and nutritional periodicities in the starfish, *Marthasterias glacialis*, from Plymouth Sound. Journal of the Marine Biological Association of the United Kingdom, 64: 461-470.

Nicol, S. 2000. Understanding krill growth and aging: the contribution of experimental studies. Canadian Journal of Fisheries and Aquatic Sciences, 57: 168-177.

Nicol, S., Stolp, M., Cochran, T., Geijsel, P., and Marshall, J. 1992. Growth and shrinkage of Antarctic krill *Euphausia superba* from the Indian Ocean sector of the Southern Ocean during summer. Marine Ecology Progress Series, 89: 175-181.

Nisbet, R. M., Muller, E. B., Lika, K., and Kooijman, S. A. L. M. 2000. From molecules to ecosystems through dynamic energy budget models. Journal of Animal Ecology, 69: 913-926.

Nizzetto, L., Macleod, M., Borgå, K., Cabrerizo, A., Dachs, J., Guardo, A. D., Ghirardello, D., Hansen, K., Jarvis, A., Lindroth, A., Ludwig, B., Monteith, D., Perlinger, J., Scheringer, M., Schwendenmann, L., Semple, K., Wick, L., Zhang, G., and Jones, K. 2010. Past, present, and future controls on levels of persistent organic pollutants in the global environment. Environmental Science & Technology, 44: 6526-6531.

Normant, M., and Lamprecht, I. 2006. Does scope for growth change as a result of salinity stress in the amphipod *Gammarus oceanicus*? Journal of Experimental Marine Biology and Ecology, 334: 158-163.

Nunes, C. D. A. P., and Jangoux, M. 2004. Reproductive cycle of the spatangoid echinoid *Echinocardium cordatum* (Echinodermata) in the southwestern North Sea. Invertebrate Reproduction & Development, 45: 41-57.

O'Connor, M. P., Kemp, S. J., Agosta, S. J., Hansen, F., Sieg, A. E., Wallace, B. P., McNair, J. N., and Dunham, A.E. 2007. Reconsidering the mechanistic basis of the metabolic theory of ecology. Oikos, 116: 1058-1072.

O'Halloran, M. J., and O'Dor, R. K. 1988. Molt cycle of male snow crabs, *Chionoecetes Opilio*, from observations of external features, setal changes, and feeding behavior. Journal of Crustacean Biology, 8: 164-176.

Oksanen, J., Blanchet, F. G., Friendly, M., Kindt, R., Legendre, P., McGlinn, D., Minchin, P. R., O'Hara, R., Simpson, G., Solymos, P., Stevens, M.H., Szoecs, E., and Wagner, H. 2017. Vegan Community Ecology Package. https://cran.r-project.org/package=vegan.

Olden, J. D., and Neff, B. D. 2001. Cross-correlation bias in lag analysis of aquatic time series. Marine Biology, 138: 1063-1070.

Paganini, A. W., Miller, N. A., and Stillman, J. H. 2014. Temperature and acidification variability reduce physiological performance in the intertidal zone porcelain crab *Petrolisthes cinctipes*. Journal of Experimental Biology, 217: 3974-3980.

Pan, M., McBeath, A. J. A., Hay, S. J., Pierce, G. J., and Cunningham, C. O. 2008. Real-time PCR assay for detection and relative quantification of *Liocarcinus depurator* larvae from plankton samples. Marine Biology, 153: 859-870.

Pan, T.-C. F., Applebaum, S. L., and Manahan, D. T. 2015. Experimental ocean acidification alters the allocation of metabolic energy. Proceedings of the National Academy of Sciences, 112: 4696-4701.

Parker, L. M., Ross, P. M., and O'Connor, W. A. 2009. The effect of ocean acidification and temperature on the fertilization and embryonic development of the Sydney rock oyster *Saccostrea glomerata* (Gould 1850). Global Change Biology, 15: 2123-2136.

Paul, A. J., and Fuji, A. 1989. Bioenergetics of the Alaskan crab *Chionoecetes bairdi* (Decapoda: Majidae. Journal of Crustacean Biology, 9: 25–36.

Pearce, C. M., Williams, S. W., Yuan, F., Castell, J. D., and Robinson, S. M. C. 2005. Effect of temperature on somatic growth and survivorship of early post-settled green sea urchins, *Strongylocentrotus droebachiensis* (Müller). Aquaculture Research, 36: 600-609.

Pearson, G. A., Lago-Leston, A., and Mota, C. 2009. Frayed at the edges: selective pressure and adaptive response to abiotic stressors are mismatched in low diversity edge populations. Journal of Ecology, 97: 450-462.

Peck, M. A., Buckley, L. J., Caldarone, E. M., and Bengtson, D. A. 2003. Effects of food consumption and temperature on growth rate and biochemical-based indicators of growth in early juvenile Atlantic cod *Gadus morhua* and haddock *Melanogrammus aeglefinus*. Marine Ecology Progress Series, 251: 233-243.

Pecquerie, L., Johnson, L. R., Kooijman, S. A. L. M., and Nisbet, R. M. 2011. Analyzing variations in life-history traits of Pacific salmon in the context of Dynamic Energy Budget (DEB) theory. Journal of Sea Research, 66: 424-433.

Pecquerie, L., Petitgas, P., and Kooijman, S. A. 2009. Modeling fish growth and reproduction in the context of the Dynamic Energy Budget theory to predict environmental impact on anchovy spawning duration. Journal of Sea Research, 62: 93-105.

Penkoff, S. J., and Thurberg, F. P. 1982. Changes in oxygen consumption of the american lobster, *Homarus americanus*, during the molt cycle. Comparative Biochemistry and Physiology Part A: Physiology, 72: 621-622.

Perry, A. L., Low, P. J., Ellis, J. R., and Reynolds, J. D. 2005. Climate change and distribution shifts in marine fishes. Science, 308: 1912-1915.

Persson, L., Claessen, D., De Roos, A. M., Byström, P., Sjögren, S., Svanbäck, R., Wahlström, E., and Westman, E. 2004. Cannibalism in a size-structured population: Energy extraction and control. Ecological Monographs, 74: 135-157.

Persson, L., and De Roos, A. M. 2006. Food-dependent individual growth and population dynamics in fishes. Journal of Fish Biology, 69: 1-20.

Peterson, C. H. 1979. Predation, competitive exclusion, and diversity in the soft-sediment benthic communities of estuaries and lagoons. *In* Ecological Processes in Coastal and Marine Systems, pp. 233-264. Ed. by R. J. Livingston. Springer US, Boston, MA.

Peterson, C. H., and Fegley, S. R. 1986. Seasonal allocation of resources to growth of shell, soma and gonads in *Mercenaria mercenaria*. The Biological Bulletin, 171: 597-610.

Pincebourde, S., Sanford, E., Casas, J., and Helmuth, B. 2012. Temporal coincidence of environmental stress events modulates predation rates. Ecology Letters, 15: 680-688.

Place, S. P., Donnell, M. J., and Hofmann, G. E. 2008. Gene expression in the intertidal mussel *Mytilus californianus*: physiological response to environmental factors on a biogeographic scale. Marine Ecology Progress Series, 356: 1-14.

Poloczanska, E. S., Brown, C. J., Sydeman, W. J., Kiessling, W., Schoeman, D. S., Moore, P. J., Brander, K., Bruno, J., Buckley, L., Burrows, M., Duarte, C., Halpern, B., Holding, J., Kappel, C., O'Connor, M., Pandolfi, J., Parmensan, C., Schwing, F., Thompson, S., and Richardson, A. 2013. Global imprint of climate change on marine life. Nature Climate Change, 3: 919-925.

Pörtner, H.-O. 2010. Oxygen- and capacity-limitation of thermal tolerance: a matrix for integrating climate-related stressor effects in marine ecosystems. The Journal of Experimental Biology, 213: 881-893.

Pörtner, H. 2001. Climate change and temperature-dependent biogeography: oxygen limitation of thermal tolerance in animals. Naturwissenschaften, 88: 137-146.

Pörtner, H. O., and Knust, R. 2007. Climate change affects marine fishes through the oxygen limitation of thermal tolerance. Science, 315: 95-97.

Posey, M., Powell, C., Cahoon, L., and Lindquist, D. 1995. Top down vs. bottom up control of benthic community composition on an intertidal tideflat. Journal of Experimental Marine Biology and Ecology, 185: 19-31.

Pouvreau, S., Bourles, Y., Lefevre, S., Gangnery, A., and Alunno-Bruscia, M. 2006. Application of a dynamic energy budget model to the Pacific oyster, *Crassostrea gigas*, reared under various environmental conditions. Journal of Sea Research, 56: 156-167.

Price, C. A., Weitz, J. S., Savage, V. M., Stegen, J., Clarke, A., Coomes, D. A., Dodds, P. S., Etienne, R., Kerkhoff, A., McCullogh, K., Niklas, K., Olff, H., and Swenson, N. 2012. Testing the metabolic theory of ecology. Ecology Letters, 15: 1465-1474.

Probst, W. N., Stelzenmüller, V., and Fock, H. O. 2012. Using cross-correlations to assess the relationship between time-lagged pressure and state indicators: an exemplary analysis of North Sea fish population indicators. ICES Journal of Marine Science, 69: 670-681.

Purcell, J. E., White, J. R., Nemazie, D. A., and Wright, D. A. 1999. Temperature, salinity and food effects on asexual reproduction and abundance of the scyphozoan *Chrysaora quinquecirrha*. Marine Ecology Progress Series, 180: 187-196.

Queirós, A. M., Fernandes, J. A., Faulwetter, S., Nunes, J., Rastrick, S. P. S., Mieszkowska, N., Artioli, Y., Yool, A., Calosi, P., Arvanitidis, C., Findlay, H., Barane, M., Cheung, W., and Widdicombe, S. 2015. Scaling up experimental ocean acidification and warming research: from individuals to the ecosystem. Global Change Biology, 21: 130-143.

Queirós, A. M., Stephens, N., Widdicombe, S., Tait, K., McCoy, S. J., Ingels, J., Rühl, S., Airs, R., Beesley, A., Carnoval, G., Cazenave, P., Dashfield, S., Hua, E., Jones, M., Lindeque, P., McNeil, C.L., Nunes, J., Krause-Jensen, D. and Somerfield, P.. 2019. Connected macroalgal-sediment systems: blue carbon and food webs in the deep coastal ocean. Ecological Monographs, 89: e01366. https://doi.org/10.1002/ecm.1366

Quetin, L. B., and Ross, R. M. 1991. Behavioral and physiological characteristics of the Antarctic krill, *Euphausia superba*. American Zoologist, 31: 49-63.

Quijón, P. A., Kelly, M. C., and Snelgrove, P. V. R. 2008. The role of sinking phytodetritus in structuring shallow-water benthic communities. Journal of Experimental Marine Biology and Ecology, 366: 134-145.

Quijón, P. A., and Snelgrove, P. V. R. 2005. Predation regulation of sedimentary faunal structure: potential effects of a fishery-induced switch in predators in a Newfoundland sub-Arctic fjord. Oecologia, 144: 125-136.

Rato, L. D., Novais, S. C., Lemos, M. F. L., Alves, L. M. F., and Leandro, S. M. 2017. *Homarus gammarus* (Crustacea: Decapoda) larvae under an ocean acidification scenario: responses across different levels of biological organization. Comparative Biochemistry and Physiology Part C: Toxicology & Pharmacology, 203: 29-38.

Raviv, S., Parnes, S., and Sagi, A. 2008. Coordination of reproduction and molt in decapods. *In* Reproductive Biology of crustaceans: case studies of decapod crustaceans: CRC Press, pp365-390.

Re, A. D., Diaz, F., Sierra, E., Rodríguez, J., and Perez, E. 2005. Effect of salinity and temperature on thermal tolerance of brown shrimp *Farfantepenaeus aztecus* (Ives)(Crustacea, Penaeidae). Journal of Thermal Biology, 30: 618-622.

Reiss, H., Cunze, S., König, K., Neumann, H., and Kröncke, I. 2011. Species distribution modelling of marine benthos: a North Sea case study. Marine Ecology Progress Series, 442: 71-86.

Reiss, H., and Kröncke, I. 2004. Seasonal variability of epibenthic communities in different areas of the southern North Sea. ICES Journal of Marine Science, 61: 882-905.

Reymond, H., and Lagardère, J. P. 1990. Feeding rhythms and food of *Penaeus japonicus* bate (Crustacea, Penaeidae) in salt marsh ponds; role of halophilic entomofauna. Aquaculture, 84: 125-143.

Richards, R. A. 2012. Phenological shifts in hatch timing of northern shrimp *Pandalus borealis*. Marine Ecology Progress Series, 456: 149-158.

Riedel, B., Stachowitsch, M., and Zuschin, M. 2008. Sea anemones and brittle stars: unexpected predatory interactions during induced in situ oxygen crises. Marine Biology, 153: 1075-1085.

Roberts, D. A., Birchenough, S. N., Lewis, C., Sanders, M. B., Bolam, T., and Sheahan, D. 2013. Ocean acidification increases the toxicity of contaminated sediments. Global Change Biology, 19: 340-351.

Robinson, L., Elith, J., Hobday, A. J., Pearson, R. G., Kendall, B. E., Possingham, H. P., and Richardson, A. J. 2011. Pushing the limits in marine species distribution modelling: lessons from the land present challenges and opportunities. Global Ecology and Biogeography, 20: 789-802.

Robinson, N. M., Nelson, W. A., Costello, M. J., Sutherland, J. E., and Lundquist, C. J. 2017. A systematic review of marine-based Species Distribution Models (SDMs) with recommendations for best practice. Frontiers in Marine Science, 4: 421. https://doi.org/10.3389/fmars.2017.00421

Rogers-Bennett, L., Dondanville, R. F., Moore, J. D., and Vilchis, L. I. 2010. Response of red abalone reproduction to warm water, starvation, and disease stressors: Implications of ocean warming. Journal of Shellfish Research, 29: 599-611, 513.

Rosland, R., Strand, Ø., Alunno-Bruscia, M., Bacher, C., and Strohmeier, T. 2009. Applying Dynamic Energy Budget (DEB) theory to simulate growth and bio-energetics of blue mussels under low seston conditions. Journal of Sea Research, 62: 49-61.

Rowley, A. F., and Pope, E. C. 2012. Vaccines and crustacean aquaculture—A mechanistic exploration. Aquaculture, 334-337: 1-11.

Rufino, M., Abelló, P., and Yule, A. B. 2004. Male and female carapace shape differences in *Liocarcinus depurator* (Decapoda, Brachyura): An application of geometric morphometric analysis to crustaceans. Italian Journal of Zoology, 71: 79-83.

Rufino, M., Abelló, P., Yule, A. B., and Torres, P. 2005. Geographic, bathymetric and inter-annual variability in the distribution of *Liocarcinus depurator* (Brachyura: Portunidae) along the Mediterranean coast of the Iberian Peninsula. Scientia Marina, 69: 503-518.

Sainte-Marie, B., Gosselin, T., Sévigny, J.-M., and Urbani, N. 2008. The snow crab mating system: Opportunity for natural and unnatural selection in a changing environment. Bulletin of Marine Science, 83: 131-161.

Sanders, T., Widdicombe, S., Calder-Potts, R., and Spicer, J. I. 2014. Environmental hypoxia but not minor shell damage affects scope for growth and body condition in the blue mussel *Mytilus edulis* (L.). Marine Environmental Research, 95: 74-80.

Sang, H. M., Fotedar, R., and Filer, K. 2011. Effects of dietary mannan oligosaccharide on the survival, growth, immunity and digestive enzyme activity of freshwater crayfish, *Cherax destructor* Clark (1936). Aquaculture Nutrition, 17: e629-e635.

Sarà, G., Romano, C., Widdows, J., and Staff, F. J. 2008. Effect of salinity and temperature on feeding physiology and scope for growth of an invasive species (*Brachidontes pharaonis* - Mollusca: Bivalvia) within the Mediterranean sea. Journal of Experimental Marine Biology and Ecology, 363: 130-136.

Saravanan, M., Lee, D.-H., and Rhee, J.-S. 2018. Effects of polychlorinated biphenyls on survival, growth, and offspring production of the mysid crustacean, *Neomysis awatschensis*. Toxicology and Environmental Health Sciences, 10: 132-138.

Sastry, A. N. 1966. Temperature effects in reproduction of the bay scallop *Aequipecten irradians* (Lamarck). The Biological Bulletin, 130: 118-134.

Sastry, A. N., and Blake, N. J. 1971. Regulation of gonad development in the bay scallop *Aequipecten irradians* (Lamarck). The Biological Bulletin, 140: 274-283.

Schoolfield, R. M., Sharpe, P. J. H., and Magnuson, C. E. 1981. Non-linear regression of biological temperature-dependent rate models based on absolute reaction-rate theory. Journal of Theoretical Biology, 88: 719-731.

Schurmann, H., and Steffensen, J. 1994. Spontaneous swimming activity of Atlantic cod *Gadus morhua* exposed to graded hypoxia at three temperatures. Journal of Experimental Biology, 197: 129-142.

Schuwerack, P. M. M., Lewis, J. W., and Jones, P. W. 2001. Pathological and physiological changes in the South African freshwater crab *Potamonautes warreni* (Calman) induced by microbial gill infestations. Journal of Invertebrate Pathology, 77: 269-279.

Scrosati, R. A., and Ellrich, J. A. 2017. Recruitment and abundance of intertidal barnacles and mussels along the Atlantic Canadian coast: pelagic influences and relationships with predator abundance. bioRxiv: 239756.

Seear, P. J., Tarling, G. A., Burns, G., Goodall-Copestake, W. P., Gaten, E., Özkaya, Ö., and Rosato, E. 2010. Differential gene expression during the moult cycle of Antarctic krill (*Euphausia superba*). BMC Genomics, 11: 582.

Serra-Diaz, J. M., Keenan, T. F., Ninyerola, M., Sabaté, S., Gracia, C., and Lloret, F. 2013. Geographical patterns of congruence and incongruence between correlative species distribution models and a process-based ecophysiological growth model. Journal of Biogeography, 40: 1928-1938.

Shin, P. K. S., Cheung, P. H., Yang, F. Y., and Cheung, S. G. 2005. Intermittent exposure to reduced oxygen levels affects prey size selection and consumption in swimming crab *Thalamita danae* Stimpson. Marine Pollution Bulletin, 51: 1003-1009.

Siikavuopio, S. I., Dale, T., Mortensen, A., and Foss, A. 2007. Effects of hypoxia on feed intake and gonad growth in the green sea urchin, *Strongylocentrotus droebachiensis*. Aquaculture, 266: 112-116.

Silliman, B. R., and Bertness, M. D. 2002. A trophic cascade regulates salt marsh primary production. Proceedings of the National Academy of Sciences, 99: 10500-10505.

Skákala, J., Ford, D., Brewin, R. J. W., McEwan, R., Kay, S., Taylor, B., de Mora, L., and Ciavatta, S. 2018. The assimilation of phytoplankton functional types for operational forecasting in the Northwest European Shelf. Journal of Geophysical Research: Oceans, 123: 5230-5247.

Sköld, M., and Gunnarsson, J. S. G. 1996. Somatic and germinal growth of the infaunal brittle stars *Amphiura filiformis* and *A. chiajei* in response to organic enrichment. Marine Ecology Progress Series, 142: 203-214.

Smith, M. T., and Addison, J. T. 2003. Methods for stock assessment of crustacean fisheries. Fisheries Research, 65: 231-256.

Smith, V. J., Brown, J. H., and Hauton, C. 2003. Immunostimulation in crustaceans: does it really protect against infection? Fish & Shellfish Immunology, 15: 71-90.

Smyth, T., Atkinson, A., Widdicombe, S., Frost, M., Allen, I., Fishwick, J., Queiros, A., Sims, D., and Barange, M. 2015. The Western Channel Observatory. Progress in Oceanography, 137, Part B: 335-341.

Snelgrove, P. V. R. 1999. Getting to the bottom of marine biodiversity: Sedimentary habitats: Ocean bottoms are the most widespread habitat on Earth and support high biodiversity and key ecosystem services. BioScience, 49: 129-138.

Soares, R., Peixoto, S., Wasielesky, W., and D'Incao, F. 2005. Feeding rhythms and diet of *Farfantepenaeus paulensis* under pen culture in Patos Lagoon estuary, Brazil. Journal of Experimental Marine Biology and Ecology, 322: 167-176.

Sokolova, I. 2004. Cadmium effects on mitochondrial function are enhanced by elevated temperatures in a marine poikilotherm, *Crassostrea virginica* Gmelin (Bivalvia: Ostreidae). Journal of Experimental Biology, 207: 2639-2648.

Sokolova, I. M. 2013. Energy-limited tolerance to stress as a conceptual framework to integrate the effects of multiple stressors. Integrative and Comparative Biology, 53: 597-608.

Solan, M., Cardinale, B. J., Downing, A. L., Engelhardt, K. A. M., Ruesink, J. L., and Srivastava, D. S. 2004. Extinction and ccosystem function in the marine benthos. Science, 306: 1177-1180.

Somerton, D. A. 1980. Fitting straight lines to Hiatt growth diagrams: a re-evaluation. ICES Journal of Marine Science, 39: 15-19.

Sorte, C. J. B., Williams, S. L., and Carlton, J. T. 2010. Marine range shifts and species introductions: comparative spread rates and community impacts. Global Ecology and Biogeography, 19: 303-316.

Spicer, J. I., Raffo, A., and Widdicombe, S. 2007. Influence of CO_2-related seawater acidification on extracellular acid–base balance in the velvet swimming crab *Necora puber*. Marine Biology, 151: 1117-1125.

Steneck, R. 1997. Fisheries-induced biological changes to the structure and function of the Gulf of Maine ecosystem. *In* Proceedings of the Gulf of Maine ecosystem dynamics scientific symposium and workshop. RARGOM Report, pp. 153-168.

Steneck, R. S., Vavrinec, J., and Leland, A. V. 2004. Accelerating trophic-level dysfunction in kelp forest ecosystems of the western North Atlantic. Ecosystems, 7: 323-332.

Stentiford, G. D., Neil, D. M., Peeler, E. J., Shields, J. D., Small, H. J., Flegel, T. W., Vlak, J. M., Jones, B., Morado, F., Moss, S., Lotz, J., Bartholomay, L., Behringer, D., Hauton, C. and Lightner, D. 2012. Disease will limit future food supply from the global crustacean fishery and aquaculture sectors. Journal of Invertebrate Pathology, 110: 141-157.

Stern, S., and Cohen, D. 1982. Oxygen consumption and ammonia excretion during the molt cycle of the freshwater prawn *Macrobrachium rosenbergii* (De Man). Comparative Biochemistry and Physiology Part A: Physiology, 73: 417-419.

Stevens, A. M., and Gobler, C. J. 2018. Interactive effects of acidification, hypoxia, and thermal stress on growth, respiration, and survival of four North Atlantic bivalves. Marine Ecology Progress Series, 604: 143-161.

Stoffer, D. 2016. astsa- Applied Statistical Time-Series Analysis. 1.7 edn. https://cran.r-project.org/package=astsa

Stumpp, M., Trübenbach, K., Brennecke, D., Hu, M. Y., and Melzner, F. 2012. Resource allocation and extracellular acid–base status in the sea urchin *Strongylocentrotus droebachiensis* in response to CO_2 induced seawater acidification. Aquatic Toxicology, 110-111: 194-207.

Stumpp, M., Wren, J., Melzner, F., Thorndyke, M. C., and Dupont, S. T. 2011. CO_2 induced seawater acidification impacts sea urchin larval development I: Elevated metabolic rates decrease scope for growth and induce developmental delay. Comparative Biochemistry and Physiology Part A: Molecular & Integrative Physiology, 160: 331-340.

Sui, Y., Kong, H., Shang, Y., Huang, X., Wu, F., Hu, M., Lin, D., Lu, W., and Wang, Y. 2016. Effects of short-term hypoxia and seawater acidification on hemocyte responses of the mussel *Mytilus coruscus*. Marine Pollution Bulletin, 108: 46-52.

Sundblad, G., Bergström, U., and Sandström, A. 2011. Ecological coherence of marine protected area networks: a spatial assessment using species distribution models. Journal of Applied Ecology, 48: 112-120.

Sutherland, J. P. 1990. Recruitment regulates demographic variation in a tropical intertidal barnacle. Ecology, 71: 955-972.

Tait, K., Airs, R. L., Widdicombe, C. E., Tarran, G. A., Jones, M. R., and Widdicombe, S. 2015. Dynamic responses of the benthic bacterial community at the Western English Channel observatory site L4 are driven by deposition of fresh phytodetritus. Progress in Oceanography, 137: 546-558.

Talmage, S. C., and Gobler, C. J. 2010. Effects of past, present, and future ocean carbon dioxide concentrations on the growth and survival of larval shellfish. Proceedings of the National Academy of Sciences, 107: 17246-17251.

Taylor, D. L., and Peck, M. A. 2004. Daily energy requirements and trophic positioning of the sand shrimp *Crangon septemspinosa*. Marine Biology, 145: 167–177.

Thomas, C. W., Crear, B. J., and Hart, P. R. 2000. The effect of temperature on survival, growth, feeding and metabolic activity of the southern rock lobster, *Jasus edwardsii*. Aquaculture, 185: 73-84.

Thomas, Y., Flye-Sainte-Marie, J., Chabot, D., Aguirre-Velarde, A., Marques, G. M., and Pecquerie, L. 2019. Effects of hypoxia on metabolic functions in marine organisms: Observed patterns and modelling assumptions within the context of Dynamic Energy Budget (DEB) theory. Journal of Sea Research, 143: 231-242.

Thomas, Y., Mazurié, J., Alunno-Bruscia, M., Bacher, C., Bouget, J.-F., Gohin, F., Pouvreau, S., and Struski, C. 2011. Modelling spatio-temporal variability of *Mytilus edulis* (L.) growth by forcing a dynamic energy budget model with satellite-derived environmental data. Journal of Sea Research, 66: 308-317.

Thorson, G. 1950. Reproductive and larval ecology of marine bottom invertebrates. Biological Reviews, 25: 1-45.

Throndsen, J. 1978. Productivity and abundance of ultra- and nanoplankton in Oslofjorden. Sarsia, 63: 273-284.

Thronson, A., and Quigg, A. 2008. Fifty-five years of fish kills in coastal Texas. Estuaries and Coasts, 31: 802-813.

Thrush, S. F. 1999. Complex role of predators in structuring soft-sediment macrobenthic communities: Implications of changes in spatial scale for experimental studies. Austral Ecology, 24: 344-354.

Todgham, A. E., and Stillman, J. H. 2013. Physiological responses to shifts in multiple environmental stressors: Relevance in a changing world. Integrative and Comparative Biology, 53: 539-544.

Traifalgar, R., Corre, V., and Serrano, A. 2013. Efficacy of dietary immunostimulants to enhance the immunological responses and Vibriosis resistance of juvenile *Penaeus monodon*. Journal of Fisheries and Aquatic Science, 8: 340-354.

Trapletti, A., Hornik, K., and LeBaron, B. 2017. Time Series Analysis. 0.10-42 edn.

Trenkel, V. M., Le Loc'h, F., and Rochet, M.-J. 2007. Small-scale spatial and temporal interactions among benthic crustaceans and one fish species in the Bay of Biscay. Marine Biology, 151: 2207-2215.

Underwood, A. J., and Fairweather, P. G. 1989. Supply-side ecology and benthic marine assemblages. Trends in Ecology & Evolution, 4: 16-20.

UNESCO 1968. Monographs on Oceanographic Methodology: Zooplankton Sampling, Paris United Nations.

Urbina, M., Paschke, K., Gebauer, P., and Chaparro, O. R. 2010. Physiological energetics of the estuarine crab *Hemigrapsus crenulatus* (Crustacea: Decapoda: Varunidae): responses to different salinity levels. Journal of the Marine Biological Association of the United Kingdom, 90: 267-273.

van der Have, T. M., and de Jong, G. 1996. Adult size in ectotherms: Temperature effects on growth and differentiation. Journal of Theoretical Biology, 183: 329-340.

van der Meer, J. 2006a. An introduction to Dynamic Energy Budget (DEB) models with special emphasis on parameter estimation. Journal of Sea Research, 56: 85-102.

van der Meer, J. 2006b. Metabolic theories in ecology. Trends in Ecology & Evolution, 21: 136-140.

van der Veer, H. W., and Bergman, M. J. N. 1987. Predation by crustaceans on a newly settled 0-group plaice *Pleuronectes platessa* population in the western Wadden Sea. Marine Ecology Progress Series, 35: 203-215.

Verslycke, T., Roast, S. D., Widdows, J., Jones, M. B., and Janssen, C. R. 2004. Cellular energy allocation and scope for growth in the estuarine mysid *Neomysis integer* (Crustacea: Mysidacea) following chlorpyrifos exposure: a method comparison. Journal of Experimental Marine Biology and Ecology, 306: 1-16.

Vilchis, L. I., Tegner, M. J., Moore, J. D., Friedman, C. S., Riser, K. L., Robbins, T. T., and Dayton, P. K. 2005. Ocean warming effects on growth, reproduction, and survivorship of southern California abalone. Ecological Applications, 15: 469-480.

Wainwright, T. C., and Armstrong, D. A. 1993. Growth patterns in the Dungeness crab (*Cancer magister* Dana): synthesis of data and comparison of models. Journal of Crustacean Biology, 13: 36-50.

Walther, K., Anger, K., and Pörtner, H. O. 2010. Effects of ocean acidification and warming on the larval development of the spider crab *Hyas araneus* from different latitudes (54° vs. 79°N). Marine Ecology Progress Series, 417: 159-170.

Wang, F., Yang, H., Gao, F., and Liu, G. 2008. Effects of acute temperature or salinity stress on the immune response in sea cucumber, *Apostichopus japonicus*. Comparative Biochemistry and Physiology Part A: Molecular & Integrative Physiology, 151: 491-498.

Weber, R. E., and Hagerman, L. 1981. Oxygen and carbon dioxide transporting qualities of hemocyanin in the hemolymph of a natant decapod *Palaemon adspersus*. Journal of Comparative Physiology, 145: 21-27.

Wehrtmann, I. S., and López, G. A. 2003. Effects of temperature on the embryonic development and hatchling size of *Betaeus emarginatus* (Decapoda: Caridea: Alpheidae). Journal of Natural History, 37: 2165-2178.

Wei, L.-Z., Zhang, X.-M., Li, J., and Huang, G.-Q. 2008. Compensatory growth of Chinese shrimp, *Fenneropenaeus chinensis* following hypoxic exposure. Aquaculture International, 16: 455-470.

Wernberg, T., Smale, D. A., and Thomsen, M. S. 2012. A decade of climate change experiments on marine organisms: procedures, patterns and problems. Global Change Biology, 18: 1491-1498.

West, A., McGrorty, S., Caldow, R., Durell, S., Yates, M., and Stillman, R. 2004. Sampling macro-invertebrates on intertidal flats to determine the potential food supply for waders. NERC/Centre for Ecology and Hydrology, 19pp. CEH project No. C02007

West, G. B., Brown, J. H., and Enquist, B. J. 2001. A general model for ontogenetic growth. Nature, 413: 628-631.

White, C. R., Cassey, P., and Blackburn, T. M. 2007. Allometric exponents do not support a universal metabolic allometry. Ecology, 88: 315-323.

Whiteley, N. M. 2011. Physiological and ecological responses of crustaceans to ocean acidification. Marine Ecology Progress Series, 430: 257-271.

Whiteley, N. M., Suckling, C. C., Ciotti, B. J., Brown, J., McCarthy, I. D., Gimenez, L., and Hauton, C. 2018. Sensitivity to near-future CO_2 conditions in marine crabs depends on their compensatory capacities for salinity change. Scientific Reports, 8: 15639. https://www.nature.com/articles/s41598-018-34089-0

Widbom, B., and Frithsen, J. B. 1995. Structuring factors in a marine soft bottom community during eutrophication-an experiment with radio-labelled phytodetritus. Oecologia, 101: 156-168.

Widdicombe, C. E., Eloire, D., Harbour, D., Harris, R. P., and Somerfield, P. J. 2010. Long-term phytoplankton community dynamics in the Western English Channel. Journal of Plankton Research, 32: 643-655.

Widdicombe, S., and Austen, M. C. 2001. The interaction between physical disturbance and organic enrichment: An important element in structuring benthic communities. Limnology and Oceanography, 46: 1720-1733.

Wieking, G., and Kröncke, I. 2005. Is benthic trophic structure affected by food quality? The Dogger Bank example. Marine Biology, 146: 387-400.

Wiklund, A.-K. E., and Sundelin, B. 2001. Impaired reproduction in the amphipods *Monoporeia affinis* and *Pontoporeia femorata* as a result of moderate hypoxia and increased temperature. Marine Ecology Progress Series, 222: 131-141.

Williams, D. M. C. B. 1980. Dynamics of the Pomacentrid community on small patch reefs in One Tree Lagoon (Great Barrier Reef). Bulletin of Marine Science, 30: 159-170.

Willmott, C., and Matsuura, K. 2005. Advantages of the mean absolute error (MAE) over the root mean square error (RMSE) in assessing average model performance. Climate Research, 30: 79-82.

Wiltshire, K. H., Kraberg, A., Bartsch, I., Boersma, M., Franke, H.-D., Freund, J., Gebühr, C., Gerdts, G., Stockmann, K., and Wichels, A. 2009. Helgoland Roads, North Sea: 45 years of change. Estuaries and Coasts, 33: 295-310.

Włodarska-Kowalczuk, M., Górska, B., Deja, K., and Morata, N. 2016. Do benthic meiofaunal and macrofaunal communities respond to seasonality in pelagial processes in an Arctic fjord (Kongsfjorden, Spitsbergen)? Polar Biology, 39: 2115-2129.

Wood, H. L., Spicer, J., Lowe, D., and Widdicombe, S. 2010. Interaction of ocean acidification and temperature; the high cost of survival in the brittlestar *Ophiura ophiura*. Marine Biology, 157: 2001-2013.

Woodin, S. A. 1999. Shallow water benthic ecology: a North American perspective of sedimentary habitats. Australian Journal of Ecology, 24: 291-301.

Worm, B., and Lotze, H. K. 2016. Chapter 13 - Marine Biodiversity and Climate Change. *In* Climate Change (Second Edition), pp. 195-212. Ed. by T. M. Letcher. Elsevier, Boston.

Wyban, J., Walsh, W. A., and Godin, D. M. 1995. Temperature effects on growth, feeding rate and feed conversion of the Pacific white shrimp (*Penaeus vannamei*). Aquaculture, 138: 267-279.

Xie, M., Sun, Y., Feng, J., Gao, Y., and Zhu, L. 2019. Predicting the toxic effects of Cu and Cd on *Chlamydomonas reinhardtii* with a DEBtox model. Aquatic Toxicology, 210: 106-116.

Yuan, X., Yang, H., Wang, L., Zhou, Y., and Gabr, H. R. 2009. Bioenergetic responses of sub-adult sea cucumber *Apostichopus japonicus* (Selenka) (Echinodermata: Holothuroidea) to temperature with special discussion regarding its southernmost distribution limit in China. Journal of Thermal Biology, 34: 315-319.

Zacherl, D., Gaines, S. D., and Lonhart, S. I. 2003. The limits to biogeographical distributions: insights from the northward range extension of the marine snail, *Kelletia kelletii* (Forbes, 1852). Journal of Biogeography, 30: 913-924.

Zamora, L. N., and Jeffs, A. G. 2012. Feeding, metabolism and growth in response to temperature in juveniles of the Australasian sea cucumber, *Australostichopus mollis*. Aquaculture, 358-359: 92-97.

Zeileis, A., Grothendieck, G., Ryan, J. A., Ulrich, J. M., and Andrews, F. 2018. Zoo: S3 Infrastructure for Regular and Irregular Time Series (Z's Ordered Observations). 1.8-4 edn.

Zhang, Q., Warwick, R. M., McNeill, C. L., Widdicombe, C. E., Sheehan, A., and Widdicombe, S. 2015. An unusually large phytoplankton spring bloom drives rapid changes in benthic diversity and ecosystem function. Progress in Oceanography, 137, Part B: 533-545.

Zhao, X., Shi, W., Han, Y., Liu, S., Guo, C., Fu, W., Chai, X., et al. 2017. Ocean acidification adversely influences metabolism, extracellular pH and calcification of an economically important marine bivalve, *Tegillarca granosa*. Marine Environmental Research, 125: 82-89.

Zühlke, R., Alvsvåg, J., de Boois, I., Cotter, J., Ehrich, S., Ford, A., Hinz, H., Jarre-Teichmann, A., Jennings, S., Kröncke, I., Lancaster, J., Piet, G. and Price, P. 2001. Epibenthic diversity in the North Sea. Senckenbergiana Maritima, 31: 269-281.